Z-nucleic acids in virus-host interactions



Layal Liverpool

Radcliffe Department of Medicine

St Edmund Hall

University of Oxford

Supervisors: Jan Rehwinkel, Ph.D.

Peter Simmonds, Ph.D.

Jonathan Maelfait, Ph.D.

Thesis submitted for the degree of Doctor of Philosophy in Infection, Immunology and Translational Medicine

Trinity Term 2019

Acknowledgements

I dedicate this thesis to my grandmother Cecilia Gaisie (*in memoriam*) and grandfather Abdul Fattah Shalabi (*in memoriam*).

I would like to acknowledge my supervisor Jan Rehwinkel and co-supervisors, Jonathan Maelfait (University of Ghent) and Peter Simmonds. I would like to thank Jan for providing me with the fantastic opportunity to join his laboratory for my DPhil and for supporting my career development. This project was established by Jonathan and I would like to thank him for his brilliant day-to-day supervision and support with experiments during the first year of my DPhil and for continuing to supervise me after he left Oxford in 2017.

I would further like to thank Natalia Sampaio and Qiannan (Kalika) Tang, both of whom supervised me at the bench after Jonathan left the lab in 2017. Natalia and Kalika have both been extremely understanding, patient and thorough supervisors as well as inspiring female mentors. I am very thankful to Natalia for supporting me through the hardest moments and for believing in me all the way through. I am very grateful to Kalika for being harsh (but fair) and for teaching me how to “stay cool” in the lab! The majority of the animal work in Chapter 3 was done by Anne Bridgeman and I would like to thank her for her invaluable help with these experiments. I would like to thank all other Rehwinkel lab members past and present for providing such a positive and motivating lab environment to work in (and for answering all my questions!): Henry Blest, Lise Chauveau, Chiara Cursi, Tamara

Davenne, Kate Dicker, Antonio Gregorio Dias Jr., Jonny Hertzog, Alice Mayer, Lea Nussbaum, Rachel Rigby, Sonja Roll, Mirjam Schilling, TOPO the tiger and the iBright™ FL1000. I can only hope that my future colleagues will be as wonderful as my colleagues in the #RehwinkelLab have been. I would especially like to thank Gregorio for his friendship.

I am extremely grateful to all of my colleagues at the MRC WIMM, including all the facility managers, technicians and administrative staff without whom none of this work would have been possible.

I would like to thank my advisor, Christoph Tang, my thesis committee members and transfer and confirmation examiners Jelena Bezbradica-Mirkovic, Persephone Borrow, Mads Gyrd-Hansen and Paul Klenerman, and my thesis examiners, Nicole Zitzmann and Nicholas Gay, for taking the time to evaluate my work.

My DPhil was funded by the Wellcome Trust as part of the Infection, Immunology and Translational Medicine (IITM) programme in Oxford. I would like to thank the directors of the IITM programme, past and present, including Keith Gull, Fiona Powrie, Helen McShane and Christoph Tang, as well as my IITM peers, especially Cherrelle Dacon and Richard Morter for their support and friendship. I would also like to thank the IITM administrator Dawn Gibbons and MSDTC administrator Louise Samson. I am grateful to the Wellcome Trust, my course directors and my primary supervisor for supporting my application for an extension, which I used to undertake a 1-month placement at The Guardian newspaper in the

science writing team as part of my British Science Association (BSA) Media Fellowship (funded by the Society for Applied Microbiology) in 2018. I would like to thank the BSA for the opportunity, as well as my mentors at The Guardian, Ian Sample and Hannah Devlin, for inspiring and motivating me.

I am a passionate science communicator and champion of public engagement with research. I would like to thank all of the past and present public engagement and communications staff who have supported me with various science communication and public engagement initiatives throughout my DPhil: Alison Brindle, Martin Christlieb, Bryony Graham, Kirsty Heber-Smith, Michaela Livingstone-Banks, Charvy Narain, Emma O'Brien and Catarina Vicente. I would also like to thank everyone who has engaged with science through our initiatives, including all my followers on Twitter @layallivs and Instagram @ScienceSpedUp.

I would like to thank my rotation supervisors Quentin Sattentau and Michael Dustin and their lab members, including my bench-side supervisors Rebecca Moore, Hila Novak and Salvatore Valvo.

I would like to thank my college adviser Eva Gluenz for her support throughout my studies. I would also like to thank the St Edmund Hall community.

I would like to thank my former colleagues at UCL, particularly Richard Milne, Greg Towers and Chris van Tulleken for inspiring my passion for virology and for believing in me from the very beginning.

I would like to thank my former supervisors at Erasmus MC Rotterdam, Jan Piet van Hamburg and Sandra Paulissen, for introducing me into the world of

scientific research, teaching me how to pipette and inspiring me to become a scientist myself.

I would like to thank Clare van der Willigen for sparking my passion for science at a very early stage. I would like to thank Adam Bushnell for teaching me how to be a writer.

Finally, I would like to thank my family and close friends for all their love and support throughout this challenging endeavour, in particular my mother, Rawia, my father, Philip, and my sister, Yasmin. Thank you Konrad, my sweetheart.

Abstract

One of the biggest threats faced by cells is infection. When a virus infects a cell, its nucleic acids can be recognised by cellular sensors, which activate potent antiviral innate immune responses, such as interferons and cell death. These initial responses are vital in preventing the spread of infection to surrounding cells. Critically, nucleic acid sensors must have mechanisms of recognising foreign, aberrant or mislocalised nucleic acids and distinguishing them from unperturbed cellular nucleic acids. Alternative conformations of nucleic acids may represent a molecular sign of virus infection that can be sensed. Double-stranded DNA and RNA can adopt different helical conformations, including the unusual Z-conformation. The existence of proteins containing Z-binding domains (ZBDs) suggests Z-nucleic acids have important but so far poorly characterised biological functions. One such protein is Z-DNA binding protein-1 (ZBP1/DAI/DLM1). Using mouse cytomegalovirus as a model, we demonstrated that ZBP1 mediates virus-induced necroptotic cell death in a manner dependent on its two ZBDs. This suggests that the trigger for ZBP1 may be a Z-conformation nucleic acid. Knock-in mice, in which the ZBDs of ZBP1 are mutated, were more susceptible to virus infection. In addition to these mouse studies, we have demonstrated that ZBP1 also activates ZBD-dependent necroptosis in human cells and established and validated an assay for screening of small molecule or viral protein antagonists of ZBP1-mediated necroptosis in a human cell line.

TABLE OF CONTENTS

Table of Contents

Chapter 1 Introduction 19

1.1 Pattern recognition by the innate immune system 19

1.2 Nucleic acid sensing: ligands and receptors 22

1.3 Z-nucleic acids 28

1.4 Z-nucleic acid binding proteins and Z-DNA binding protein-1 31

1.5 Nucleic acid sensors and programmed cell death 36

1.6 Necroptosis 42

1.7 ZBP1-mediated necroptosis 50

1.8 Viral antagonism of necroptosis 53

1.9 Thesis aims 55

Chapter 2 Materials and methods 57

2.1 Mice 57

2.2 Cells 58

2.3 Plasmids, oligonucleotides and reagents 59

2.4 Viruses 64

2.5 RT-QPCR 66

2.6 Cell viability and necroptosis assays 67

2.7 Western blotting 69

2.8 Flow cytometry 70

2.9 Confocal microscopy 70

2.10 Statistics 71

Chapter 3 Results I Sensing of viral and endogenous RNA by mouse ZBP1 induces necroptosis 72

3.1 Z-nucleic acid binding is essential for ZBP1-mediated MCMV^{M45mutRHIM}-induced cell death 74

3.2 ZBP1-mediated, ZBD-dependent MCMV^{M45mutRHIM}-induced cell death is necroptotic 80

3.3 ZBP1-mediated, ZBD-dependent MCMV^{M45mutRHIM}-induced necroptosis is independent of type I IFN signalling 82

3.4 ZBP1 ZBD mutant knock-in mice fail to restrict MCMV^{M45mutRHIM} and cells from these animals do not undergo virus-induced necroptosis 86

3.5 MVA and MHV68 may induce ZBP1-mediated cell death 94

3.6 Discussion 96

Chapter 4 Results II ZBP1 mediates necroptosis in human cells 100

4.1 Ectopic ZBP1 expression in human cells induces spontaneous cell death 103

4.2 Reconstitution of the ZBP1 necrosome in human cells 113

4.3 A novel tool to detect inhibitors of the human ZBP1 necrosome 118

4.4 Discussion 123

Chapter 5 Results III A targeted screen for viral protein inhibitors of the human ZBP1 necrosome 128

5.1 Testing candidate VZV proteins for inhibition of ZBP1-mediated RIPK3 auto-phosphorylation 130

5.2 Screening of ZIKV proteins for inhibition of ZBP1-mediated RIPK3 auto-phosphorylation 133

5.3 Discussion 137

Chapter 6 Conclusions 141

References 145

Appendix I Supplementary figures 163

Appendix II Science communication & public engagement 175

Appendix III Publications 178

LIST OF FIGURES

FIGURE 1. NUCLEIC ACID SENSORS RECOGNISE VIRUS INFECTION AND TRIGGER TYPE I IFN INDUCTION. 23
FIGURE 2. STRUCTURAL REPRESENTATIONS OF B-DNA AND Z-DNA. 30
FIGURE 3. Z-NUCLEIC ACID BINDING PROTEINS AND THEIR DOMAINS. 33
FIGURE 4. DNA SENSORS AND PROGRAMMED CELL DEATH. 39
FIGURE 5. RNA SENSORS AND PROGRAMMED CELL DEATH. 42
FIGURE 6. TNF SIGNALLING PATHWAYS. 46
FIGURE 7. ZBP1-MEDIATED VIRUS-INDUCED NECROPTOSIS. 51
FIGURE 8. VIRAL ANTAGONISM OF ZBP1-MEDIATED NECROPTOSIS. 54
FIGURE 9. MUTATIONS INTRODUCED INTO THE TWO ZBDS (ZA1A2) OF MOUSE ZBP1. 76
FIGURE 10. ZBP1-MEDIATED MCMV^{M45MUTRHIM}-INDUCED REDUCTION IN CELL VIABILITY IS ZBD DEPENDENT. 77
FIGURE 11. KINETICS OF ZBP1-MEDIATED ZBD-DEPENDENT MCMV^{M45MUTRHIM}-INDUCED CELL DEATH. 79
FIGURE 12. ZBP1-MEDIATED VIRUS-INDUCED CELL DEATH IS RESCUED BY PHARMACOLOGICAL INHIBITION OF RIPK3 BUT NOT RIPK1. 81
FIGURE 13. ZBP1 RESTRICTS MCMV^{M45MUTRHIM} REPLICATION BY INDUCING NECROPTOSIS, BUT NOT TYPE I IFN EXPRESSION. 83
FIGURE 14. ZBP1-MEDIATED VIRUS-INDUCED CELL DEATH IS NOT AFFECTED BY IFNAR1 BLOCKADE. 85
FIGURE 15. KNOCK-IN OF ZBP1^{ZA1A2MUT} DOES NOT AFFECT *ZBP1* EXPRESSION. 86
FIGURE 16. KNOCK-IN OF ZBP1^{ZA1A2MUT} ABROGATES MCMV^{M45MUTRHIM}-INDUCED NECROPTOSIS. 88
FIGURE 17. KNOCK-IN OF ZBP1^{ZA1A2MUT} INCREASES THE RATE OF MCMV^{M45MUTRHIM} GENOME REPLICATION. 89

FIGURE 18. *ZBP1*$^{ZA1A2MUT/ZA1A2MUT}$ MICE ARE LESS ABLE TO CONTROL MCMV^{M45MUTRHIM} SPREAD TO THE SPLEEN. 90
FIGURE 19. INCREASED MCMV^{M45MUTRHIM} SPREAD TO THE SPLEEN IN *ZBP1*$^{ZA1A2MUT/ZA1A2MUT}$ MICE IS ASSOCIATED WITH INCREASED CYTOKINE INDUCTION. 92
FIGURE 20. *SPATA2*$^{-/-}$ MICE CONTROL MCMV^{M45MUTRHIM} SPREAD TO THE SPLEEN. 93
FIGURE 21. MVA AND MHV68 INDUCE A ZBP1-MEDIATED REDUCTION IN CELL VIABILITY. 94
FIGURE 22. MVA AND MHV68 INDUCE A ZBP1-MEDIATED CELL MEMBRANE PERMEABILISATION. 95
FIGURE 23. CONSERVATION OF KEY AMINO ACIDS IN ZBP1 ZBDS FROM HUMAN TO MOUSE. 100
FIGURE 24. PROTEIN EXPRESSION LEVELS OF ZBP1, RIPK3 AND MLKL IN DIFFERENT HUMAN CELL LINES. 103
FIGURE 25. ECTOPIC ZBP1 EXPRESSION IN HT-29 CELLS IS CYTOTOXIC. 105
FIGURE 26. ZBP1 HAS A PREDOMINANTLY CYTOPLASMIC LOCALISATION IN TRANSFECTED HEK293T CELLS. 107
FIGURE 27. CO-TRANSFECTION OF ZBP1, RIPK3 AND MLKL INDUCES CELL MEMBRANE PERMEABILISATION IN HEK293T. 108
FIGURE 28. DOSE TITRATIONS OF ZBP1, RIPK3 AND MLKL TRANSFECTIONS IN HEK293T. 110
FIGURE 29. CO-TRANSFECTION OF ZBP1, RIPK3 AND MLKL REDUCES CELL VIABILITY IN HEK293T 112
FIGURE 30. SCHEMATIC OF ZBP1-MEDIATED NECROPTOSIS ASSAY IN HEK293T. 113
FIGURE 31. ZBP1 MEDIATES RIPK3 PHOSPHORYLATION IN A ZBD-DEPENDENT MANNER. 115

FIGURE 32. ZBP1-MEDIATED ZBD-DEPENDENT RIPK3 PHOSPHORYLATION REQUIRES RIPK3 KINASE ACTIVITY. 117
FIGURE 33. ZBP1-MEDIATED ZBD-DEPENDENT RIPK3 AUTO-PHOSPHORYLATION IS INHIBITED BY MCMV M45 FRAGMENTS AND HSV-1 ICP6..... 120
FIGURE 34. RHIM-DEPENDENT INHIBITION OF ZBP1-MEDIATED ZBD-DEPENDENT RIPK3 AUTO-PHOSPHORYLATION BY AN M45 FRAGMENT. 122
FIGURE 35. VZV ORF20 CONTAINS A PUTATIVE RHIM. 131
FIGURE 36. VZV ORFS 19 AND 20 DO NOT INHIBIT ZBP1-MEDIATED ZBD-DEPENDENT RIPK3 AUTO-PHOSPHORYLATION. 132
FIGURE 37. ZIKV PROTEINS NS5, NS3, NS4A, NS4A-2K-NS4B, NS4B AND 2K-NS4B DO NOT INHIBIT ZBP1-MEDIATED ZBD-DEPENDENT RIPK3 AUTO-PHOSPHORYLATION..... 135
FIGURE 38. INFECTION WITH ZIKV DOES NOT INHIBIT ZBP1-MEDIATED ZBD-DEPENDENT RIPK3 AUTO-PHOSPHORYLATION. 136

LIST OF TABLES

TABLE 1. LIST OF PRIMERS 60

TABLE 2. LIST OF PRIMARY ANTIBODIES USED FOR WESTERN BLOTTING..... 61

ABBREVIATIONS

ABCF1	ATP binding cassette subfamily F member 1
ACTB	β-Actin
ADAR1	Adenosine deaminase acting on RNA-1
ADP	Adenosine diphosphate
AIM2	Absent in melanoma 2
ALS	Amyotrophic lateral sclerosis
AP-1	Activator protein 1
ATP	Adenosine triphosphate
Bax	Bcl-2-associated X protein
Bcl-2	B-cell lymphoma 2
CARD	Caspase activation and recruitment domain
Cas9	CRISPR associated protein 9
cDNA	Complementary DNA
CDR	Cytosolic DNA receptor
CD4	Cluster of differentiation 4
CD8	Cluster of differentiation 8
cGAMP	Cyclic guanosine monophosphate-adenosine monophosphate
cGAS	cGAMP synthase
CRISPR	Clustered regularly interspaced short palindromic repeats
CTL	Cytotoxic T-lymphocyte

CVB	Coxsackie B virus
DAI	DNA-dependent activator of IFN-regulatory factors
DDX41	DEAD-box helicase 41
DHX9	DExH-box helicase 9
DHX36	DExH-box helicase 36
DNA	Deoxyribonucleic acid
DNA-PK	DNA protein kinase
DNase II	Deoxyribonuclease II
dsRNA	Double-stranded RNA
EAE	Experimental autoimmune encephalomyelitis
ESCRT-III	Endosomal sorting complexes required for transport III
EV	Empty vector
FADD	Fas-associated protein with death domain
FISH	Fluorescence *in situ* hybridisation
FRET	Fluorescence resonance energy transfer
GAPDH	Glyceraldehyde 3-phosphate dehydrogenase
gB	Glycoprotein B
GSDMD	Gasdermin D
HCMV	Human cytomegalovirus
HEK293T	Human embryonic kidney 293 large T antigen
HIV-1	Human immunodeficiency virus type 1

HLA	Human leukocyte antigen
HRP	Horse radish peroxidase
hSMART	Human sensor for MLKL activation by RIPK3 based on FRET
HSV1	Herpes simplex virus 1
HSV2	Herpes simplex virus 2
IAP	Inhibitor of apoptosis
IAV	Influenza A virus
ICP6	Infected cell protein 6
ICP10	Infected cell protein 10
IE1	Immediate early 1
IE3	Immediate early 3
IFI16	IFN gamma inducible protein 16
Ifi44	IFN-induced protein 44
Ifit1	IFN-induced protein with tetratricopeptide repeats 1
IFN	Interferon
IFNAR1	IFN alpha and beta receptor subunit 1
IL-1β	Interleukin 1β
IL-18	Interleukin 18
IRF1	IFN regulatory factor 1
IRF3	IFN regulatory factor 3
ISG	IFN stimulated gene

LPS	Lipopolysaccharide
LRRFIP1	Leucine-rich repeat binding flightless II interacting protein 1
MAPK	Mitogen-activated protein kinase
MAVS	mitochondrial antiviral signalling protein
MCMV	Mouse cytomegalovirus
MDA5	Melanoma differentiation-associated protein 5
MDDC	Monocyte-derived dendritic cells
MEF	Mouse embryonic fibroblast
MHC	Major Histocompatibility
MHV68	Murine gammaherpes virus 68
MLKL	Mixed lineage kinase like
MOI	Multiplicity of infection
MRE11	Meiotic Recombination 11
MS	Multiple sclerosis
MVA	Modified vaccinia Ankara
MyD88	Myeloid differentiation primary response 88
Nec-1	Necrostatin-1
NFκB	Nuclear factor kappa-light-chain-enhancer of activated B cells
NS	Non structural
OASL1	2'-5'-oligoadenylate synthetase-like 1
ORF	Open reading frame

PAMP	Pathogen-associated molecular pattern
PARP	Poly (ADP-ribose) polymerase
PBS	Phosphate buffered saline
PCR	Polymerase chain reaction
PKR	Protein kinase R
PKZ	Protein kinase Z
PRR	Pattern recognition receptor
PUMA	p53 upregulated modulator of apoptosis
RHIM	RIP homotypic interaction motif
RIG-I	Retinoic acid inducible gene I
RIP	Receptor interacting protein
RIPK1	RIP kinase 1
RIPK3	RIP kinase 3
RLR	RIG-I like receptor
RNA	Ribonucleic acid
RT-qPCR	Real time quantitative PCR
SDS-PAGE	Sodium dodecyl sulphate polyacrylamide gel electrophoresis
SMAC	Second mitochondria-derived activator of caspase
STAT1	Signal transducer and activator of transcription 1
STING	Stimulator of IFN genes
SPATA2	Spermatogenesis associated protein 2

TANK	TNF receptor associated factor family member associated NFκB activator
TBK1	TANK-binding kinase 1
THP1	Tohoku Hospital Pediatrics-1
TNF	Tumour necrosis factor
TLR	Toll-like receptor
TRADD	Tumour necrosis factor receptor type 1-associated DEATH domain protein
TREX1	Three-prime repair exonuclease 1
TRIF	TIR domain-containing adapter inducing IFNβ
UL45	Unique long 45
vIRA	Viral inhibitor of RIP activation
VV	Vaccinia virus
VZV	Varicella zoster virus
WT	Wildtype
ZBD	Z-binding domain
ZBP1	Z-DNA binding protein 1
ZIKV	Zika virus
zVAD	carbobenzoxy-valyl-alanyl-aspartyl-[O-methyl]-fluoromethylketone

CHAPTER 1 INTRODUCTION

1.1 PATTERN RECOGNITION BY THE INNATE IMMUNE SYSTEM

One of the biggest threats facing cells and multi-cellular organisms is infection. The immune system evolved as a defence mechanism against infection and encompasses everything from cell-autonomous innate immunity, to the system of highly specialised immune cells acting in concert within multicellular organisms. Infectious agents can come in various different forms such as bacteria, fungi, viruses and parasites. The immune system must therefore be capable of recognising and responding to a huge variety of potential invaders. At the level of cell-autonomous innate immunity, this is achieved using a system of pattern recognition receptors (PRRs), which recognise pathogen-associated molecular patterns (PAMPs). In addition to PRRs, constitutively expressed cellular restriction factors, anti-microbial peptides, autophagy and cytolysis form important cell-intrinsic barriers against infection (Randow et al. 2013). Upon detection of an invading pathogen, PRRs can signal the activation of cell-autonomous innate immune responses, which serve to restrict the infection and, in the case of multi-cellular organisms, limit the spread of the infection to surrounding cells. This theory of pattern recognition was first proposed by Charles Janeway in 1989 (Janeway 1989) and was subsequently confirmed by the discovery of *Toll* in flies and related PRRs in mammals (Lemaitre et al. 1996; Medzhitov et al. 1997), which was recognised by

the 2011 Nobel Prize in Physiology or Medicine, jointly awarded to Ralph Steinman, Jules Hoffman and Bruce Beutler.

The 2011 Nobel Prize further highlighted the establishment of a link between innate and adaptive immunity. Broadly speaking, the immune system can be divided into two arms, called innate and adaptive. Innate immune cells are phagocytic and include polymorphonuclear cells such as neutrophils, basophils and eosinophils as well as non-polymorphonuclear cells such as macrophages and dendritic cells. Adaptive immune cells are lymphocytes, called T-cells and B-cells because they derive from the thymus and bone marrow, respectively. Whereas innate immune cells rely on germ-line encoded PRRs, which are broadly specific, lymphocytes utilise somatically encoded receptors, which recognise peptides called antigens, derived from proteins from pathogens, in a highly specific manner. Importantly, cell-autonomous innate immunity is not restricted to innate immune cells. Indeed, most cell lineages have the capacity to defend themselves against infection (Randow et al. 2013). The innate immune system represents the first line of defence against an invading pathogen, however, if cell-autonomous innate immune responses and phagocytosis fail to result in pathogen clearance, innate immune cells can recruit lymphocytes to the site of infection. Crucially, phagocytes possess the ability to process and present antigens to lymphocytes via Major Histocompatibility (MHC) molecules, encoded by Human Leukocyte Antigen (HLA) genes. In particular, dendritic cells form a vital bridge between innate and adaptive immunity, by migrating from sites of infection to secondary lymphoid organs where lymphocytes

reside. Activated lymphocytes migrate to sites of infection and execute highly targeted effector functions such as killing of infected cells by cytotoxic T-lymphocytes (CTLs) and the secretion of neutralising antibodies by differentiated B-cells called plasma cells. Antibodies facilitate phagocytic killing via Fc-receptors and can also neutralise pathogens directly.

Viruses are obligate intracellular pathogens; absolutely dependent on their host cells for replication. As a result, viruses have an extremely intimate interaction with their host cells. Viruses in essence are nucleic acids, DNA or RNA, contained within an outer protein shell. Given the relative simplicity of viruses, the primary virus-associated molecular pattern, which cells have evolved to recognise is their nucleic acids. In doing so, cells have overcome the challenge of distinguishing their own endogenous or “self” nucleic acids with those from invading pathogens like viruses.

A key remaining question in the field of innate immunity and nucleic acid sensing pertains to the precise molecular mechanisms by which cells discriminate between self and foreign nucleic acids. Failure to make this distinction accurately can result not only in viral diseases, but also in auto-inflammatory pathologies (Barber 2015), mediated by inappropriate responses to self nucleic acids. Moreover, nucleic acids from dying cancer cells can be sensed to activate anti-tumour immune responses (Ohkuri et al. 2014). The molecular pathways involved in nucleic acid detection and innate immune activation therefore present interesting therapeutic targets for a multitude of diseases.

1.2 NUCLEIC ACID SENSING: LIGANDS AND RECEPTORS

Nucleic acids, DNA and RNA, are the biological molecules essential to all known forms of life. Nucleic acids are polymers in which each monomer is a nucleotide. Nucleotides are composed of a 5-carbon sugar, a phosphate group and a nitrogenous base. The sugar can be ribose, making the resulting polymer a ribonucleic acid (RNA), or deoxyribose, making the resulting polymer a deoxyribonucleic acid (DNA). The nitrogenous base can be adenosine (A), thymidine (T) in DNA or uracil (U) in RNA, guanosine (G) or cytosine (C). Nucleic acids from invading pathogens can be sensed to activate potent cell-intrinsic innate immune responses. Nucleic acid sensors, specifically, are proteins that detect perturbations in cellular nucleic acid homeostasis through direct binding to unusual, foreign, aberrant or mislocalised nucleic acids inside cells. Moreover, nucleic acid sensors are essential and non-redundant for the induction of innate immune signalling pathways. Nucleic acid sensing is particularly important in the context of viral infection where a key innate immune response is the induction of type I interferons (IFNs) (McNab et al. 2015), which signal autocrine and paracrine to set up a cellular antiviral state (Figure 1). As such, type I IFNs not only restrict viruses in the infected cell but also limit their spread to surrounding cells. In addition to type I IFN induction, several nucleic acid sensors and proteins involved in downstream signalling activate other innate immune responses such as translational arrest (Yan

& Z. J. Chen 2012) or programmed cell death (Mocarski et al. 2012). Following detection of a virus infection, the induction of programmed cell death pathways such as apoptosis, serves to eliminate the virus-infected cell, thereby preventing the spread of the infection to surrounding cells and protecting the whole organism.

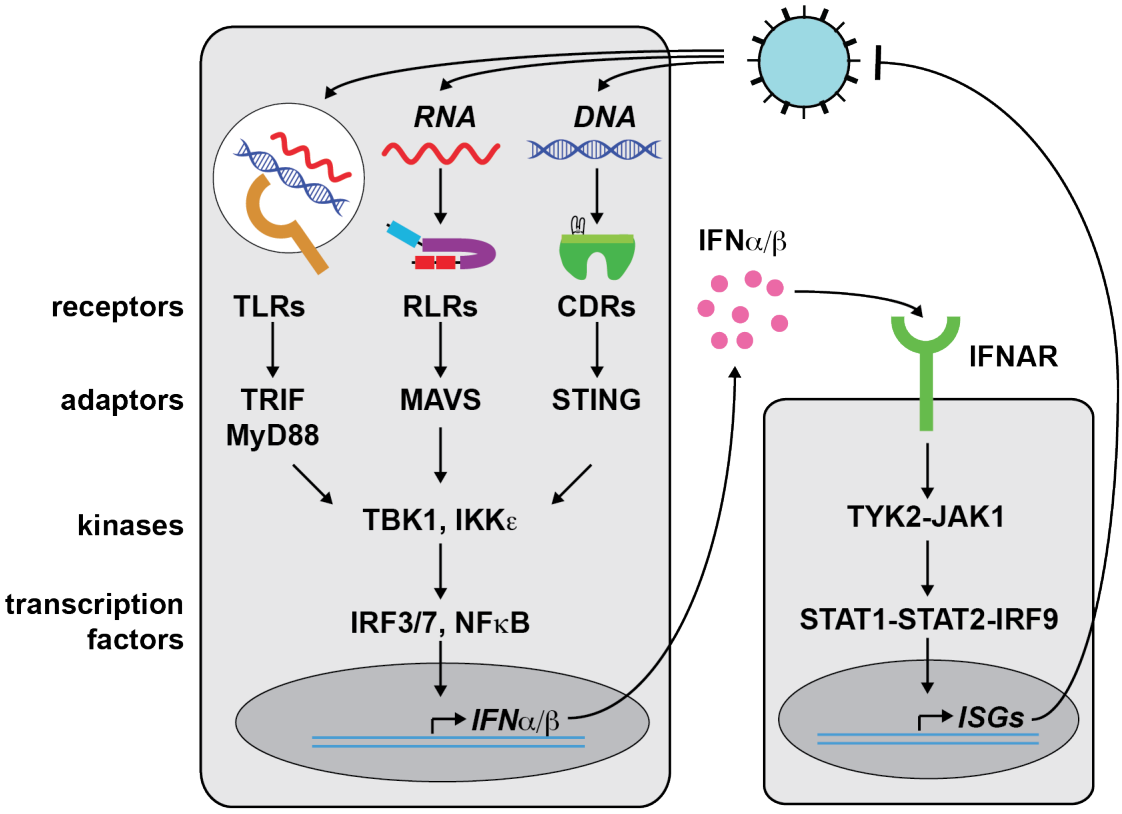


Figure 1. Nucleic acid sensors recognise virus infection and trigger type I IFN induction.

Taken from Jan Rehwinkel. Cellular nucleic acid sensors include endosomal TLRs and cytosolic RLRs and CDRs, and can induce type I IFN upon sensing of virus infection. Type I IFN signals autocrine and paracrine via IFNAR to set up a cellular antiviral state.

Nucleic acid sensors face the significant challenge of distinguishing foreign nucleic acids from an abundance of self nucleic acids present inside cells.

Understanding the precise mechanisms governing this self versus non-self-discrimination is therefore a key goal in the field. Nucleic acid sensors can broadly be divided into DNA and RNA sensors, although RNA:DNA hybrids are also PAMPs that can be sensed (Mankan et al. 2014; Rigby et al. 2014). The first nucleic acid sensors to be described were from the Toll-like receptor (TLR) family and have an endosomal localisation within the cell (Figure 1). These include the endosomal DNA sensor TLR9, which specifically recognises CpG dinucleotides (Hemmi et al. 2000), and the endosomal RNA sensors TLR3 and TLR7/8 (Kariko et al. 2004; Heil 2004; Diebold et al. 2004). Since the TLRs were first discovered (Medzhitov et al. 1997), numerous cytosolic DNA and RNA sensors have been described. The cytosolic nucleic acid sensors can generally be grouped into cytosolic DNA receptors (CDRs) and retinoic acid inducible gene I (RIG-I) like receptors (RLRs), which sense DNA and RNA respectively to activate type I IFN (Figure 1). Known mechanisms of self versus non-self discrimination by DNA and RNA sensors can be broadly divided into three categories, reviewed in (Schlee & G. Hartmann 2016): compartmentalisation of self nucleic acids within the cell, chemical modifications present on viral but not self nucleic acids and structural differences between viral and cellular nucleic acids. The following paragraphs will elaborate on these mechanisms and highlight well-characterised examples.

One mechanism by which nucleic acid sensors discriminate self from foreign nucleic acids is that DNA is usually compartmentalised in organelles, namely the nucleus and mitochondria, whereas the majority of the described innate immune

DNA sensors have a cytoplasmic or endosomal localisation. TLR9 recognises unmethylated CpG DNA from various pathogens including bacteria, parasites and viruses (Kumagai et al. 2008; Ghosh & Stumhofer 2013). The discovery that TLR9 is localised to endosomal compartments (Hemmi et al. 2000) raised the question of how DNA from viruses that enter through non-endosomal routes, for instance direct plasma membrane fusion, are sensed. This initiated the hunt for a cytosolic DNA sensor, the existence of which was validated by reports in 2006 of innate immune responses to DNA in cells from Myeloid differentiation primary response 88 (MyD88) knock-out mice (Ishii et al. 2006; Stetson & Medzhitov 2006). It is now understood that the presence of DNA in the cytosol, for instance viral DNA, activates cytosolic DNA sensors like cyclic guanosine monophosphate-adenosine monophosphate (cGAMP) synthase (cGAS). cGAS is essential for the type I IFN response to cytosolic double-stranded DNA (dsDNA) derived from microorganisms (Chen et al., 2016; Sun et al., 2013). Active cGAS synthesises the second messenger cGAMP (Wu et al., 2013), hence its nomenclature. cGAMP binds to and activates stimulator of IFN genes (STING). Active STING then engages TANK-binding kinase 1 (TBK1), which in turn phosphorylates the transcription factor IFN regulatory factor 3 (IRF3), eventually leading to type I IFN gene transcription (Chen et al., 2016). In addition to sensing DNA from multiple viruses (Q. Chen et al. 2016), cGAS has been implicated in many auto-inflammatory diseases where it is thought that inappropriate sensing of endogenous DNA by cGAS underlies pathology (Ablasser et al., 2014; Gao et al., 2015; Gray et al., 2015; Mackenzie et al., 2016; Maelfait et al., 2016). This is

consistent with the well understood role of cytoplasmic and endosomal nucleases like Three-prime repair exonuclease 1 (TREX1) and DNase II, which negatively regulate innate immune DNA sensing (Y.-G. Yang et al. 2007; Ablasser et al. 2014). Indeed, loss of these nucleases in humans and mice is associated with auto-inflammatory disease, presumably mediated by the accumulation of self DNA (Morita et al. 2004; Crow et al. 2006). DNA damage that results in leakage of nuclear or mitochondrial DNA into the cytosol is also associated with cGAS activation in multiple pathologies (T. Li & Z. J. Chen 2018). How inappropriate cGAS activation is avoided during the cell cycle, when the nuclear envelope breaks down, remains to be elucidated. Of note, two studies independently demonstrated that micronuclei, which arise when the cell cycle progresses after induction of double-stranded DNA breaks, were required for the downstream activation of the cGAS/STING DNA sensing pathway and associated inflammatory signalling (Mackenzie et al. 2017) (Mackenzie et al. 2017; Harding et al. 2017). Prior to the discovery of cGAS, many other cytosolic DNA sensors were described, including DAI (Takaoka et al. 2007), AIM2 (Burckstummer et al. 2009; Hornung et al. 2009; Roberts et al. 2009; Fernandes-Alnemri et al. 2009), IFI16 (Unterholzner et al. 2010), LRRFIP1 (P. Yang et al. 2010), DHX9 (T. Kim et al. 2010), DHX36 (T. Kim et al. 2010), DDX41 (Z. Zhang et al. 2011), Ku70 (X. Zhang et al. 2011), DNA-PK (Ferguson et al. 2012), ABCF1 (Lee et al. 2013), STING (Abe et al. 2013) and MRE11 (Kondo et al. 2013). Some of these proteins will be discussed in more detail in subsequent sections.

TLR3 and TLR7/8 sense RNA in endosomes (Tatematsu et al. 2018), which, in the absence of infection, are normally RNA free. However, given the presence of normal cellular RNA in other regions such as the cytosol, additional mechanisms of self versus non-self discrimination other than compartmentalisation are particularly important for RNA sensors to avert spontaneous activation in response to self RNA. An additional mechanism of self versus non-self discrimination relies upon recognition of the presence or absence of chemical modifications on nucleic acids, for example, the RNA sensor RIG-I recognises phosphate moieties present on viral but not cellular RNA species (Rehwinkel & Reis e Sousa 2010). In addition to containing two or three phosphate groups at the 5'-end, RIG-I stimulatory RNAs lack 5'-cap methylation, which is present on cellular cytosolic RNAs, and contain base-pairing adjacent to the 5'-end (Rehwinkel & Reis e Sousa 2010). These features are all specific to viral RNAs (Baum et al. 2010; Rehwinkel et al. 2010; Goubau et al. 2014), enabling effective discrimination from cellular RNAs by RIG-I. RIG-I belongs to the RLR family of receptors, which also includes melanoma differentiation-associated protein 5 (MDA5). RIG-I and MDA5 share similar domains, including two domains involved in RNA binding, a DExD/H-box RNA helicase domain and a C-terminal domain, as well as two N-terminal caspase activation and recruitment domains (CARDs) required for signalling. CARDs enable both RIG-I and MDA5 to interact with key signalling adaptor protein mitochondrial antiviral signalling protein (MAVS), which induces type I IFN. Despite these structural similarities, RIG-I and MDA5 sense different virus infections and, unlike

RIG-I, the mechanisms by which MDA5 discriminates viral and self RNA are less well understood, but evidence suggests recognition of RNA length and structure are important (Dias Junior et al. 2019). Indeed, a third way sensors distinguish viral from self nucleic acids is based on structural differences. The best characterised example of this is the double-stranded RNA (dsRNA) structure commonly associated with virus infection, which is recognised by RIG-I, MDA5, protein kinase R (PKR) and oligoadenylate synthases in the cytosol (Hur 2019), and by TLR3 in endosomes (Alexopoulou et al. 2001). In addition to genomic RNA from dsRNA viruses, dsRNA intermediates produced during replication of single stranded RNA viruses or during overlapping transcription that occurs during replication of some DNA viruses (Colby & Duesberg 1969; Willis et al. 2011), can also be sensed to activate antiviral responses. In accordance, alternative conformations of nucleic acids, such as Z-conformation DNA or RNA (Z-DNA/Z-RNA), may also represent structural PAMPs that can be sensed.

1.3 Z-NUCLEIC ACIDS

Nucleic acids can exist in multiple conformations, including traditional Watson-Crick-Franklin double helices (Watson & Crick 1953) and Z-DNA/Z-RNA (A. H. Wang et al. 1979; Hall et al. 1984). Z-nucleic acids have a “zigzag” conformation because the orientation of every second nucleotide pair is altered relative to the sugar-phosphate backbone (**Figure 2**). Specifically, whereas all

bases in B-DNA/A-RNA are in the *anti*-conformation, every other nucleotide in Z-DNA/Z-RNA double helices is in the *syn*-conformation. The result is that the phosphate groups in Z-nucleic acids are closer together than in B-DNA/A-RNA. Inside cells under physiological conditions, the electrostatic repulsion of these charged phosphate groups means that the B-DNA conformation is most favourable. However, under high salt conditions this electrostatic repulsion is reduced and the Z-conformation is stabilised. Chemical modifications, for example cytosine methylation, also stabilise the Z-conformation (Behe & Felsenfeld 1981). The Z-conformation represents a higher energy state than B-DNA/A-RNA and, since purines (adenosine and guanine) can form the *syn*-conformation without an energy penalty, the specific nucleotide sequence is a key determinant of the energy required for the transition to the Z-conformation. A study found that sequences with alternating purines and pyrimidines, particularly alternating guanine and cytosine residues, were more readily converted to the Z-conformation (A. H. Wang et al. 1984). However, the Z-conformation can still form without an alternating purine-pyrimidine sequence in solution (Feigon et al. 1985).

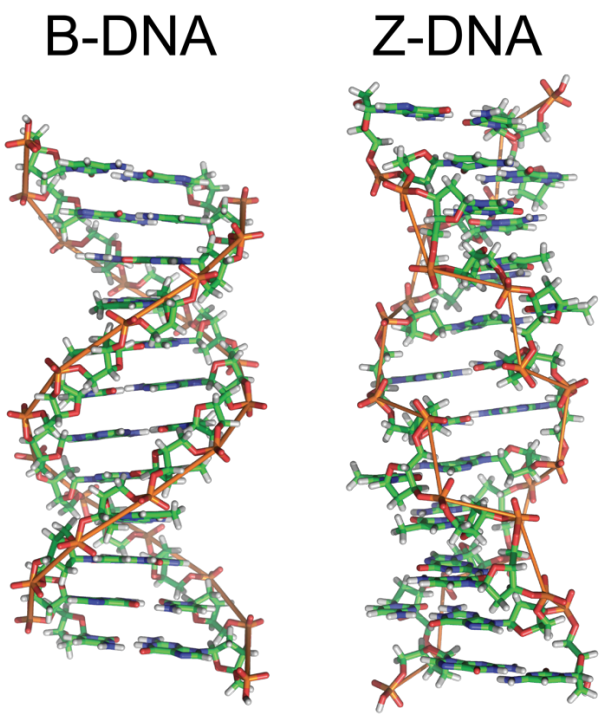


Figure 2. Structural representations of B-DNA and Z-DNA.

Modified from Zephyris (Richard Wheeler), 9 February 2007, In Wikipedia: en.wikipedia.org, retrieved 4 June 2019. The structures of B-DNA and Z-DNA are depicted. Z-DNA was discovered by Alexander Rich in 1979. It contains a left-handed helix-turn and adopts a zig-zag (Z) conformation. The glycosidic bond of every other base is in the *syn*-conformation. As a result, every other base is 'flipped out' of the helix. dsRNA can also adopt the Z-conformation.

The instability of Z-nucleic acids under standard cellular conditions has made them challenging to study in this context, however, there is evidence to suggest that Z-nucleic acids are biologically relevant (Rich & S. Zhang 2003; Herbert 2019). For example, spermine, spermidine and cytosine methylation, all of which have been shown to stabilise Z-DNA *in vitro* (Behe & Felsenfeld 1981), exist inside living cells. Negative supercoiling of DNA, another aspect of biological systems, requires energy and has been shown to stabilise the Z-conformation (Haniford & Pulleyblank

1983). During transcription, the DNA behind the moving RNA polymerase gets unwound and is subjected to negative torsional strain, which stabilises Z-DNA (Liu & J. C. Wang 1987). The discovery that Z-DNA-specific antibodies are found in human autoimmune diseases, namely systemic lupus erythematosus (Lafer et al. 1981), provides further evidence of a biological role for Z-DNA. Moreover, anti-Z-DNA antibodies stain DNA in transcriptionally active regions inside *Drosophila* polytene chromosomes (Lancillotti et al. 1987) and mammalian cell nuclei (Wittig et al. 1989). Z-RNA is less well characterised than Z-DNA (Herbert 2019). Shortly after Z-RNA was first discovered (Hall et al. 1984), structural studies revealed its similar conformation to Z-DNA (Teng et al. 1989; Davis et al. 1990). Like Z-DNA, Z-RNA is also immunogenic (Hardin et al. 1988). Z-RNA specific antibodies have been isolated from mice and rabbits, although some of these antibodies recognised both Z-RNA and Z-DNA. Z-RNA-specific antibodies stain the cytoplasm of eukaryotic cells visualised by immunofluorescent microscopy, suggesting that Z-RNA exists in fixed cells (Zarling et al. 1987).

1.4 Z-NUCLEIC ACID BINDING PROTEINS AND Z-DNA BINDING PROTEIN-1

Consistent with a biological role for Z-nucleic acids, four proteins containing Z-nucleic acid binding domains (ZBDs) have been described to date (**Figure 3**). However, the role of Z-nucleic acids and ZBDs in biology remains incompletely

understood. All four described ZBD-containing proteins have been implicated in virus-host interactions. These include the human RNA-editing enzyme adenosine deaminase acting on RNA-1 (ADAR1), the vaccinia virus (VV) innate immune evasion protein E3L, the fish ortholog of the human double-stranded RNA sensor and antiviral effector protein kinase R (PKR) called PKZ, and Z-DNA binding protein-1 (ZBP1/DAI/DLM1), a redundant (Z. Wang et al. 2008; Lippmann et al. 2008; Ishii et al. 2008) DNA sensor (Takaoka et al. 2007) and a mediator of a virus-induced inflammatory cell death called necroptosis (Upton et al. 2012) (**Figure 3**). This section will summarise what is known about ZBDs and ZBD-containing proteins with particular emphasis on ZBP1, which is the focus of this thesis.

The first ZBD-containing protein to be identified was ADAR1 p150 (Herbert et al. 1995). This IFN-inducible form of ADAR1 contains a ZBD, called Zα1, as well as a Zβ domain, which shares some similarities with Zα1 but cannot bind to Z-DNA (**Figure 3**). ADAR1 p110 is a truncated, constitutively expressed and non-IFN-inducible form of the protein, which lacks Zα1. ADAR1 additionally contains three dsRNA binding domains (dsRBDs) and a deaminase domain, which mediate its RNA binding and editing functions, respectively (U. Kim et al. 1994) (**Figure 3**). ADAR1 has been implicated in the editing of certain transcripts in cells and it is therefore possible that the ZBD enables targeting of ADAR1 p150 to Z-DNA, which forms only in transcriptionally active genes (Herbert & Rich 2001). Given that ZBDs can bind to Z-RNA (Placido et al. 2007), in addition to Z-DNA, it is also possible that ADAR1 p150 binds Z-RNA, although this has not yet been investigated.

Interestingly, mutations in ADAR1 that reduce Z-nucleic acid binding or that impair deaminase activity cause interferonopathies such as Aicardi-Goutières Syndrome (Rice et al. 2012).

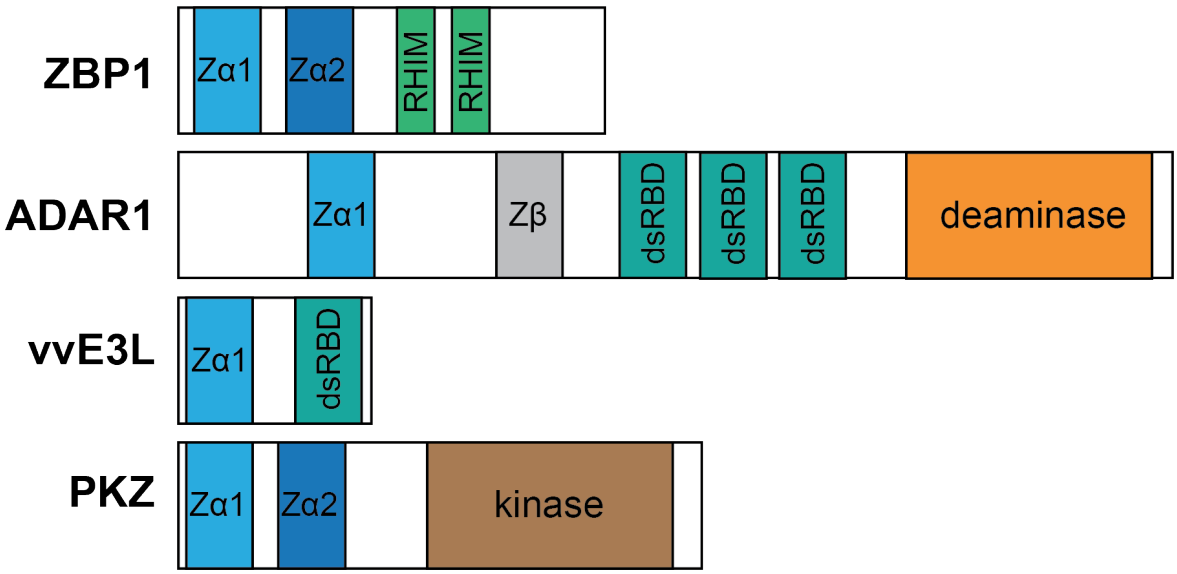


Figure 3. Z-nucleic acid binding proteins and their domains.

To date, 4 known proteins have been described containing Z-nucleic acid binding domains (ZBDs). All ZBDs are structurally very similar, but only Zα1 and Zα2 can physically interact with Z-conformation nucleic acids. ZBP1 contains one Zα1 and one Zα2 domain, which enable specific binding to Z-conformation nucleic acids. ZBP1 additionally contains a RIP homotypic interaction motif (RHIM) domain, a protein-protein interaction domain, which signals necroptosis induction by mediating an interaction with RIPK3. ADAR1 is a dsRNA-specific adenosine deaminase and contains 3 sequential dsRNA binding domains (dsRBDs). E3L is encoded by Vaccinia virus (VV) and antagonises the antiviral response. PKZ is the fish orthologue of PKR, a mammalian translational inhibitor. All 4 proteins function in antiviral immunity.

The co-crystal structure of ADAR1 Zα1 and Z-DNA (Schwartz 1999) enabled the identification of key residues within the ZBD that are required for Z-nucleic acid binding, which in turn led to the discovery of other ZBD-containing proteins

(Schwartz et al. 2001). The binding of Zα1 to Z-DNA is sequence independent and relies instead on contacts formed between Zα1 and the “zigzag” sugar-phosphate backbone, thereby providing specificity for the Z-conformation (Schwartz 1999). Specifically, a single base contact is made to guanine in the *syn*-conformation - a feature specific to Z-conformation nucleic acids. In addition, a helix-turn-helix motif is used by Zα1 to contact Z-DNA, however, this motif is also frequently used by proteins to interact with B-DNA. The Zα1 domain found in ADAR1 is additionally found in ZBP1, E3L and PKZ, however, ZBP1 and PKZ both have an additional ZBD called Zα2 (**Figure 3**). Key asparagine and tyrosine residues in Zα1 and Zα2, which are required for maintaining the ZBD fold and contacting DNA are conserved between all the ZBD-containing proteins (Schwartz et al. 2001). The two ZBDs of ZBP1 can bind Z-DNA together and binding of B-DNA by both Zα1 and Zα2 can mediate a conversion from B-DNA to Z-DNA (Ha et al. 2008). Z-RNA ZBDs bind to Z-RNA in a similar way to Z-DNA, but with differences in solvation due to the 2′-OH group of RNA (Herbert 2019).

VV E3L, an antagonist of PKR (Chang et al. 1992) and the type I interferon (IFN) response (Beattie et al. 1995), contains a single ZBD (Zα1) and a single dsRBD (**Figure 3**). VV is a large, double-stranded DNA virus whose replication is cytoplasmic. During replication, overlapping transcription forms dsRNA intermediates, which can trigger PKR leading to translational arrest (Willis et al. 2011). E3L is thought to antagonise PKR activation by sequestering dsRNA (Romano et al. 1998). *In vitro* studies have shown that the C-terminal dsRBD of E3L

is required for antagonism of PKR and the type I IFN response (Shors & Jacobs 1997), but conflicting studies suggest it is actually the N-terminal ZBD required for these functions (Romano et al. 1998; Cao et al. 2012; Thakur et al. 2014). Moreover, the E3L ZBD is required for pathogenesis of VV in mice (Brandt & Jacobs 2001). Interestingly, ZBDs from ADAR1 or ZBP1 functionally substitute for the E3L ZBD in mouse infection models (Y.-G. Kim et al. 2003). More recently, the E3L ZBD has been proposed to mediate antagonism of ZBP1-mediated necroptosis by the VV Western Reserve strain through the sequestration of ZBP1 ligands (Koehler et al. 2017). The study reported that a virus with an N-terminal deletion in E3L, that removes the ZBD, activates ZBP1-mediated necroptosis in mouse and human cells, whereas its wildtype counterpart does not.

ZBP1 was first identified in 1999 as the product of a gene that is up-regulated in activated mouse macrophages following stimulation with interferon-γ (IFNγ) or lipopolysaccharide (LPS) (Fu et al. 1999). It was subsequently discovered to bind to Z-DNA, hence it's nomenclature (Schwartz et al. 2001), and to be capable of inducing a B-DNA to Z-DNA transition (Ha et al. 2008). Of note, in addition to its two N-terminal ZBDs, ZBP1 contains two C-terminal RIP homotypic interaction motifs (RHIM), which mediate necroptosis activation (**Figure 3**). In 2007, ZBP1 was reported to sense B-DNA in the cytosol for type I IFN induction and named DNA-dependent activator of interferon regulatory factors (DAI) (Takaoka et al. 2007). However, this function of ZBP1 was subsequently shown to be redundant in human cells and in mice (Z. Wang et al. 2008; Lippmann et al. 2008; Ishii et al. 2008).

Moreover, this was followed by the discovery of cGAS as a critical and non-redundant cytosolic DNA sensor in humans and mice (Sun et al., 2013). Since then, accumulating evidence from us and others instead implicates ZBP1 as an RNA sensor of virus infection and activator of antiviral necroptotic cell death in mice and humans (Upton et al. 2012; Thapa et al. 2016; Kuriakose et al. 2016; Sridharan et al. 2017; Maelfait et al. 2017; Koehler et al. 2017; Guo et al. 2018) (see Appendix).

1.5 NUCLEIC ACID SENSORS AND PROGRAMMED CELL DEATH

There is an accumulating body of evidence that several nucleic acid sensors can activate programmed cell death pathways, such as apoptosis, as a cell-intrinsic innate immune response. Programmed cell death describes the activation of one of a number of intracellular processes that result in the death of the cell in a controlled manner. For instance, apoptosis can be induced in cells extrinsically, upon ligation of death receptors, or intrinsically, upon the release of cytochrome C from the mitochondria (Elmore 2007). Programmed cell death is essential for the survival of multicellular organisms through the removal of damaged, malignant and infected cells and also plays an important role in removing excess cells during organismal development. Apoptosis does not involve the release of cellular cytoplasmic contents whereas other programmed cell death pathways, such as necroptosis and pyroptosis, culminate in the release of cytoplasmic contents into the extracellular environment where these can trigger inflammation. This section will highlight

several examples of DNA and RNA sensors that activate programmed cell death pathways. ZBP1, which we and others have demonstrated is an RNA sensor that activates antiviral necroptotic cell death (Upton et al. 2012; Thapa et al. 2016; Kuriakose et al. 2016; Sridharan et al. 2017; Maelfait et al. 2017; Koehler et al. 2017; Guo et al. 2018) (see Appendix), and the necroptosis pathway are reviewed in section 1.7.

Several studies report that programmed cell death, particularly apoptosis, can be activated downstream of the cGAS-STING DNA sensing pathway (Figure 4). Tang *et al.* show that natural and artificial STING agonists, including variants of cGAMP, induce intrinsic apoptosis in malignant B-cells (Tang et al., 2016). STING agonist-induced apoptosis is not re-capitulated by treatment with recombinant IFNβ suggesting that this is unlikely to be an indirect effect of signalling through the type I IFN receptor. In T-cells, STING activation blocks proliferation and triggers cell death characterised by increased expression of pro-apoptotic genes (Cerboni et al. 2017; Larkin et al. 2017; Gulen et al. 2017). Moreover, human fibroblasts undergo STING-dependent apoptosis upon detection of DNA from herpes simplex virus 1 (HSV-1) and human cytomegalovirus (HCMV) (Diner et al., 2016). In hepatocytes, endoplasmic reticulum stress triggers apoptosis in a STING- and IRF3-dependent manner (Iracheta-Vellve et al., 2016; Petrasek et al., 2013). Finally, cGAMP treatment induces STING-dependent cell death in the monocytic cell line THP1, although the mechanism of cell death remains to be elucidated (Cerboni et al., 2017).

Absent in melanoma 2 (AIM2) has been implicated as a sensor of cytosolic DNA from invading DNA viruses and bacteria as well as self-derived cytosolic DNA (Choubey and Panchanathan, 2017; Hornung et al., 2009; Muruve et al., 2008). In response to binding to DNA, AIM2 activates the inflammasome (Figure 4) (Burckstummer et al., 2009; Fernandes-Alnemri et al., 2009; Hornung et al., 2009; Roberts et al., 2009). The inflammasome is a large protein complex that facilitates activation of caspase-1 by auto-proteolytic cleavage. Active caspase-1 in turn cleaves and thereby matures the pro-inflammatory cytokines IL-18 and IL-1β (Schroder and Tschopp, 2010). Inflammasome activation also results in the induction of pyroptosis, a caspase-1-dependent inflammatory form of cell death. Pyroptosis involves cell swelling, lysis and ultimately the release of cytoplasmic content (Shi et al., 2017). The active forms of IL-18 and IL-1β mediate downstream inflammation and immune responses and, given that they are not released by the canonical secretory pathway via the Golgi apparatus, their release is thought to be dependent on pyroptosis (Lamkanfi and Dixit; Sharma and Kanneganti, 2016; Shi et al., 2017). Mechanistically, cleavage by caspase-1 leads to the release of an N-terminal gasdermin D (GSDMD) fragment that forms pores in the cell membrane and thereby initiates pyroptotic cell death (Kayagaki et al., 2015; Liu et al., 2016; Shi et al., 2017; Shi et al., 2015). GSDMD deficiency abrogates pyroptosis in response to poly(dA:dT), a synthetic dsDNA that is sensed by AIM2 (Kayagaki et al., 2015; Shi et al., 2015). In addition to pyroptosis, AIM2 has been implicated in

apoptosis in a recent study (Chen et al., 2017), which demonstrated a pro-apoptotic and anti-proliferative effect of AIM2 in colorectal cancer cells.

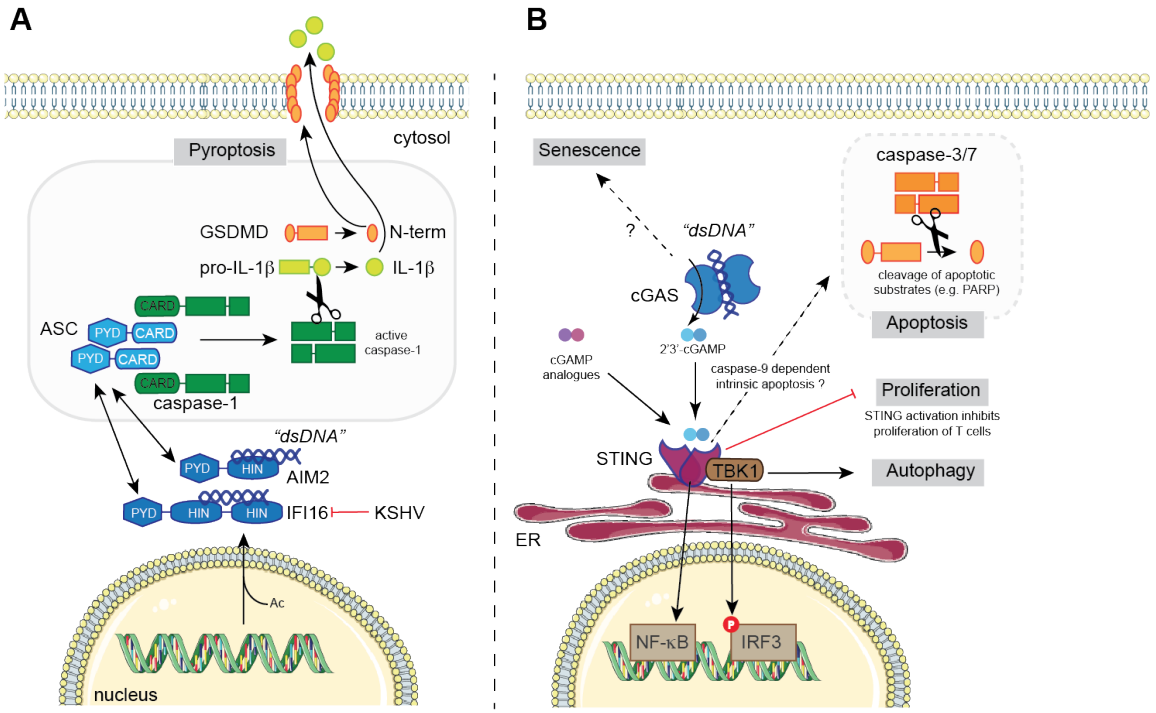


Figure 4. DNA sensors and programmed cell death.

Taken from Maelfait, Liverpool & Rehwinkel (manuscript in preparation) (see Appendix). DNA sensors can activate programmed cell death pathways, including apoptosis and pyroptosis.

TLR9 has also been linked to cell death. TLR9 is strongly activated by DNA molecules containing CpG dinucleotides, which are commonly found in bacteria but are usually methylated in vertebrates (Hacker et al., 2002). In a 2010 study, stimulation of neuroblastoma cells with TLR9 ligands was found to induce apoptosis (Brignole et al., 2010). Indeed, treatment with CpG induces cell death that is characterised by cleavage of caspase 3 and 7 and, which is rescued by

pharmacological pan-caspase inhibition (Brignole et al., 2010). Down-regulation of TLR9 using RNA interference protects dendritic cells from CpG induced apoptosis. In nude mice with neuroblastoma, treatment with CpG prolongs long-term survival suggesting an important potential application for CpG oligonucleotides in cancer therapy (Brignole et al., 2010). The use of nude mice, which lack a fully functioning adaptive immune system, is consistent with T-cell-independent cytolysis of the cancer cells. Of note, a number of other studies have linked TLR9 with apoptosis induction and revealed that TLR9 is not only pro-apoptotic, but also blocks apoptosis depending on the cellular context (El Kebir et al., 2014; Fischer et al., 2005; He et al., 2011a; Xiang et al., 2015; Zheng et al., 2008). For instance, murine macrophages exposed to environmental stress undergo increased apoptosis and a 2015 study (Xiang et al., 2015) found that deficiency of TLR9 attenuates macrophage apoptosis and is associated with down-regulation of caspase-3 and poly (ADP-ribose) polymerase (PARP) cleavage.

Alongside their important role in the induction of type I IFN as a response to virus infection, RLRs have also been reported to activate apoptosis (Figure 5). Transfection of MDA5 and RIG-I-stimulatory RNAs into cells induces apoptosis, in addition to type I IFN (Rintahaka et al. 2008; Poeck et al. 2008; Besch et al. 2009). RLR-triggered apoptosis, activated during virus infection, can benefit the host through the elimination of virus-infected cells (Chattopadhyay & Sen 2017; P. Li et al. 2016; van den Boorn & G. Hartmann 2013; Yu et al. 2016). Mechanistically, RLR triggered apoptosis is dependent on MAVS and IRF3, as is the case with IFN

induction (Besch et al. 2009; Chattopadhyay et al. 2010), however complex formation between MAVS and IRF3 differs upstream of these two signalling outcomes. In the case of type I IFN induction, MAVS facilitates TBK1-mediated IRF3 phosphorylation, which is necessary for the transcriptional induction of type I IFNs. For apoptosis induction, MAVS instead forms a larger complex that facilitates IRF3 modification through the addition of linear ubiquitin chains, which results in IRF3 translocation to mitochondria where it triggers cell-intrinsic apoptosis and cytochrome C release mediated by the pro-apoptotic protein Bax (Chattopadhyay et al. 2010; Chattopadhyay et al. 2016; Chattopadhyay & Sen 2017).

The RNA sensor TLR3 signals via TIR domain-containing adapter inducing IFNβ (TRIF) to induce type I IFNs and pro-inflammatory cytokines through NF-κB and IRF3 mediated transcriptional activation (Yamamoto et al. 2002; Yamamoto et al. 2003; Oshiumi et al. 2003; Hoebe et al. 2003). Like ZBP1, TRIF contains a C-terminal RHIM and can therefore interact with receptor interacting protein kinase 1 (RIPK1) to activate NF-κB (Meylan et al. 2004) or various programmed cell death pathways downstream of TLR3 ligation (Figure 5) (Maelfait et al. 2008; Weber et al. 2010; Feoktistova et al. 2011; He et al. 2011; Estornes et al. 2012; Kaiser et al. 2013). During virus infection, dsRNA ligands activate TLR3 and mutations in TLR3 or TRIF have been linked to herpes simplex virus 1 (HSV1) and influenza A virus (IAV) encephalitis in humans (Hidaka et al. 2006; S.-Y. Zhang et al. 2007; Sancho-Shimizu et al. 2011). In mice infected with IAV, TLR3 triggers cell death in the lungs and contributes to immunopathology (Le Goffic et al. 2006; Zinngrebe et al. 2016).

TLR3-mediated cell death can additionally be induced by treatment of small intestinal epithelial cells with poly(I:C) (McAllister et al. 2013) or following RNA release from cells damaged by ionising radiation (Takemura et al. 2014).

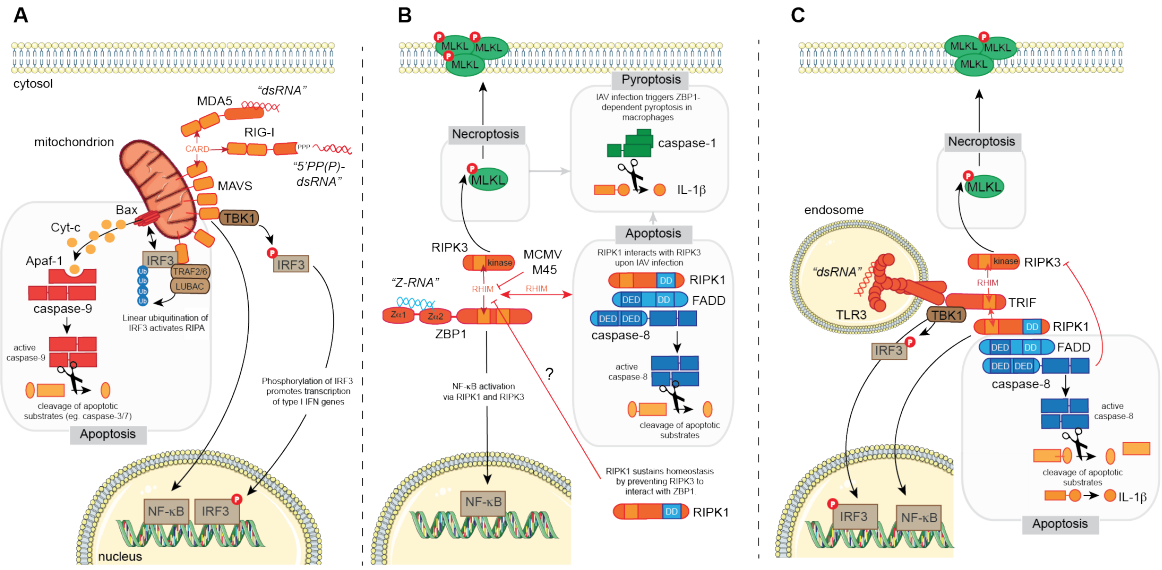


Figure 5. RNA sensors and programmed cell death.

Taken from Maelfait, Liverpool & Rehwinkel (manuscript in preparation) (see Appendix). RNA sensors can activate programmed cell death pathways, including apoptosis, necroptosis and pyroptosis.

1.6 NECROPTOSIS

Necroptosis is a form of programmed necrosis. Previously, apoptosis was thought to be the only programmed cell death pathway and necrosis was seen as unregulated; however, evidence from genetic, biochemical and functional studies, and the discovery of specific pharmacological inhibitors of necrosis, have specified this process as a molecularly controlled form of inflammatory cell death (Pasparakis

& Vandenabeele 2015). The most well characterised forms of molecularly controlled necrosis are pyroptosis and necroptosis. Pyroptosis and necroptosis are both inflammatory forms of cell death characterised by cell membrane lysis and the release of cellular contents into the extracellular environment (Pasparakis & Vandenabeele 2015). Pyroptosis is activated downstream of the inflammasome, which can have various upstream triggers. Mechanistically, caspase-1 mediates the catalytic conversion of the cytokines IL-18 and IL-1β into their active forms, whose release depend on pyroptosis (Lamkanfi and Dixit; Sharma and Kanneganti, 2016; Shi et al., 2017). Caspase-1 initiates pyroptosis by cleaving gasdermin D (GSDMD), whose N-terminal fragment then forms pores in the cell membrane resulting in cell lysis (Kayagaki et al., 2015; Liu et al., 2016; Shi et al., 2017; Shi et al., 2015). During necroptosis, the pseudokinase mixed lineage kinase like (MLKL) becomes phosphorylated and forms oligomers that, like GSDMD, form pores in the cell membrane causing cell lysis (Sun et al. 2012; Zhao et al. 2012; Dondelinger et al. 2014). This section will focus on necroptosis, which is activated downstream of ZBP1 sensing of virus infection (Upton et al. 2012; Thapa et al. 2016; Kuriakose et al. 2016; Sridharan et al. 2017; Maelfait et al. 2017; Koehler et al. 2017; Guo et al. 2018) (see Appendix).

Central players in the necroptosis pathway are receptor interacting protein kinase 3 (RIPK3) and its pseudokinase substrate, mixed lineage kinase like (MLKL). Once activated by upstream signals, RIPK3 phosphorylates MLKL triggering its oligomerisation (Sun et al. 2012; Zhao et al. 2012). MLKL oligomers form pores in

the cell membrane, resulting in necrotic cell death (Dondelinger et al. 2014). Inositol phosphate kinases are required for MLKL oligomerisation and localisation to the plasma membrane (Dovey et al. 2018). However, MLKL activation is not a point of no return, as active MLKL can be shed from cells in exosomes, circumventing necroptotic cell death (Gong et al. 2017). RIPK3 is a RHIM-containing protein and its activation is triggered by RHIM-RHIM interactions with upstream signalling proteins. RHIM-containing proteins that can activate RIPK3 include RIPK1 (Cho et al. 2009; Kaiser et al. 2011; Oberst et al. 2011), TRIF (He et al. 2011; Kaiser et al. 2013) and ZBP1 (Upton et al. 2012). Mechanistically, these RHIM-containing proteins directly bind RIPK3 and facilitate RIPK3 phosphorylation and consequent activation. The necrosome is the complex formed between RIPK3 and the activating RHIM-containing protein, which is canonically RIPK1 (Vandenabeele et al. 2010). RIPK1 kinase activity is required for RIPK1 or TRIF mediated necroptosis activation (Holler et al. 2000; Chan et al. 2003; Y. Lin et al. 2004); however, ZBP1 can mediate necroptosis independently of RIPK1 kinase activity by acting as a scaffold for RIPK3 auto-phosphorylation (He et al. 2011; Kaiser et al. 2013; Upton et al. 2012). Hereafter, the term ZBP1 necrosome is used to refer to the non-canonical ZBP1-RIPK3 signalling complex specifically.

Necroptosis induced by tumour necrosis factor (TNF) binding its receptor is well studied and is mediated through the formation of a canonical RIPK1-RIPK3 necrosome. TNF signalling can induce inflammatory and pro-survival gene expression through a receptor-bound complex that activates NFκB, AP-1 and MAPK

signalling; however, under certain conditions it can induce cell death instead (Figure 6) (Pasparakis & Vandenabeele 2015). When brakes on apoptosis are released, for example following treatment with the translation inhibitor cycloheximide, a different complex, including TRADD, FADD and caspase-8, forms and mediates caspase-8 driven apoptosis independently of RIPK1 (Kelliher et al. 1998; Micheau & Tschopp 2003; L. Wang et al. 2008). When inhibitor of apoptosis proteins (IAP) are additionally inhibited, for example by treatment with SMAC-mimetics, RIPK1 drives apoptosis by forming a complex with RIPK3, FADD and caspase-8 (L. Wang et al. 2008). In this context, apoptosis requires RIPK1 kinase activity, whereas RIPK3 acts as a scaffold protein in the complex, which is referred to as the ripoptosome (Feoktistova et al. 2011; Tenev et al. 2011). Necroptosis can only occur when apoptosis is inhibited, because caspase-8 controls RIPK1 and RIPK3 levels by proteolysis (Y. Lin et al. 1999; Feng et al. 2007). However, when apoptosis is inhibited, for example by the pan-caspase inhibitor zVAD or by genetic ablation of caspase-8, a RIPK1-RIPK3 necrosome can form and necroptosis mediated by RIPK1 and RIPK3 kinase activity can occur (Cho et al. 2009; Kaiser et al. 2011; Oberst et al. 2011). In addition to TNF receptors, necroptosis can be activated downstream of PRR ligation, including of TLR3, TLR4 and ZBP1 (Meylan et al. 2004; He et al. 2011; Upton et al. 2012) (see section 1.5). ZBP1-mediated necroptosis is reviewed in section 1.7.

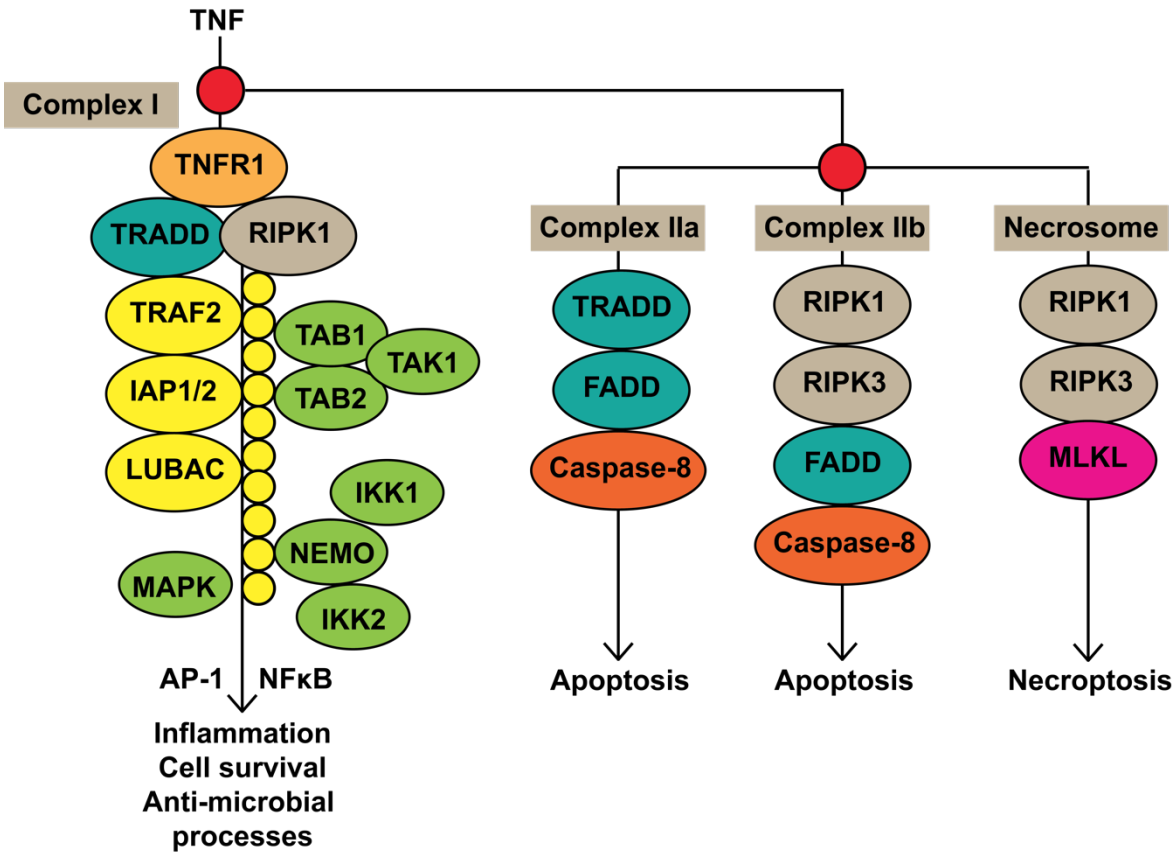


Figure 6. TNF signalling pathways.

Modified from Pasparakis & Vandenabeele 2015. TNF binding its receptor can induce inflammation, cell survival, anti-microbial processes and cell death pathways, including apoptosis and necroptosis.

Necroptosis forms a key innate immune response to viral infection by eliminating virus-infected cells (Mocarski et al. 2015; Upton et al. 2017). In fact, clearance of infected or damaged cells by cytolysis is an evolutionarily ancient strategy for the elimination of pathogens and preservation of health in multicellular organisms. Prior to the discovery of necroptosis, apoptosis was identified as a critical mechanism by which infected cells were eliminated (Yatim & Albert 2011).

Evidence for this is the evolution of a plethora of viral proteins dedicated to antagonising apoptosis in host cells (Hardwick 1998; Galluzzi et al. 2008; Upton & Chan 2014). Given that so many viruses encode inhibitors of apoptosis, virus infected cells are often driven towards necroptosis instead. Early evidence of the importance of cell death in viral control was the demonstration that overexpression of the anti-apoptotic protein B-cell lymphoma 2 (Bcl-2) is sufficient to turn a lytic virus into a persistent one (Levine et al. 1993). The importance of necroptosis in viral defence became clear later when several groups independently demonstrated that caspase blockade did not always rescue virus-induced cell death, but rather increased the amount of cell death in certain cell lines, for example in the mouse L929 cell line (Vercammen et al. 1998; M. Li & Beg 2000; Jaattela & Tschopp 2003; Vandenabeele et al. 2010). This phenomenon can now be explained by the fact that inhibition of apoptosis, for example by virally encoded proteins or pharmacological caspase blockade, sensitises cells to necroptosis (Y. Lin et al. 1999; Feng et al. 2007). This was initially only observed in certain cell lines because not all cell lines express sufficient amounts of the key necroptosis mediators RIPK3 and MLKL (Vercammen et al. 1998; M. Li & Beg 2000; Jaattela & Tschopp 2003; Vandenabeele et al. 2010). Since this discovery, multiple viruses have been shown to activate necroptosis in infected cells (Mocarski et al. 2015; Upton et al. 2017). For example, VV-infected cells become sensitised to TNF-driven necroptosis (Cho et al. 2009). Multiple herpes viruses activate necroptosis, including mouse cytomegalovirus (MCMV), HCMV and herpes simplex viruses 1 and 2 (HSV1/2)

(Upton et al. 2010; Omoto et al. 2015; Guo et al. 2015). In the examples described thus far, necroptosis induction has a protective role for the host by facilitating the elimination of virus-infected cells. However, excessive antiviral necroptosis may also contribute to immunopathology in certain contexts and even be detrimental to the host. For instance, HIV-1 infection has been reported to activate necroptosis in CD4 and CD8 T-cells and, in chronic HIV, necroptosis contributes to dysfunctional CD8 T-cell proliferation (Pan et al. 2014; Gaiha et al. 2014). Influenza A virus (IAV) induces multiple cell death pathways during infection, including necroptosis (Nogusa et al. 2016), which has been reported to benefit (Thapa et al. 2016) and harm (Kuriakose et al. 2016) host survival post-infection in different *in vivo* studies. Whether necroptosis is beneficial or harmful to the host may depend on various factors, for example one could speculate that necroptosis may be an effective way of limiting virus spread initially; however, if the virus is able to persist, then chronic necroptosis may ultimately result in host tissue damage.

Necroptosis is a medically important pathway, which, in addition to antiviral innate immunity, has been implicated in several non-communicable diseases (Galluzzi et al. 2017; Yuan et al. 2019; Degterev et al. 2019). As a consequence, there is significant interest from the pharmaceutical industry in drugs that target the necroptosis pathway (Degterev et al. 2019). Necrostatin-1 (Nec-1), which inhibits RIPK1, is a prime example (Degterev et al. 2005). Indeed, the kinases RIPK1 and RIPK3 provide promising drug targets because the kinase structure is highly amenable for the development of specific pharmacological small molecule

inhibitors. Nec-1 was found to be protective in animal models of ischaemic brain injury and myocardial infarction (Degterev et al. 2005; C. C. T. Smith et al. 2007). Moreover, necroptosis exacerbates cell death and neuroinflammation in several neurogenerative diseases, including multiple sclerosis, amyotrophic lateral sclerosis (ALS), Parkinson's disease and Alzheimer's disease (Ofengeim et al. 2015; Ito et al. 2016; Ofengeim et al. 2017; Caccamo et al. 2017; Iannielli et al. 2018). Tissue samples from cortical lesions of MS patients, and from mice with an experimental autoimmune encephalomyelitis (EAE) model of MS, showed reduced levels of active caspase-8, which may sensitise these cells to necroptosis (Ofengeim et al. 2015). In a genetic mouse model of ALS, RIPK1 has been shown to mediate axonal degeneration via promotion of necroptosis and inflammation (Ito et al. 2016). In Parkinson's disease models, pharmacological inhibition of necroptosis protects from dopaminergic neuronal cell death and reveals a potential link between mitochondrial defects and necroptosis activation (Iannielli et al. 2018). Necroptosis has also been reported to activate a response in microglia that promotes disease in Alzheimer's and levels of RIPK1 in post-mortem samples from individuals with late-onset Alzheimer's disease are increased compared to controls, and correlate with disease severity (Ofengeim et al. 2017; Caccamo et al. 2017). Drugs targeting RIPK1 are being clinically tested and may be used for the treatment of neurological conditions in humans in future (Weisel et al. 2017).

1.7 ZBP1-MEDIATED NECROPTOSIS

The first evidence that ZBP1 can activate RIPK3-MLKL driven necroptosis came in a study from Upton and colleagues, which found that ZBP1 complexes with RIPK3 via RHIM-RHIM interactions to activate RIPK1-independent virus-induced necroptosis (Upton et al. 2012). Type I IFN-induced ZBP1 expression sensitises cells to necroptosis induced by an MCMV mutant virus lacking viral inhibitor of RIP activation (vIRA), which is normally employed by MCMV to antagonise RIPK3-driven necroptosis (Upton et al. 2010). This MCMV mutant virus is attenuated in wildtype mice, but rescued in *Ripk3*$^{-/-}$ mice (Upton et al. 2010). This virus is similarly attenuated in *Zbp1*$^{-/-}$ mice, consistent with a ZBP1-RIPK3 complex as the target of vIRA (Upton et al. 2012). Importantly, ZBP1-mediated virus-induced necroptosis was not rescued by Nec-1, indicating that the ZBP1 necrosome forms independently of RIPK1. Following on from this discovery, studies from us and others have revealed the molecular mechanism by which MCMV infection is sensed by ZBP1 to activate necroptosis (Figure 7) (Maelfait et al. 2017; Sridharan et al. 2017) (see Appendix), and ZBP1 has been shown to mediate necroptosis in response to infection by several other viruses (Thapa et al. 2016; Kuriakose et al. 2016; Koehler et al. 2017; Guo et al. 2018). These results are described in detail in this thesis.

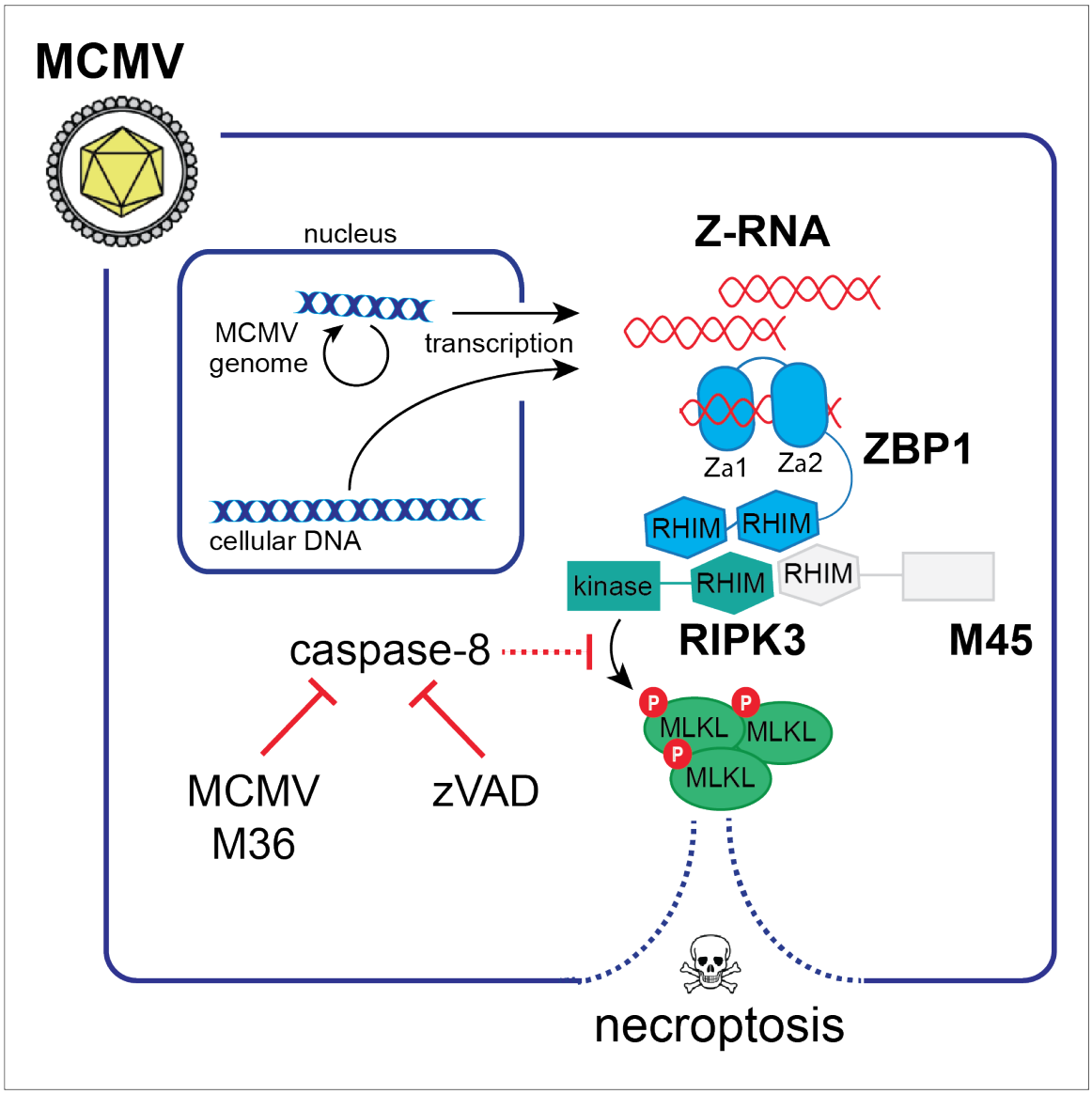


Figure 7. ZBP1-mediated virus-induced necroptosis.

Taken from Maelfait *et al* 2017 (see Appendix). ZBP1 senses MCMV infection and activates RIPK3-MLKL driven necroptotic cell death.

In addition to virus-induced necroptosis, ZBP1 has additionally been implicated in necroptosis-associated inflammation in mice deficient in RIPK1 (J. Lin et al. 2016; Newton et al. 2016). Alongside its kinase-dependent pro-necroptotic

role (Cho et al. 2009; Kaiser et al. 2011; Oberst et al. 2011), RIPK1 also has a kinase-independent anti-necroptotic role in regulating necroptosis activation (Kaiser et al. 2011; Dillon et al. 2014; Dannappel et al. 2014). The anti-necroptotic function of RIPK1 is important for preventing inflammation in epithelial barriers during late embryonic development in mice (Kaiser et al. 2011; Dillon et al. 2014). Knock-in of RHIM-mutant RIPK1 causes perinatal lethality in mice that is rescued by RIPK3, MLKL or ZBP1 deficiency (J. Lin et al. 2016; Newton et al. 2016). Moreover, adult mice with an epidermis-specific knock-out of RIPK1 develop necroptosis mediated skin inflammation, which is rescued by MLKL or ZBP1 knock-out (J. Lin et al. 2016; Newton et al. 2016). This phenotype is mediated by ZBP1-RIPK3 driven necroptosis, which occurs in keratinocytes. Under normal conditions, RIPK1 prevents ZBP1 from interacting with RIPK3 and activating necroptosis via RHIM-RHIM interactions, but when the RIPK1 RHIM is mutated this brake on ZBP1-mediated necroptosis is released (J. Lin et al. 2016; Newton et al. 2016). Precisely what activates ZBP1 in this context, in the absence of infection, remains to be investigated. In addition to RIPK1, other proteins have been implicated in the regulation of ZBP1-mediated necroptosis, including IFN regulatory factor 1 (IRF1) (Kuriakose et al. 2018) and p53 upregulated modulator of apoptosis (PUMA) (D. Chen et al. 2018). Whereas IRF1 positively regulates ZBP1 at the transcriptional level during IAV infection of mice (Kuriakose et al. 2018), PUMA is reported to amplify necroptosis in human and mouse cells by triggering the activation of cytosolic DNA sensors (D. Chen et al. 2018).

1.8 VIRAL ANTAGONISM OF NECROPTOSIS

Given the continuous evolutionary arms race between virus and host, best described by the Red Queen hypothesis (Van Valen 1973), it is unsurprising that viruses have evolved mechanisms of antagonising necroptosis (Figure 8). The first evidence of viral antagonism of necroptosis was the identification of the MCMV M45 gene, which encodes the necroptosis inhibitor vIRA (Upton et al. 2010). Like ZBP1 and RIPK3, vIRA contains a RHIM domain, which enables it to antagonise ZBP1-RIPK3-mediated necroptosis. MCMV^{M45mutRHIM}, a mutant lacking a functional vIRA, induces necroptosis in a ZBP1-dependent manner (Upton et al. 2012). Necroptosis occurs only when apoptosis is inhibited (Y. Lin et al. 1999; Feng et al. 2007) and, as with many other viruses, MCMV encodes an apoptosis inhibitor called *M36*, which antagonises caspase-8 (Ebermann et al. 2012). HCMV encodes an antagonist, which inhibits necroptosis at a stage downstream of MLKL phosphorylation (Omoto et al. 2015). HSV1 and HSV2 encode infected cell proteins 6 (ICP6) and 10 (ICP10), respectively, which inhibit both apoptosis and necroptosis in infected human cells (Guo et al. 2015). ICP6 and ICP10 can inhibit apoptosis directly by interacting with caspase-8, and the same proteins inhibit necroptosis via a distinct, RHIM-dependent mechanism similar to that employed by MCMV vIRA (Guo et al. 2015). VV encodes a large number of innate immune evasion proteins, including anti-apoptotic proteins (G. L. Smith et al. 2013). VV has also been reported

to antagonise necroptosis using the E3L protein, which contains a ZBD (Koehler et al. 2017). To date, E3L is the only reported viral antagonist of necroptosis that does not contain a RHIM. In the present study, we explore whether other viruses encode as yet unknown antagonists of ZBP1-mediated necroptosis.

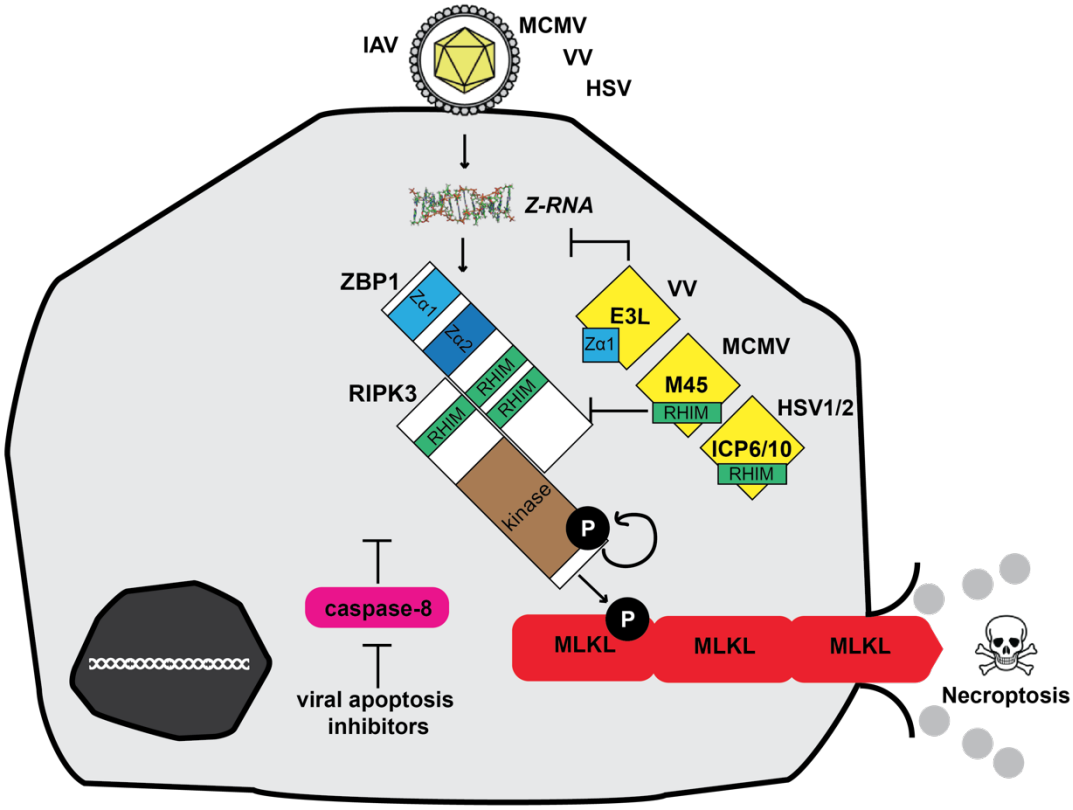


Figure 8. Viral antagonism of ZBP1-mediated necroptosis.

MCMV, IAV, VV and HSV1/2 are sensed by ZBP to activate necroptosis. MCMV, VV and HSV1/2 encode antagonists of ZBP1-mediated necroptosis (M45, E3L and ICP6/10 respectively). An IAV encoded antagonist of ZBP1-mediated necroptosis has not been identified.

1.9 THESIS AIMS

The aims of the research presented in this thesis were to (a) investigate the mechanism by which mouse ZBP1 recognises MCMV to activate antiviral necroptotic cell death, (b) investigate whether ZBP1-mediated necroptosis is relevant in humans, (c) develop and validate an assay to measure human ZBP1-mediated necroptosis activation and (d) employ said assay to identify novel viral protein inhibitors of human ZBP1-mediated necroptosis activation.

Since the commencement of these studies, evidence has been accumulating that ZBP1 is a critical cellular innate immune receptor for the detection of multiple mammalian viruses (DeFilippis, Alvarado, Sali, Rothenburg & Früh 2010a; Upton et al. 2012; Thapa et al. 2016; Kuriakose et al. 2016; Koehler et al. 2017; Guo et al. 2018; Daniels et al. 2019). However, the majority of studies on virus-induced ZBP1-mediated necroptosis have been conducted in the mouse system, with equivalent functions of ZBP1 in humans remaining less characterised (Upton et al. 2012; Thapa et al. 2016; Kuriakose et al. 2016; Sridharan et al. 2017; Maelfait et al. 2017; Koehler et al. 2017; Guo et al. 2018). The establishment of experimental tools for the study of human ZBP1-mediated necroptosis is important, particularly as necroptosis is increasingly being implicated in a broad spectrum of human pathologies beyond antiviral immunity (Galluzzi et al. 2017; Yuan et al. 2019; Degterev et al. 2019).

Altogether, the results presented in this thesis (a) demonstrate that MCMV-induced ZBP1-mediated necroptosis requires ZBP1 Z-nucleic acid binding function

(Chapter 3 Results I) (Maelfait et al. 2017) (see Appendix), (b) demonstrate that ZBP1 mediates ZBD-dependent necroptosis in human cells (Chapter 4 Results II) and (c) describe the development and validation of a novel assay measuring ZBP1-mediated necroptosis activation in human cells (Chapter 4 Results II). This human ZBP1-mediated necroptosis assay was (d) employed to screen candidate viral protein antagonists from two medically relevant human pathogens (Chapter 5 Results III).

CHAPTER 2 MATERIALS AND METHODS

2.1 MICE

All mice were on the C57Bl/6 background. *Zbp1* is located on chromosome 2 (GenBank NM_021394.2; Ensembl ENSMUSG00000027514). *Zbp1*$^{Zα1α2mut/Zα1α2mut}$ transgenic mice were generated by Cyagen through genetic modification of C57Bl/6 embryonic stem (ES) cells by Cre-Lox recombination (Maelfait et al. 2017) (see Appendix). Modified ES cells were injected into blastocysts and transplanted into pseudopregnant females to produce founder males for breeding (Maelfait et al. 2017) (see Appendix). Genotyping of *Zbp1*$^{Zα1α2mut/Zα1α2mut}$ transgenic mice was performed using primers provided by Cyagen (Maelfait et al. 2017) (see Appendix) and sequencing was performed by Source Bioscience. *Spata2*$^{-/-}$ mice were a gift from Mads Gyrd-Hansen, University of Oxford. Mouse work was performed by Jonathan Maelfait, now at Ghent University, or Anne Bridgeman, University of Oxford, as indicated in the figure legends. This work was performed in accordance with the UK Animals (Scientific Procedures) Act 1986 and approved by a project license granted by the UK Home Office (PPL No. 40/3583) and was also approved by the Institutional Animal Ethics Committee Review Board at the University of Oxford.

2.2 CELLS

NIH3T3 cells were gifts from Caetano Reis e Sousa, The Francis Crick Institute, London. Immortalised *Zbp1*$^{-/-}$ MEFs were generated by Jonathan Maelfait (Maelfait et al. 2017) (see Appendix) from primary *Zbp1*$^{-/-}$ MEFs, which were originally a gift from Ken Ishii, Osaka University. Primary MEFs from wildtype, heterozygous and homozygous *Zbp1*^{Zα1α2mut} mice were from embryos extracted from the uterine horns of pregnant mice sacrificed at day 12.5-14.5 post-coitus by Jonathan Maelfait (Maelfait et al. 2017) (see Appendix). TLA-HEK293T cells were from Open Biosystems. Other HEK293T cells were from ATCC or were gifts from Caetano Reis e Sousa, Veit Hornung, LMU Munich or Greg Towers, University College London. HT-29 cells were a gift from Lars Fugger, University of Oxford. Human monocyte derived dendritic cell lysates were a gift from Alison Simmons, University of Oxford.

All cells were cultured in DMEM (Sigma Aldrich) supplemented with 10% heat-inactivated foetal calf serum (Sigma Aldrich) and 2mM L-glutamine (Thermo Fisher Scientific), with the exception of primary MEFs, where the culture medium was additionally supplemented with 50 U/mL penicillin-streptomycin (Thermo Fisher Scientific). All cells were grown at 37°C, 5% CO_2, and 20% O_2, with the exception of primary MEFs, which were grown at 37°C, 5% CO_2 and 3% O_2. The absence of mycoplasma contamination was confirmed monthly for all cells by Lucetta™ test (Lonza) and Hoechst staining.

2.3 PLASMIDS, OLIGONUCLEOTIDES AND REAGENTS

Plasmids & oligonucleotides:

Mouse *Zbp1* constructs were gateway cloned into pLenti6.3/TO/V5-DEST (Thermo Fisher Scientific) by Jonathan Maelfait from pCMV-SPORT6-Zbp1 (PlasmID clone: MmCD00314236, Harvard Medical School) (Maelfait et al. 2017) (see Appendix). Human *ZBP1* (CCDS13461.1) constructs were synthesised by GeneArt® and gateway cloned (Table 1) into pLenti6.3/TO/V5-DEST (Thermo Fisher Scientific) or pLenti6 (Addgene plasmid-17293-sequence-8556). Human *RIPK3* (NM_006871.3) construct in pLenti6/FLAG/puro was a gift from Yves Dondelinger and Mathieu Bertrand, University of Ghent. Human *MLKL* (CCDS32487.1) construct was TOPO cloned (Table 1) into pcDNA3.1/V5/His (Thermo Fisher Scientific) from pENTRC-hMLKL, which was a gift from Yves Dondelinger and Mathieu Bertrand. FLAG-ICP6(HSV1_KOS) (KM222723.1) was synthesised by GeneArt® in pcDNA3.1. M45 constructs were gateway cloned (Table 1) into pLenti6.3/TO/V5-DEST (Thermo Fisher Scientific) from pCMV/Tag5A-M45(MCMV-K181) or a RHIM-mutant version, both of which were gifts from Jason Upton, University of Austin. ZIKV protein coding sequences were gateway cloned into pLenti6.3/TO/V5-DEST by Jonny Hertzog, Antonio Gregorio Dias Jr and Rachel Rigby, University of Oxford (GenBank accession KU527068) using a strain from Brazil (Hertzog et al. 2018). VZV ORFs 19 and 20 were gateway cloned from VZV rOka (PMID 8394020) infected cells into pLenti6.3/TO/V5-DEST (Thermo Fisher Scientific) by Jonny Hertzog. Empty vector constructs

(pLenti6.3/TO/V5-DEST/empty and pcDNA3.1/empty) were generated by Jonny Hertzog (unpublished). All plasmid DNA was amplified using the Qiagen Maxiprep Kit. All constructs were sequence-verified by sequencing by Source BioScience using Source Bioscience stock primers.

Table 1. List of primers

Primer	**Sequence (5' to 3')**
Mouse *Zbp1*-Exon2(Zα1) fwd	TGACCACTGTAACCAATGCCACCT
Mouse *Zbp1*-Exon2(Zα1) rvs	GACCTGAAACCTGACCTTCCCAAC
Mouse *Zbp1*-Exon3(Zα2) fwd	TGGTGTCGTCGTTCCTGTCTGCTT
Mouse *Zbp1*-Exon3(Zα2) rvs	CTCGTGGCTCTTAATGTGCGTGTAG
Human *ZBP1* untagged (without STOP codon) fwd	GCCGCCATGGCCCAGGCTCCTGCTGA
Human *ZBP1* untagged (without STOP codon) rvs	AATCCCACCTCCCCACCAGCTC
Human *ZBP1* untagged (with STOP codon) fwd	GCCGCCATGGCCCAGGCTCCTGCTGA
Human *ZBP1* untagged (with STOP codon) rvs	CTAAATCCCACCTCCCCACCAGCTCCC CTC
Human *ZBP1* untagged (with STOP codon, linker and FLAG-tag) fwd	GCCGCCATGGCCCAGGCTCCTGCTGA

Human *ZBP1* untagged (with STOP codon, linker and FLAG-tag) rvs	CTACTTGTCGTCATCGTCTTTGTAGTCT CCTCCTCCTCCTCCAATCCCACCTCCCC ACCAGCTCCCCTC
Human *MLKL* fwd	CTTAGAAAGGTGGAGAGTTTCTTTA
Human *MLKL* rvs	CTACTTAGAAAAGGTGGAGAGTTTCTTT AAGATT
MCMV *M45* 90aa & 277aa fragments fwd	GCCGCCATGGATCGCCAGCCCAAAG
MCMV 90aa fragment rvs	GGTCTTGGGGTAGCTCCTGCG
MCMV 277aa fragment rvs	GTACAGGAGGGGATCAGCTTTGGC

Antibodies:

Primary antibodies used for western blotting are listed in the table below (Table 2). Secondary antibodies used for western blotting were: HRP conjugated donkey anti-mouse, donkey anti-rabbit and donkey anti-rat antibodies (VWR International). Neutralising anti-IFNAR1 (clone MAR1-5A3, Biolegend) was used at 0.5µg/mL. Anti-V5-APC (clone AB_2532221, Thermo Fisher Scientific) was used at 2.5µg/mL. Anti-V5-FITC (clone AB_2556567, Thermo Fisher Scientific) was used at 2.5µg/mL.

Table 2. List of primary antibodies used for western blotting.

Antigen	**Clone**	**Host**	**Dilution**	**Supplier**
Mouse & Human ZBP1	Zippy1	Mouse	1:1000	Adipogen

Mouse pS345 MLKL	polyclonal	Rabbit	1:1000	Abcam
Mouse MLKL	3H1	Rat	1:1000	
Mouse MLKL (for oligomers)	polyclonal	Rabbit	1:2000	Sigma Aldrich
Human MLKL	D2I6N	Rabbit	1:1000	Cell Signalling Technologies
MCMV IE1	monoclonal	Mouse	1:1000	Qiyi Tang, Ponce School of Medicine
Mouse and Human β-Actin (ACTB)	AC-15	Mouse (HRP-coupled)	1:500,000	Sigma Aldrich
Human STAT1	Y2H3	Rabbit	1:1000	Cell Signalling Technologies
Human RIPK3	E1Z1D	Rabbit	1:1000	Cell Signalling Technologies
Human pS227 RIPK3	EPR9627	Rabbit	1:2000	Abcam
Human GAPDH	14C10	Rabbit (HRP-coupled)	1:5000	Cell Signalling Technologies

V5-tag	polyclonal	Rabbit (HRP-coupled)	1:5000	Thermo Fisher Scientific
FLAG-tag	M2	Mouse (HRP-coupled)	1:1000	Sigma Aldrich
ZIKV NS5	Polyclonal (serum)	Rabbit	1:500	Andres Merits, University of Tartu

Other reagents:

Mouse TNF (PeproTech) and zVAD (Z-VAD-FMK) (Enzo Life Sciences) were used at final concentrations of 30ng/mL and 20μM respectively. The cell impermeable dyes YOYO-3 Iodide (0.25μM) and SYTOX GREEN (25nM) were from Thermo Fisher Scientific. Dimethylsulfoxide (DMSO) was from Sigma Aldrich. Necrostatin-1 (Enzo Life Sciences) and GSK'872 (Calbiochem) were used at 30μM and 3μM, respectively, or as indicated in the figure legends. IFN-A/D was purchased from Sigma-Aldrich or R&D Systems and used at 100 U/mL. Blasticidin S HCl (Thermo Fisher Scientific) for antibiotic selection of transduced HT-29 cells was used at 10μg/mL. LIVE/DEAD™ Aqua Fixable Dead Cell Stain was from Thermo Fisher Scientific. OptiMEM (Thermo Fisher Scientific) and FuGENE® 6 (Promega) were used for transfection of HEK293T cells at 45μL and 5.4μL respectively per μg

of DNA transfected. ProLong Diamond antifade mountant with DAPI was from Thermo Fisher Scientific. Lambda phosphatase kit was from New England Biolabs.

2.4 VIRUSES

Lentiviruses used to transduce NIH3T3, immortalised *Zbp1*$^{-/-}$ MEFs (Chapter 3 Results I) (Maelfait et al. 2017) (see Appendix) and HT-29 cells (Chapter 4 Results II) were produced in TLA HEK293T cells by transfection of the aforementioned pLenti6.3/TO/V5-DEST (Thermo Fisher Scientific) transducing vectors in the presence of Virapower packaging mix (Thermo Fisher Scientific). Cell culture medium was changed 24h post-transfection and, 48h post-transfection, the supernatant containing lentiviruses was collected and filtered (0.22µm). Lentiviral transduction of cells was performed by inoculating cells with increasing doses of lentivirus in the presence of 10µg/mL polybrene (Sigma Aldrich), followed by selection of transduced cells with 10µg/mL blasticidin (Thermo Fisher Scientific).

MCMV (wildtype K181 strain and MCMV^{M45mutRHIM}) (Upton et al. 2010), was a gift from Edward Mocarski, Emory University, Atlanta, and Jason Upton, University of Austin. MCMV was propagated in immortalised *Zbp1*$^{-/-}$ MEFs infected with an MOI of 0.1 and then concentrated by ultracentrifugation (30,000 *g*) of supernatants collected from virus-infected cells at 100% cytopathic effect (CPE) (Maelfait et al. 2017) (see Appendix). MCMV titers were determined by plaque assays performed in technical duplicate (Maelfait et al. 2017) (see Appendix). Specifically, MCMV was

titered on primary *Zbp1*^{Zα1α2mut} MEFs, in the presence of a 1:1 ratio of cell culture medium and carboxymethylcellulose (CMC) (Sigma Aldrich), and incubated for 6 days before fixation of cells with 4% formaldehyde (Sigma Aldrich) solution and staining with 0.5% crystal violet (Sigma Aldrich) solution to enable visualisation of plaques. Plaques were counted manually and titers were recorded as plaque forming units (PFU) per mL of virus. In the *in vivo* MCMV infection experiments in Chapter 3 Results I, harvested spleens were homogenised in cell culture medium with acid-washed glass beads (Sigma Aldrich) at speed 5.0 in a FastPrep-24 (MP Biomedicals), and supernatants were then cleared by centrifugation (200 *g*, 3min). Virus titers were determined from the homogenised spleen supernatants by plaque assay as described above. To minimise bias, I was blinded to the infection status of the mice from which the spleens were extracted until the plaque assay was completed.

MVA and MHV68 were gifts from Michael Way (The Francis Crick Institute, London) and Anne Bridgeman (University of Oxford) respectively.

Total RNA from A549 cells infected with ZIKV/H.sapiens/Brazil/PE243/2015 (GenBank accession KX197192.1) (Hertzog et al. 2018) was a gift from Alain Kohl, University of Glasgow, and was used to generate infectious ZIKV, which was propagated in and titered on A549-BVDVNPro cells by Mirjam Schilling, University of Oxford.

2.5 RT-QPCR

After lysis of cells in RLT buffer (Qiagen) containing 1:100 2-mercaptoethanol (Sigma Aldrich) and homogenisation using a Qiashredder (Qiagen), RNA was purified using RNeasy columns with a DNase I (Qiagen) digestion step. For RNA purification from mouse livers, liver sections were homogenised at speed 5.0 in a FastPrep-24 (MP Biomedicals) in RLT buffer (Qiagen) containing 1:100 2-mercaptoethanol (Sigma Aldrich), with the addition of acid-washed glass beads (Sigma Aldrich), and RNA was then purified from supernatants cleared by centrifugation (200 *g*, 3min). cDNA synthesis was performed with SuperScript II reverse transcriptase (Thermo Fisher Scientific) and oligo(dT) primers (Ambion). Where DNA was extracted, cells were lysed in AL-buffer (Qiagen) and incubated with proteinase K (Qiagen) at 56°C for 10 min, and DNA was then purified using DNeasy blood and tissue columns (Qiagen). 15 ng DNA was amplified using TaqMan universal PCR (Applied Biosystems) master mixes on a 7,800 real-time PCR system (Applied Biosystems). mRNA expression data were normalised to *Gapdh* and analysed by the comparative Ct method. A plasmid encoding a fragment of the MCMV glycoprotein B (gB) gene (pGEMTeasy-MCMV-gB) was used as a standard for determining the viral genome copy numbers (Vliegen et al. 2003). The lower detection limit was 30 molecules. The following Taqman RT-qPCR probes and primers were used: *Ifi44* (Mm00505670_m1, Applied Biosystems), *Ifit1* (Mm00515153_m1, Applied Biosystems), *Oasl1* (Mm00455081_m1, Applied Biosystems), *Ifnb1* (Mm00439552_s1, Applied Biosystems), *Gapdh* (Cat. no.

4352932E, Applied Biosystems), *Il1b* (Mm00434228_m1, Applied Biosystems), *Zbp1* (Mm01247052_m1, Applied Biosystems), *Tnf* (Mm00492606_m1, Applied Biosystems) gB forward primer (5'-AGGGCTTGGAGAGGACCTACA-3'), gB reverse primer (5'-GCCCGTCGGCAGTCTAGTC-3') and gB probe (5'FAM_AGCTAGACGACAGCCAACGCAACGA_3'TAMRA).

2.6 CELL VIABILITY AND NECROPTOSIS ASSAYS

To assess endpoint cellular ATP content as a proxy for cell viability, NIH3T3 cells, immortalised *Zbp1*$^{-/-}$ MEFs or HEK293T cells seeded at 5,000 cells per well in a 96-well plate were treated, infected or transfected as described in the figure legends and, 24h later (or 48h later for HEK293T cells), removed from the incubator and incubated at room temperature for 30min before lysing with CellTiter-Glo® reagent (Promega), which was added directly into the cell culture medium at a ratio of 1:1. 50uL was then transferred into a white 96-well luminometer plate and luminescence, proportional to cellular ATP content, was measured using a GloMax® 96-well plate luminometer (Promega).

To measure cell death kinetics, NIH3T3 cells or immortalised *Zbp1*$^{-/-}$ MEFs (reconstituted or not with ZBP1) seeded at 5,000 cells per well in a 96-well plate, were treated or infected as described in the figure legends and, at the same time, a cell impermeable dye (YOYO-3 Iodide (0.25μM) or SYTOX GREEN (25nM) (Thermo Fisher Scientific)) was added to the cell culture medium. HEK293T cells

were seeded at 20,000 cells per well in a 96-well plate and then transfected as described in the figure legends. 24h post transfection, SYTOX GREEN was added to the cell culture medium. After addition of the cell impermeable dye, all cells were then placed in an in-incubator imaging system (IncuCyte®) and imaged hourly by automated microscopy for 24h. Cell permeabilisation was measured as uptake of the cell impermeable dye by cells over the 24h that followed. The number of stained cells per image at a given time point was counted automatically using the IncuCyte® analysis software, which was trained with example images from each experiment. Where indicated, untreated cells were lysed with PBS + 0.125% Triton-X100 (Sigma Aldrich) after the last time point and the number of stained cells in this condition set to 100%.

For the human ZBP1-mediated necroptosis assay in HEK293T (Chapter 4 Results II & Chapter 5 Results III), cells seeded at 1,000,000 cells per well in a 6-well plate, with 3mL of fresh cell culture medium per well, were co-transfected with plasmid expression constructs encoding ZBP1 (1µg), RIPK3-FLAG (0.3µg) and MLKL (0.3µg), with or without a plasmid encoding a V5-tagged candidate viral antagonist or positive control (0-5µg). Transfection was performed using 45µL of OptiMEM (Thermo Fisher Scientific) and 5.4µL of FuGENE® 6 (Promega) per µg of DNA. The total amount of DNA transfected per well was kept constant for all the different conditions using appropriate empty vector plasmid DNA as indicated in the figure legends. 24h post transfection cells were harvested and lysates analysed by

SDS-PAGE and western blotting (described in section 2.7) with an anti-pRIPK3 antibody (pSer-227) (described in section 2.3) to measure RIPK3 phosphorylation.

2.7 WESTERN BLOTTING

In the relevant experiments described in Chapter 3 Results I, cells were lysed in 20mM Trizma base (plus HCl to pH 7), 100mM NaCl, 60mM $Na_4P_2O_7$, 100mM NaF, 10μM $ZnCl_2$, 1% NP40, protease inhibitors (Cell Signalling Technologies Techologies) and phosphatase inhibitor cocktail 3 (Sigma Aldrich). In the relevant experiments described in Chapter 4 Results II and Chapter 5 Results III, cells were lysed in 50mM Trizma base (plus HCl to pH 7.4), 150mM NaCl, 1% NP-40, 0.5% deoxycholate, 0.1% SDS, protease inhibitors (Cell Signalling Technologies) and phosphatase inhibitor cocktail 3 (Sigma Aldrich). Protein lysates were cleared by centrifugation at 16,000 *g* for 10min. Protein lysates were denatured and reduced by heating at 95°C for 3min with 25% LDS sample buffer (NuPage, Thermo Fisher Scientific) and 10% 2-mercaptoethanol (Sigma Aldrich), and then run on Bis-Tris SDS-PAGE gels (NuPAGE, Thermo Fisher Scientific) in MOPS buffer (NuPage, Thermo Fisher Scientific) at 180V. Gels were transferred to nitrocellulose membranes (Perkin Elmer) at 100V for 1-1.5h in Transfer Buffer (NuPage, Thermo Fisher Scientific) with 10% methanol or in transfer buffer containing 25mM Trizma base and 192mM glycine with 20% methanol. Membranes were blocked and incubated with antibodies in Tris-buffered saline (10mM Trizma base (plus HCl to

pH 7.4) and 140mM NaCl) with 0.1% Tween-20 (Sigma Aldrich) plus 5% non-fat dried milk (Sigma Aldrich) or, for phospho-blotting, 5% bovine serum albumin (Sigma Aldrich). Primary and secondary antibodies used for Western blotting are described in Section 2.3. Membranes were developed using Western Lightning® Plus-ECL, Enhanced Chemiluminescence Substrate (Perkin Elmer) and either developed on hyperfilm (GE Healthcare) or using an iBright™ FL1000 (Thermo Fisher Scientific).

2.8 FLOW CYTOMETRY

Flow cytometry was performed using the Attune NxT Flow Cytometer (Thermo Fisher Scientific). HT-29 cells were stained with LIVE/DEAD™ Aqua Fixable Dead Cell Stain (Thermo Fisher Scientific), fixed with 4% formaldehyde (Thermo Fisher Scientific), permeabilised with 0.5% triton-X100 (Sigma Aldrich) and stained with anti-V5 conjugated to APC (Thermo Fisher Scientific). The gating strategy used is shown in **Figure S3**. Data were analysed using FlowJo.

2.9 CONFOCAL MICROSCOPY

HEK293T seeded at 75,000 cells per well in a 24 well plate, on coverslips coated with poly-L-lysine, were transfected using OptiMEM (Thermo Fisher Scientific) and FuGENE® 6 (Promega) as described in the figure legends and 24h later fixed with 4% formaldehyde (Thermo Fisher Scientific), permeabilised with

0.25% TritonX100 (Sigma Aldrich) and washed with 0.1 M glycine, before incubating with anti-V5-FITC (clone AB_2556567, Thermo Fisher Scientific) at 2.5µg/mL for 3h at room temperature. After washing with PBS, slides were mounted using ProLong Diamond antifade mountant with DAPI (ThermoFisher Scientific). Prepared slides were imaged using the Zeiss 780 LSM inverted microscope. Images were analysed using ImageJ.

2.10 STATISTICS

Statistical analysis was performed in GraphPad Prism v7.00 as detailed in the figure legends.

CHAPTER 3 RESULTS I
SENSING OF VIRAL AND ENDOGENOUS RNA BY MOUSE ZBP1 INDUCES NECROPTOSIS

Necroptosis is a programmed cell death pathway that mediates host defence through the elimination of virus-infected cells (Mocarski et al. 2015). In accordance with Red Queen dynamics (Van Valen 1973), viruses have evolved to suppress necroptosis during infection of host cells. The MCMV-host interaction is a well-characterised example. MCMV is sensed by ZBP1 to activate RIPK3-MLKL-mediated necroptosis (Upton et al. 2012). Upon MCMV detection, ZBP1 engages RIPK3 via RHIM-RHIM interactions, resulting in RIPK3 auto-phosphorylation and consequent activation. Of note, whereas ZBP1-mediated necroptosis is independent of RIPK1 (Upton et al. 2012), ZBP1 has been reported to induce NFκB activation via RIPK1 and RIPK3 (Kaiser et al. 2008; Rebsamen et al. 2009), both of which can bind to ZBP1 via RHIM-RHIM interactions. Once activated, RIPK3 phosphorylates the pseudokinase MLKL, which oligomerises and forms pores in the cell membrane leading to inflammatory cell death (Sun et al. 2012; Zhao et al. 2012; Dondelinger et al. 2014). This necroptotic cell death serves to eliminate the virus-infected cell, thus preventing the spread of infection to surrounding cells and protecting the whole organism.

Unsurprisingly, MCMV has evolved to inhibit virus-induced necroptosis, using a function encoded by *M45* (Upton et al. 2008; Upton et al. 2010). *M45*

encodes viral inhibitor of RIP activation (vIRA), hereafter referred to as M45, which contains a RHIM domain and can thereby out-compete the RHIM-RHIM interaction between ZBP1 and RIPK3, preventing ZBP1-mediated RIPK3 activation and downstream cell death (Upton et al. 2012). It follows that a virus with mutations in four key residues of the RHIM domain of M45 (MCMV^{M45mutRHIM}) fails to antagonise ZBP1-mediated necroptosis and consequently activates cell death (Upton et al. 2012). As a result, this M45 mutant virus is attenuated in wildtype mice (Upton et al. 2012). Necroptosis can only occur when apoptosis is inhibited (Kaiser et al. 2011; Oberst et al. 2011; H. Zhang et al. 2011) and, in the context of MCMV^{M45mutRHIM} infection, this is mediated through the inhibition of pro-apoptotic caspase-8 by the product of another MCMV gene, *M36* (Ebermann et al. 2012). In uninfected cells, apoptosis inhibition can also be achieved pharmacologically, for instance by treatment with the pan-caspase inhibitor zVAD. Furthermore, mouse *Zbp1* is an ISG (Shaw et al. 2017) and so is up-regulated during virus infection (Maelfait et al. 2017) (see Appendix).

Following on from the previously mentioned studies of Upton and colleagues, a key remaining question pertained to the precise mechanism by which MCMV^{M45mutRHIM} infection is detected by ZBP1 to induce necroptosis. In particular, the aim of the research detailed in this chapter was to examine which domains and residues of ZBP1 were required for sensing of MCMV infection. ZBP1 is one of only four proteins known to contain one or more ZBDs, which enable specific binding of nucleic acids in the Z-conformation (Herbert et al. 1995; Schwartz 1999). Hence,

the underlying hypothesis being tested in this study was that ZBP1 recognises a Z-conformation nucleic acid, which accumulates during virus infection, via its two ZBDs. The recognition of Z-nucleic acids, and the ability to distinguish these from classical B-DNA or A-RNA, may represent a mechanism of self vs non-self discrimination employed by host cells.

In this chapter, I detail the results that I contributed to a now published study (Maelfait et al. 2017) (see Appendix), which adds to an accumulating body of evidence demonstrating that, during virus infection, ZBP1 senses nascent RNA via its two ZBDs and then activates RIPK3-MLKL-mediated necroptosis to restrict viral replication. Thapa *et al* reported that mouse ZBP1 senses influenza A virus (IAV) RNA to activate cell death (Thapa et al. 2016), a finding which our results confirmed in a different infection model, namely MCMV. Another group independently showed that mouse ZBP1 senses IAV to activate cell death but concluded that IAV proteins rather than RNA trigger ZBP1 (Kuriakose et al. 2016).

3.1 Z-NUCLEIC ACID BINDING IS ESSENTIAL FOR ZBP1-MEDIATED MCMV^{M45MUTRHIM}-INDUCED CELL DEATH

To investigate whether ZBP1-mediated MCMV^{M45mutRHIM}-induced necroptosis is ZBD-dependent, NIH3T3 cells stably expressing wildtype mouse ZBP1 (ZBP1^{WT}) or a ZBD mutant form of the protein (ZBP1^{Zα1α2mut}) (**Figure 9**) were infected with MCMV^{M45mutRHIM} at a multiplicity of infection (MOI) of 10 and, after 24h,

cellular ATP content was measured as a proxy for viability using the CellTiter-Glo® Luminescence Cell Viability assay (Figure 10). ATP indicates the presence of metabolically active cells and the amount of ATP present is directly proportional to the number of viable cells present in culture. A proprietary recombinant luciferase enzyme catalyses the conversion of beetle luciferin to oxyluciferin, in a reaction that uses ATP and produces light. The amount of light produced can be measured using a luminometer and is proportional to the number of viable cells. Mouse *Zbp1* constructs were gateway cloned into a lentiviral vector by Jonathan Maelfait and the same mutations shown in Figure 9 were introduced into the two ZBDs (Zα1 and Zα2) to generate a ZBD mutant construct ($ZBP1^{Z\alpha1\alpha2mut}$). In $ZBP1^{Z\alpha1\alpha2mut}$, key asparagine and tyrosine residues in the ZBP1 ZBDs (N46 and Y50 in Zα1 and N122 and N126 in Zα2) have been mutated to alanine (Figure 9). Previous X-ray crystallography studies identified these four amino acid residues to be essential for Z-nucleic acid binding by ZBDs *in vitro* (Herbert et al. 1995; Schwartz 1999). NIH3T3 cells were selected for this study because they are a necroptosis competent mouse cell line (Upton et al. 2012), which do not express ZBP1 endogenously, enabling them to be reconstituted with $ZBP1^{WT}$ or $ZBP1^{Z\alpha1\alpha2mut}$ by lentiviral transduction (Maelfait et al. 2017) (see Appendix). Importantly, protein expression levels of $ZBP1^{WT}$ and $ZBP1^{Z\alpha1\alpha2mut}$ in these stably transduced NIH3T3 cells were equal (Maelfait et al. 2017) (see Appendix).

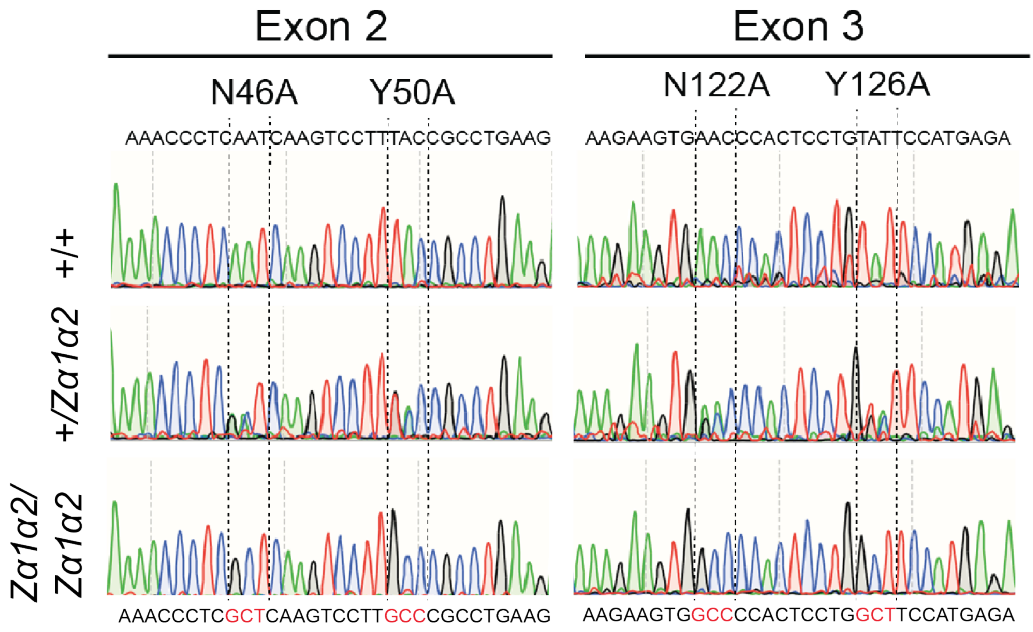


Figure 9. Mutations introduced into the two ZBDs (Zα1α2) of mouse ZBP1.

Modified from Maelfait *et al* 2017 (see Appendix). DNA fragments encompassing exon 2 (Zα1) or exon 3 (Zα2) were PCR-amplified from genomic DNA from primary MEFs of the indicated genotypes and were then sequenced.

Tumour necrosis factor (TNF) binding its receptor can trigger apoptosis, but when apoptosis is inhibited by viral antagonists or by the pan-caspase inhibitor zVAD, TNF signalling induces necroptosis instead. In accordance, whereas untreated cells remained viable after 24h, cells treated with a combination of TNF and zVAD displayed a considerable reduction in viability, which was independent of ZBP1 expression (**Figure 10**). Conversely, ZBP1^{WT} expressing cells treated with zVAD alone or infected with MCMV^{M45mutRHIM} significantly lost viability compared to untransduced cells (**Figure 10**). In both cases, the observed reduction in cell

viability was ZBD-dependent because ZBP1^{Zα1α2mut} expressing cells behaved similarly to untransduced cells (**Figure 10**).

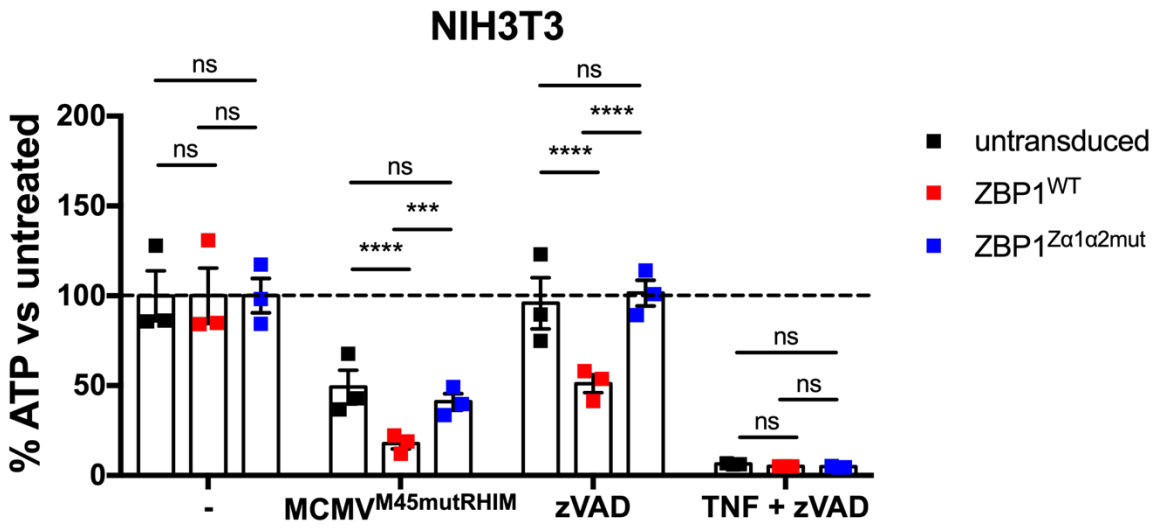


Figure 10. ZBP1-mediated MCMV^{M45mutRHIM}-induced reduction in cell viability is ZBD dependent.

NIH3T3 cells ectopically expressing wildtype *Mus musculus* ZBP1 (ZBP1^{WT}) or a ZBD mutant (ZBP1^{Zα1α2mut}) were infected with MCMV^{M45mutRHIM} at MOI 10 or treated with zVAD (20μM) alone or in combination with TNF (30ng/mL) (TNF + zVAD). After 24h, cell viability (% ATP) was assessed by the CellTiter-Glo® assay. Means are pooled from 3 independent experiments each performed in technical triplicate and error bars represent ± standard error of the mean. Asterisks represent significant differences as determined by Two-way analysis of variance with Tukey's correction applied for multiple comparisons (ns = P>0.05, * = P≤0.05, ** = P≤0.01, *** = P≤0.001, **** = P≤0.0001).

To investigate the kinetics of ZBP1-mediated, ZBD-dependent virus-induced cell death, the experiment was repeated and uptake of a cell-impermeable DNA stain (YOYO-3) was monitored hourly by automated microscopy for 24h, using an in-incubator imaging system (IncuCyte®) (**Figure 11**). Cell membrane rupture,

which occurs during necroptosis, enables cell impermeable DNA stains such as YOYO-3 to enter cells and stain their DNA. To measure cell death, uptake of YOYO-3 by cells can therefore be quantified by automated microscopy (IncuCyte®). Untreated cells (media only) remained viable for the experiment duration (**Figure 11**A). Before the last time point, these cells were lysed with Triton-X100 and the number of YOYO-3+ cells after this was set to 100%. Cells treated with the combination of TNF and zVAD rapidly underwent cell death, irrespective of their transduction status (**Figure 11**B). Conversely, by 8h post-infection with $MCMV^{M45mutRHIM}$ (**Figure 11**C), a considerable proportion of $ZBP1^{WT}$-expressing cells, but not of $ZBP1^{Zα1α2mut}$-expressing or untransduced cells, had lost membrane integrity, consistent with ZBP1-mediated and ZBD-dependent virus-induced cell death.

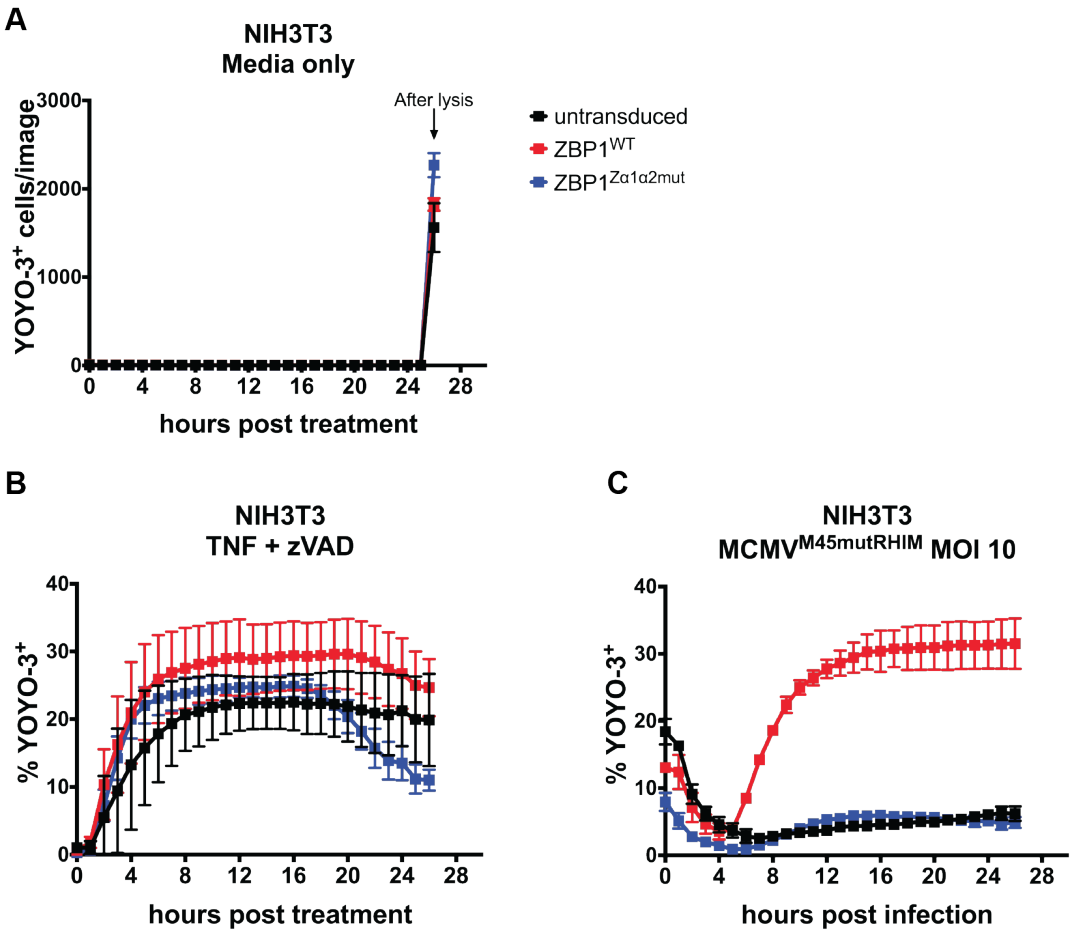


Figure 11. Kinetics of ZBP1-mediated ZBD-dependent MCMV^{M45mutRHIM}-induced cell death.

NIH3T3 cells ectopically expressing wildtype *Mus musculus* ZBP1 (ZBP1^{WT}) or a ZBD mutant (ZBP1^{Zα1α2mut}) were either (A) left untreated, (B) treated with zVAD (20μM) in combination with TNF (30ng/uL) (TNF + zVAD) or (C) infected with MCMV^{M45mutRHIM} at MOI 10. Cell death was measured hourly by automated microscopy (IncuCyte®), as uptake of a cell impermeable DNA stain (YOYO-3). Before the last time point, the cells in (A) were lysed with Triton-X100 and the number of YOYO-3+ cells after this (indicated by the arrow) was set to 100% for (B) and (C). The number of YOYO-3$^+$ cells/image in (A), or the percentage of YOYO3$^+$ cells in (B-C), is plotted on the y-axis. Means in (A-C) are from 1 experiment performed in technical triplicate and error bars represent ± 1 standard deviation. These results were reproduced by Jonathan Maelfait in at least 3 independent experiments published in Maelfait *et al* 2017 (see Appendix).

Altogether, these data demonstrate that sensing of MCMV^{M45mutRHIM} requires intact ZBP1 ZBDs, suggesting that the ZBP1 ligand may indeed be a Z-nucleic acid. Parallel lines of investigation by Jonathan Maelfait revealed that ZBP1 cross-links to RNA in a ZBD-dependent way and that ZBP1-dependent cell death requires RNA transcription but not viral DNA synthesis, leading to the hypothesis that the ligand for ZBP1 in this context may be Z-RNA (Maelfait et al. 2017) (see Appendix).

3.2 ZBP1-MEDIATED, ZBD-DEPENDENT MCMV^{M45MUTRHIM}-INDUCED CELL DEATH IS NECROPTOTIC

To identify the precise mechanism of ZBP1-mediated virus-induced cell death in this context, NIH3T3 cells stably expressing ZBP1^{WT} were infected with MCMV^{M45mutRHIM}, in the presence or absence of pharmacological inhibitors of RIPK3 or RIPK1 and, after 24h, cell viability was assessed as previously using the CellTiter-Glo® assay (**Figure 12**). GSK'872 (Kaiser et al. 2013) and Nec-1 (Degterev et al. 2005) inhibit RIPK3 and RIPK1 kinase activity respectively.

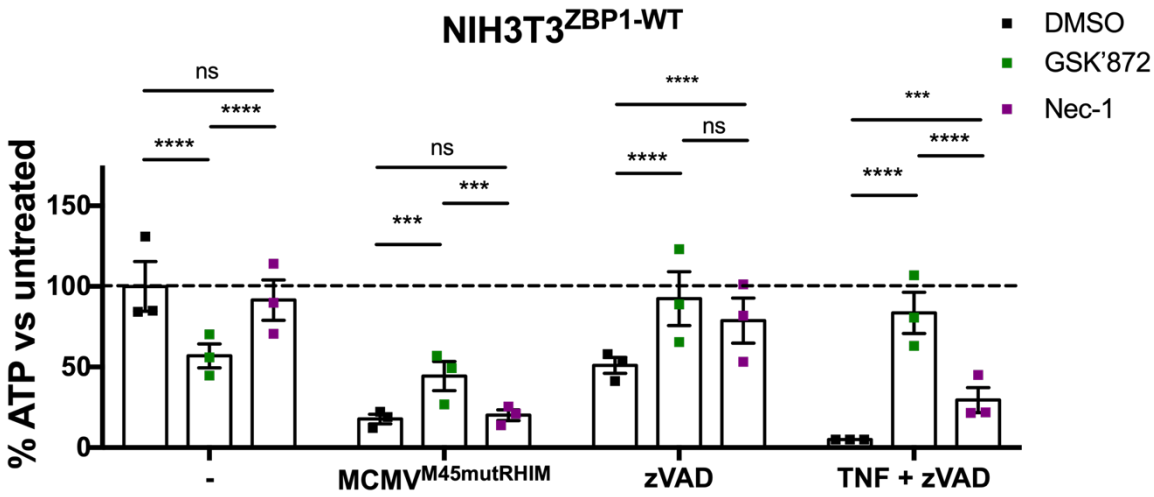


Figure 12. ZBP1-mediated virus-induced cell death is rescued by pharmacological inhibition of RIPK3 but not RIPK1.

NIH3T3 cells ectopically expressing wildtype *Mus musculus* ZBP1 (ZBP1^{WT}) were infected with MCMV^{M45mutRHIM} at MOI 10 or treated with zVAD (20μM) alone or in combination with TNF (30ng/uL) (TNF + zVAD) in the presence of either a DMSO vehicle, the RIPK3 inhibitor GSK'872 (3μM) or the RIPK1 inhibitor Necrostatin-1 (Nec-1) (30μM). After 24h, cell viability (% ATP) was measured by the CellTiter-Glo® assay. Means are pooled from 3 independent experiments each performed in technical triplicate and error bars represent ± standard error of the mean. Asterisks represent significant differences as determined by Two-way analysis of variance with Tukey's correction applied for multiple comparisons (ns = P>0.05, * = P≤0.05, ** = P≤0.01, *** = P≤0.001, **** = P≤0.0001).

Cell death induced by MCMV^{M45mutRHIM}, zVAD or TNF and zVAD in combination was rescued by pharmacological inhibition of RIPK3 (GSK'872), consistent with necroptosis as the mechanism (Figure 12). Interestingly, whereas RIPK1 inhibition (Nec-1) rescued cell death induced in the presence of zVAD, it only partially rescued cell death induced by TNF and zVAD combined, and it did not rescue cell death induced by MCMV^{M45mutRHIM}. This suggests that the precise mechanism of necroptosis activation may differ according to the origin of the ZBP1 ligand as endogenous or viral.

3.3 ZBP1-MEDIATED, ZBD-DEPENDENT MCMV^{M45MUTRHIM}-INDUCED NECROPTOSIS IS INDEPENDENT OF TYPE I IFN SIGNALLING

MCMV^{M45mutRHIM} infection induced a type I IFN response, as detected by measuring ISG expression levels in immortalised *Zbp1*$^{-/-}$ MEFs (**Figure 13**) (Maelfait et al. 2017) (see Appendix). *Ifit1*, *Ifi44* and *Oasl1* were induced upon viral infection and their levels were similar irrespective of whether cells were reconstituted or not with wildtype or ZBD mutant ZBP1 (**Figure 13**). Reconstituted immortalised *Zbp1*$^{-/-}$ MEFs were generated and validated by Jonathan Maelfait by anti-ZBP1 western blot (Maelfait et al. 2017) (see Appendix). These results demonstrate that ZBP1 and its ZBDs, whilst required for necroptosis induction, do not modulate the induction of type I IFN during viral infection.

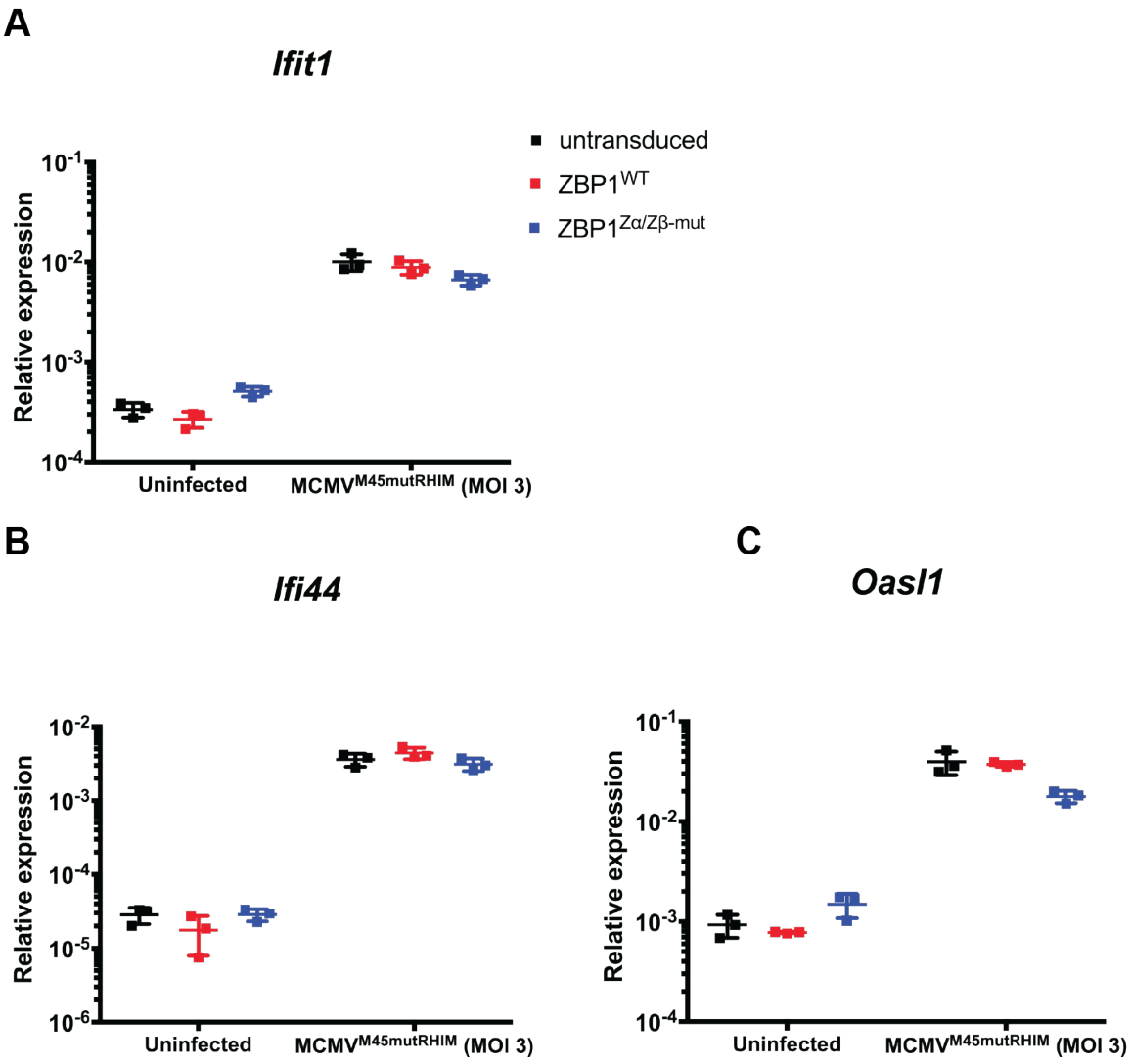


Figure 13. ZBP1 restricts MCMV^{M45mutRHIM} replication by inducing necroptosis, but not type I IFN expression.

Immortalised *Zbp1*$^{-/-}$ MEFs reconstituted with wildtype *Mus musculus* ZBP1 (ZBP1^{WT}) or a ZBD mutant (ZBP1^{Zα1α2mut}) were infected with MCMV^{M45mutRHIM} at an MOI of 4. Cells were harvested 8h post infection and (A) *Ifit1*, (B) *Ifi44* and (C) *Oasl1* mRNA expression levels measured by RT-qPCR and are shown relative to *Gapdh*. Means in (A-C) are representative of 1 experiment performed in triplicate and error bars represent ± 1 standard deviation. Cells were infected and harvested by Jonathan Maelfait. These results were reproduced by Jonathan Maelfait in an additional experiment, which is also published in Maelfait *et al* 2017 (see Appendix).

Given that MCMV induces a type I IFN response (**Figure 13**), the next goal was to investigate the possibility that IFN-induced endogenous transcripts could be providing the ligand for ZBP1 activation. To test this, immortalised *Zbp1*$^{-/-}$ MEFs reconstituted with wildtype ZBP1 were infected with MCMV^{M45mutRHIM} in the presence or absence of neutralising antibodies against the type I IFN receptor (anti-IFNAR1). IFNAR1 blockade had no effect on MCMV^{M45mutRHIM}-induced cell death (**Figure 14**A). As a control, to confirm that the anti-IFNAR1 antibody did in fact inhibit type I IFN induced transcription in this experiment, ISG expression levels were additionally measured by RT-qPCR. As expected, IFNAR1 blockade had no effect on *IFNβ* expression (**Figure 14**B), but did lead to a reduction in the expression levels of the ISGs *Ifi44* and *Ifit1* (**Figure 14**B). Some ISG expression remained after treatment with the anti-IFNAR1 antibody, even when higher doses of antibody were used (data not shown). Taken together, these results suggest MCMV^{M45mutRHIM}-induced necroptosis induction is independent of type I IFN signalling.

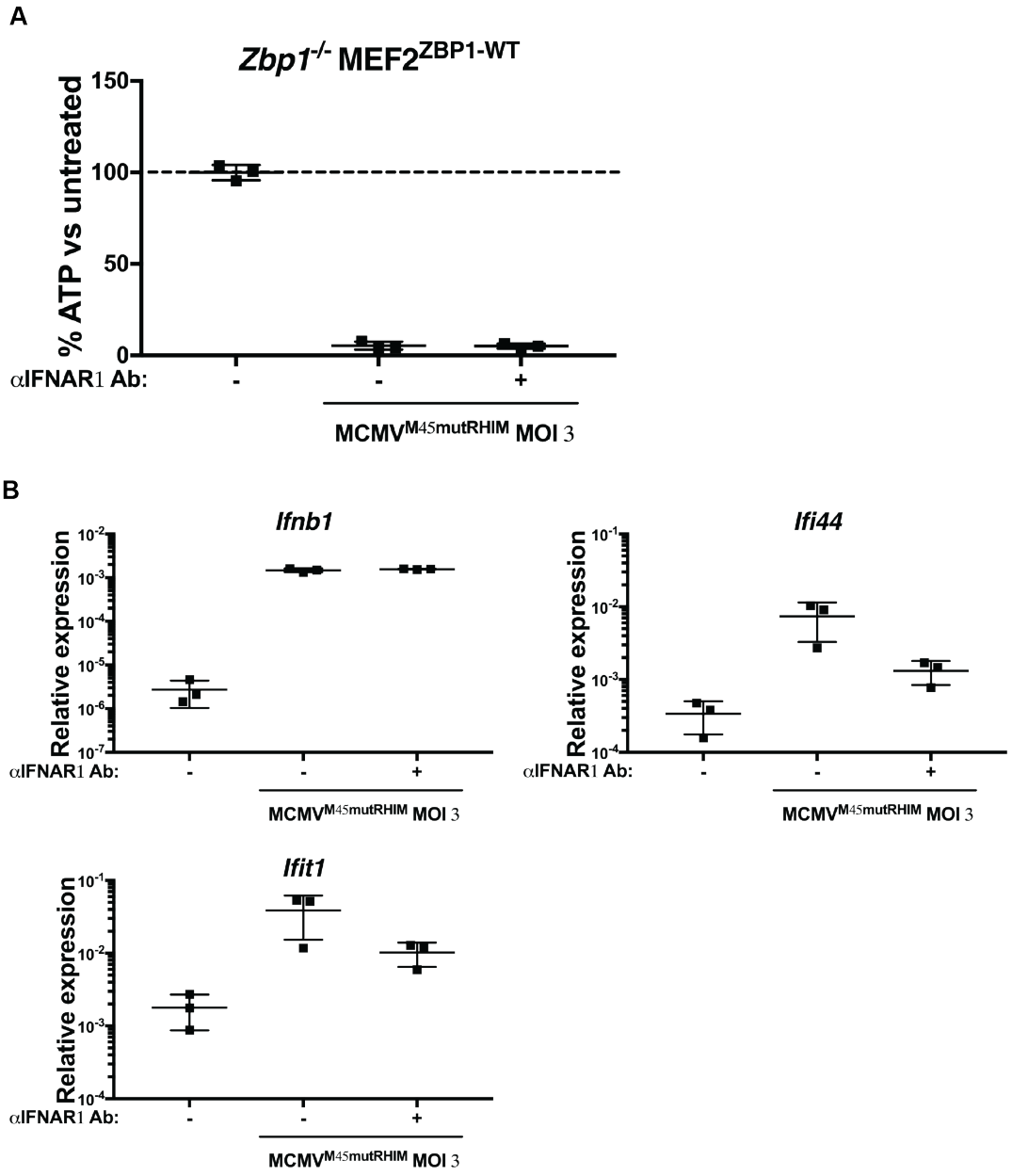


Figure 14. ZBP1-mediated virus-induced cell death is not affected by IFNAR1 blockade.

Immortalised *Zbp1*$^{-/-}$ MEFs were reconstituted with wildtype ZBP1 and then infected with MCMV^{M45mutRHIM} in the presence or absence of an IFNAR1 blocking antibody (0.5µg/mL). (A) After 24h, cell viability (% ATP) was assessed by the CellTiter-Glo® assay. (B) After 8h, cells treated in parallel were harvested and *Ifnb1*, *Ifit1* and *Ifi44* mRNA expression levels were measured by RT-qPCR. Means in (A) and (B) are from 1 representative experiment of 2 independent experiments each performed in technical triplicate and error bars represent ± 1 standard deviation (see Figure S1 for data from repeat experiment).

3.4 ZBP1 ZBD MUTANT KNOCK-IN MICE FAIL TO RESTRICT MCMV^{M45MUTRHIM} AND CELLS FROM THESE ANIMALS DO NOT UNDERGO VIRUS-INDUCED NECROPTOSIS

In order to test the relevance of ZBP1-mediated, ZBD-dependent sensing and virus-induced necroptosis *in vivo*, a knock-in mouse model was generated (Maelfait et al. 2017) (see Appendix) in which the ZBDs of ZBP1 were mutated as shown in **Figure 9**. Cells from these *Zbp1*$^{Zα1α2mut/Zα1α2mut}$ knock-in animals expressed similar levels of *Zbp1* compared to cells from wildtype mice after treatment with type I IFN (**Figure 15**).

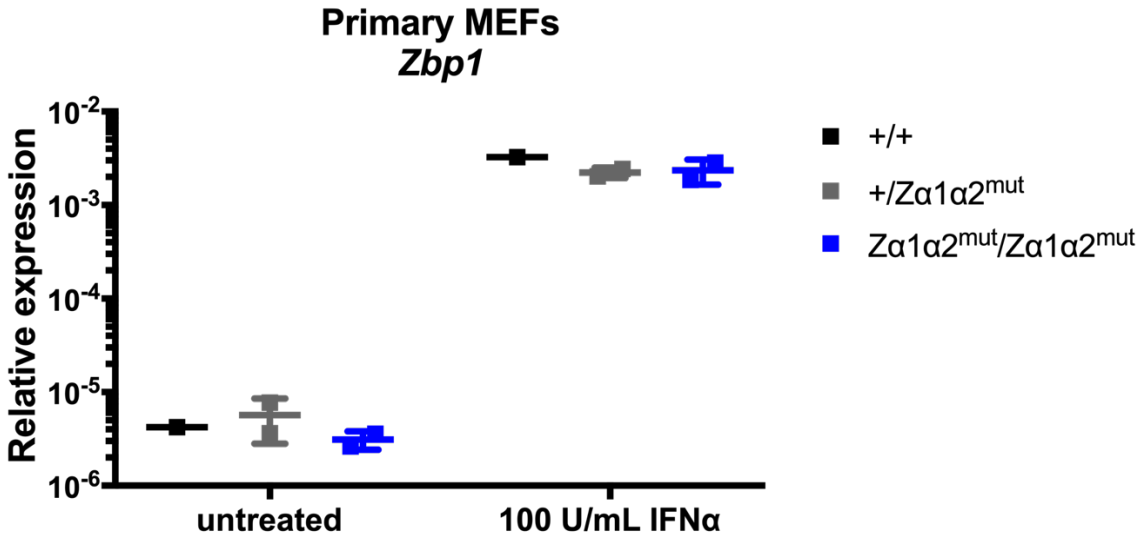


Figure 15. Knock-in of ZBP1^{Zα1α2mut} does not affect *Zbp1* expression.

Primary MEFs isolated from *Zbp1* wildtype (+/+), heterozygous (+/Zα1α2mut) or homozygous mutant (Zα1α2mut/Zα1α2mut) C57BL/6 mice were treated or not with 100 U/mL recombinant type I IFN (IFN-A/D) and after 16h, *Zbp1* mRNA expression was measured by qPCR. Means are representative of 1 experiment, with biological duplicates for the heterozygous and homozygous mutant mice and error bars represent ± 1 standard deviation.

In contrast to their wildtype counterparts, MLKL phosphorylation (**Figure 16**A) and oligomerisation (**Figure 16**B) were absent in cells from *Zbp1*$^{Zα1α2mut/Zα1α2mut}$ mice 16h after MCMV^{M45mutRHIM}-infection, reflecting an absence of ZBP1-mediated MLKL activation. Cells from *Zbp1*$^{Zα1α2mut/Zα1α2mut}$ mice still phosphorylated MLKL following treatment with a combination of TNF and zVAD (**Figure 16**C), however, demonstrating that the necroptosis machinery downstream of ZBP1 was intact. In cells from wildtype mice, the MCMV protein immediate early 1 (IE1) was detected at 8h post infection, but was completely absent by 16h (**Figure 16**B) – the same time point at which ZBP1-mediated MLKL activation was detected in these cells (**Figure 16**B, C). The opposite occurred in cells from *Zbp1*$^{Zα1α2mut/Zα1α2mut}$ mice, where the absence of MLKL activation at 16h post infection was associated with increased IE1 expression compared to cells from wildtype mice (**Figure 16**B, C). These data demonstrate that the lack of ZBP1-mediated necroptosis activation in cells from *Zbp1*$^{Zα1α2mut/Zα1α2mut}$ mice is associated with increased viral replication.

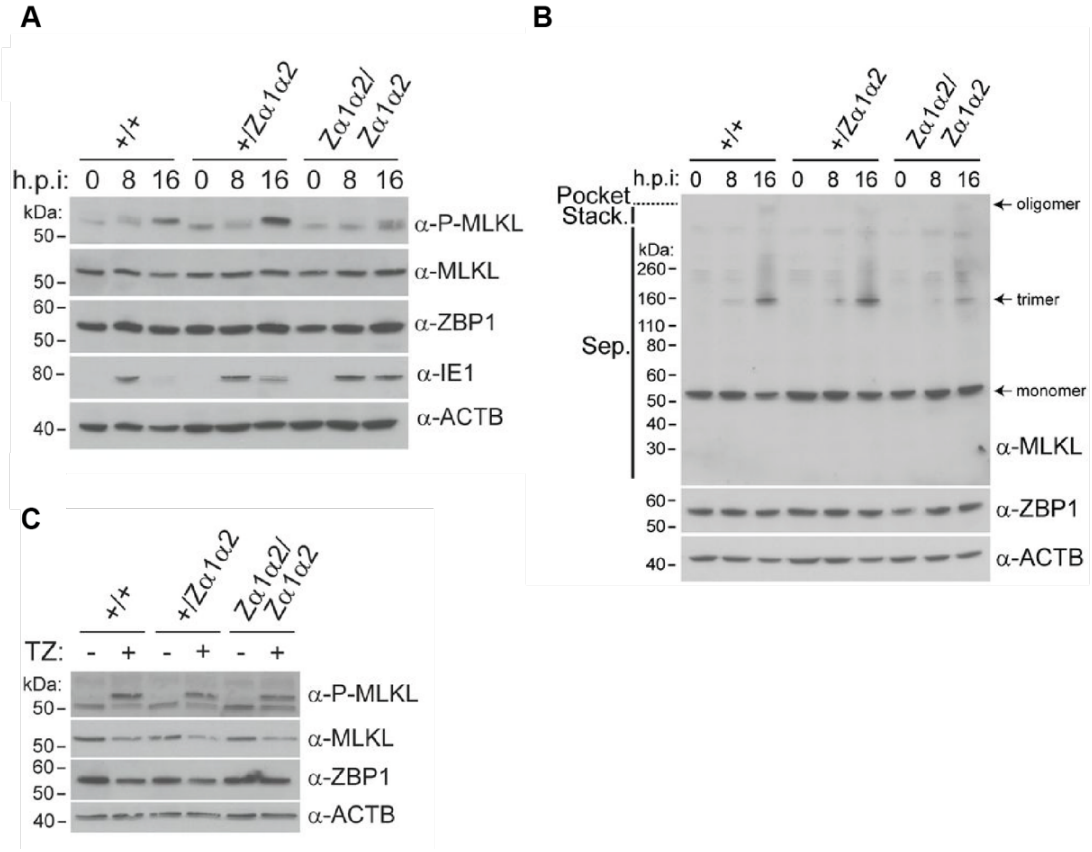


Figure 16. Knock-in of ZBP1^{Zα1α2mut} abrogates MCMV^{M45mutRHIM}-induced necroptosis.

Taken from Maelfait *et al* 2017 (see Appendix). Primary MEFs isolated from *Zbp1* wildtype (+/+), heterozygous (+/Zα1α2mut) or homozygous mutant (Zα1α2mut/Zα1α2mut) C57BL/6 mice were (A, B) infected with MCMV^{M45mutRHIM} at an MOI of 3 and protein expression was measured by SDS-PAGE and western blotting at the indicated time points post-infection, or (C) treated or not with the combination of TNF and zVAD (TZ) and protein expression was measured by SDS-PAGE and western blotting after 8h. In (A-C), data shown are from 1 experiment. Cells were infected, treated and harvested by Jonathan Maelfait. Animal work was conducted by Jonathan Maelfait. These results were reproduced by Jonathan Maelfait in an additional experiment.

To directly measure the effect of ZBP1^{Zα1α2mut} knock-in on viral genome replication, primary MEFs from *Zbp1*$^{Zα1α2mut/Zα1α2mut}$ mice were infected with MCMV^{M45mutRHIM} and copy numbers of the MCMV gene glycoprotein B (gB) were measured by RT-qPCR. 4 days post infection, copy numbers of MCMV gB were

significantly increased in *Zbp1*$^{Zα1α2mut/Zα1α2mut}$ mice compared to heterozygous or wildtype mice. This suggests that MCMV^{M45mutRHIM} genome replication occurs at an increased rate in cells from *Zbp1*$^{Zα1α2mut/Zα1α2mut}$ mice compared to wildtype or heterozygous animals (**Figure 17**). Altogether, these data provide further evidence that the failure to induce ZBP1-mediated necroptosis in cells from *Zbp1*$^{Zα1α2mut/Zα1α2mut}$ mice results in poorer control of viral replication.

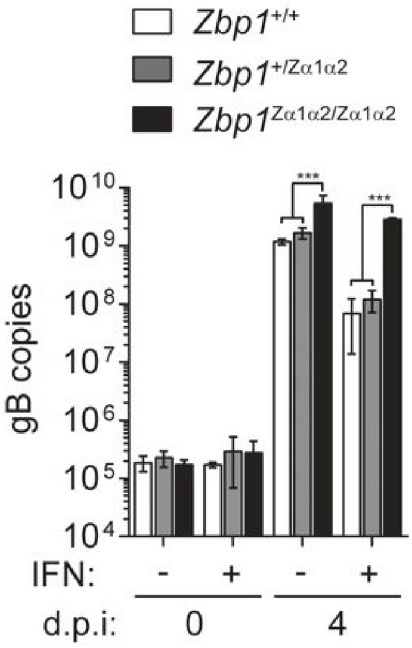


Figure 17. Knock-in of ZBP1^{Zα1α2mut} increases the rate of MCMV^{M45mutRHIM} genome replication.

Taken from Maelfait *et al* 2017 (see Appendix). Primary MEFs of the indicated genotypes were treated or not with 100 U/mL of recombinant type I IFN (IFN-A/D) for 16 h. DNA samples were collected at 0 and 4 days post infection (d.p.i) and analysed by qPCR (0 d.p.i = samples collected at the time of infection i.e. uninfected cells). MCMV glycoprotein B (gB) copy numbers were derived from a titration using defined amounts of gB plasmid. Means are representative of 3 independent experiments and error bars represent ± SD. Asterisks represent significant differences as determined by Two-way analysis of variance with Tukey's correction applied for multiple comparisons (ns = P>0.05, * = P≤0.05, ** = P≤0.01, *** = P≤0.001, **** = P≤0.0001). Cells were infected and harvested by Jonathan Maelfait.

Both wildtype (*Zbp1*$^{+/+}$) and *Zbp1*$^{Zα1α2mut/Zα1α2mut}$ mice allowed replication of wildtype MCMV, as determined by measuring viral titre in the spleen 4 days post-intraperitoneal infection (**Figure 18**). However, whereas MCMV^{M45mutRHIM} was unable to spread to the spleen in wildtype mice, infectious virus was recovered from the spleens of *Zbp1*$^{Zα1α2mut/Zα1α2mut}$ mice (**Figure 18**), suggesting that Z-nucleic acid binding by ZBP1 is required for antiviral defence *in vivo*. This phenotype was observed in males and females.

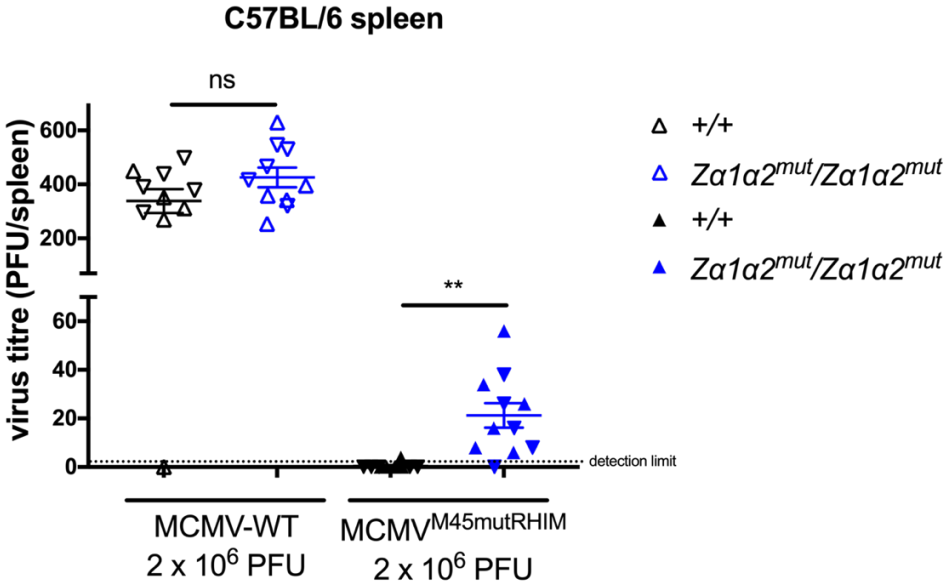


Figure 18. *Zbp1*$^{Zα1α2mut/Zα1α2mut}$ mice are less able to control MCMV^{M45mutRHIM} spread to the spleen.

Zbp1 wildtype (+/+) or ZBD mutant (Zα1α2mut/Zα1α2mut) C57BL/6 littermate mice were infected or not as indicated with 2 x 10^6 PFU of wildtype MCMV (MCMV-WT) or MCMV^{M45mutRHIM} by intraperitoneal injection. 4 days post-infection mice were sacrificed and viral titres in spleens were determined by plaque assay. Each data point represents one mouse. Means are pooled from 2 independent experiments: one with male mice (upward-facing triangles) and one with female mice (downward-facing triangles). The dotted horizontal line indicates the detection limit. Error bars represent ± standard error of the

mean. Asterisks represent significant differences as determined by Student's t-test with Welch's correction (ns = P>0.05, * = P≤0.05, ** = P≤0.01, *** = P≤0.001, **** = P≤0.0001). Animal work was conducted by Anne Bridgeman.

Wildtype MCMV replicates to higher titres than MCMV^{M45mutRHIM}, which is attenuated in wildtype mice (**Figure 18**), and this correlated with higher induction of cytokines by MCMV compared to MCMV^{M45mutRHIM} in infected wildtype animals (**Figure 19**). In line with this, the observed partial rescue of MCMV^{M45mutRHIM} titres in the spleens of *Zbp1*$^{Zα1α2mut/Zα1α2mut}$ mice was associated with a significantly increased induction of the inflammatory cytokine *Il1b*, as well as of *Zbp1*, in the livers of these animals (**Figure 19**).

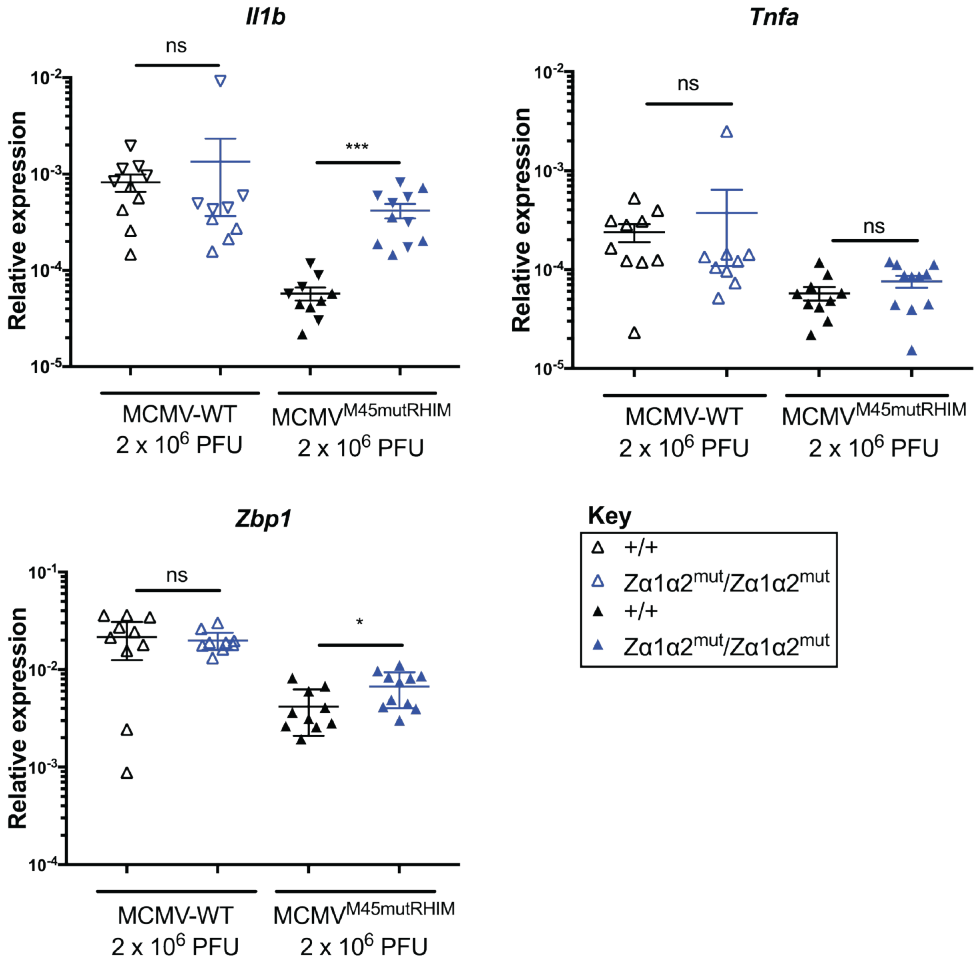


Figure 19. Increased MCMV^{M45mutRHIM} spread to the spleen in *Zbp1*$^{Zα1α2mut/Zα1α2mut}$ mice is associated with increased cytokine induction.

Zbp1 wildtype (+/+) or ZBD mutant (Zα1α2mut/Zα1α2mut) C57BL/6 littermate mice were infected as in Figure 18. 4 days post-infection mice were sacrificed and *Il1b*, *Tnfa* and *Zbp1* mRNA expression levels in livers harvested 4 days post-infection were measured by RT-qPCR relative to *Gapdh*. Each data point represents one mouse. Means are pooled from 2 independent experiments: one with male mice (upward-facing triangles) and one with female mice (downward-facing triangles). Error bars represent ± standard error of the mean. Asterisks represent significant differences as determined by Student's t-test with Welch's correction (ns = P>0.05, * = P≤0.05, ** = P≤0.01, *** = P≤0.001, **** = P≤0.0001). Animal work was conducted by Anne Bridgeman.

Spermatogenesis associated protein 2 (SPATA2) has been implicated in inflammatory signalling and necroptosis (Elliott et al. 2016; Wagner et al. 2016).

Based on this we hypothesised that SPATA2 deficient mice may phenocopy *Zbp1*$^{Zα1α2mut/Zα1α2mut}$ knock-in mice upon MCMV^{M45mutRHIM} infection. However, MCMV^{M45mutRHIM} failed to replicate to significant levels in either wildtype or *Spata2*$^{-/-}$ mice (Figure 20), suggesting SPATA2 may not be required for ZBP1-mediated virus-induced necroptosis *in vivo*. In contrast, virus replication was detectable in wildtype primary MEFs that were infected *in vitro* as a control (Figure 20).

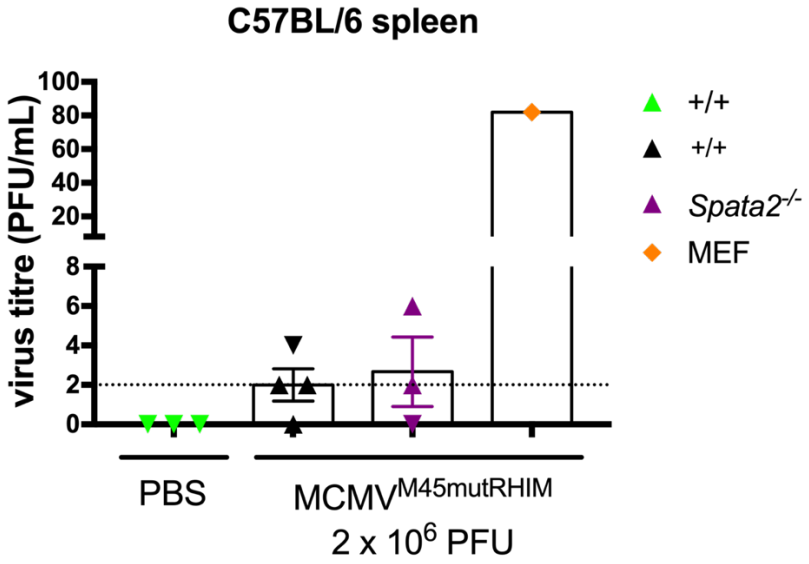


Figure 20. *Spata2*$^{-/-}$ mice control MCMV^{M45mutRHIM} spread to the spleen.

Wildtype (+/+) or *Spata2*$^{-/-}$ C57BL/6 littermate mice were infected or not as indicated with 2 x 10^6 PFU of MCMV^{M45mutRHIM} by intraperitoneal injection. 4 days post-infection mice were sacrificed and viral titres in spleens were determined by plaque assay. Each triangle-shaped data point represents one mouse. As a positive control for the plaque assay, cells were directly infected with MCMV^{M45mutRHIM} at an MOI of 0.01. Means are pooled from 1 experiment with male (upward-facing triangles) and female (downward-facing triangles) mice. The dotted horizontal line indicates the detection limit. Error bars represent ± standard error of the mean. Animal work was conducted by Anne Bridgeman.

3.5 MVA AND MHV68 MAY INDUCE ZBP1-MEDIATED CELL DEATH

To investigate whether ZBP1 senses other viruses to activate cell death, immortalised *Zbp1*$^{-/-}$ MEFs were reconstituted or not with wildtype ZBP1 (ZBP1^{WT}) (Maelfait et al. 2017) (see Appendix) and infected at MOI 5 with modified vaccinia Ankara (MVA), murine gammaherpes virus 68 (MHV68) or MCMV^{M45mutRHIM} (**Figure 21**). After 24h, a larger reduction in cell viability was observed in virus-infected cells reconstituted with ZBP1 compared to ZBP1-deficient cells, consistent with virus-induced cell death mediated by ZBP1. Treatment with zVAD alone also induced ZBP1-mediated cell death, whereas treatment with the combination of TNF and zVAD induced cell death in both cell types irrespective of ZBP1 expression.

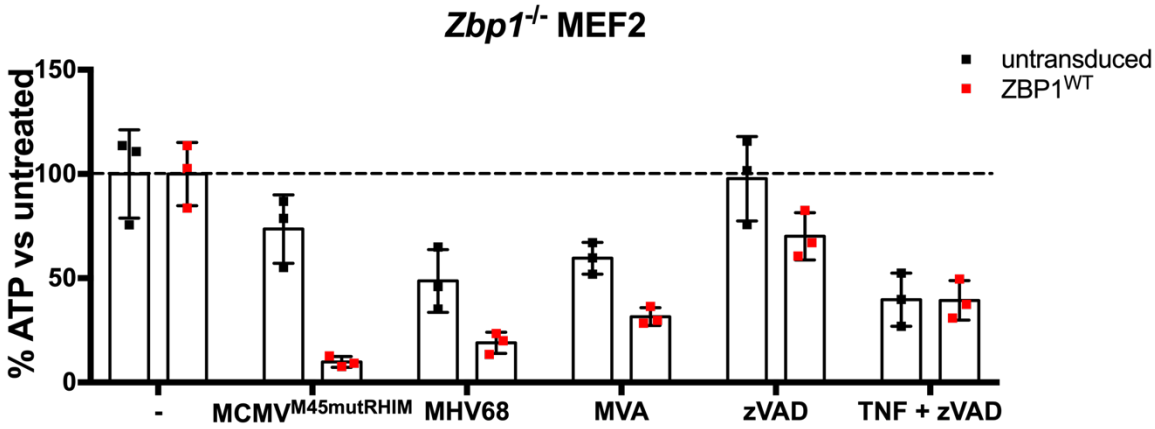


Figure 21. MVA and MHV68 induce a ZBP1-mediated reduction in cell viability.

Immortalised *Zbp1*$^{-/-}$ MEFs were reconstituted or not with wildtype ZBP1 (ZBP1^{WT}) and then either infected with the viruses indicated at MOI 5 or treated with zVAD (20μM) alone or in combination with TNF (30ng/mL) (TNF + zVAD). After 24h, cell viability (% ATP) was measured by the CellTiter-Glo® assay. Means are from 1 experiment performed in technical triplicate and error bars represent ± 1 standard deviation.

To examine the kinetics of this cell death, cells treated in the same way were imaged hourly, in the presence of a cell impermeable DNA stain (SYTOX GREEN). ZBP1-mediated MVA-induced cell death was detected after 4hpi whereas ZBP1-mediated cell death induced by MHV68 and MCMV^{M45mutRHIM} was detected slightly later, after 8hpi. Whereas MVA did not induce cell death in ZBP1-deficient cells, MHV68 did induce some cell death, and this was increased further in cells reconstituted with ZBP1.

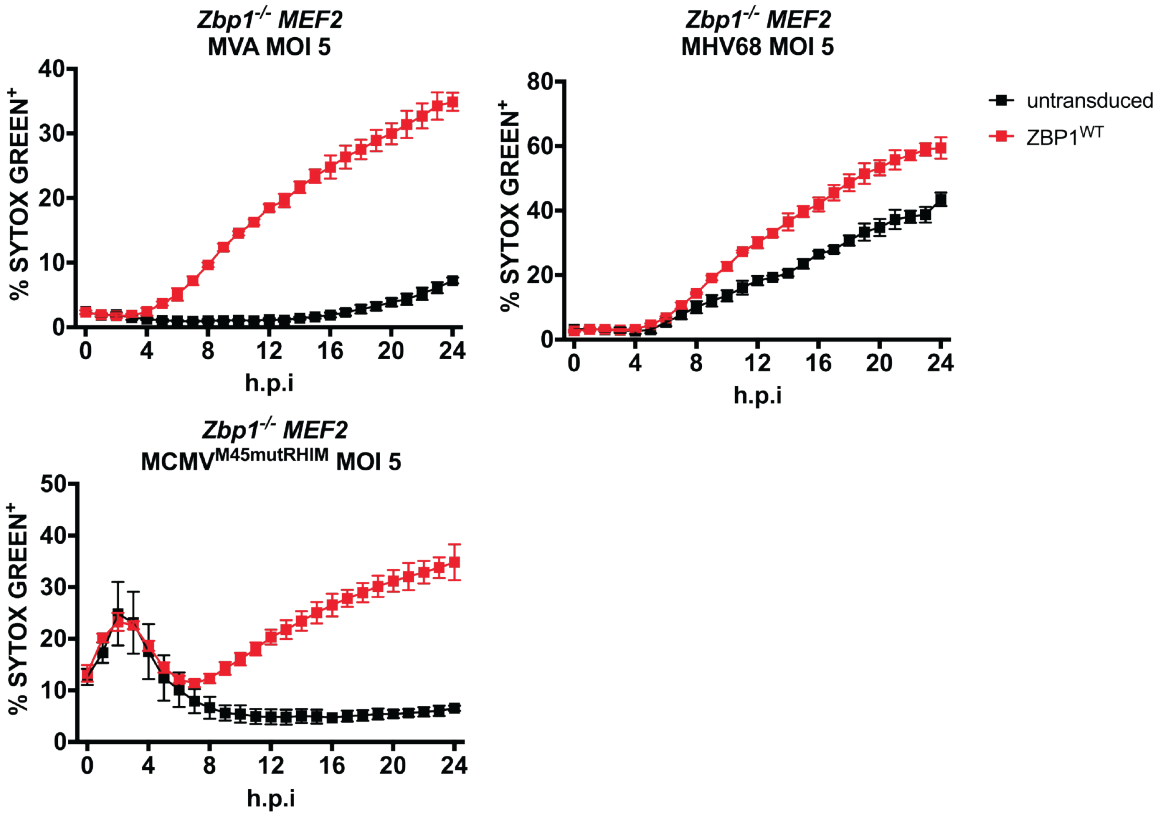


Figure 22. MVA and MHV68 induce a ZBP1-mediated cell membrane permeabilisation.

Immortalised *Zbp1*$^{-/-}$ MEFs were reconstituted or not with wildtype ZBP1 (ZBP1^{WT}) and then infected with the viruses indicated at MOI 5. Cell death was measured hourly over 24h by

automated microscopy (IncuCyte®), as uptake of a cell impermeable DNA stain (SYTOX GREEN). Means are from 1 experiment performed in technical triplicate and error bars represent ± standard deviation.

These preliminary results suggest that ZBP1 may sense MVA and MHV68, in addition to MCMV (Upton et al. 2012) and IAV (Thapa et al. 2016; Kuriakose et al. 2016), to activate cell death in mouse cells. However, repeat experiments would be necessary for the statistical significance of these results to be determined.

3.6 DISCUSSION

This chapter described the results that I contributed to a published study (Maelfait et al. 2017) (see Appendix), which demonstrated that, in the context of virus infection, ZBP1 senses RNA via its two ZBDs and then activates RIPK3-MLKL-mediated necroptosis to restrict viral replication. In addition to these published results, I also described additional results confirming that ZBD-dependent sensing by ZBP1 is relevant in an *in vivo* infection model and preliminary data suggesting that ZBP1 may sense other viruses, in addition to MCMV (Upton et al. 2012) and IAV (Thapa et al. 2016; Kuriakose et al. 2016).

Mutation of key residues in the ZBP1 ZBDs (Figure 9), that are required for Z-nucleic acid binding (Herbert et al. 1995; Schwartz 1999), prevented sensing of $MCMV^{M45mutRHIM}$ and the consequent induction of necroptotic antiviral cell death (Figure 10, Figure 11 & **Figure 12**). These results are consistent with the hypothesis that the ligand for ZBP1 during $MCMV^{M45mutRHIM}$ infection is a Z-nucleic acid. Indeed,

experiments performed in parallel by Jonathan Maelfait demonstrated that ZBP1 cross-links to RNA in a ZBD-dependent manner and that necroptosis induced by ZBP1 during virus infection is prevented by treatment with the transcription inhibitor Actinomycin D early post-infection (Maelfait et al. 2017) (see Appendix). One might therefore speculate that the ligand for ZBP1 is a Z-RNA, which is generated as a consequence of virus infection. My attempts to visualise Z-RNA in virus-infected cells using immunofluorescent confocal microscopy did not yield conclusive results as, due to the instability of Z-RNA, a suitable positive control for Z-RNA staining with the anti-Z-DNA antibody tested was lacking (data not shown). In the future, chemicals that stabilise Z-RNA, such as the recently developed 2'-*O*-Methyl-8-methylguanosine (Balasubramaniyam et al. 2018), and Z-RNA specific antibodies could enable visualisation of Z-RNA in virus-infected cells.

Since ZBP1 binds to RNA (Maelfait et al. 2017) (see Appendix) and induces necroptosis (Figure 10, Figure 11 & **Figure 12**) in uninfected cells treated only with the pan-caspase inhibitor zVAD, the origin of this RNA as viral or endogenous remains to be fully elucidated. Given that type I IFN receptor blockade did not rescue MCMV^{M45mutRHIM}-induced cell death (Figure 14), it is unlikely that ZBP1 is sensing IFN-induced endogenous transcripts. However, it is conceivable that virus infection alters cellular RNA homeostasis in such a way as to trigger ZBP1 activation. Alternatively, the ZBP1 agonist may differ in uninfected versus virus-infected cells, potentially explaining the differing sensitivity of zVAD-treated versus MCMV^{M45mutRHIM}-infected ZBP1-expressing cells to pharmacological RIPK1

inhibition (Figure 12). Silencing of MCMV immediate early 3 (IE3), which is required for the generation of early transcripts by the virus, partially rescued necroptosis activation induced by MCMV^{M45mutRHIM} infection (Maelfait et al. 2017) (see Appendix). Moreover, a mutant virus lacking functional IE3 fails to activate ZBP1-mediated necroptosis (Sridharan et al. 2017). Together, these results indicate that an early viral transcript may be the agonist for ZBP1 during infection with MCMV^{M45mutRHIM}. In future, ZBP1 immunoprecipitation and RNA sequencing may enable the ZBP1 ligand to be more precisely identified and defined.

Cells from *Zbp1*$^{Zα1α2mut/Zα1α2mut}$ mice failed to induce ZBP1-mediated necroptosis in response to MCMV^{M45mutRHIM} infection (Figure 16), resulting in poorer control of viral replication (Figure 16 & Figure 17), which most likely explains the observed increase in spread of virus to the spleen in these animals (Figure 18). Compared to wildtype MCMV, MCMV^{M45mutRHIM} was attenuated in wildtype mice as expected, however, knock-in of *Zbp1*$^{Zα1α2mut/Zα1α2mut}$ did not completely rescue MCMV^{M45mutRHIM} titres in the spleen to the levels seen in the spleens of mice infected with wildtype MCMV (Figure 18). One explanation might be that M45 has another function, unrelated to its role in necroptosis antagonism, that is required for viral replication. This other function of M45 may be inadvertently affected by mutating the RHIM domain. M45 additionally contains a non-functional ribonucleoside-diphosphate reductase large subunit-like domain (Lembo et al. 2004), which may mediate this other cryptic function. Alternatively, there may be compensatory mechanisms in *Zbp1*$^{Zα1α2mut/Zα1α2mut}$ mice that enable some restriction of virus

replication to continue. The increase in MCMV^{M45mutRHIM} spread to the spleen in *Zbp1*$^{Zα1α2mut/Zα1α2mut}$ mice correlated with an increase in inflammatory cytokine expression in the liver (Figure 19), likely due to the increased amount of virus replication generating more ligands for pattern recognition receptors.

Preliminary results indicate that ZBP1 may sense other viruses, namely MVA and MHV68 (Figure 21, Figure 22), in addition to MCMV (Upton et al. 2012) and IAV (Thapa et al. 2016; Kuriakose et al. 2016). In fact, since these data were generated (Figure 21, Figure 22), mouse ZBP1 has additionally been shown to sense VV Western Reserve (Koehler et al. 2017) and HSV1/2 (Guo et al. 2018) to activate necroptosis, and, recently, Zika virus (ZIKV) to activate a cellular antiviral metabolic state (Daniels et al. 2019). Altogether, the findings presented in this chapter contribute to a rapidly expanding literature implicating ZBP1 as a critical and specific sensor of infection by multiple mammalian viruses.

CHAPTER 4 RESULTS II
ZBP1 MEDIATES NECROPTOSIS IN HUMAN CELLS

All of the studies of ZBP1 discussed in Chapter 3 were performed in mice or mouse cells. Comparatively little is known about whether ZBP1-mediated necroptosis is important for antiviral defence in humans. The key residues required for Z-nucleic acid binding within the ZBDs of ZBP1 (Herbert et al. 1995; Schwartz 1999) are highly conserved from human to mouse (Figure 23) and, in an unbiased systematic approach to determine the antiviral effects of over 350 IFN-stimulated genes, human ZBP1 was shown to prevent replication of multiple RNA and DNA viruses, including Coxsackie B virus (CVB), Sindbis virus, hepatitis C virus and VV (Schoggins et al. 2011; Schoggins et al. 2014). Subsequent studies have specifically implicated human ZBP1 as a sensor of VV (Koehler et al. 2017), IAV (B. M. Hartmann et al. 2017) and HSV (Guo et al. 2018) for activation of RIPK3-driven antiviral cell death.

UniProtKB	Zα1	Zα2
Q9H171_HUMAN	KRELNQVLYRMKK	AKDVNRDLYRMKS
F6XT26_CANLF	KKKLNQVLYRLMK	AKDVNRDLYDMRK
E1BIH9_BOVIN	KKKLNQLLHKMKQ	AKEVNPDLYAMRD
A5GFP5_PIG	KKKLNQVLHRMKK	AKEVNRDLYAMRN
A2APF7_MOUSE	KKTLNQVLYRLKK	AKEVNPLLYSMRN

Figure 23. Conservation of key amino acids in ZBP1 ZBDs from human to mouse.

Taken from Maelfait *et al* 2017 (see Appendix). ZBP1 sequences from the indicated species were aligned using Clustal Omega and the sequence context of the conserved asparagine and tyrosine residues (highlighted) involved in Z-nucleic acid binding is shown.

In accordance with Red Queen dynamics (Van Valen 1973), one might reasonably predict that viruses sensed by ZBP1 are likely to encode antagonists of ZBP1 signalling. For instance, MCMV encodes M45, which prevents a critical RHIM-RHIM interaction between ZBP1 and RIPK3 that is required to induce necroptosis in mice (Upton et al. 2012). An equivalent antagonist from IAV has not been identified, however, one study reported that the HA genomic segment from pandemic H1N1 IAVs could mediate antagonism of RIPK3-driven necroptosis in human dendritic cells (B. M. Hartmann et al. 2017). Unlike MCMV, IAV is not a mouse pathogen. Thus, if an IAV-encoded protein antagonist equivalent to MCMV M45 does exist, it may be species-restricted, explaining why it has not been detected in studies conducted exclusively in mice or mouse cells (Thapa et al. 2016; Kuriakose et al. 2016). This is the case for HSV1 and HSV2, which encode ICP6 and ICP10 respectively, both of which contain RHIM domains. ICP6/10 can inhibit the RHIM-RHIM interaction between ZBP1 and RIPK3 in human, but not mouse, cells (Guo et al. 2015; Guo et al. 2018). In fact, ICP6 instead activates necroptosis in mouse cells infected with HSV1 (Guo et al. 2018). In contrast to ICP6, M45 is not species-restricted and can antagonise ZBP1-RIPK3 driven necroptosis in both mouse and human cells (Guo et al. 2015). In addition to RHIM-mediated antagonism of ZBP1-driven necroptosis, another potential inhibitory mechanism has been identified. The VV protein E3L contains an N-terminal ZBD (Zα1) (**Figure 3**), which has been proposed to enable antagonism of ZBP1 activation through the sequestration of ZBP1 ligands (Koehler et al. 2017). A virus with an N-terminal

deletion in E3L, which removes the ZBD, activates ZBP1-mediated necroptosis in mouse and human cells, whereas the corresponding wildtype virus does not (Koehler et al. 2017).

In addition to detection of RNA in the context of virus infection, mouse ZBP1 senses endogenous RNA to activate cell death (Maelfait et al. 2017) (see Appendix & Chapter 3 Results I). Whether human ZBP1 also senses endogenous nucleic acids is not known. The present chapter details the reconstitution of the human ZBP1 necrosome in a human cell line, demonstrating that ectopic expression of core human ZBP1 necrosome constituents was sufficient to activate necroptosis, which required intact ZBP1 ZBDs. This may suggest the presence of an endogenous ligand for ZBP1 in human cells. This system also provides an experimental tool with which proteins and small molecules can be screened for their ability to inhibit human ZBP1 necrosome activation, for example to identify novel viral antagonists of this pathway. This chapter describes the establishment of this human ZBP1-mediated necroptosis assay and screening platform, with proof-of-concept experiments demonstrating that this assay can detect known viral protein and small molecule inhibitors of ZBP1-driven necroptosis.

4.1 ECTOPIC ZBP1 EXPRESSION IN HUMAN CELLS INDUCES SPONTANEOUS CELL DEATH

In order to identify a suitable system for studying human ZBP1, protein expression levels of ZBP1, RIPK3 and MLKL – key necroptosis mediators – were measured in four sub-lines of human embryonic kidney 293T cells (HEK293T), in a human colorectal adenocarcinoma cell line (HT-29) and in primary human monocyte-derived dendritic cells (MDDC) by SDS-PAGE and western blotting (Figure 24).

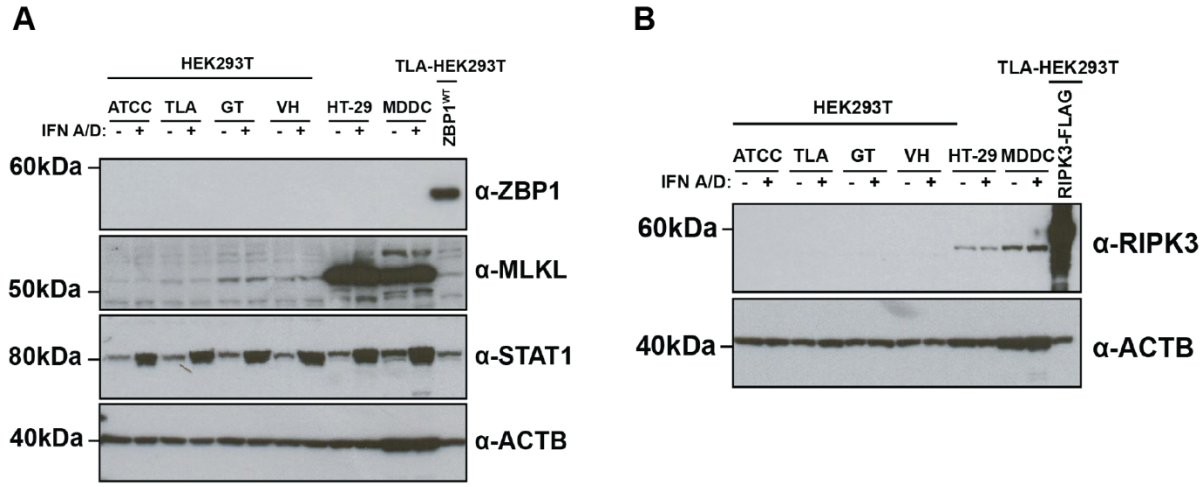


Figure 24. Protein expression levels of ZBP1, RIPK3 and MLKL in different human cell lines.

(A-B) Cells were treated or not with 100U/mL recombinant type I IFN (IFN-A/D) as indicated for 16h and then harvested and analysed by SDS-PAGE and western blotting. Four different sub-lines of HEK293T were tested, including: cells obtained directly from ATCC (ATCC), TLA-HEK293T cells (TLA) and HEK293T cells that were gifts from Greg Towers (GT) or Veit Hornung (VH). HT-29 cells and human monocyte-derived dendritic cells (MDDC) were also tested. As positive controls, lysates from TLA-HEK293T cells transfected for 24h with ZBP1 or RIPK3 were also included. Data in (A) and (B) are from 1 representative experiment of 3 independent experiments (see Figure S2 for data from repeat experiments).

Although type I IFN-induced ZBP1 protein expression has previously been reported in HT-29 cells (Koehler et al. 2017), in the present study, ZBP1 was neither detected at baseline nor after treatment with type I IFN in lysates from any of the human cells tested (Figure 24A). This is consistent with data from another study demonstrating that, unlike the mouse protein, human ZBP1 is not type I IFN inducible (Shaw et al. 2017). In contrast to ZBP1, the ISG STAT1 was detected at baseline in all cells tested and was increased following type I IFN treatment as expected (Figure 24A). ZBP1 was detected in lysates from HEK293T cells in which ZBP1 was ectopically expressed by transient transfection (Figure 24A). RIPK3 and MLKL were not detected to significant levels in lysates from HEK293T cells, but were detected in lysates from HT-29 cells and primary human MDDCs, as well as in lysates from transiently transfected HEK293T cells (Figure 24A-B).

HT-29 cells are necroptosis competent because they express RIPK3 and MLKL endogenously (Omoto et al. 2015) (Figure 24A-B) and are therefore commonly used in necroptosis studies. To investigate whether human ZBP1 activates necroptosis, HT-29 cells were stably transduced with wildtype human ZBP1 ($ZBP1^{WT}$) or a ZBD-mutant (N46A & Y50A in Zα1 and N141A & Y145A in Zα2) containing equivalent point mutations to those that were introduced in mouse ZBP1 in Chapter 3 ($ZBP1^{Zα1α2mut}$) (**Figure 25**). After antibiotic selection of successfully transduced cells, a spontaneous cell death phenotype was observed in the $ZBP1^{WT}$-expressing cells, which was absent from cells expressing $ZBP1^{Zα1α2mut}$ or mock transduced cells (EV) (**Figure 25**A). As a result of this

spontaneous cell death, ZBP1^{WT}-expressing cells grew more slowly in culture than their ZBP1^{Zα1α2mut} or mock transduced counterparts (Figure 25A). Unsurprisingly, the proportion of ZBP1^{WT}-expressing cells decreased from this polyclonal population of transduced cells over time, since toxicity of the protein provided a selective advantage to any cells that spontaneously lost ZBP1^{WT} expression (Figure 25B-C).

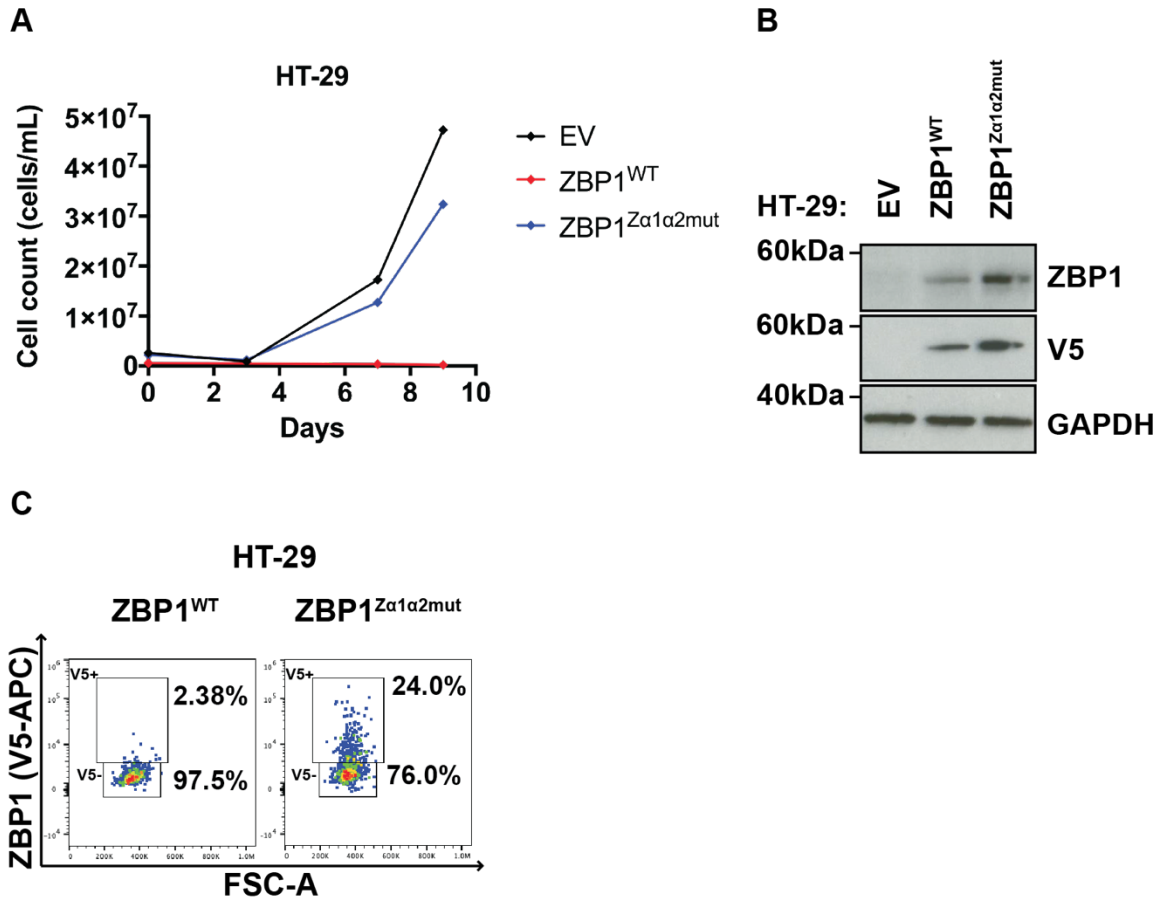


Figure 25. Ectopic ZBP1 expression in HT-29 cells is cytotoxic.

(A-C) HT-29 cells were transduced with empty vector (EV), ZBP1^{WT}-V5 or ZBP1^{Zα1α2mut}-V5, using lentiviruses. (A) After antibiotic selection of transduced cells, surviving cells were

trypsinised, resuspended and counted a total of four times during the 10-day period that followed. Cell counts (cells/mL) are plotted over time (days). (B) Lysates from transduced cells (after antibiotic selection) were analysed by SDS-PAGE and western blotting. (C) Transduced cells were stained with an anti-V5 antibody conjugated to APC and analysed by flow cytometry. See Figure S3 for gating strategy. Data in (A-C) are from 1 experiment.

Given that HT-29 stably expressing wildtype ZBP1 could not survive in cell culture (**Figure 25**), the next aim was to identify a more tractable model for studying human ZBP1-mediated necroptosis. An advantage of using the HT-29 cells was that they expressed RIPK3 and MLKL endogenously (**Figure 24**), however, this simultaneously rendered them hypersensitive to ZBP1-mediated cell death (**Figure 25**). The HT-29 cells carried the additional disadvantage of being unamenable to transfection (data not shown). Conversely, HEK293T cells, which naturally lack ZBP1, RIPK3 and MLKL, can be readily transfected. To investigate their suitability as an alternative model, HEK293T cells were transfected with plasmid expression constructs encoding V5-tagged $ZBP1^{WT}$ or $ZBP1^{Z\alpha1\alpha2mut}$, and then imaged by confocal microscopy 24h later (Figure 26). Both $ZBP1^{WT}$ and $ZBP1^{Z\alpha1\alpha2mut}$ expressing cells were viable, as expected, and the cellular localisation of $ZBP1^{Z\alpha1\alpha2mut}$ was similar to $ZBP1^{WT}$, suggesting that mutation of the ZBDs does not affect the predominantly cytoplasmic cellular localisation of ZBP1 (Figure 26).

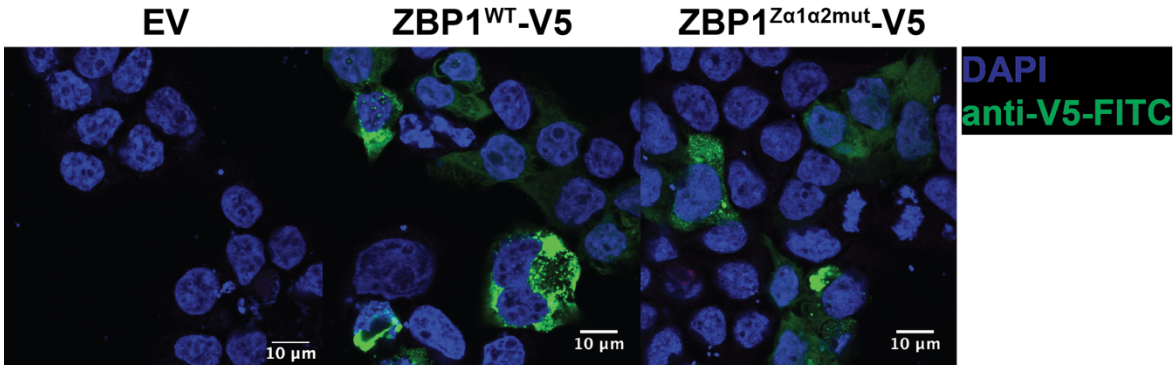


Figure 26. ZBP1 has a predominantly cytoplasmic localisation in transfected HEK293T cells.

HEK293T cells on coverslips were transfected with either an empty vector control plasmid (EV) or V5-tagged human ZBP1 wildtype ($ZBP1^{WT}$) or ZBD mutant ($ZBP1^{Zα1α2mut}$) and 24h post transfection cells were fixed, permeabilised and stained (DAPI and anti-V5-FITC) before imaging by confocal microscopy. Images (display range 0-4095) from 1 representative experiment of 2 independent experiments are shown (see Figure S4 for data from repeat experiment).

To further examine human ZBP1-mediated ZBD-dependent cytotoxicity, HEK293T cells were reconstituted with either an equivalent amount of empty vector plasmid DNA (EV), or with plasmid expression constructs encoding RIPK3 and MLKL with or without $ZBP1^{WT}$, by transient transfection. Uptake of a cell impermeable DNA stain (SYTOX GREEN) was then monitored hourly by automated microscopy (IncuCyte®) for 24h starting at 24h post-transfection (Figure 27). A significantly higher number of cells transfected with $ZBP1^{WT}$, in addition to RIPK3 and MLKL, underwent a ZBP1-dependent cell membrane permeabilisation over the 24h following transfection, as compared to cells transfected with RIPK3 and MLKL only or mock transfected cells (Figure 27).

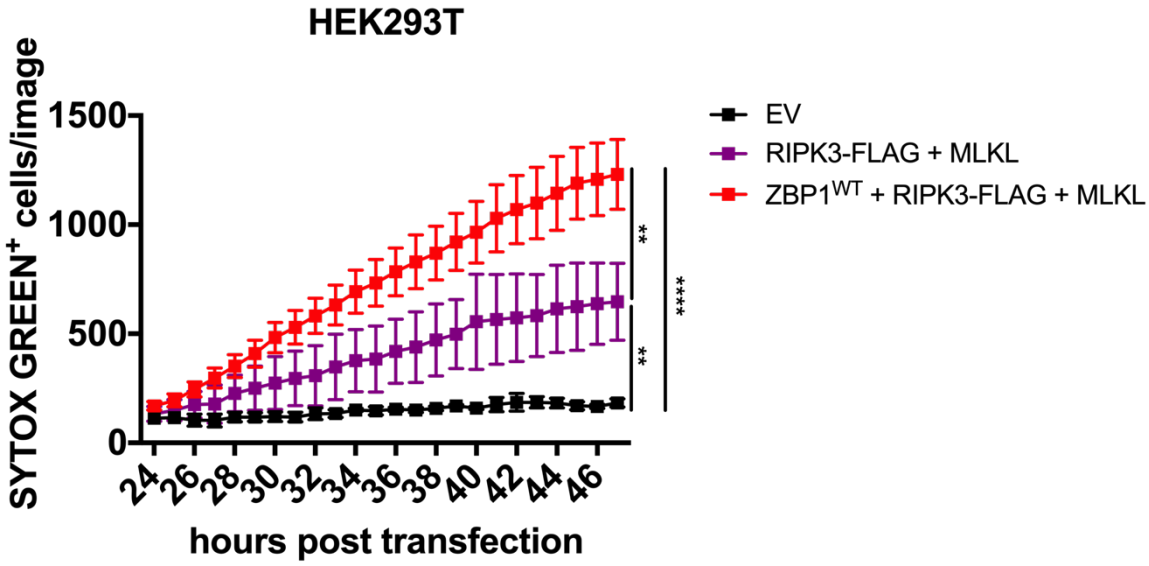


Figure 27. Co-transfection of ZBP1, RIPK3 and MLKL induces cell membrane permeabilisation in HEK293T.

HEK293T cells at 20,000 cells/well in a 96-well plate were co-transfected with empty vector (EV) or plasmids encoding RIPK3 (11.1ng/well) and MLKL (11.1ng/well), with or without ZBP1 (33.3ng/well). 24h post-transfection a cell impermeable DNA stain (SYTOX GREEN) was added to the cell culture medium and uptake of this dye was monitored hourly for a further 24h by microscopy (IncuCyte®). Means are pooled from 2-4 independent experiments and error bars represent ± standard error of the mean. Asterisks represent significant differences as determined by repeated measures ANOVA with Friedman test (ns = P>0.05, * = P≤0.05, ** = P≤0.01, *** = P≤0.001, **** = P≤0.0001).

Dose titrations of the individual expression constructs revealed that increasing doses of EV, ZBP1 or RIPK3 alone are not sufficient to induce cell death, whereas expression of MLKL alone induces some cell death at higher plasmid concentrations (of 33.3ng/well and above) (Figure 28A). Although neither RIPK3 nor MLKL expression alone were sufficient to induce cell death at lower plasmid concentrations, co-expression of these proteins lowered the threshold for cell death

induction (Figure 28B). When ZBP1 was additionally co-expressed at higher concentrations (33.3ng/well or more), the threshold for cell death induction was further lowered (Figure 28B), consistent with ZBP1-mediated RIPK3-MLKL driven cell death.

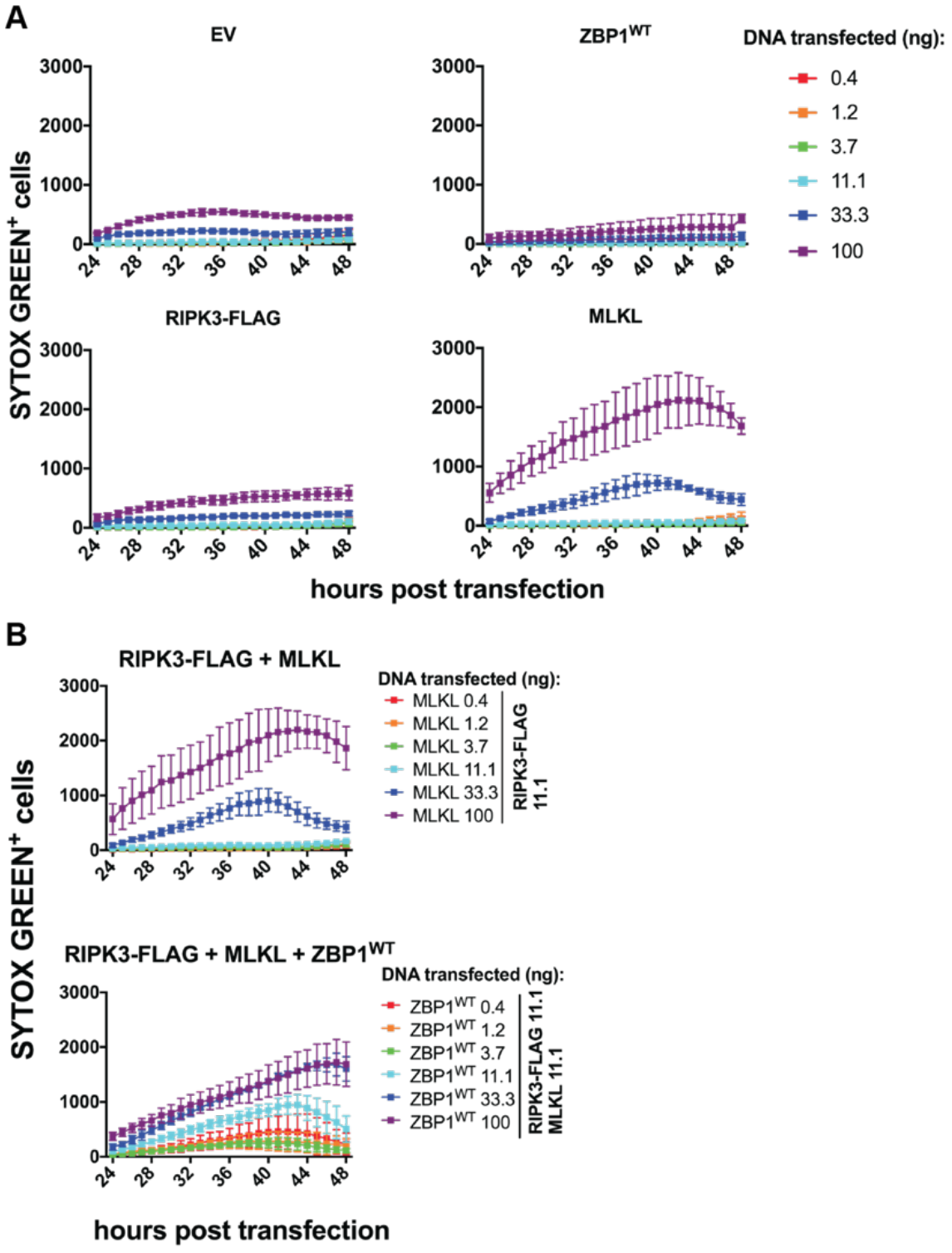


Figure 28. Dose titrations of ZBP1, RIPK3 and MLKL transfections in HEK293T.

HEK293T cells at 20,000 cells/well in a 96-well plate were transfected with dose titrations of plasmids encoding empty vector (EV), ZBP1, RIPK3-FLAG or MLKL in (A) and the indicated combinations of these plasmids in (B). 24h post-transfection a cell impermeable DNA stain (SYTOX GREEN) was added to the cell culture medium and uptake of this dye was monitored hourly for 24h by automated microscopy (IncuCyte®). SYTOX GREEN+ cells per image are plotted over time (hours post transfection). Means in (A) and (B) are representative of 1 independent experiment performed in triplicate and error bars represent ± 1 standard deviation.

To quantify the proportion of cells dying in a ZBP1-dependent way and to confirm that this cell death was also ZBD-dependent, HEK293T cells were transfected and 24h post-transfection cell viability was assessed using the CellTiter-Glo® assay described in Chapter 3 (Figure 29). Intracellular ATP content was reduced by 12% 24h post-transfection with RIPK3 and MLKL, compared to 28% post-transfection with $ZBP1^{WT}$, RIPK3 and MLKL, and 16% after transfection with $ZBP1^{Z\alpha1\alpha2mut}$, RIPK3 and MLKL (Figure 29). However, despite this numerical trend of a greater reduction in cell viability when ZBP1 is present and when the ZBD is intact, none of these differences were statistically significant.

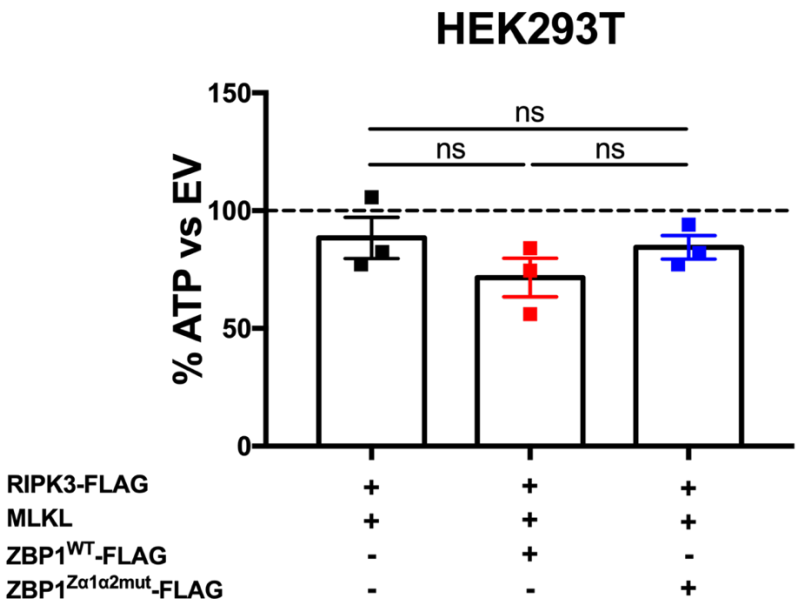


Figure 29. Co-transfection of ZBP1, RIPK3 and MLKL reduces cell viability in HEK293T.

HEK293T cells were transfected with plasmids encoding the indicated proteins. 48h post-transfection, cells were harvested and viability assessed using the CellTiter-Glo® assay. Percentage ATP (% ATP) relative to cells transfected with an empty vector control plasmid (EV) is on the y-axis. Means are pooled from 3 independent experiments and error bars represent ± standard error of the mean. Asterisks represent significant differences as determined by One Way ANOVA with Kruskal-Wallis test and Dunn's multiple comparisons test (ns = P>0.05, * = P≤0.05, ** = P≤0.01, *** = P≤0.001, **** = P≤0.0001. From left to right on the graph: column A vs column B, p=0.6991 (ns); column A vs column C, p>0.9999 (ns); column B vs column C, p=0.8902 (ns)).

Altogether, the results presented in this section demonstrate that ectopic expression of ZBP1 in necroptosis competent human cell lines is sufficient to activate cell death. The next goal was to define the mechanism of ZBP1-mediated cell death and to fully determine whether its activation was ZBD-dependent.

4.2 RECONSTITUTION OF THE ZBP1 NECROSOME IN HUMAN CELLS

A human ZBP1-mediated necroptosis assay was developed with the aims of determining the upstream triggers of ZBP1-mediated cell death and, ultimately, developing a screening platform to identify viral protein antagonists of ZBP1-mediated necroptosis activation (**Figure 30**).

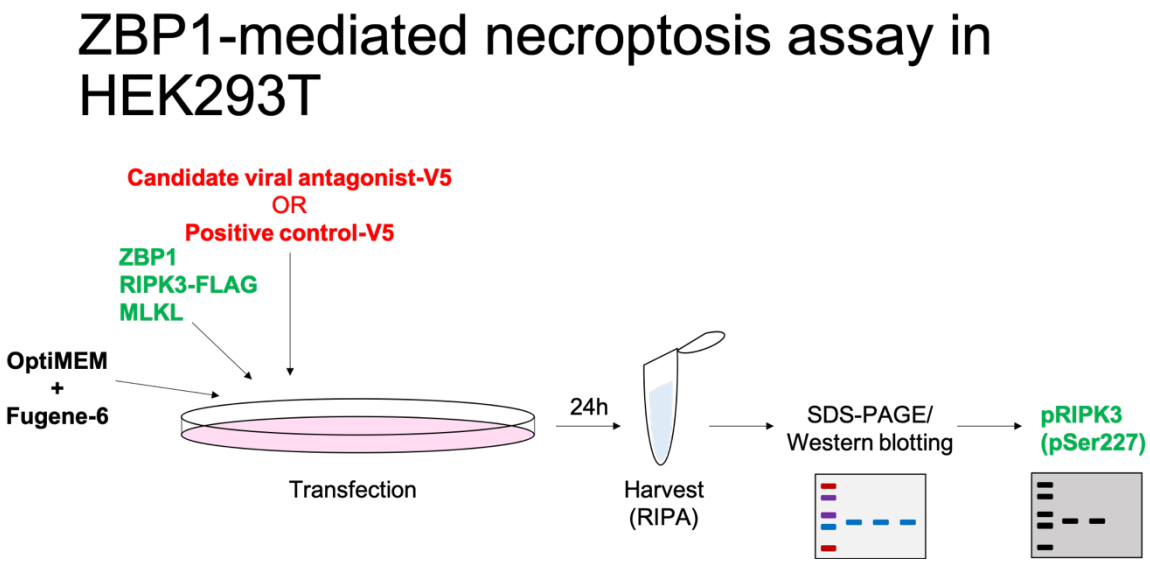


Figure 30. Schematic of ZBP1-mediated necroptosis assay in HEK293T.

HEK293T cells seeded at 1,000,000 cells per well in a 6-well plate are co-transfected with plasmid expression constructs encoding ZBP1 (1µg), RIPK3-FLAG (0.3µg) and MLKL (0.3µg), with or without a plasmid encoding a V5-tagged candidate viral antagonist or positive control (0-5µg). 24h post transfection cells are harvested and lysates analysed by SDS-PAGE and western blotting with an anti-pRIPK3 antibody (pSer-227) to measure RIPK3 phosphorylation.

To interrogate the precise mechanism of ZBP1-mediated cell death activated in HEK293T reconstituted with ZBP1^{WT}, RIPK3 and MLKL, lysates from transfected

cells were analysed by SDS-PAGE and western blotting (**Figure 31**). Interestingly, there was a ZBP1-mediated, ZBD-dependent reduction in total RIPK3 detection and a corresponding retardation of RIPK3 migration through the gel (Figure 31A), consistent with post-translational modification of the protein. To activate necroptosis, ZBP1 forms a RHIM-RHIM interaction with RIPK3, providing a scaffold for RIPK3 auto-phosphorylation and activation (Cho et al. 2009). Specifically, RIPK3 phosphorylation on serine-227 (pSer-227) is essential for necroptosis induction (W. Chen et al. 2013). Active RIPK3 phosphorylates MLKL (Sun et al. 2012; Zhao et al. 2012), triggering MLKL oligomerisation and consequent pore formation in the cell membrane (Dondelinger et al. 2014), which leads to necroptotic cell death. To investigate whether RIPK3 was being phosphorylated in a ZBP1-mediated ZBD-dependent way, phosphorylation of RIPK3 on serine-227 (pSer-227) was measured before and after treatment of the lysates with lambda-phosphatase (λPP) (Figure 31B-C). Indeed, a λPP-sensitive band corresponding to phosphorylated RIPK3 (pRIPK3) was present only in lysates from cells that received $ZBP1^{WT}$, and not in lysates from cells that received $ZBP1^{Z\alpha1\alpha2mut}$, in combination with RIPK3 and MLKL (Figure 31B-C). A ZBP1-mediated ZBD-dependent reduction in total MLKL was also observed (Figure 31A), which could potentially be explained by a reduction of antibody binding due to a post-translational modification of MLKL, such as phosphorylation. However, neither phosphorylation of MLKL nor MLKL oligomerisation could be detected by western blot, potentially due to limitations of the antibodies available (data not shown).

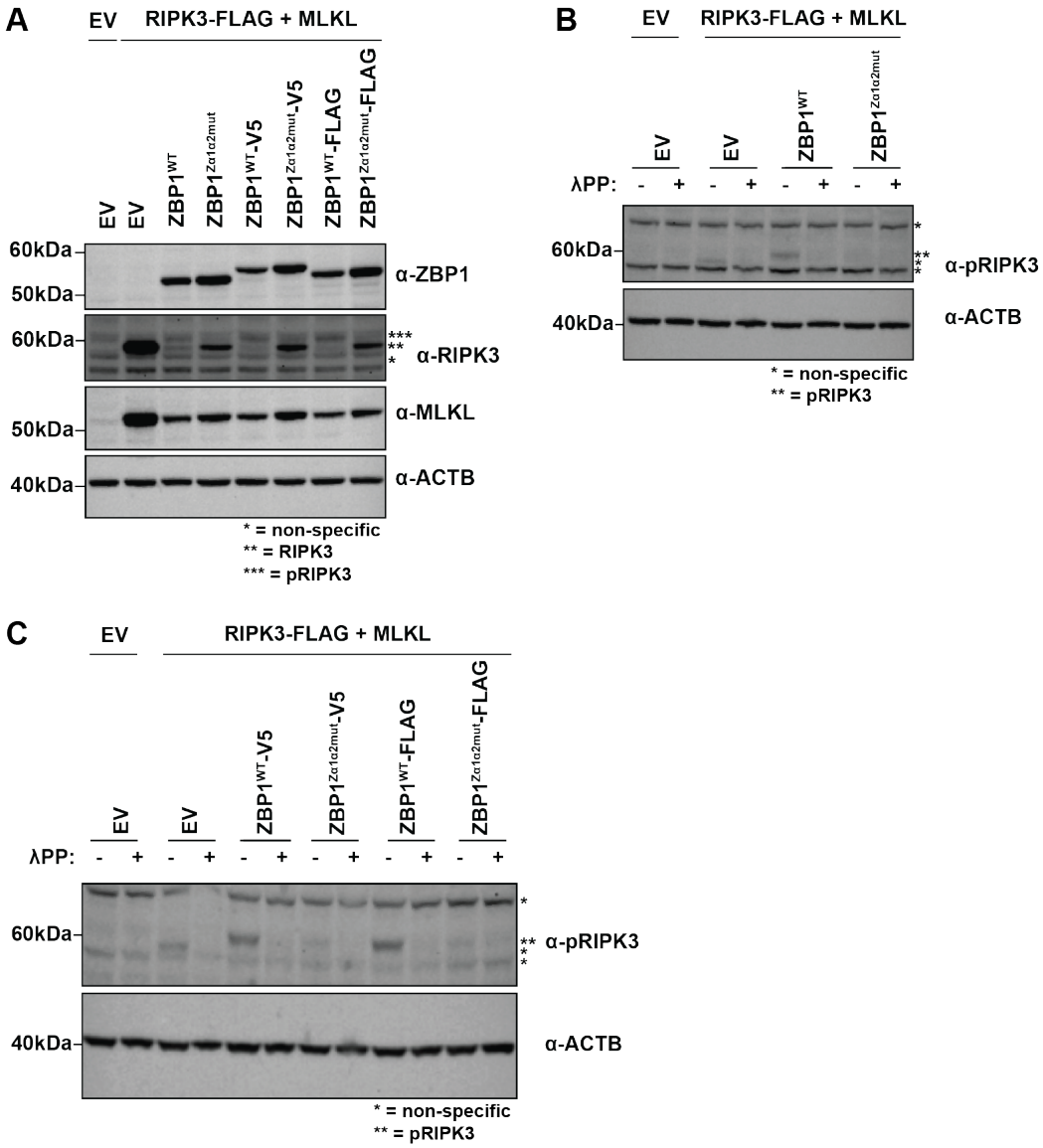


Figure 31. ZBP1 mediates RIPK3 phosphorylation in a ZBD-dependent manner.

(A-C) HEK293T cells were co-transfected with plasmids encoding empty vector (EV) or RIPK3 and MLKL, with or without untagged, V5-tagged or FLAG-tagged ZBP1 wildtype ($ZBP1^{WT}$) or ZBD mutant ($ZBP1^{Z\alpha1\alpha2mut}$). 24h post-transfection, cells were harvested and lysates that were treated or not with lambda-phosphatase (λPP) as indicated were analysed by SDS-PAGE and western blotting with anti-pRIPK3 antibody (pSer-227) and the other antibodies indicated. Data are from 1 representative experiment of 3 independent experiments (see Figure S5 and Figure S6 for data from other experiments).

To determine whether RIPK3 auto-phosphorylation was the mechanism of ZBP1-mediated, ZBD-dependent RIPK3 phosphorylation being activated in transfected HEK293T cells, cells were transfected in the presence of a dose titration of the pharmacological RIPK3 kinase inhibitor GSK'872 (Kaiser et al. 2013) and protein expression analysed as in the previous experiment (Figure 32). GSK'872 inhibited ZBP1-mediated, ZBD-dependent RIPK3 phosphorylation in a dose-dependent manner, demonstrating that RIPK3 kinase activity is required for RIPK3 phosphorylation in this context (Figure 32). Moreover, the fact that a known small molecule inhibitor of necroptosis (GSK'872) showed an effect in this assay suggests that it could be utilised to screen other candidate small molecule inhibitors of this pathway in future.

Altogether, these data demonstrate reconstitution of the human ZBP1 necrosome in HEK293T cells by transient transfection. Importantly, human ZBP1 necrosome activation, measured by RIPK3 auto-phosphorylation, is dependent on intact ZBP1 ZBDs. This may suggest that ZBP1-mediated necroptosis activation in this context is ligand-binding dependent and not the result of ectopic ZBP1 expression alone.

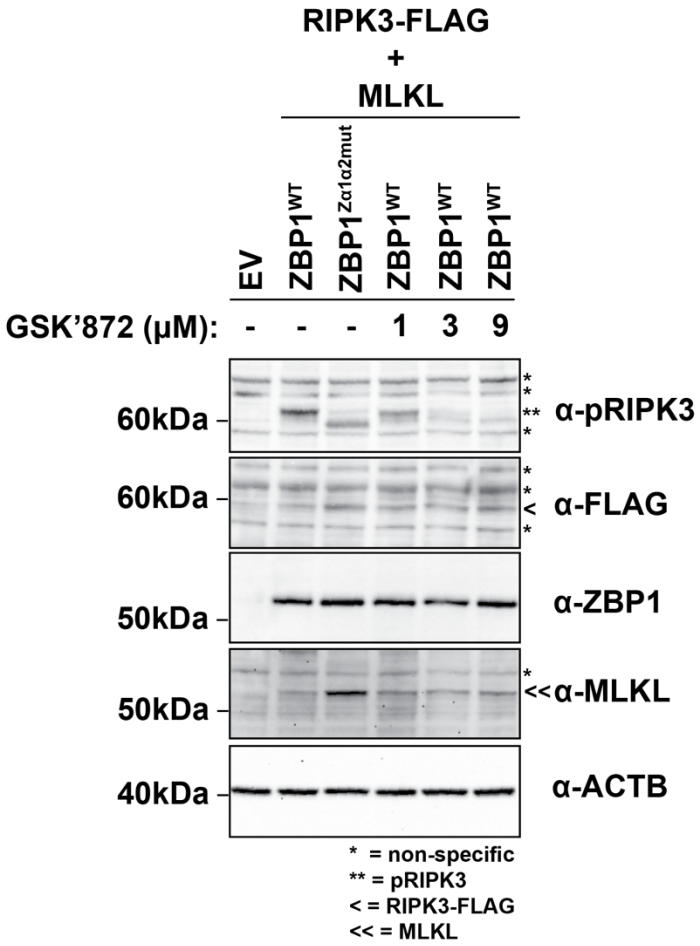


Figure 32. ZBP1-mediated ZBD-dependent RIPK3 phosphorylation requires RIPK3 kinase activity.

HEK293T cells were co-transfected with plasmids encoding empty vector (EV) or RIPK3, MLKL and ZBP1 wildtype ($ZBP1^{WT}$) or ZBD mutant ($ZBP1^{Zα1α2mut}$), with or without a dose titration of the pharmacological RIPK3 inhibitor GSK'872. 24h post-transfection, cells were harvested and lysates analysed by SDS-PAGE and western blotting with anti-pRIPK3 antibody (pSer-227) and the other antibodies indicated. Data are from 1 representative experiment of 3 independent experiments (see Figure S7 for repeat experiments).

4.3 A NOVEL TOOL TO DETECT INHIBITORS OF THE HUMAN ZBP1 NECROSOME

Transient co-transfection of ZBP1, RIPK3 and MLKL is sufficient to reconstitute a ligand-binding dependent human ZBP1 necrosome in HEK293T cells, characterised by RIPK3 auto-phosphorylation on serine-227 (pSer-227). The activation of this ZBP1 necrosome can be antagonised by a described small molecule pharmacological inhibitor of RIPK3 (GSK'872). To explore whether this ZBP1-mediated necroptosis assay could additionally be employed as a tool to detect protein-mediated inhibition of the human ZBP1 necrosome, the next aim was to co-transfect a described viral protein inhibitor of ZBP1-mediated RIPK3 activation together with ZBP1, RIPK3 and MLKL and to measure ZBP1-mediated, ZBD-dependent RIPK3 auto-phosphorylation as previously. MCMV M45 can inhibit necroptosis in human cells (Guo et al. 2015). The RHIM domain of M45 interferes with the RHIM-RHIM interaction between ZBP1 and RIPK3. Full-length M45 was cloned and sequence-verified but could not be detected at protein level after transient transfection of a plasmid expression construct in HEK293T cells (data not shown). However, truncated forms of M45, comprised of either the 90 or 277 N-terminal amino acids (M45-90aa or M45-277aa), retain the ability to inhibit necroptosis in human cells (Pham et al. 2018). Like MCMV M45, HSV1 ICP6 also inhibits ZBP1-mediated necroptosis in human cells via a RHIM-dependent mechanism (Guo et al. 2018). To determine whether M45-90aa, M45-277aa or ICP6 could inhibit ZBP1-mediated necroptosis activation in transfected HEK293T, these

proteins were co-expressed with ZBP1, RIPK3 and MLKL, and RIPK3 phosphorylation was measured by western blotting. Co-expression of M45-90aa, M45-277aa or ICP6 inhibited ZBP1-mediated RIPK3 auto-phosphorylation as expected (Figure 33), despite the fact that M45-90aa was not detected at protein level by western blot (anti-V5) at the dose transfected in this experiment (1µg). Of note, M45-90aa was detectable by western blot (anti-V5) in subsequent experiments where higher doses (3-5µg) were transfected (Chapter 5 Results III). In the same experiment, RHIM-mutants of M45-90aa and M45-277aa ($M45^{mutRHIM}$-90aa and $M45^{mutRHIM}$-277aa) did not inhibit RIPK3 phosphorylation, although neither $M45^{WT}$-90aa nor $M45^{mutRHIM}$-90aa were detectable at protein level and $M45^{mutRHIM}$-277aa was expressed at slightly lower levels than its wildtype counterpart (anti-V5) (Figure 33). M45-90aa and M45-277aa constructs were in the same lentiviral vector (pLenti6.3/TO/V5-DEST), whereas FLAG-ICP6 was in a different expression vector (pcDNA3.1). To control for this, the experiment in Figure 33 was performed using two empty vector controls (EV^1 and EV^2) corresponding to each of these plasmid vectors. The results were not influenced by vector (Figure 33).

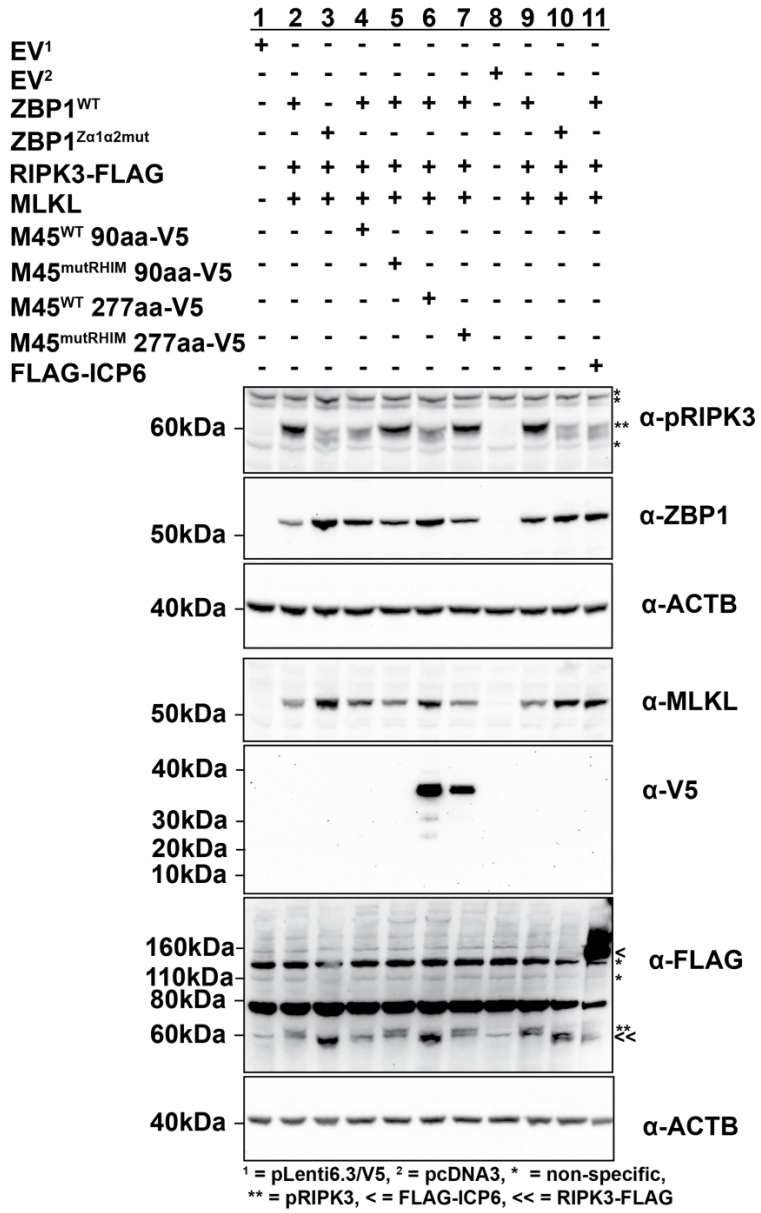


Figure 33. ZBP1-mediated ZBD-dependent RIPK3 auto-phosphorylation is inhibited by MCMV M45 fragments and HSV-1 ICP6.

HEK293T cells were co-transfected with plasmids encoding empty vector (EV) or RIPK3, MLKL and ZBP1, with or without 1µg of plasmid encoding C-terminally V5-tagged wildtype or RHIM-mutant 90 or 277 amino acid RHIM-encompassing M45 fragments ($M45^{WT}$-90aa-V5, $M45^{mutRHIM}$-90aa-V5, $M45^{WT}$-277aa-V5 or $M45^{mutRHIM}$-277aa-V5) or N-terminally FLAG-tagged HSV-1 ICP6 (FLAG-ICP6). 24h post-transfection, cells were harvested and lysates analysed by SDS-PAGE and western blotting with anti-pRIPK3 antibody (pSer-227) and the other antibodies indicated. Data are from 1 representative experiment of 2 independent experiments (see Figure S8 for repeat experiment).

In order to directly ascertain the mechanism of necroptosis inhibition by the M45 fragments, the aforementioned experiment was repeated with a dose titration of wildtype or RHIM-mutant M45-277aa (Figure 34). Whereas wildtype M45-277aa ($M45^{WT}$-277aa) inhibited ZBP1-mediated RIPK3 phosphorylation in a dose-dependent manner, the RHIM-mutant ($M45^{mutRHIM}$-277aa) did not inhibit, even when protein expression levels were equivalent to wildtype (anti-V5) (Figure 34). This demonstrates that $M45^{WT}$-277aa inhibits ZBP1-mediated RIPK3 phosphorylation in a RHIM-dependent way.

Altogether, these results demonstrate that reconstitution of the human ZBP1 necrosome in HEK293T cells provides a novel tool for detection of protein-mediated inhibition of this pathway, including by the described viral protein inhibitors HSV-1 ICP6 and MCMV M45 N-terminal 90 and 277 amino acid fragments. These proteins could therefore serve as positive controls in a screen to identify novel protein inhibitors of ZBP1-mediated RIPK3 auto-phosphorylation.

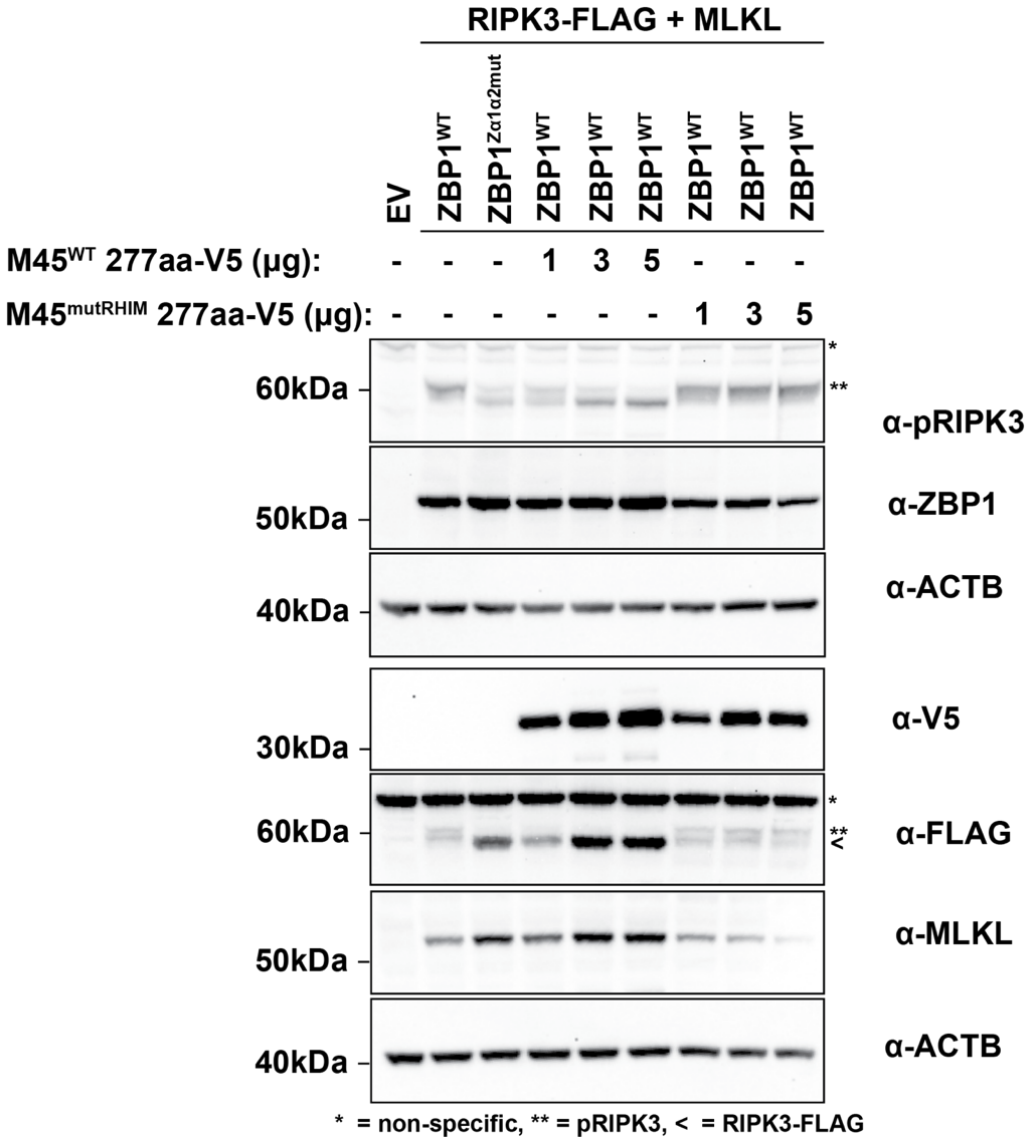


Figure 34. RHIM-dependent inhibition of ZBP1-mediated ZBD-dependent RIPK3 auto-phosphorylation by an M45 fragment.

HEK293T cells were co-transfected with plasmids encoding empty vector (EV) or RIPK3, MLKL and ZBP1, with or without a dose titration of a wildtype or RHIM-mutant 277-amino acid fragment of M45 ($M45^{WT}$-277aa or $M45^{mutRHIM}$-277aa). 24h post-transfection, cells were harvested and lysates analysed by SDS-PAGE and western blotting with anti-pRIPK3 antibody (pSer-227) and the other antibodies indicated. Data are representative of 3 independent experiments (see Figure S9 and Figure S10 for repeat experiments).

4.4 DISCUSSION

The results presented in this chapter demonstrate that human ZBP1 can mediate necroptosis (**Figure 25** & **Figure 27**). This finding was independently corroborated in another study (Sridharan et al. 2017). Ectopic expression of human ZBP1 alone is sufficient to drive necroptosis activation in competent cells (**Figure 25**), and, as was observed with mouse ZBP1 (Maelfait et al. 2017) (see Appendix & Chapter 3 Results I), human ZBP1-mediated necroptosis activation is ZBD-dependent (**Figure 31**). In evidence, mutation of key residues within the human ZBP1 ZBDs, required for Z-nucleic acid binding (Y. Yang et al. 2014), abrogated ZBP1-mediated RIPK3 auto-phosphorylation (**Figure 31** & **Figure 32**) and cell death (**Figure 25**). These data are consistent with the presence of an endogenous ligand for ZBP1 in human cells. However, another possible explanation could be that a ZBP1 ligand is generated as a consequence of the lentiviral transduction (**Figure 25**) and plasmid transfection (**Figure 27** & **Figure 31**) processes. It is not known whether lentiviruses are sensed by ZBP1 for necroptosis activation, but there has been one report of ZBP1-mediated tumour cell death after electrotransfer of plasmid DNA (Znidar et al. 2018). Whereas there is evidence that the ligand for mouse ZBP1 is an RNA species (Thapa et al. 2016; Maelfait et al. 2017; Sridharan et al. 2017) (see Appendix), the human ZBP1 ligand has not been identified. It is important to note that the aforementioned experiments were all performed in human cell lines expressing human ZBP1 ectopically. In future, it will be informative to study ZBP1 in primary

human cells, such as lymph node and splenic cells, where it is endogenously expressed (Rothenburg et al. 2002). Such samples are currently challenging to obtain as spleens, for example, can only be taken from deceased individuals, and lymph nodes are only usually extracted in cases of serious infection, such as tonsillitis, where there is inflammation of the tissue. Technologies such as CRISPR/Cas9 (Jinek et al. 2012; Cong et al. 2013) could be utilised to knock-in ZBD mutations and investigate the role of Z-nucleic acid binding in ZBP1-mediated necroptosis activation in primary human cells.

Despite the presence of a significantly higher number of dead cells after reconstitution of the ZBP1 necrosome in HEK293T cells (**Figure 27**), assessment of cell viability revealed that the difference in the proportion of non-viable cells was not statistically significant (**Figure 29**). This could be explained by the transfection efficiency, which the confocal imaging data would indicate was approximately 40% (**Figure 26**). Even if all successfully transfected cells lost their viability, these cells most likely represented only a fraction of the total number of cells present. To overcome this limitation, RIPK3 phosphorylation was measured directly (**Figure 31**), with the advantage that this event is specific to necroptosis activation and requires successful transfection of only two plasmids (ZBP1 and RIPK3). MLKL was still co-transfected in order to enable subsequent measurement of MLKL phosphorylation and oligomerisation – events that are also specific to necroptosis and occur downstream of RIPK3 activation. However, although ZBP1 did mediate ZBD-dependent RIPK3 auto-phosphorylation

(**Figure 31** & **Figure 32**), neither MLKL phosphorylation nor oligomerisation were detected (data not shown). There was an observed reduction in total MLKL that correlated with RIPK3 phosphorylation (**Figure 31**, **Figure 32**, **Figure 33** & **Figure 34**), indicating that the MLKL may have been rapidly degraded following its activation or post-translationally modified such that the epitope recognised by the antibody was altered. Whether MLKL is degraded after activation is not known but active MLKL does undergo post-translational changes including phosphorylation and oligomerisation (Sun et al. 2012; Zhao et al. 2012; Dondelinger et al. 2014), and incorporation of MLKL into exosomes has been identified as a mechanism by which it is removed from cells (Gong et al. 2017). If improved antibodies (anti human MLKL & anti human pMLKL) are generated in future, these lysates could be re-analysed to measure MLKL activation, which has the advantage of being specific to necroptosis and directly upstream of cell death.

Altogether, the ZBP1-mediated necroptosis assay established in HEK293T has a number of limitations. Firstly, ectopic expression of the proteins of interest (ZBP1, RIPK3 and MLKL) is limited by transfection efficiency, and does not entirely recapitulate the behaviour of endogenously expressed proteins. Secondly, HEK293T cells are an immortalised cell line and so do not recapitulate the behaviour of primary human cells, since immortalisation necessitates significant alteration of the genome and dysregulation of multiple cellular pathways (Shen et al. 2008; Stepanenko & Dmitrenko 2015). Finally, although

this assay can detect antagonists of ZBP1-mediated RIPK3 auto-phosphorylation (**Figure 32** & **Figure 33**), it will not reveal antagonists of MLKL or of the RIPK3-MLKL interaction, which are downstream of RIPK3 auto-phosphorylation. Hence, any viral proteins which function as antagonists downstream of RIPK3 auto-phosphorylation would not be detected by the assay.

In spite of its aforementioned limitations, the ZBP1-mediated necroptosis assay established in HEK293T successfully detected known inhibitors of ZBP1-RIPK3 driven necroptosis activation, including the small molecule inhibitor GSK'872 (Kaiser et al. 2013) (**Figure 32**) as well as described viral protein inhibitors M45-90aa, M45-277aa and ICP6 (Upton et al. 2012; Pham et al. 2018; Guo et al. 2018) (**Figure 33**), all of which antagonised ZBP1-mediated ZBD-dependent RIPK3 auto-phosphorylation as expected. Mechanistically, antagonism by M45-277aa was RHIM-mediated (**Figure 33** & **Figure 34**), in consistence with the published literature (Upton et al. 2008; Upton et al. 2010; Upton et al. 2012). This assay therefore represents a useful tool with which small molecules and proteins could be assayed for their ability to antagonise ZBP1-mediated ZBD-dependent necroptosis activation. The current read-out of western blotting is less high-throughput than direct measurement of cell death, however, measuring RIPK3 phosphorylation is more specific to necroptosis activation. In future, if suitable antibodies are available, this assay could be adapted to include an alternative, more high-throughput read-out, such as flow cytometry or confocal microscopy with intracellular staining for phosphorylated

RIPK3 and MLKL. Alternatively, a recently developed sensor for MLKL activation by RIPK3 based on fluorescence resonance energy transfer (FRET) (hSMART) (Murai et al. 2018), could potentially be adapted to study ZBP1-mediated necroptosis in human cells in future.

CHAPTER 5 RESULTS III
A TARGETED SCREEN FOR VIRAL PROTEIN INHIBITORS OF THE HUMAN ZBP1 NECROSOME

The previous chapter (Chapter 4 Results II) described the establishment of a novel assay, which was able to detect known small molecule and viral protein inhibitors of human ZBP1-mediated RIPK3 auto-phosphorylation in transfected HEK293T cells. This assay is summarised in Figure 30. The present chapter details results obtained from applying this method in the form of a targeted screen, with the aim of identifying as yet unknown viral protein inhibitors of ZBP1-mediated necroptosis activation. The viral proteins tested in the screen were from varicella zoster virus (VZV) and Zika virus (ZIKV), based on hypotheses that these viruses may encode antagonists of ZBP1-mediated necroptosis activation.

VZV, like MCMV and HSV1, is a herpes virus. Given that MCMV and HSV1 are both sensed by ZBP1 (Upton et al. 2012; Guo et al. 2018), it was hypothesised that ZBP1 may also sense other members of the herpes virus family and, in turn, that these viruses may encode antagonists of ZBP1-mediated necroptosis. Two candidates that were considered were human cytomegalovirus (HCMV), which is a betaherpesvirus like MCMV, and VZV, which is an alphaherpesvirus like HSV. HCMV is the human equivalent of MCMV, although it is not known whether HCMV activates ZBP1-mediated necroptosis. One report implicates ZBP1 as a sensor of HCMV but for type I IFN induction rather than for necroptosis activation (DeFilippis,

Alvarado, Sali, Rothenburg & Früh 2010a). HCMV UL45 does not share the same function as MCMV M45 in antagonism of ZBP1-RIPK3 mediated necroptosis (Omoto et al. 2015). HCMV does, however, suppress TNF or MCMV driven necroptosis activation in human cells using a function encoded by IE1, which inhibits necroptosis at a stage downstream of MLKL phosphorylation (Omoto et al. 2015). HCMV therefore inhibits necroptosis via a distinct mechanism from MCMV and HSV. Whether VZV is sensed by ZBP1 is not known. Given that other herpes viruses are sensed by ZBP1 (DeFilippis, Alvarado, Sali, Rothenburg & Früh 2010b; Upton et al. 2012; Guo et al. 2018), we hypothesised that VZV may also be recognised via this sensing pathway and that the virus may therefore encode an antagonist. One aim of this study was therefore to test candidate VZV proteins for their ability to inhibit human ZBP1 necrosome activation. Two candidates were selected from a VZV ORF library (Hertzog et. al. unpublished), based on their similarity to known viral inhibitors of ZBP1-mediated necroptosis.

In addition to DNA viruses, including several herpesviruses (DeFilippis, Alvarado, Sali, Rothenburg & Früh 2010a; Upton et al. 2012; Guo et al. 2018) and VV (Koehler et al. 2017), ZBP1 has also been reported to sense RNA viruses, including IAV (Thapa et al. 2016; Kuriakose et al. 2016) and, recently, ZIKV (Daniels et al. 2019). Mouse ZBP1 was implicated as a sensor of ZIKV, not for RIPK3-mediated necroptosis induction, but for RIPK3-driven activation of an antiviral cellular metabolic state (Daniels et al. 2019). Whether human ZBP1 senses ZIKV or whether ZIKV induces necroptosis are not known. However, West Nile virus

(WNV), another flavivirus, has previously been reported to activate necrosis (Chu & Ng 2003), as well as RIPK3-driven neuroinflammation (Daniels et al. 2017). We hypothesised that ZIKV may be sensed by ZBP1 in humans and that the virus may therefore encode an inhibitor of ZBP1-mediated RIPK3 activation. The second aim of this study was thus to screen a library of expression constructs for individual ZIKV proteins (Hertzog et al. 2018) for their ability to inhibit human ZBP1 necrosome activation.

5.1 TESTING CANDIDATE VZV PROTEINS FOR INHIBITION OF ZBP1-MEDIATED RIPK3 AUTO-PHOSPHORYLATION

Like MCMV M45 (Lembo et al. 2004) and HSV1/2 ICP6/10 (Cameron et al. 1988), VZV open-reading frame 19 (ORF19) (Spector et al. 1987; Heineman & Cohen 1994) contains a ribonucleoside-diphosphate reductase large subunit-like domain. Since M45 (Upton et al. 2012) and ICP6/10 (Guo et al. 2018) are also antagonists of ZBP1-RIPK3 mediated necroptosis, we hypothesised that VZV ORF19 may have the same dual functionality. A second hypothesis was that VZV ORF20 may antagonise ZBP1-RIPK3 mediated necroptosis, because it contains a putative RHIM (Figure 35).

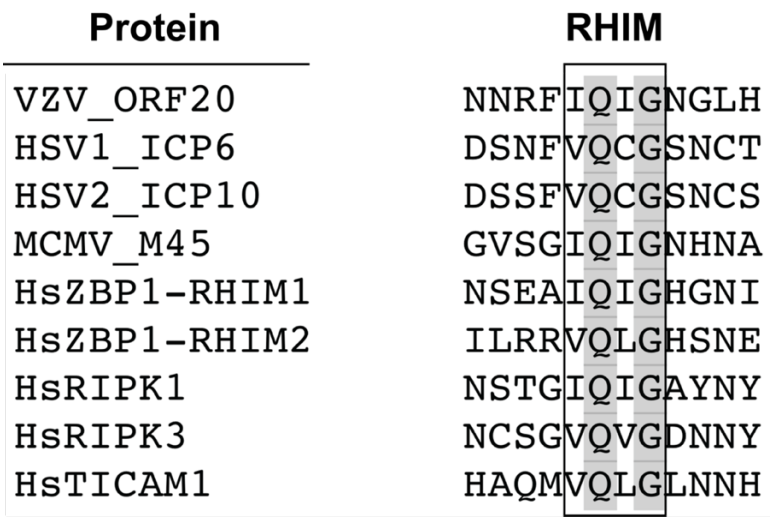


Figure 35. VZV ORF20 contains a putative RHIM.

RHIM-encompassing amino acid sequence fragments from the following viral and *Homo sapien* (Hs) proteins were aligned using Clustal Omega and the conserved glutamine and glycine residues are highlighted: VZV ORF20, HSV1 ICP6, HSV2 ICP10, MCMV M45, human ZBP1 (RHIM1 and RHIM2), human RIPK1, human RIPK3 and human TICAM1.

To test both of these ideas, HEK293T cells were co-transfected with ZBP1, RIPK3 and MLKL, as previously, with or without V5-tagged VZV ORF19, VZV ORF20 or, as a positive control, M45-90aa. 24h post transfection, cells were harvested and analysed by SDS-PAGE and western blotting (Figure 36). ZBP1-mediated ZBD-dependent RIPK3 auto-phosphorylation was still detected after co-expression of either VZV ORF19 or VZV ORF20 with ZBP1, RIPK3 and MLKL, whereas co-expression of M45-90aa with the same proteins prevented RIPK3 phosphorylation at both doses of plasmid tested (Figure 36). Importantly, this functional difference cannot be explained by differences in protein expression as M45-90aa, VZV ORF19 and VZV ORF20 were all expressed at equivalent levels (anti-V5) (Figure 36). Thus, these data do not support the hypothesis that either

VZV ORF19 or VZV ORF20 are antagonists of human ZBP1-mediated necroptosis activation.

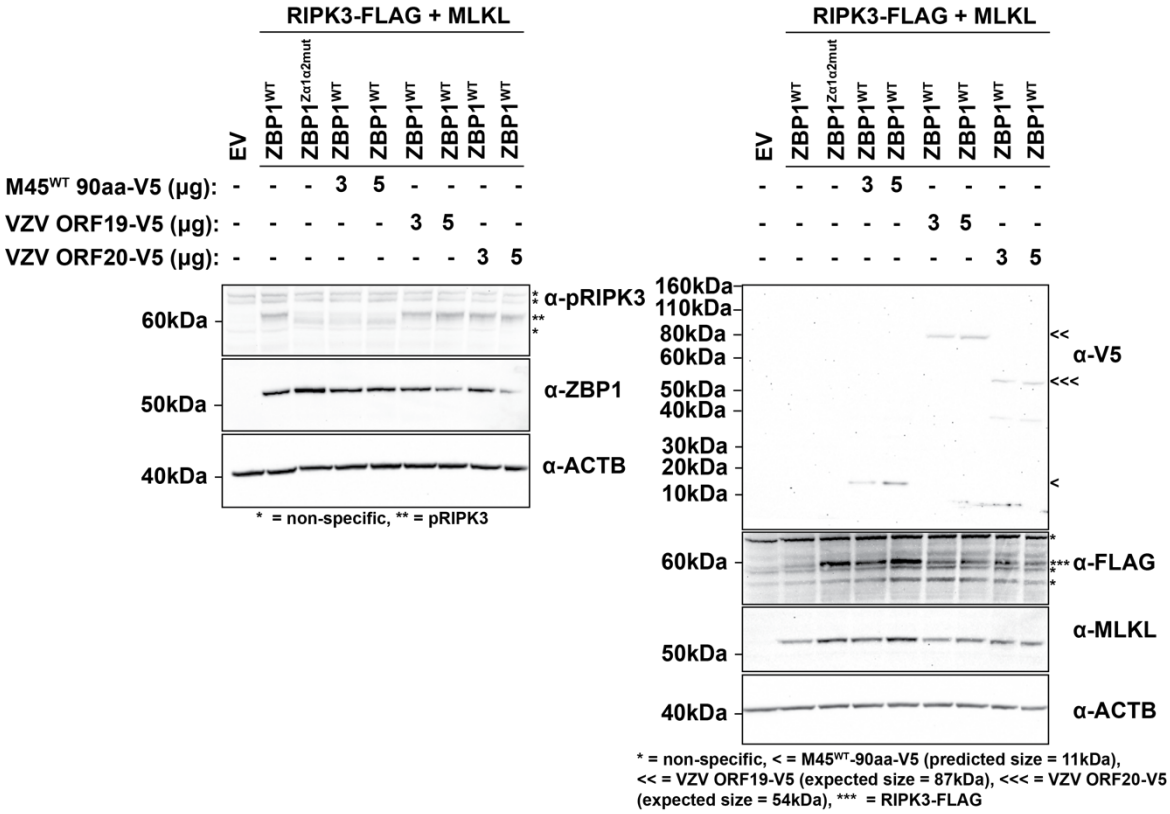
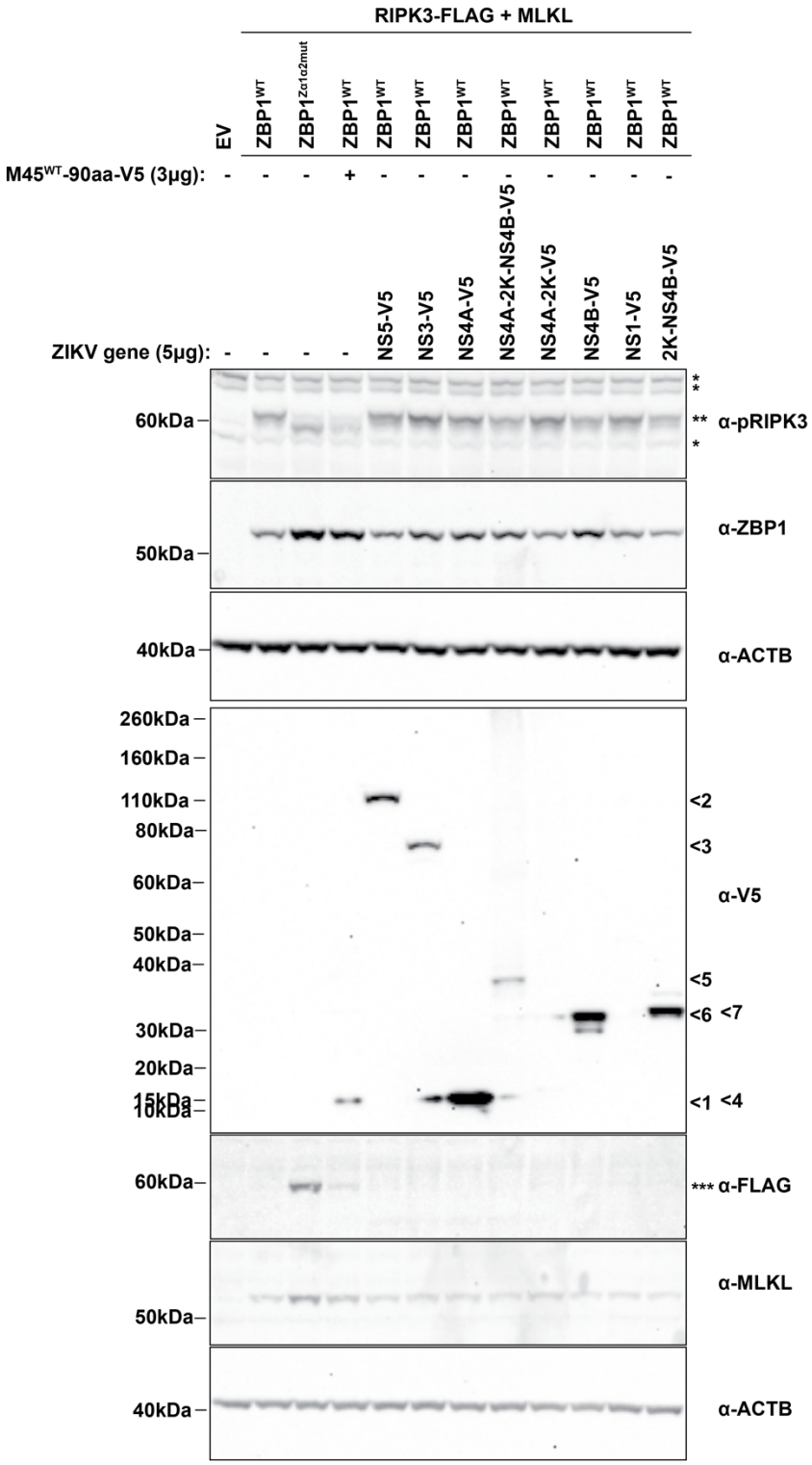


Figure 36. VZV ORFs 19 and 20 do not inhibit ZBP1-mediated ZBD-dependent RIPK3 auto-phosphorylation.

HEK293T cells were co-transfected with plasmids encoding empty vector (EV) or RIPK3, MLKL and ZBP1, with or without a dose titration of plasmid encoding V5-tagged 90-amino acid fragment of M45 ($M45^{WT}$-90aa), VZV ORF19 or VZV ORF20. 24h post-transfection, cells were harvested and lysates analysed by SDS-PAGE and western blotting with anti-pRIPK3 antibody (pSer-227) and the other antibodies indicated. Data are representative of 3 independent experiments (see Figure S11 and Figure S12 for repeat experiments).

5.2 SCREENING OF ZIKV PROTEINS FOR INHIBITION OF ZBP1-MEDIATED RIPK3 AUTO-PHOSPHORYLATION

To investigate whether any ZIKV proteins are antagonists of ZBP1-mediated necroptosis, HEK293T cells were co-transfected with ZBP1, RIPK3 and MLKL, as previously, with or without a plasmid encoding a V5-tagged ZIKV protein or, as a positive control, M45-90aa. 24h post transfection, cells were harvested and analysed by SDS-PAGE and western blotting (**Figure 37**). Of the 13 ZIKV protein coding sequences in the initial library (Hertzog et al. 2018), only 6 produced proteins that were detectable by western blot (anti-V5) after plasmid transfection of HEK293T: NS5, NS3, NS4A, NS4A-2K-NS4B, NS4B and 2K-NS4B (**Figure 37**). NS4A-2K, NS1, capsid, prM, NS2A, NS2B and envelope were not detected (**Figure 37** & data not shown). Despite the fact that these 6 ZIKV proteins were expressed at levels equivalent to or higher than M45-90aa, none of these proteins inhibited ZBP1-mediated ZBD-dependent RIPK3 auto-phosphorylation, whereas M45-90aa did (**Figure 37**).



* = non-specific, ** = pRIPK3, <1 = M45WT-90aa (11kDa), <2 = NS5 (103kDa), <3 = NS3 (70kDa), <4 = NS4A (16kDa), <5 = NS4A-2K-NS4B (~40kDa), <6 = NS4B, <7 = 2K-NS4B (~30kDa), *** = RIPK3-FLAG

Figure 37. ZIKV proteins NS5, NS3, NS4A, NS4A-2K-NS4B, NS4B and 2K-NS4B do not inhibit ZBP1-mediated ZBD-dependent RIPK3 auto-phosphorylation.

HEK293T cells were co-transfected with plasmids encoding empty vector (EV) or RIPK3, MLKL and ZBP1, with or without a dose titration of plasmid encoding V5-tagged 90-amino acid fragment of M45 ($M45^{WT}$-90aa) or the ZIKV proteins indicated. 24h post-transfection, cells were harvested and lysates analysed by SDS-PAGE and western blotting with anti-pRIPK3 antibody (pSer-227) and the other antibodies indicated. Data are representative of 2 independent experiments (see Figure S13 for repeat experiment).

In a preliminary experiment aimed at further investigating whether ZIKV inhibits ZBP1-mediated necroptosis, HEK293T cells were co-transfected with plasmids encoding ZBP1, RIPK3 and MLKL, and then infected with ZIKV at an MOI of 0.5 or 2.5 after 6h. Cells were harvested at 24 and 48h time points post-infection for analysis by SDS-PAGE and western blotting. ZIKV NS5 expression was detected 24h post infection in lysates from cells that were infected at the higher MOI of 2.5; however, no inhibition of ZBP1-mediated ZBD-dependent RIPK3 auto-phosphorylation was detected. Therefore, no evidence was found in favour of the hypothesis that ZIKV encodes an antagonist of the human ZBP1 necrosome (**Figure 37** & **Figure 38**).

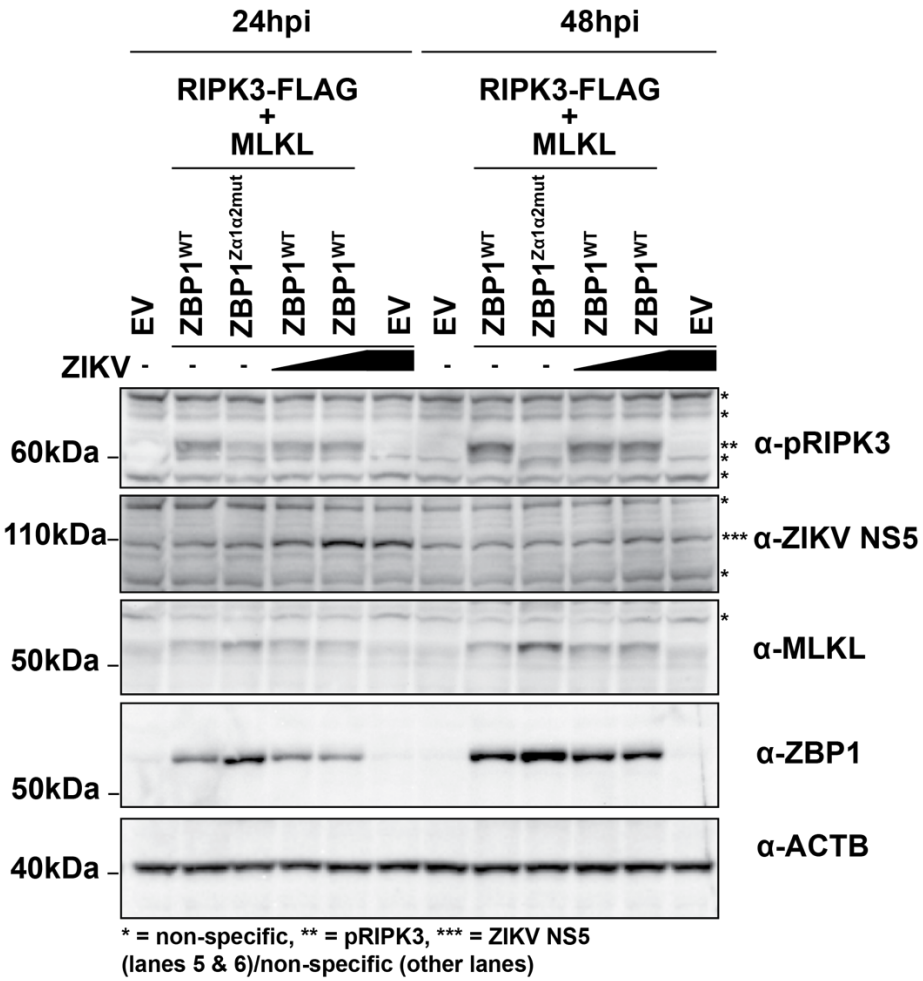


Figure 38. Infection with ZIKV does not inhibit ZBP1-mediated ZBD-dependent RIPK3 auto-phosphorylation.

HEK293T cells were co-transfected with plasmids encoding empty vector (EV) or RIPK3, MLKL and ZBP1, and then, 6h post transfection, infected or not with ZIKV at MOI 0.5 or 2.5. 24h and 48h post-transfection, cells were harvested and lysates analysed by SDS-PAGE and western blotting with anti-pRIPK3 antibody (pSer-227) and the other antibodies indicated. Data are from 1 experiment. ZIKV infection was performed in BSL-3 by Mirjam Schilling.

5.3 DISCUSSION

The general aim of the study described in the present chapter was to apply the novel screening approach developed in Chapter 4 to identify viral protein antagonists of human ZBP1-necrosome activation. Specific aims were to test the hypotheses that selected proteins from VZV and ZIKV are capable of antagonising ZBP1-mediated RIPK3 auto-phosphorylation. However, none of the VZV or ZIKV proteins tested were found to inhibit ZBP1-mediated RIPK3 auto-phosphorylation as measured in the assay by western blotting; nonetheless, positive controls behaved as expected in multiple repeat experiments (**Figure 36** & **Figure 37**), substantiating the evidence that this assay can detect known inhibitors of this pathway. Moreover, these results demonstrate how this screen could be implemented to identify novel protein inhibitors of this pathway in future.

We hypothesised that VZV may encode an antagonist of ZBP1-mediated RIPK3 auto-phosphorylation, because ZBP1 senses other herpes viruses, which encode antagonists of the ZBP1-RIPK3 interaction (Upton et al. 2012; Guo et al. 2018), and because two VZV proteins (VZV ORF19 and VZV ORF20) were found to share common features with these known herpes virus-encoded antagonists. These features include the presence of a ribonucleoside-diphosphate reductase large subunit domain in VZV ORF19 (Heineman & Cohen 1994), and a putative RHIM in VZV ORF20 (**Figure 35**). Whereas the positive control M45-90aa inhibited ZBP1-mediated RIPK3 auto-phosphorylation robustly at the doses tested, both VZV ORFs 19 and 20 failed to inhibit, even when expressed at equivalent levels to the

positive control (**Figure 36**). It is important to note, however, that ectopic expression of these VZV ORFs does not fully recapitulate infection with the whole virus, where the kinetics of protein expression and amounts of protein produced during infection may influence how these viral proteins interact with host proteins. In future, infection of susceptible, necroptosis competent cells with VZV may help to more definitively determine whether the virus encodes an inhibitor of necroptosis. If this is the case, the ZBP1-mediated necroptosis assay could be utilised to screen a VZV ORF library (Hertzog et. al. unpublished) to potentially identify the antagonist in question.

A library of expression constructs for individual ZIKV proteins (Hertzog et al. 2018) was additionally screened for inhibition of ZBP1-mediated RIPK3 auto-phosphorylation; however, only 6 of 13 expression constructs in the library produced proteins that were detectable by western blot (anti-V5). Why the remaining 7 proteins were not expressed is not clear and perhaps highlights a limitation of using a transient transfection-based assay with multiple plasmids being transfected simultaneously. An alternative approach that could be taken in future would be lentiviral transduction of cells with various ZIKV expression constructs followed by co-transfection with ZBP1, RIPK3 and MLKL. Importantly, conclusions could still be drawn for the 6 ZIKV proteins that were expressed, which included NS5, NS3, NS4A, NS4A-2K-NS4B, NS4B and 2K-NS4B. The ZIKV genome consists of a single open-reading frame, which encodes a polyprotein from which all the structural and non-structural (NS) proteins are cleaved by a combination of viral and host proteases (Di Serio et al. 2012). NS5 contains a methyltransferase domain and an

RNA-dependent RNA polymerase domain, and has been implicated in innate immune antagonism by ZIKV (Issur et al. 2009; Grant et al. 2016; Hertzog et al. 2018). NS3 is a serine protease, which has been implicated in translational repression (Hou et al. 2017). NS4A and NS4B, which may be expressed individually or as various fusion proteins with the linker peptide 2K, have been reported to inhibit neurogenesis and induce autophagy (Liang et al. 2016). Of these 6 ZIKV proteins, none inhibited ZBP1-mediated RIPK3 auto-phosphorylation, despite all being expressed at levels equivalent to or higher than the positive control, M45-90aa (**Figure 37**). Infection of transfected cells with ZIKV in a preliminary experiment did not inhibit ZBP1-mediated RIPK3 auto-phosphorylation either (**Figure 38**). However, infection of HEK293T cells in this experiment, measured as NS5 expression by western blot, was relatively low and was detected only at the highest MOI of 2.5 at 24h post infection (**Figure 38**). In future, a recently developed fluorescent cell based ZIKV infection system (McFadden et al. 2018) might be employed to sort ZIKV infected cells and ask whether these cells are more resistant to pharmacologically induced necroptosis compared to uninfected cells.

It is important to note that the failure of the VZV and ZIKV proteins tested to inhibit ZBP1-mediated RIPK3 auto-phosphorylation does not exclude the possibility that any of these proteins is capable of antagonising necroptosis activation at a level downstream of RIPK3 auto-phosphorylation, such as MLKL phosphorylation, oligomerisation or membrane permeabilisation. For instance, HCMV encodes an inhibitor that acts downstream of MLKL phosphorylation (Omoto et al. 2015).

Moreover, it has been reported that even MLKL-mediated membrane permeabilisation is not a point of no return when it comes to necroptosis induction (Gong et al. 2017). MLKL can instead be released from the cell in exosomes in an endosomal sorting complexes required for transport (ESCRT)-III dependent manner, rescuing the cell in question from necroptotic cell death (Gong et al. 2017). Whether viruses can hijack this process as a mechanism of evading ZBP1-mediated necroptosis is not known.

CHAPTER 6 CONCLUSIONS

The results presented in this thesis demonstrate that the ZBDs of ZBP1 are required for necroptosis activation, a finding supported by data from multiple other studies (Thapa et al. 2016; Kuriakose et al. 2016; Sridharan et al. 2017; Maelfait et al. 2017). We (Maelfait et al. 2017) and others (Sridharan et al. 2017) found that mouse ZBP1 uses its ZBDs to sense MCMV infection, and then engages RIPK3 via RHIM-RHIM interactions to activate necroptotic antiviral cell death. We further demonstrated that ZBP1 mediates necroptosis in human cells, another discovery that was independently corroborated (Sridharan et al. 2017). We found that both mouse and human ZBP1 activated necroptosis in the absence of infection, suggesting the presence of endogenous ZBP1 ligands in mouse and human cells. This phenomenon was harnessed to develop a human ZBP1-mediated necroptosis assay in HEK293T cells, which measures ZBP1-mediated RIPK3 auto-phosphorylation induced after ectopic expression of these proteins by transient transfection. This human ZBP1-mediated necroptosis assay responded to known small molecule and viral protein inhibitors of ZBP1-mediated RIPK3 auto-phosphorylation repeatedly and robustly; however, implementation of the assay in a targeted screen to identify viral protein antagonists of this pathway yielded negative results.

The crucial role of the ZBDs in ZBP1-mediated necroptosis induction suggests that Z-conformation nucleic acids may represent an important pathogen

and danger associated molecular pattern for innate immune activation. In mice, the ZBP1 ligand appears to be an RNA species (Maelfait et al. 2017); however, the human ZBP1 ligand has not yet been identified. In future, the ZBP1 ligand may be further characterised, for example through ZBP1 immunoprecipitation and sequencing experiments, to better define the ZBP1 ligand, as well confocal microscopy and, potentially, RNA FISH experiments to investigate the origin of this ligand in both infected and uninfected cells. Agonists for pattern recognition receptors can provide useful adjuvants for vaccination (Vasou et al. 2017). Antiviral necroptosis serves not only to eliminate virus infected cells from the body but also to trigger inflammation, which activates both innate and adaptive immune responses (Pasparakis & Vandenabeele 2015). Thus, based on the hypothesis that the ZBP1 agonist is a Z-conformation nucleic acid, it may be interesting to investigate the potential of Z-nucleic acids as novel vaccine adjuvants in the future. Given the instability of Z-nucleic acids, this would most likely require the use of chemically stabilized Z-DNA or Z-RNA.

There have been relatively few studies examining whether human ZBP1 mediates necroptosis and if ZBP1 sensing is relevant during virus infection of human cells (Sridharan et al. 2017; Koehler et al. 2017; Guo et al. 2018; Daniels et al. 2019). We demonstrated, through ectopic expression of ZBP1, RIPK3 and MLKL, that ZBP1 mediates necroptosis in human cells and, mechanistically, that human ZBP1 mediates ZBD-dependent RIPK3 auto-phosphorylation. Despite being unable to study endogenous ZBP1 in human cells, we were able to show that human

ZBP1 shares a similar activation mechanism with the mouse protein, suggesting it may be possible to extend findings from mouse studies to humans. A key difference between mouse and human ZBP1 is that the mouse protein is type I IFN inducible whereas its human counterpart is not (Shaw et al. 2017). Precisely how ZBP1 expression is induced in human cells remains to be elucidated and will be important for future studies of human ZBP1 in primary cells. Our findings additionally suggest that ectopic ZBP1 expression in necroptosis competent cells is more toxic in human than in mouse cells. Whether this is also the case in primary human cells remains to be investigated and may provide further insight into the function of ZBP1 in humans.

Transient co-transfection of human ZBP1, RIPK3 and MLKL in HEK293T cells was sufficient to reconstitute a ZBD-dependent ZBP1 necrosome characterised by auto-phosphorylation of RIPK3 on serine 227 (pSer-227). Human ZBP1-mediated RIPK3 auto-phosphorylation was sensitive to pharmacological RIPK3 kinase inhibition by a described small molecule inhibitor, and to protein-mediated inhibition of the RHIM-RHIM interaction by described viral antagonists of this pathway. This assay therefore provides a novel tool for the identification of small molecule or protein inhibitors of human ZBP1 necrosome activation. Results from applying this assay in a targeted screen of candidate VZV and ZIKV proteins were negative; however, positive controls consistently functioned as expected, validating the assay as a potentially useful tool for identifying novel antagonists of ZBP1 signalling in future. We were also able to identify key limitations of this assay,

including its reliance on ectopic expression of proteins and its inability to detect inhibitors that act downstream of RIPK3 auto-phosphorylation in the necroptosis signalling cascade. As such, whether any of the VZV or ZIKV proteins tested inhibit the RIPK3-MLKL interaction or downstream events cannot be deduced from our data. A future, improved iteration of the human ZBP1-mediated necroptosis assay, which enables higher throughput screening will be an important tool in a landscape where necroptosis is being increasingly implicated in human diseases (Galluzzi et al. 2017; Yuan et al. 2019; Degterev et al. 2019).

In conclusion, this study provides important insight into the mechanism of ZBP1 activation upstream of necroptosis induction, which occurs in both the presence and absence of virus infection, revealing a potential role for Z-conformation nucleic acids in innate immune activation. This study also demonstrates the conservation of ZBP1 function and activation mechanism from human to mouse, and reports the development and validation of a novel tool to identify inhibitors of human ZBP1 necrosome activation. Remaining questions pertain to the precise identity of the ZBP1 ligand and its origin in different settings, the regulation and role of ZBP1 in humans, whether there are more viruses that are sensed by ZBP1 and the mechanisms employed by viruses to antagonise ZBP1 in host cells. Altogether, the results presented in this thesis contribute to a fast growing literature wherein ZBP1 emerges as an essential and specific pattern recognition receptor for sensing of virus infection in mammalian cells.

REFERENCES

Abe, T. et al., 2013. STING recognition of cytoplasmic DNA instigates cellular defense. *Molecular Cell*, 50(1), pp.5–15.

Ablasser, A. et al., 2014. TREX1 deficiency triggers cell-autonomous immunity in a cGAS-dependent manner. *The Journal of Immunology*, 192(12), pp.5993–5997.

Alexopoulou, L. et al., 2001. Recognition of double-stranded RNA and activation of NF-κB by Toll-like receptor 3. *Nature*, 413, pp.732 EP –.

Balasubramaniyam, T. et al., 2018. 2'-O-Methyl-8-methylguanosine as a Z-Form RNA Stabilizer for Structural and Functional Study of Z-RNA. *Molecules (Basel, Switzerland)*, 23(10).

Barber, G.N., 2015. STING: infection, inflammation and cancer. *Nat Rev Immunol*, 15(12), pp.760–770.

Baum, A., Sachidanandam, R. & Garcia-Sastre, A., 2010. Preference of RIG-I for short viral RNA molecules in infected cells revealed by next-generation sequencing. *Proceedings of the National Academy of Sciences*, 107(37), pp.16303–16308.

Beattie, E. et al., 1995. Reversal of the interferon-sensitive phenotype of a vaccinia virus lacking E3L by expression of the reovirus S4 gene. *Journal of Virology*, 69(1), pp.499–505.

Behe, M. & Felsenfeld, G., 1981. Effects of methylation on a synthetic polynucleotide: the B--Z transition in poly(dG-m5dC).poly(dG-m5dC). *Proc Natl Acad Sci USA*, 78(3), p.1619.

Besch, R. et al., 2009. Proapoptotic signaling induced by RIG-I and MDA-5 results in type I interferon-independent apoptosis in human melanoma cells. *The Journal of clinical investigation*, 119(8), pp.2399–2411.

Brandt, T.A. & Jacobs, B.L., 2001. Both carboxy- and amino-terminal domains of the vaccinia virus interferon resistance gene, E3L, are required for pathogenesis in a mouse model. *Journal of Virology*, 75(2), pp.850–856.

Burckstummer, T. et al., 2009. An orthogonal proteomic-genomic screen identifies AIM2 as a cytoplasmic DNA sensor for the inflammasome., 10(3), pp.266–272.

Caccamo, A. et al., 2017. Necroptosis activation in Alzheimer's disease. *Nature neuroscience*.

Cameron, J.M. et al., 1988. Ribonucleotide reductase encoded by herpes simplex virus is a determinant of the pathogenicity of the virus in mice and a valid antiviral target. *Journal of General Virology*, 69 (Pt 10), pp.2607–2612.

Cao, H. et al., 2012. Innate Immune Response of Human Plasmacytoid Dendritic Cells to Poxvirus Infection Is Subverted by Vaccinia E3 via Its Z-DNA/RNA Binding Domain T. Volker, ed. *PLoS ONE*, 7(5), p.e36823.

Cerboni, S. et al., 2017. Intrinsic antiproliferative activity of the innate sensor STING in T lymphocytes. *Journal of Experimental Medicine*, 214(6), pp.1769–1785.

Chan, F.K.-M. et al., 2003. A role for tumor necrosis factor receptor-2 and receptor-interacting protein in programmed necrosis and antiviral responses. *Journal of Biological Chemistry*, 278(51), pp.51613–51621.

Chang, H.W., Watson, J.C. & Jacobs, B.L., 1992. The E3L gene of vaccinia virus encodes an inhibitor of the interferon-induced, double-stranded RNA-dependent protein kinase. *Proceedings of the National Academy of Sciences*, 89(11), pp.4825–4829.

Chattopadhyay, S. & Sen, G.C., 2017. RIG-I-like receptor-induced IRF3 mediated pathway of apoptosis (RIPA): a new antiviral pathway. *Protein & cell*, 8(3), pp.165–168.

Chattopadhyay, S. et al., 2016. Ubiquitination of the Transcription Factor IRF-3 Activates RIPA, the Apoptotic Pathway that Protects Mice from Viral Pathogenesis. *Immunity*, 44(5), pp.1151–1161.

Chattopadhyay, S. et al., 2010. Viral apoptosis is induced by IRF-3-mediated activation of Bax. *The EMBO journal*, 29(10), pp.1762–1773.

Chen, D. et al., 2018. PUMA amplifies necroptosis signaling by activating cytosolic DNA sensors. *Proceedings of the National Academy of Sciences*.

Chen, Q., Sun, L. & Chen, Z.J., 2016. Regulation and function of the cGAS-STING pathway of cytosolic DNA sensing., 17(10), pp.1142–1149.

Chen, W. et al., 2013. Diverse sequence determinants control human and mouse receptor interacting protein 3 (RIP3) and mixed lineage kinase domain-like (MLKL) interaction in necroptotic signaling. *Journal of Biological Chemistry*, 288(23), pp.16247–16261.

Cho, Y. et al., 2009. Phosphorylation-Driven Assembly of the RIP1-RIP3 Complex Regulates Programmed Necrosis and Virus-Induced Inflammation. *Cell*, 137(6), pp.1112–1123.

Chu, J.J.H. & Ng, M.L., 2003. The mechanism of cell death during West Nile virus infection is dependent on initial infectious dose. *Journal of General Virology*, 84(Pt 12), pp.3305–3314.

Colby, C. & Duesberg, P.H., 1969. Double-stranded RNA in Vaccinia Virus Infected Cells. *Nature*, 222(5197), pp.940–944.

Cong, L. et al., 2013. Multiplex genome engineering using CRISPR/Cas systems. *Science (New York, N.Y.)*, 339(6121), pp.819–823.

Crow, Y.J. et al., 2006. Mutations in the gene encoding the 3“-5” DNA exonuclease TREX1 cause Aicardi-Goutieres syndrome at the AGS1 locus. *Nature genetics*, 38(8), pp.917–920.

Daniels, B.P. et al., 2017. RIPK3 Restricts Viral Pathogenesis via Cell Death-Independent Neuroinflammation. *Cell*, 169(2), pp.301–313.e11.

Daniels, B.P. et al., 2019. The Nucleotide Sensor ZBP1 and Kinase RIPK3 Induce the Enzyme IRG1 to Promote an Antiviral Metabolic State in Neurons. *Immunity*, 50(1), pp.64–76.e4.

Dannappel, M. et al., 2014. RIPK1 maintains epithelial homeostasis by inhibiting apoptosis and necroptosis. *Nature*, 513(7516), pp.90–94.

Davis, P. W. et al., 1990. Adamiak, R. W. & Tinoco, I. Z-RNA: the solution NMR structure of r(CGCGCG). *Biopolymers* 29, 109–122

DeFilippis, V.R., Alvarado, D., Sali, T., Rothenburg, S. & Früh, K., 2010a. Human cytomegalovirus induces the interferon response via the DNA sensor ZBP1. *Journal of Virology*, 84(1), pp.585–598.

DeFilippis, V.R., Alvarado, D., Sali, T., Rothenburg, S. & Früh, K., 2010b. Human Cytomegalovirus Induces the Interferon Response via the DNA Sensor ZBP1. *Journal of Virology*, 84(1), pp.585–598.

Degterev, A. et al., 2005. Chemical inhibitor of nonapoptotic cell death with therapeutic potential for ischemic brain injury. *Nature chemical biology*, 1(2), pp.112–119.

Degterev, A., Ofengeim, D. & Yuan, J., 2019. Targeting RIPK1 for the treatment of human diseases. *Proc Natl Acad Sci USA*, p.201901179.

Di Serio, F. et al., 2012. Virus Taxonomy: Ninth Report of the International Committee on Taxonomy of Viruses. In pp. 1221–1234.

Dias Junior, A.G., Sampaio, N.G. & Rehwinkel, J., 2019. A Balancing Act: MDA5 in Antiviral Immunity and Autoinflammation. *Trends in microbiology*, 27(1), pp.75–85.

Diebold, S.S. et al., 2004. Innate antiviral responses by means of TLR7-mediated recognition of single-stranded RNA. *Science (New York, N.Y.)*, 303(5663), pp.1529–1531.

Dillon, C.P. et al., 2014. RIPK1 blocks early postnatal lethality mediated by caspase-8 and RIPK3. *Cell*, 157(5), pp.1189–1202.

Dondelinger, Y. et al., 2014. MLKL Compromises Plasma Membrane Integrity by Binding to Phosphatidylinositol Phosphates. *Cell Reports*, 7(4), pp.971–981.

Dovey, C.M. et al., 2018. MLKL Requires the Inositol Phosphate Code to Execute Necroptosis. *Molecular Cell*, 70(5), pp.936–948.e7.

Ebermann, L. et al., 2012. Block of death-receptor apoptosis protects mouse cytomegalovirus from macrophages and is a determinant of virulence in immunodeficient hosts. *PLoS Pathogens*, 8(12), p.e1003062.

Elliott, P.R. et al., 2016. SPATA2 Links CYLD to LUBAC, Activates CYLD, and Controls LUBAC Signaling. *Molecular Cell*, 63(6), pp.990–1005.

Elmore, S., 2007. Apoptosis: a review of programmed cell death. *Toxicologic pathology*, 35(4), pp.495–516.

Estornes, Y. et al., 2012. dsRNA induces apoptosis through an atypical death complex associating TLR3 to caspase-8. *Cell Death and Differentiation*, 19(9), pp.1482–1494.

Feigon, J. et al., 1985. Z-DNA forms without an alternating purine-pyrimidine sequence in solution. *Science (New York, N.Y.)*, 230(4721), pp.82–84.

Feng, S. et al., 2007. Cleavage of RIP3 inactivates its caspase-independent apoptosis pathway by removal of kinase domain. *Cellular signalling*, 19(10), pp.2056–2067.

Feoktistova, M. et al., 2011. cIAPs block Ripoptosome formation, a RIP1/caspase-8 containing intracellular cell death complex differentially regulated by cFLIP isoforms. *Molecular Cell*, 43(3), pp.449–463.

Ferguson, B.J. et al., 2012. DNA-PK is a DNA sensor for IRF-3-dependent innate immunity. *eLife*, 1, p.e00047.

Fernandes-Alnemri, T. et al., 2009. AIM2 activates the inflammasome and cell death in response to cytoplasmic DNA. *Nature*, 458(7237), pp.509–513.

Fu, Y. et al., 1999. Cloning of DLM-1, a novel gene that is up-regulated in activated macrophages, using RNA differential display. *Gene*, 240(1), pp.157–163.

Gaiha, G.D. et al., 2014. Dysfunctional HIV-specific CD8(+) T cell proliferation is associated with increased caspase-8 activity and mediated by necroptosis. *Immunity*, 41(6), pp.1001–1012.

Galluzzi, L. et al., 2017. Necroptosis: Mechanisms and Relevance to Disease. *Annu. Rev. Pathol. Mech. Dis.*, 12(1), pp.103–130.

Galluzzi, L. et al., 2008. Viral control of mitochondrial apoptosis. *PLoS Pathogens*, 4(5), p.e1000018.

Ghosh, D. & Stumhofer, J.S., 2013. Do you see what I see: Recognition of protozoan parasites by Toll-like receptors. *Current immunology reviews*, 9(3), pp.129–140.

Gong, Y.-N. et al., 2017. ESCRT-III Acts Downstream of MLKL to Regulate Necroptotic Cell Death and Its Consequences. *Cell*, 169(2), pp.286–300.e16.

Goubau, D. et al., 2014. Antiviral immunity via RIG-I-mediated recognition of RNA bearing 5'-diphosphates. *Nature*, 514(7522), pp.372–375.

Grant, A. et al., 2016. Zika Virus Targets Human STAT2 to Inhibit Type I Interferon Signaling. *Cell Host & Microbe*, 19(6), pp.882–890.

Gulen, M.F. et al., 2017. Signalling strength determines proapoptotic functions of STING. *Nature Communications*, 8(1), p.427.

Guo, H. et al., 2015. Herpes Simplex Virus Suppresses Necroptosis in Human Cells. *Cell Host & Microbe*, 17(2), pp.243–251.

Guo, H. et al., 2018. Species-independent contribution of ZBP1/DAI/DLM-1-triggered necroptosis in host defense against HSV1. *Cell Death & Disease*, 9(8), p.816.

Ha, S.C. et al., 2008. The crystal structure of the second Z-DNA binding domain of human DAI (ZBP1) in complex with Z-DNA reveals an unusual binding mode to Z-DNA. *Proceedings of the National Academy of Sciences of the United States of America*, 105(52), pp.20671–20676.

Hall, K. et al., 1984. "Z-RNA--"a left-handed RNA double helix. *Nature*, 311(5986), pp.584–586.

Haniford, D.B. & Pulleyblank, D.E., 1983. Facile transition of poly[d(TG)·d(CA)] into a left-handed helix in physiological conditions. *Nature*, 302(5909), pp.632–634.

Hardin, C. C. et al., 1988. Characterization of anti-Z-RNA polyclonal antibodies: epitope properties and recognition of Z-DNA. *Biochemistry* 27, 4169–4177.

Harding, S.M. et al., 2017. Mitotic progression following DNA damage enables pattern recognition within micronuclei. *Nature*, 548, pp.466 EP –.

Hardwick, J.M., 1998. Viral interference with apoptosis. *Seminars in cell & developmental biology*, 9(3), pp.339–349.

Hartmann, B.M. et al., 2017. Pandemic H1N1 influenza A viruses suppress immunogenic RIPK3-driven dendritic cell death. *Nature Communications*, 8(1), p.1931.

He, S. et al., 2011. Toll-like receptors activate programmed necrosis in macrophages through a receptor-interacting kinase-3-mediated pathway. *Proceedings of the National Academy of Sciences*, 108(50), pp.20054–20059.

Heil, F., 2004. Species-Specific Recognition of Single-Stranded RNA via Toll-like Receptor 7 and 8. *Science (New York, N.Y.)*, 303(5663), pp.1526–1529.

Heineman, T.C. & Cohen, J.I., 1994. Deletion of the varicella-zoster virus large subunit of ribonucleotide reductase impairs growth of virus in vitro. *Journal of Virology*, 68(5), pp.3317–3323.

Hemmi, H. et al., 2000. A Toll-like receptor recognizes bacterial DNA. *Nature*, 408(6813), pp.740–198.

Herbert, A., 2019. Z-DNA and Z-RNA in human disease. *Communications Biology*, 2(1), p.7.

Herbert, A. & Rich, A., 2001. The role of binding domains for dsRNA and Z-DNA in the in vivo editing of minimal substrates by ADAR1. *Proc Natl Acad Sci USA*, 98(21), p.12132.

Herbert, A. et al., 1995. Chicken double-stranded RNA adenosine deaminase has apparent specificity for Z-DNA. *Proceedings of the National Academy of Sciences*, 92(16), pp.7550–7554.

Hertzog, J. et al., 2018. Infection with a Brazilian isolate of Zika virus generates RIG-I stimulatory RNA and the viral NS5 protein blocks type I IFN induction and signaling. *European journal of immunology*, 48(7), pp.1120–1136.

Hidaka, F. et al., 2006. A missense mutation of the Toll-like receptor 3 gene in a patient with influenza-associated encephalopathy. *Clinical immunology (Orlando, Fla.)*, 119(2), pp.188–194.

Hoebe, K. et al., 2003. Identification of Lps2 as a key transducer of MyD88-independent TIR signalling. *Nature*, 424(6950), pp.743–748.

Holler, N. et al., 2000. Fas triggers an alternative, caspase-8-independent cell death pathway using the kinase RIP as effector molecule., 1(6), pp.489–495.

Hornung, V. et al., 2009. AIM2 recognizes cytosolic dsDNA and forms a caspase-1-activating inflammasome with ASC. *Nature*, 458(7237), pp.514–518.

Hou, S. et al., 2017. Zika Virus Hijacks Stress Granule Proteins and Modulates the Host Stress Response. *Journal of Virology*, 91(16).

Hur, S., 2019. Double-Stranded RNA Sensors and Modulators in Innate Immunity. *Annual Review of Immunology*, 37(1), pp.349–375.

Iannielli, A. et al., 2018. Pharmacological Inhibition of Necroptosis Protects from Dopaminergic Neuronal Cell Death in Parkinson's Disease Models. *Cell Reports*, 22(8), pp.2066–2079.

Ishii, K.J. et al., 2006. A Toll-like receptor-independent antiviral response induced by double-stranded B-form DNA., 7(1), pp.40–48.

Ishii, K.J. et al., 2008. TANK-binding kinase-1 delineates innate and adaptive immune responses to DNA vaccines. *Nature*, 451(7179), pp.725–729.

Issur, M. et al., 2009. The flavivirus NS5 protein is a true RNA guanylyltransferase that catalyzes a two-step reaction to form the RNA cap structure. *RNA (New York, N.Y.)*, 15(12), pp.2340–2350.

Ito, Y. et al., 2016. RIPK1 mediates axonal degeneration by promoting inflammation and necroptosis in ALS. *Science (New York, N.Y.)*, 353(6299), pp.603–608.

Jaattela, M. & Tschopp, J., 2003. Caspase-independent cell death in T lymphocytes., 4(5), pp.416–423.

Janeway, C.A.J., 1989. Approaching the asymptote? Evolution and revolution in immunology. *Cold Spring Harbor symposia on quantitative biology*, 54 Pt 1, pp.1–13.

Jinek, M. et al., 2012. A programmable dual-RNA-guided DNA endonuclease in adaptive bacterial immunity. *Science (New York, N.Y.)*, 337(6096), pp.816–821.

Kaiser, W.J. et al., 2011. RIP3 mediates the embryonic lethality of caspase-8-deficient mice. *Nature*, 471(7338), pp.368–372.

Kaiser, W.J. et al., 2013. Toll-like receptor 3-mediated necrosis via TRIF, RIP3, and MLKL. *The Journal of biological chemistry*, 288(43), pp.31268–31279.

Kaiser, W.J., Upton, J.W. & Mocarski, E.S., 2008. Receptor-interacting protein homotypic interaction motif-dependent control of NF-kappa B activation via the DNA-dependent activator of IFN regulatory factors. *The Journal of Immunology*, 181(9), pp.6427–6434.

Kariko, K. et al., 2004. mRNA is an endogenous ligand for Toll-like receptor 3. *Journal of Biological Chemistry*, 279(13), pp.12542–12550.

Kelliher, M.A. et al., 1998. The death domain kinase RIP mediates the TNF-induced NF-kappaB signal. *Immunity*, 8(3), pp.297–303.

Kim, T. et al., 2010. Aspartate-glutamate-alanine-histidine box motif (DEAH)/RNA helicase A helicases sense microbial DNA in human plasmacytoid dendritic cells. *Proceedings of the National Academy of Sciences*, 107(34), pp.15181–15186.

Kim, U. et al., 1994. Molecular cloning of cDNA for double-stranded RNA adenosine deaminase, a candidate enzyme for nuclear RNA editing. *Proceedings of the National Academy of Sciences of the United States of America*, 91(24), pp.11457–11461.

Kim, Y.-G. et al., 2003. A role for Z-DNA binding in vaccinia virus pathogenesis. *Proceedings of the National Academy of Sciences*, 100(12), pp.6974–6979.

Koehler, H. et al., 2017. Inhibition of DAI-dependent necroptosis by the Z-DNA binding domain of the vaccinia virus innate immune evasion protein, E3. *Proceedings of the National Academy of Sciences of the United States of America*, 114(43), pp.11506–11511.

Kondo, T. et al., 2013. DNA damage sensor MRE11 recognizes cytosolic double-stranded DNA and induces type I interferon by regulating STING trafficking. *Proceedings of the National Academy of Sciences*, 110(8), pp.2969–2974.

Kumagai, Y., Takeuchi, O. & Akira, S., 2008. TLR9 as a key receptor for the recognition of DNA. *Toll-like Receptor and Pattern Sensing for Evoking Immune Response*, 60(7), pp.795–804.

Kuriakose, T. et al., 2018. IRF1 Is a Transcriptional Regulator of ZBP1 Promoting NLRP3 Inflammasome Activation and Cell Death during Influenza Virus Infection. *The Journal of Immunology*, 200(4), pp.1489–1495.

Kuriakose, T. et al., 2016. ZBP1/DAI is an innate sensor of influenza virus triggering the NLRP3 inflammasome and programmed cell death pathways. *Sci. Immunol.*, 1(2), pp.aag2045–aag2045.

Lafer, E.M. et al., 1981. Antibodies specific for left-handed Z-DNA. *Proc Natl Acad Sci USA*, 78(6), p.3546.

Lancillotti, F. et al., 1987. Z-DNA in transcriptionally active chromosomes. *Proceedings of the National Academy of Sciences of the United States of America*, 84(6), pp.1560–1564.

Larkin, B. et al., 2017. Cutting Edge: Activation of STING in T Cells Induces Type I IFN Responses and Cell Death. *Journal of immunology (Baltimore, Md. : 1950)*, p.ji1601999.

Le Goffic, R. et al., 2006. Detrimental contribution of the Toll-like receptor (TLR)3 to influenza A virus-induced acute pneumonia. *PLoS Pathogens*, 2(6), p.e53.

Lee, M.N. et al., 2013. Identification of regulators of the innate immune response to cytosolic DNA and retroviral infection by an integrative approach. 14(2), pp.179–185.

Lemaitre, B. et al., 1996. The Dorsoventral Regulatory Gene Cassette spätzle/Toll/cactus Controls the Potent Antifungal Response in Drosophila Adults. *Cell*, 86(6), pp.973–983.

Lembo, D. et al., 2004. The ribonucleotide reductase R1 homolog of murine cytomegalovirus is not a functional enzyme subunit but is required for pathogenesis. *Journal of Virology*, 78(8), pp.4278–4288.

Levine, B. et al., 1993. Conversion of lytic to persistent alphavirus infection by the bcl-2 cellular oncogene. *Nature*, 361(6414), pp.739–742.

Li, M. & Beg, A.A., 2000. Induction of necrotic-like cell death by tumor necrosis factor alpha and caspase inhibitors: novel mechanism for killing virus-infected cells. *Journal of Virology*, 74(16), pp.7470–7477.

Li, P. et al., 2016. Stimulating the RIG-I pathway to kill cells in the latent HIV reservoir following viral reactivation. *Nature Medicine*, 22(7), pp.807–811.

Li, T. & Chen, Z.J., 2018. The cGAS–cGAMP–STING pathway connects DNA damage to inflammation, senescence, and cancer. *J Exp Med*, 215(5), p.1287.

Liang, Q. et al., 2016. Zika Virus NS4A and NS4B Proteins Deregulate Akt-mTOR Signaling in Human Fetal Neural Stem Cells to Inhibit Neurogenesis and Induce Autophagy. *Cell stem cell*, 19(5), pp.663–671.

Lin, J. et al., 2016. RIPK1 counteracts ZBP1-mediated necroptosis to inhibit inflammation. *Nature*, 540(7631), pp.124–128.

Lin, Y. et al., 1999. Cleavage of the death domain kinase RIP by caspase-8 prompts TNF-induced apoptosis. *Genes & development*, 13(19), pp.2514–2526.

Lin, Y. et al., 2004. Tumor necrosis factor-induced nonapoptotic cell death requires receptor-interacting protein-mediated cellular reactive oxygen species accumulation. *Journal of Biological Chemistry*, 279(11), pp.10822–10828.

Lippmann, J. et al., 2008. IFNbeta responses induced by intracellular bacteria or cytosolic DNA in different human cells do not require ZBP1 (DLM-1/DAI). *Cellular Microbiology*, 10(12), pp.2579–2588.

Liu, L.F. & Wang, J.C., 1987. Supercoiling of the DNA template during transcription. *Proceedings of the National Academy of Sciences*, 84(20), pp.7024–7027.

Mackenzie, K.J. et al., 2017. cGAS surveillance of micronuclei links genome instability to innate immunity. *Nature*, 548(7668), pp.461–465.

Maelfait, J. et al., 2017. Sensing of viral and endogenous RNA by ZBP1/DAI induces necroptosis. *The EMBO journal*, p.e201796476.

Maelfait, J. et al., 2008. Stimulation of Toll-like receptor 3 and 4 induces interleukin-1beta maturation by caspase-8. *Journal of Experimental Medicine*, 205(9), pp.1967–1973.

Mankan, A.K. et al., 2014. Cytosolic RNA:DNA hybrids activate the cGAS-STING axis. *The EMBO journal*, 33(24), pp.2937–2946.

McAllister, C.S. et al., 2013. TLR3, TRIF, and caspase 8 determine double-stranded RNA-induced epithelial cell death and survival in vivo. *The Journal of Immunology*, 190(1), pp.418–427.

McFadden, M.J. et al., 2018. A Fluorescent Cell-Based System for Imaging Zika Virus Infection in Real-Time. *Viruses*, 10(2), p.95.

McNab, F. et al., 2015. Type I interferons in infectious disease. *Nat Rev Immunol*, 15(2), pp.87–103.

Medzhitov, R., Preston-Hurlburt, P. & Janeway, C.A.J., 1997. A human homologue of the Drosophila Toll protein signals activation of adaptive immunity. *Nature*, 388(6640), pp.394–397.

Meylan, E. et al., 2004. RIP1 is an essential mediator of Toll-like receptor 3-induced NF-kappa B activation., 5(5), pp.503–507.

Micheau, O. & Tschopp, J., 2003. Induction of TNF receptor I-mediated apoptosis via two sequential signaling complexes. *Cell*, 114(2), pp.181–190.

Mocarski, E.S., Guo, H. & Kaiser, W.J., 2015. Necroptosis: The Trojan horse in cell autonomous antiviral host defense. *Virology*, 479-480, pp.160–166.

Mocarski, E.S., Upton, J.W. & Kaiser, W.J., 2012. Viral infection and the evolution of caspase 8-regulated apoptotic and necrotic death pathways. *Nature reviews. Immunology*, 12(2), pp.79–88.

Morita, M. et al., 2004. Gene-targeted mice lacking the Trex1 (DNase III) 3“-->5” DNA exonuclease develop inflammatory myocarditis. *Molecular and cellular biology*, 24(15), pp.6719–6727.

Murai, S. et al., 2018. A FRET biosensor for necroptosis uncovers two different modes of the release of DAMPs. *Nature Communications*, 9(1), pp.4457–4457.

Newton, K. et al., 2016. RIPK1 inhibits ZBP1-driven necroptosis during development. *Nature*, 540(7631), pp.129–133.

Nogusa, S. et al., 2016. RIPK3 Activates Parallel Pathways of MLKL-Driven Necroptosis and FADD-Mediated Apoptosis to Protect against Influenza A Virus. *Cell Host & Microbe*, 20(1), pp.13–24.

Oberst, A. et al., 2011. Catalytic activity of the caspase-8-FLIP(L) complex inhibits RIPK3-dependent necrosis. *Nature*, 471(7338), pp.363–367.

Ofengeim, D. et al., 2015. Activation of necroptosis in multiple sclerosis. *Cell Reports*, 10(11), pp.1836–1849.

Ofengeim, D. et al., 2017. RIPK1 mediates a disease-associated microglial response in Alzheimer's disease. *Proceedings of the National Academy of Sciences*, 114(41), pp.E8788–E8797.

Ohkuri, T. et al., 2014. STING contributes to antiglioma immunity via triggering type I IFN signals in the tumor microenvironment. *Cancer immunology research*, 2(12), pp.1199–1208.

Omoto, S. et al., 2015. Suppression of RIP3-dependent Necroptosis by Human Cytomegalovirus. *Journal of Biological Chemistry*, 290(18), pp.11635–11648.

Oshiumi, H. et al., 2003. TIR-containing adapter molecule (TICAM)-2, a bridging adapter recruiting to toll-like receptor 4 TICAM-1 that induces interferon-beta. *Journal of Biological Chemistry*, 278(50), pp.49751–49762.

Pan, T. et al., 2014. Necroptosis Takes Place in Human Immunodeficiency Virus Type-1 (HIV-1)-Infected CD4+ T Lymphocytes G. Poli, ed. *PLoS ONE*, 9(4), p.e93944.

Pasparakis, M. & Vandenabeele, P., 2015. Necroptosis and its role in inflammation. *Nature*, 517(7534), pp.311–320.

Pham, C.L. et al., 2018. Viral M45 and necroptosis-associated proteins form heteromeric amyloid assemblies. *EMBO Reports*.

Placido, D. et al., 2007. A left-handed RNA double helix bound by the Z alpha domain of the RNA-editing enzyme ADAR1. *Structure (London, England : 1993)*, 15(4), pp.395–404.

Poeck, H. et al., 2008. 5'-Triphosphate-siRNA: turning gene silencing and Rig-I activation against melanoma. *Nature Medicine*, 14(11), pp.1256–1263.

Randow, F., MacMicking, J.D. & James, L.C., 2013. Cellular self-defense: how cell-autonomous immunity protects against pathogens. *Science (New York, N.Y.)*, 340(6133), pp.701–706.

Rebsamen, M. et al., 2009. DAI/ZBP1 recruits RIP1 and RIP3 through RIP homotypic interaction motifs to activate NF-κB. *EMBO Reports*, 10(8), pp.916–922.

Rehwinkel, J. & Reis e Sousa, C., 2010. RIGorous detection: exposing virus through RNA sensing. *Science (New York, N.Y.)*, 327(5963), pp.284–286.

Rehwinkel, J. et al., 2010. RIG-I detects viral genomic RNA during negative-strand RNA virus infection. *Cell*, 140(3), pp.397–408.

Rice, G.I. et al., 2012. Mutations in ADAR1 cause Aicardi-Goutières syndrome associated with a type I interferon signature. *Nature genetics*, 44(11), pp.1243–1248.

Rich, A. & Zhang, S., 2003. Z-DNA: the long road to biological function. *Nature Reviews Genetics*, 4(7), pp.566–572.

Rigby, R.E. et al., 2014. RNA:DNA hybrids are a novel molecular pattern sensed by TLR9. *The EMBO journal*, 33(6), pp.542–558.

Rintahaka, J. et al., 2008. Cytosolic antiviral RNA recognition pathway activates caspases 1 and 3. *The Journal of Immunology*, 180(3), pp.1749–1757.

Roberts, T.L. et al., 2009. HIN-200 proteins regulate caspase activation in response to foreign cytoplasmic DNA. *Science (New York, N.Y.)*, 323(5917), pp.1057–1060.

Romano, P.R. et al., 1998. Inhibition of double-stranded RNA-dependent protein kinase PKR by vaccinia virus E3: role of complex formation and the E3 N-terminal domain., 18(12), pp.7304–7316. Available at: http://www.pubmedcentral.nih.gov/articlerender.fcgi?artid=109312&tool=pmcentrez&rendertype=abstract.

Rothenburg, S. et al., 2002. Complex regulation of the human gene for the Z-DNA binding protein DLM-1. *Nucleic acids research*, 30(4), pp.993–1000.

Sancho-Shimizu, V. et al., 2011. Herpes simplex encephalitis in children with autosomal recessive and dominant TRIF deficiency. *The Journal of clinical investigation*, 121(12), pp.4889–4902.

Schlee, M. & Hartmann, G., 2016. Discriminating self from non-self in nucleic acid sensing. *Nat Rev Immunol*, 16(9), pp.566–580.

Schoggins, J.W. et al., 2011. A diverse range of gene products are effectors of the type I interferon antiviral response. *Nature*, 472(7344), pp.481–485. Available

at: http://eutils.ncbi.nlm.nih.gov/entrez/eutils/elink.fcgi?dbfrom=pubmed&id=21478870&retmode=ref&cmd=prlinks.

Schoggins, J.W. et al., 2014. Pan-viral specificity of IFN-induced genes reveals new roles for cGAS in innate immunity. *Nature*, 505(7485), pp.691–695.

Schwartz, T., 1999. Crystal Structure of the Z Domain of the Human Editing Enzyme ADAR1 Bound to Left-Handed Z-DNA. *Science*, 284(5421), pp.1841–1845.

Schwartz, T. et al., 2001. Structure of the DLM-1-Z-DNA complex reveals a conserved family of Z-DNA-binding proteins. *Nature structural biology*, 8(9), pp.761–765.

Shaw, A.E. et al., 2017. Fundamental properties of the mammalian innate immune system revealed by multispecies comparison of type I interferon responses H. Malik, ed. *PLOS Biology*, 15(12), p.e2004086.

Shen, C. et al., 2008. The tumorigenicity diversification in human embryonic kidney 293 cell line cultured in vitro. *Biologicals : journal of the International Association of Biological Standardization*, 36(4), pp.263–268.

Shors, T. & Jacobs, B.L., 1997. Complementation of deletion of the vaccinia virus E3L gene by the Escherichia coli RNase III gene. *Virology*, 227(1), pp.77–87.

Smith, C.C.T. et al., 2007. Necrostatin: a potentially novel cardioprotective agent? *Cardiovascular drugs and therapy*, 21(4), pp.227–233.

Smith, G.L. et al., 2013. Vaccinia virus immune evasion: mechanisms, virulence and immunogenicity. *The Journal of general virology*, 94(Pt 11), pp.2367–2392.

Spector, T. et al., 1987. Ribonucleotide reductase induced by varicella zoster virus. Characterization, and potentiation of acyclovir by its inhibition. *Biochemical pharmacology*, 36(24), pp.4341–4346.

Sridharan, H. et al., 2017. Murine cytomegalovirus IE3-dependent transcription is required for DAI/ZBP1-mediated necroptosis. *EMBO Reports*, p.e201743947.

Stepanenko, A.A. & Dmitrenko, V.V., 2015. HEK293 in cell biology and cancer research: phenotype, karyotype, tumorigenicity, and stress-induced genome-phenotype evolution. *Gene*, 569(2), pp.182–190.

Stetson, D.B. & Medzhitov, R., 2006. Recognition of cytosolic DNA activates an IRF3-dependent innate immune response. *Immunity*, 24(1), pp.93–103.

Sun, L. et al., 2012. Mixed Lineage Kinase Domain-like Protein Mediates Necrosis Signaling Downstream of RIP3 Kinase. *Cell*, 148(1-2), pp.213–227.

Takaoka, A. et al., 2007. DAI (DLM-1/ZBP1) is a cytosolic DNA sensor and an activator of innate immune response. *Nature*, 448(7152), pp.501–505.

Takemura, N. et al., 2014. Blockade of TLR3 protects mice from lethal radiation-induced gastrointestinal syndrome. *Nature Communications*, 5, p.3492.

Tatematsu, M. et al., 2018. Extracellular RNA Sensing by Pattern Recognition Receptors. *Journal of Innate Immunity*, 10(5-6), pp.398–406.

Tenev, T. et al., 2011. The Ripoptosome, a signaling platform that assembles in response to genotoxic stress and loss of IAPs. *Molecular Cell*, 43(3), pp.432–448.

Teng, M. K. et al., 1989. Effects of the O2' hydroxyl group on Z-DNA conformation: structure of Z-RNA and (araC)- [Z-DNA]. *Biochemistry* 28, 4923–4928

Thakur, M., Seo, E.J. & Dever, T.E., 2014. Variola virus E3L Zα domain, but not its Z-DNA binding activity, is required for PKR inhibition. *RNA (New York, N.Y.)*, 20(2), pp.214–227.

Thapa, R.J. et al., 2016. DAI Senses Influenza A Virus Genomic RNA and Activates RIPK3-Dependent Cell Death. *Cell Host & Microbe*.

Unterholzner, L. et al., 2010. IFI16 is an innate immune sensor for intracellular DNA. 11(11), pp.997–1004.

Upton, J.W. & Chan, F.K.-M., 2014. Staying alive: cell death in antiviral immunity. *Molecular Cell*, 54(2), pp.273–280.

Upton, J.W., Kaiser, W.J. & Mocarski, E.S., 2008. Cytomegalovirus M45 cell death suppression requires receptor-interacting protein (RIP) homotypic interaction motif (RHIM)-dependent interaction with RIP1. *Journal of Biological Chemistry*, 283(25), pp.16966–16970.

Upton, J.W., Kaiser, W.J. & Mocarski, E.S., 2012. DAI/ZBP1/DLM-1 complexes with RIP3 to mediate virus-induced programmed necrosis that is targeted by murine cytomegalovirus vIRA. *Cell Host & Microbe*, 11(3), pp.290–297.

Upton, J.W., Kaiser, W.J. & Mocarski, E.S., 2010. Virus inhibition of RIP3-dependent necrosis. *Cell Host & Microbe*, 7(4), pp.302–313.

Upton, J.W., Shubina, M. & Balachandran, S., 2017. RIPK3-driven cell death during virus infections. *Immunological Reviews*, 277(1), pp.90–101.

van den Boorn, J.G. & Hartmann, G., 2013. Turning tumors into vaccines: co-opting the innate immune system. *Immunity*, 39(1), pp.27–37.

Van Valen, L., 1973. Van Valen.1973 - Evol Theor.pdf. *Evolutionary Theory*, 1, pp.1–30.

Vandenabeele, P. et al., 2010. The role of the kinases RIP1 and RIP3 in TNF-induced necrosis. *Science signaling*, 3(115), p.re4.

Vasou, A. et al., 2017. Targeting Pattern Recognition Receptors (PRR) for Vaccine Adjuvantation: From Synthetic PRR Agonists to the Potential of Defective Interfering Particles of Viruses. *Viruses*, 9(7), p.186.

Vercammen, D. et al., 1998. Inhibition of caspases increases the sensitivity of L929 cells to necrosis mediated by tumor necrosis factor. *Journal of Experimental Medicine*, 187(9), pp.1477–1485.

Vliegen, I. et al., 2003. Improved detection and quantification of mouse cytomegalovirus by real-time PCR. *Virus Research*, 98(1), pp.17–25.

Wagner, S.A. et al., 2016. SPATA2 links CYLD to the TNF-alpha receptor signaling complex and modulates the receptor signaling outcomes. *The EMBO journal*, 35(17), pp.1868–1884.

Wang, A.H. et al., 1984. AT base pairs are less stable than GC base pairs in Z-DNA: the crystal structure of d(m5CGTAm5CG). *Cell*, 37(1), pp.321–331.

Wang, A.H. et al., 1979. Molecular structure of a left-handed double helical DNA fragment at atomic resolution. *Nature*, 282(5740), pp.680–686.

Wang, L., Du, F. & Wang, X., 2008. TNF-alpha induces two distinct caspase-8 activation pathways. *Cell*, 133(4), pp.693–703.

Wang, Z. et al., 2008. Regulation of innate immune responses by DAI (DLM-1/ZBP1) and other DNA-sensing molecules. *Proceedings of the National Academy of Sciences of the United States of America*, 105(14), pp.5477–5482.

Watson, J.D. & Crick, F.H., 1953. Molecular structure of nucleic acids; a structure for deoxyribose nucleic acid. *Nature*, 171(4356), pp.737–738.

Weber, A. et al., 2010. Proapoptotic signalling through Toll-like receptor-3 involves TRIF-dependent activation of caspase-8 and is under the control of inhibitor of apoptosis proteins in melanoma cells. *Cell Death and Differentiation*, 17(6), pp.942–951.

Weisel, K. et al., 2017. Randomized clinical study of safety, pharmacokinetics, and pharmacodynamics of RIPK1 inhibitor GSK2982772 in healthy volunteers. *Pharmacology research & perspectives*, 5(6), p.e00365.

Willis, K.L., Langland, J.O. & Shisler, J.L., 2011. Viral double-stranded RNAs from vaccinia virus early or intermediate gene transcripts possess PKR activating function, resulting in NF-kappaB activation, when the K1 protein is absent or mutated. *Journal of Biological Chemistry*, 286(10), pp.7765–7778.

Wittig, B., Dorbic, T. & Rich, A., 1989. The level of Z-DNA in metabolically active, permeabilized mammalian cell nuclei is regulated by torsional strain. *The Journal of Cell Biology*, 108(3), p.755.

Yamamoto, M. et al., 2002. Cutting edge: a novel Toll/IL-1 receptor domain-containing adapter that preferentially activates the IFN-beta promoter in the Toll-like receptor signaling. *The Journal of Immunology*, 169(12), pp.6668–6672.

Yamamoto, M. et al., 2003. Role of adaptor TRIF in the MyD88-independent toll-like receptor signaling pathway. *Science (New York, N.Y.)*, 301(5633), pp.640–643.

Yan, N. & Chen, Z.J., 2012. Intrinsic antiviral immunity., 13(3), pp.214–222.

Yang, P. et al., 2010. The cytosolic nucleic acid sensor LRRFIP1 mediates the production of type I interferon via a β-catenin-dependent pathway. 11(6), pp.487–494.

Yang, Y. et al., 2014. Solution structure of the free Zalpha domain of human DLM-1 (ZBP1/DAI), a Z-DNA binding domain. *Journal of Biomolecular NMR*, 60(2-3), pp.189–195.

Yang, Y.-G., Lindahl, T. & Barnes, D.E., 2007. Trex1 exonuclease degrades ssDNA to prevent chronic checkpoint activation and autoimmune disease. *Cell*, 131(5), pp.873–886.

Yatim, N. & Albert, M.L., 2011. Dying to replicate: the orchestration of the viral life cycle, cell death pathways, and immunity. *Immunity*, 35(4), pp.478–490.

Yu, X. et al., 2016. Activation of the MDA-5-IPS-1 Viral Sensing Pathway Induces Cancer Cell Death and Type I IFN-Dependent Antitumor Immunity. *Cancer research*, 76(8), pp.2166–2176.

Yuan, J., Amin, P. & Ofengeim, D., 2019. Necroptosis and RIPK1-mediated neuroinflammation in CNS diseases. *Nature Reviews Neuroscience*, 20(1), pp.19–33.

Zarling, D. A. et al., 1987. Cytoplasmic Z-RNA. *Proc. Natl Acad. Sci.* USA 84, 6117–6121.

Zhang, H. et al., 2011. Functional complementation between FADD and RIP1 in embryos and lymphocytes. *Nature*, 471(7338), pp.373–376.

Zhang, S.-Y. et al., 2007. TLR3 deficiency in patients with herpes simplex encephalitis. *Science (New York, N.Y.)*, 317(5844), pp.1522–1527.

Zhang, X. et al., 2011. Cutting edge: Ku70 is a novel cytosolic DNA sensor that induces type III rather than type I IFN. *The Journal of Immunology*, 186(8), pp.4541–4545.

Zhang, Z. et al., 2011. The helicase DDX41 senses intracellular DNA mediated by the adaptor STING in dendritic cells. 12(10), pp.959–965.

Zhao, J. et al., 2012. Mixed lineage kinase domain-like is a key receptor interacting protein 3 downstream component of TNF-induced necrosis. *Proc Natl Acad Sci USA*, 109(14), p.5322.

Zinngrebe, J. et al., 2016. --LUBAC deficiency perturbs TLR3 signaling to cause immunodeficiency and autoinflammation. *J Exp Med*, 213(12), p.2671.

Znidar, K. et al., 2018. Tumor cell death after electrotransfer of plasmid DNA is associated with cytosolic DNA sensor upregulation. *Oncotarget*, 9(27), pp.18665–18681.

APPENDIX I SUPPLEMENTARY FIGURES

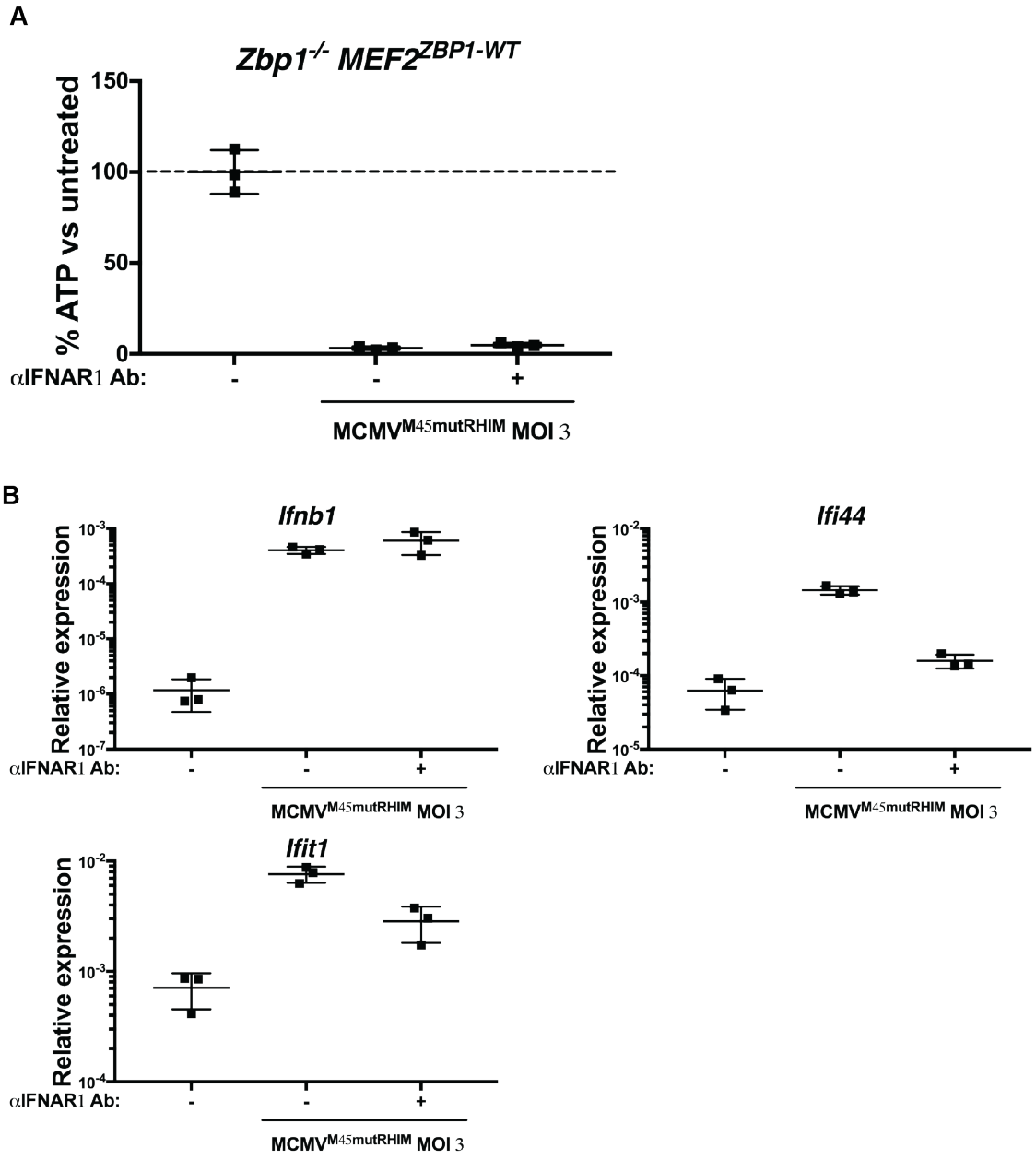


Figure S1. ZBP1-mediated virus-induced cell death is not affected by IFNAR1 blockade.

Immortalised *Zbp1*$^{-/-}$ MEFs were reconstituted with wildtype ZBP1 and then infected with MCMV^{M45mutRHIM} or treated with a combination of TNF + zVAD in the presence or absence of an IFNAR1 blocking antibody. (A) After 24h, cell viability (% ATP) was assessed by the CellTiter-Glo® assay. (B) At 8h, cells treated in parallel were harvested and *Ifnb1*, *Ifit1* and *Ifi44* mRNA expression levels were measured by qPCR. Means in (A) and (B) are from 1 representative experiment of 2 independent experiments each performed in triplicate and error bars represent ± 1 standard deviation (see Figure 14).

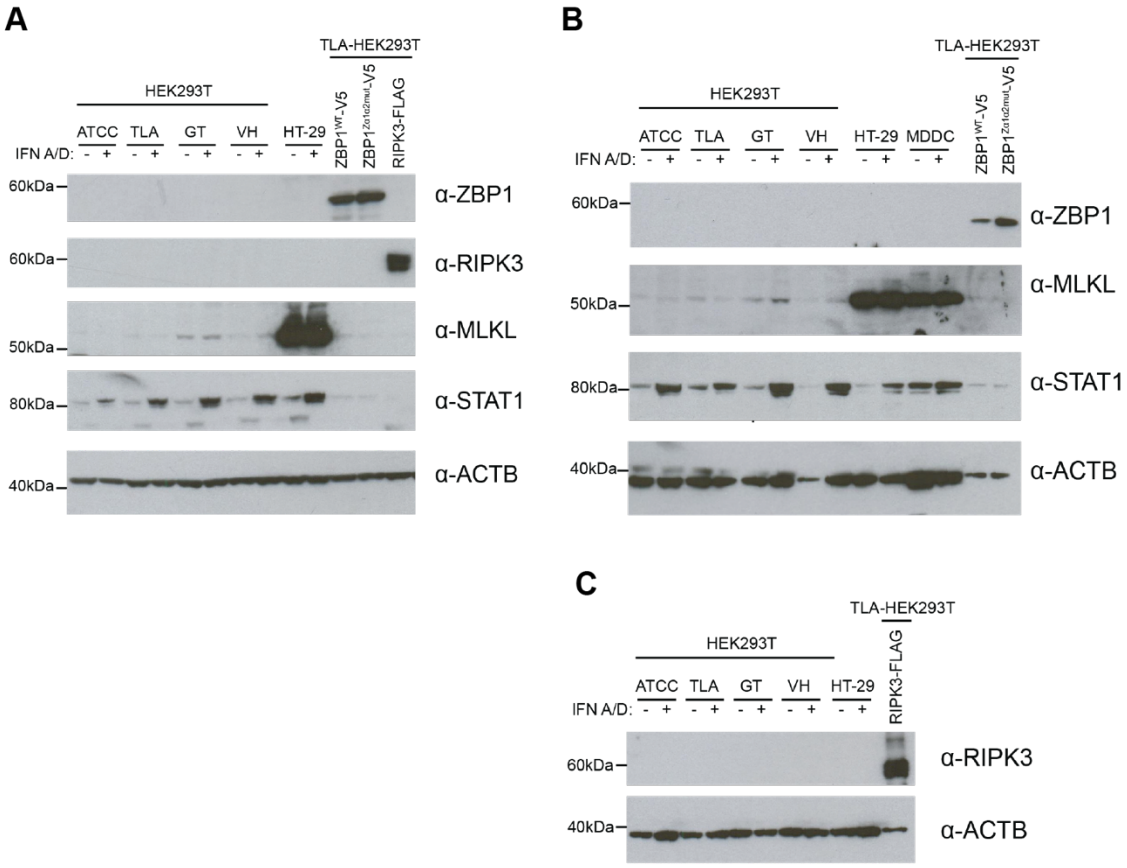


Figure S2. Protein expression levels of ZBP1, RIPK3 and MLKL in various human cell types.

(A-C) Cells were treated or not with 100U/mL recombinant type I IFN (IFN-A/D) as indicated for 16h and then harvested and analysed by SDS-PAGE and western blotting. Four different sub-lines of HEK293T were tested, including: cells obtained directly from ATCC (ATCC), TLA-HEK293T cells (TLA) and HEK293T cells that were gifts from Greg Towers (GT) and Veit Hornung (VH). (A-C) HT-29 cells and (B) human monocyte-derived dendritic cells (MDDC) were also tested. (A-C) As positive controls, lysates from TLA-HEK293T cells transfected for 24h with ZBP1 or RIPK3 were also included. Data in (A) and (B-C) are each from 1 experiment of a total of 3 independent experiments (see Figure 24).

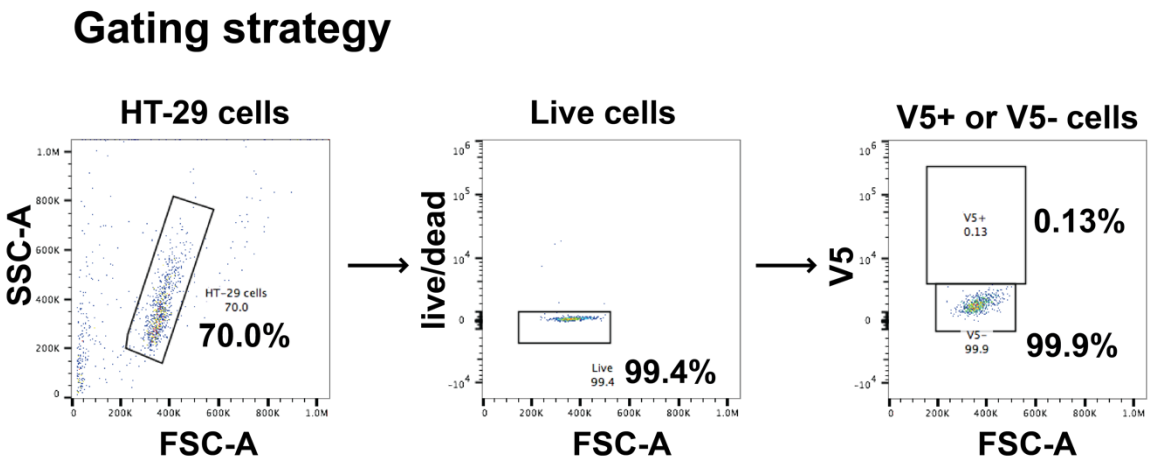


Figure S3. Ectopic ZBP1 expression in HT-29 cells is cytotoxic.

HT-29 cells were transduced with empty vector (EV), ZBP1^{WT}-V5 or ZBP1^{Zα1α2mut}-V5, using lentiviruses. EV transduced HT-29 cells were stained or not with aqua live/dead and an anti-V5 antibody conjugated to APC and analysed by flow cytometry (see Figure 25C). The gating strategy is shown here on stained EV transduced cells, which were V5-negative.

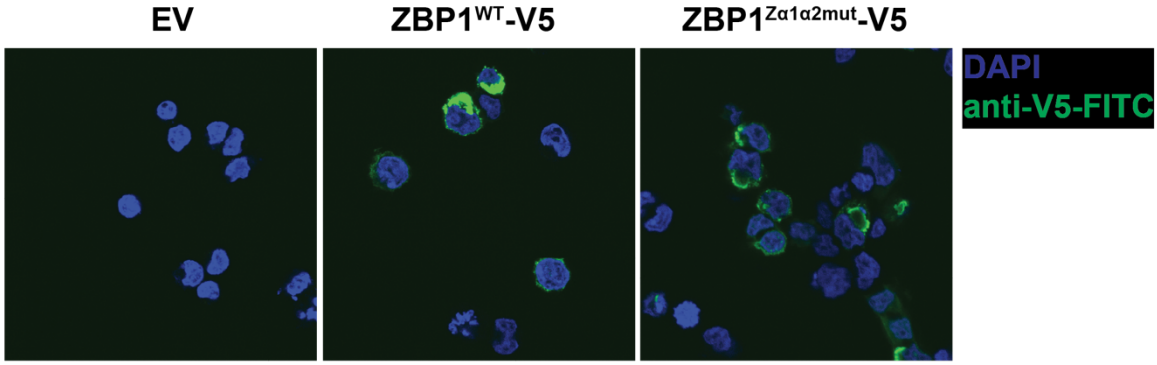


Figure S4. ZBP1 has a predominantly cytoplasmic localisation in transfected HEK293T cells.

HEK293T cells on coverslips were transfected with either an empty vector control plasmid (EV) or V5-tagged human ZBP1 wildtype (ZBP1^{WT}) or ZBD mutant (ZBP1^{Zα1α2mut}) and cells were fixed, permeabilised and stained (DAPI and anti-V5-FITC) before imaging by confocal microscopy. Images (display range 0-4095) from 1 representative experiment of 2 independent experiments are shown. (see Figure 26).

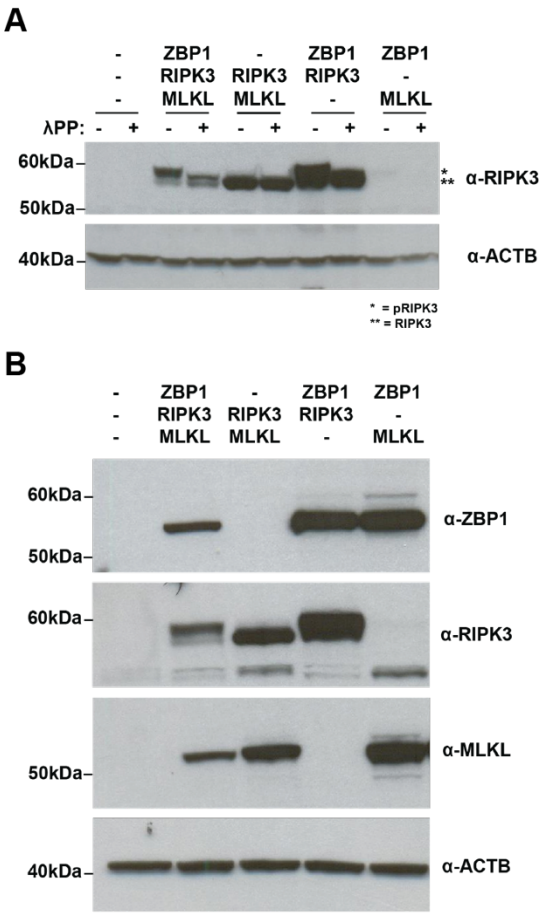


Figure S5. ZBP1 mediates RIPK3 phosphorylation in a ZBD-dependent manner.

(A-B) HEK293T cells were co-transfected with plasmids encoding empty vector (EV) or RIPK3 and MLKL, with or without untagged ZBP1 wildtype ($ZBP1^{WT}$). 24h post-transfection, cells were harvested and lysates were analysed by SDS-PAGE and western blotting with the antibodies indicated. Data shown are from 1 experiment of 3 independent experiments (see Figure 31 and Figure S6).

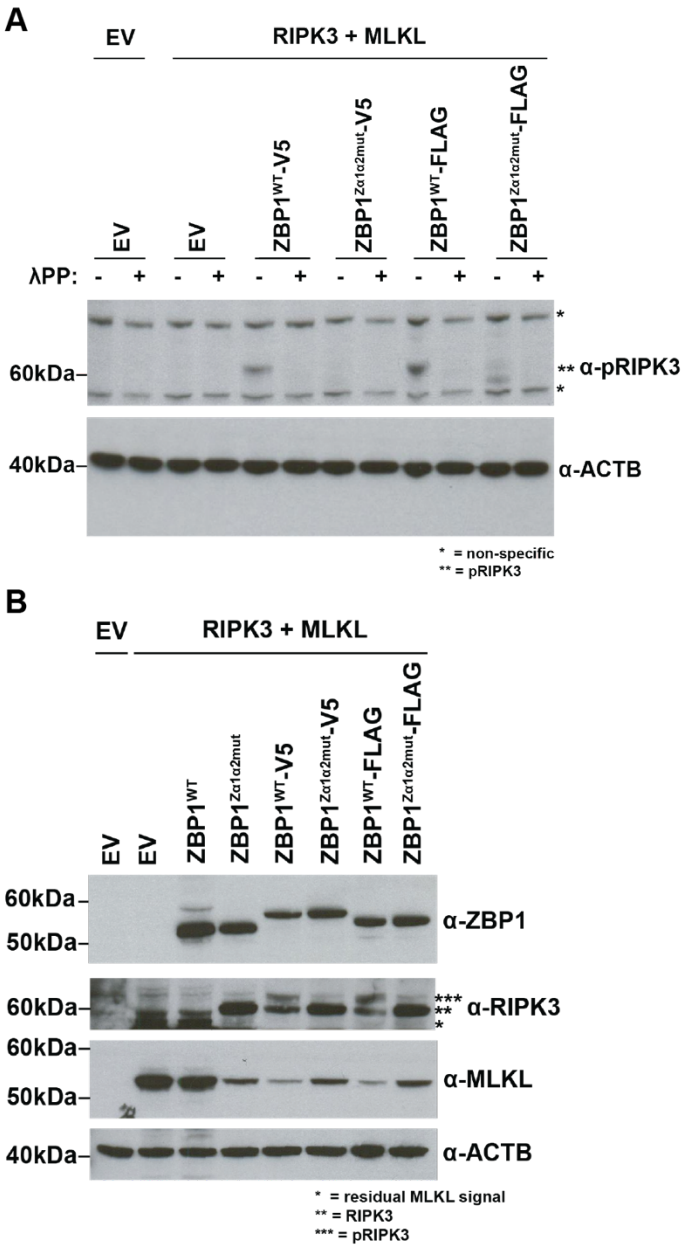


Figure S6. ZBP1 mediates RIPK3 phosphorylation in a ZBD-dependent manner.

(A-B) HEK293T cells were co-transfected with plasmids encoding empty vector (EV) or RIPK3 and MLKL, with or without untagged, V5-tagged or FLAG-tagged ZBP1 wildtype ($ZBP1^{WT}$) or ZBD mutant ($ZBP1^{Zα1α2mut}$). 24h post-transfection, cells were harvested and lysates that were treated or not with lambda-phosphatase (λPP) as indicated were analysed by SDS-PAGE and western blotting with anti-pRIPK3 antibody (pSer-227) and the other antibodies indicated. Data are from 1 representative experiment of 3 independent experiments (see Figure 31 and Figure S5).

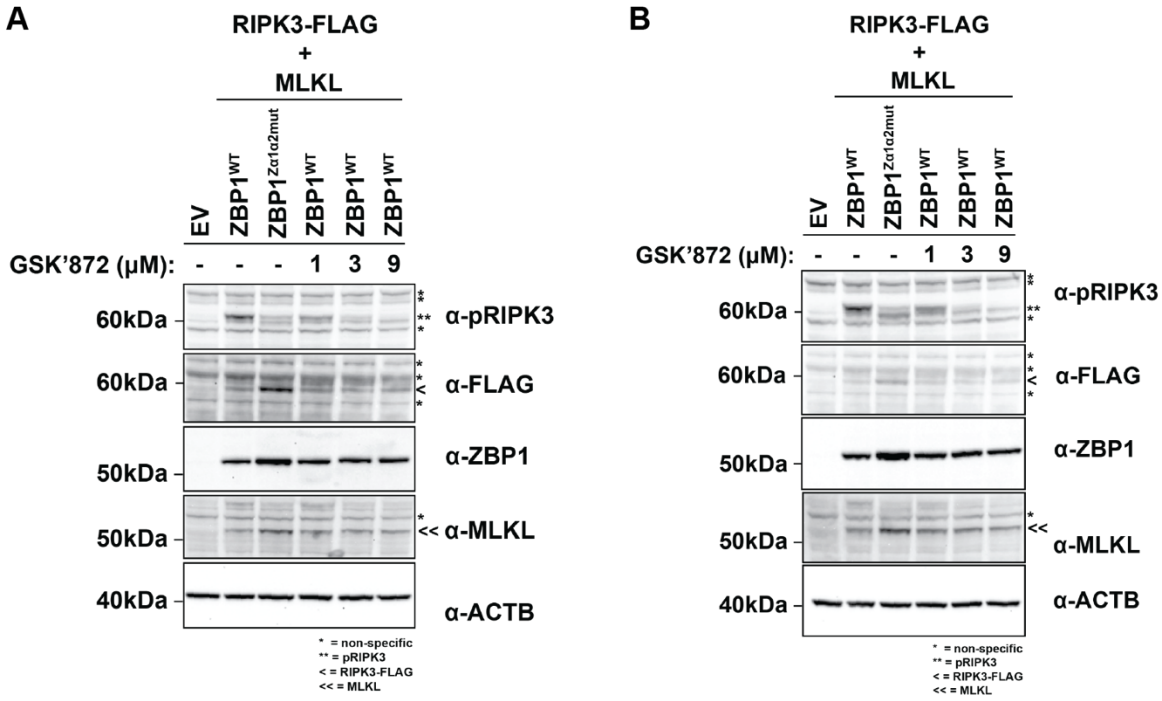


Figure S7. ZBP1-mediated RIPK3 phosphorylation requires RIPK3 kinase activity.

(A-B) HEK293T cells were co-transfected with plasmids encoding empty vector (EV) or RIPK3, MLKL and ZBP1 wildtype ($ZBP1^{WT}$) or ZBD mutant ($ZBP1^{Zα1α2mut}$), with or without a dose titration of the pharmacological RIPK3 inhibitor GSK'872. 24h post-transfection, cells were harvested and lysates analysed by SDS-PAGE and western blotting with anti-pRIPK3 antibody (pSer-227) and the other antibodies indicated. Data in (A) and (B) are each from 1 experiment of a total of 3 independent experiments (see Figure 32).

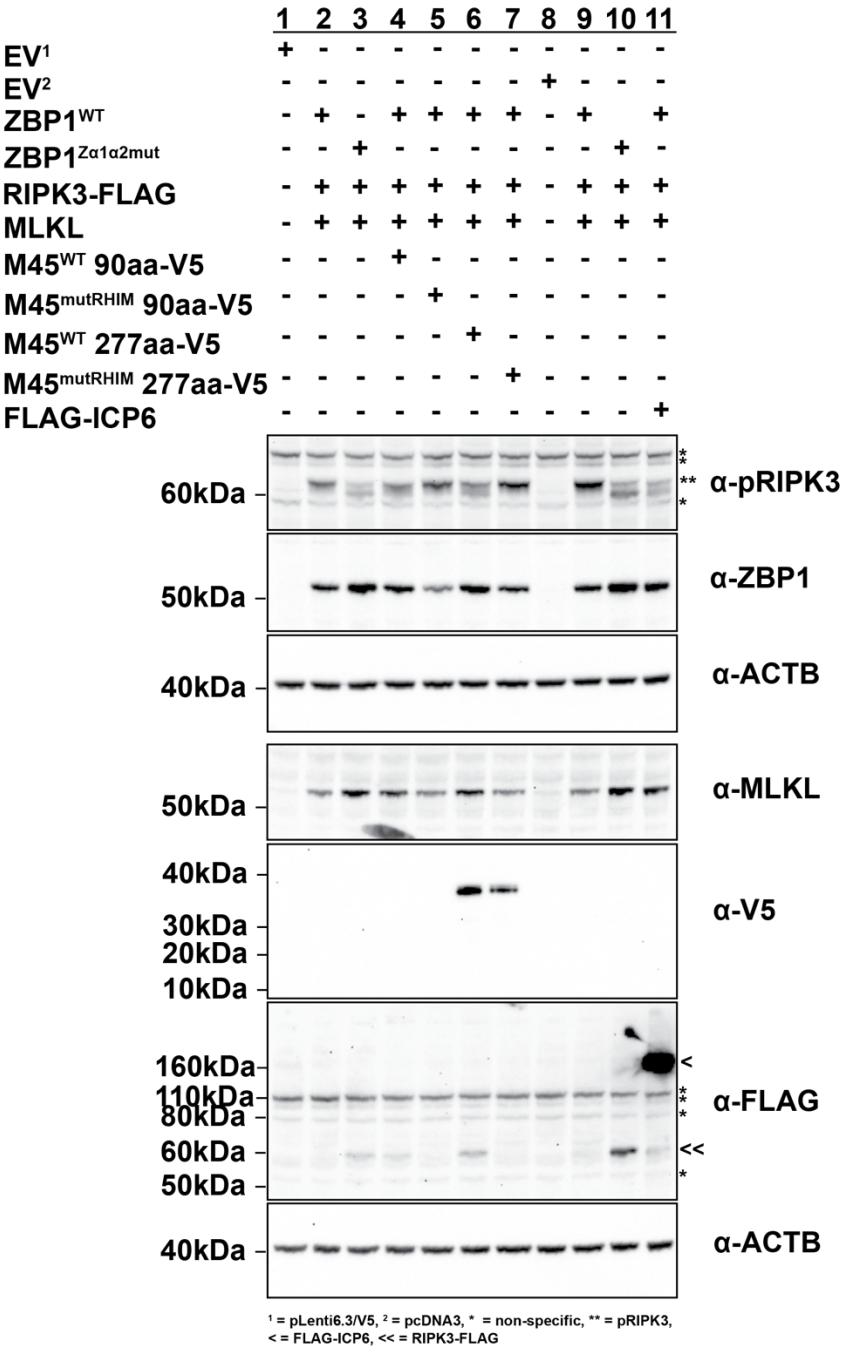


Figure S8. ZBP1-mediated RIPK3 auto-phosphorylation is inhibited by MCMV M45 fragments and HSV-1 ICP6.

HEK293T cells were co-transfected with plasmids encoding empty vector (EV) or RIPK3, MLKL and ZBP1, with or without C-terminally V5-tagged wildtype or RHIM-mutant 90 or 277 amino acid RHIM-encompassing M45 fragments ($M45^{WT}$-90aa-V5, $M45^{mutRHIM}$-90aa-V5, $M45^{WT}$-277aa-V5 or $M45^{mutRHIM}$-277aa-V5) or N-terminally FLAG-tagged HSV-1 ICP6

(FLAG-ICP6). 24h post-transfection, cells were harvested and lysates analysed by SDS-PAGE and western blotting with anti-pRIPK3 antibody (pSer-227) and the other antibodies indicated. Data are from 1 experiment of 2 independent experiments (see Figure 33).

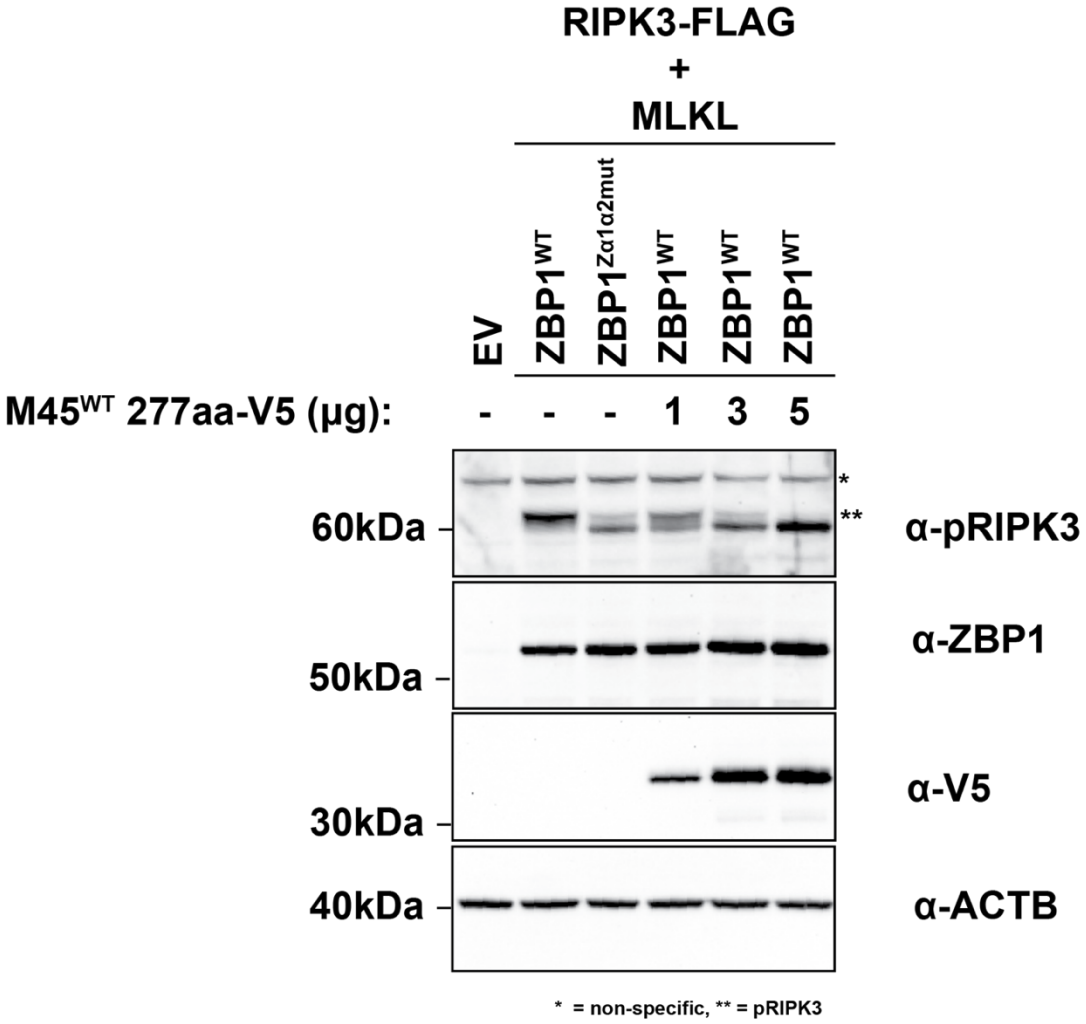


Figure S9. RHIM-dependent inhibition of ZBP1-mediated RIPK3 auto-phosphorylation by an M45 fragment.

HEK293T cells were co-transfected with plasmids encoding empty vector (EV) or RIPK3, MLKL and ZBP1, with or without a dose titration of a wildtype or RHIM-mutant 277-amino acid fragment of M45 ($M45^{WT}$-277aa or $M45^{mutRHIM}$-277aa). 24h post-transfection, cells were harvested and lysates analysed by SDS-PAGE and western blotting with anti-pRIPK3 antibody (pSer-227) and the other antibodies indicated. Data are representative of 3 independent experiments (see Figure 34 and Figure S10).

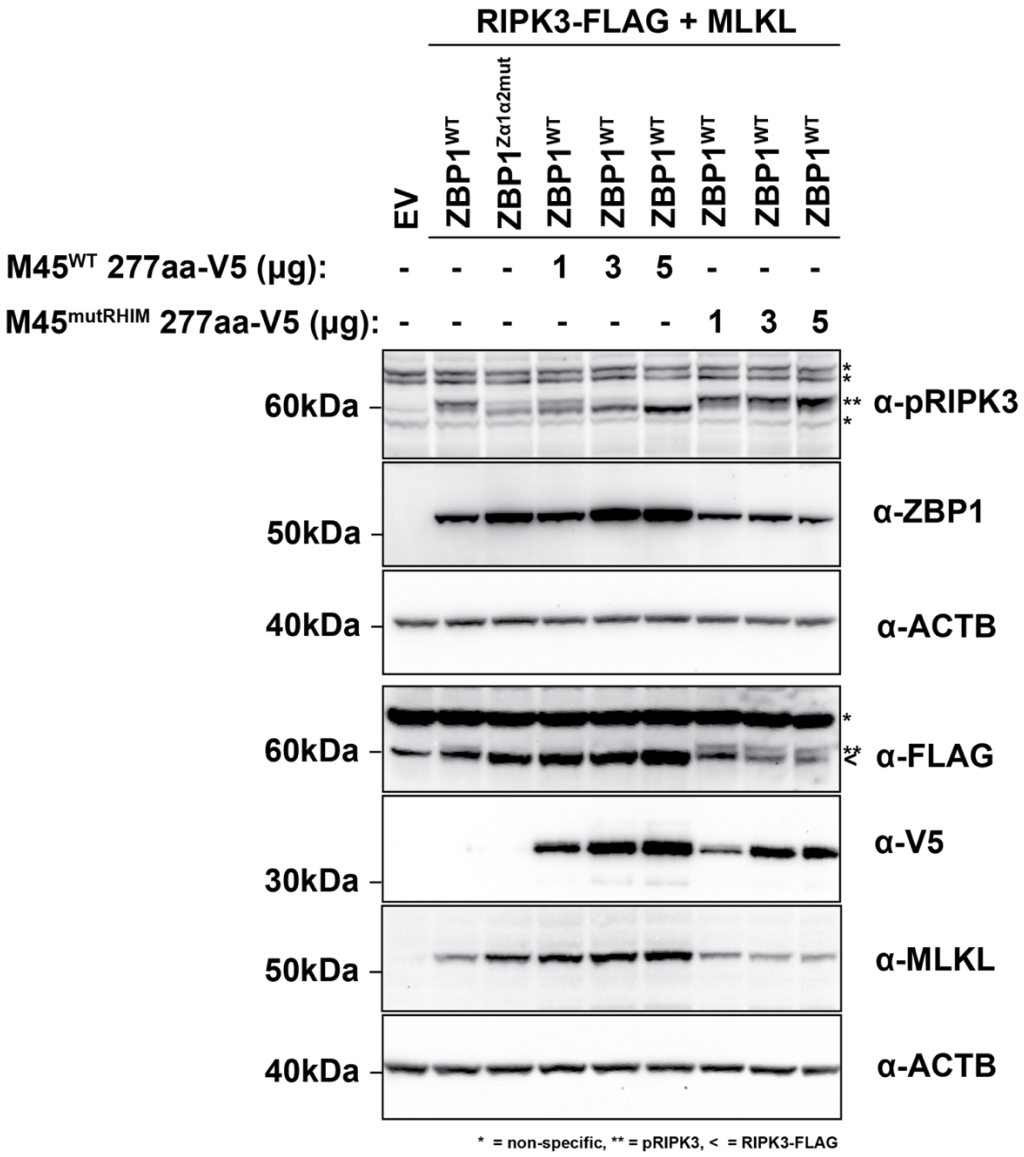


Figure S10. RHIM-dependent inhibition of ZBP1-mediated RIPK3 auto-phosphorylation by an M45 fragment.

HEK293T cells were co-transfected with plasmids encoding empty vector (EV) or RIPK3, MLKL and ZBP1, with or without a dose titration of a wildtype or RHIM-mutant 277-amino acid fragment of M45 ($M45^{WT}$-277aa or $M45^{mutRHIM}$-277aa). 24h post-transfection, cells were harvested and lysates analysed by SDS-PAGE and western blotting with anti-pRIPK3 antibody (pSer-227) and the other antibodies indicated. Data are representative of 3 independent experiments (see Figure 34 and Figure S10).

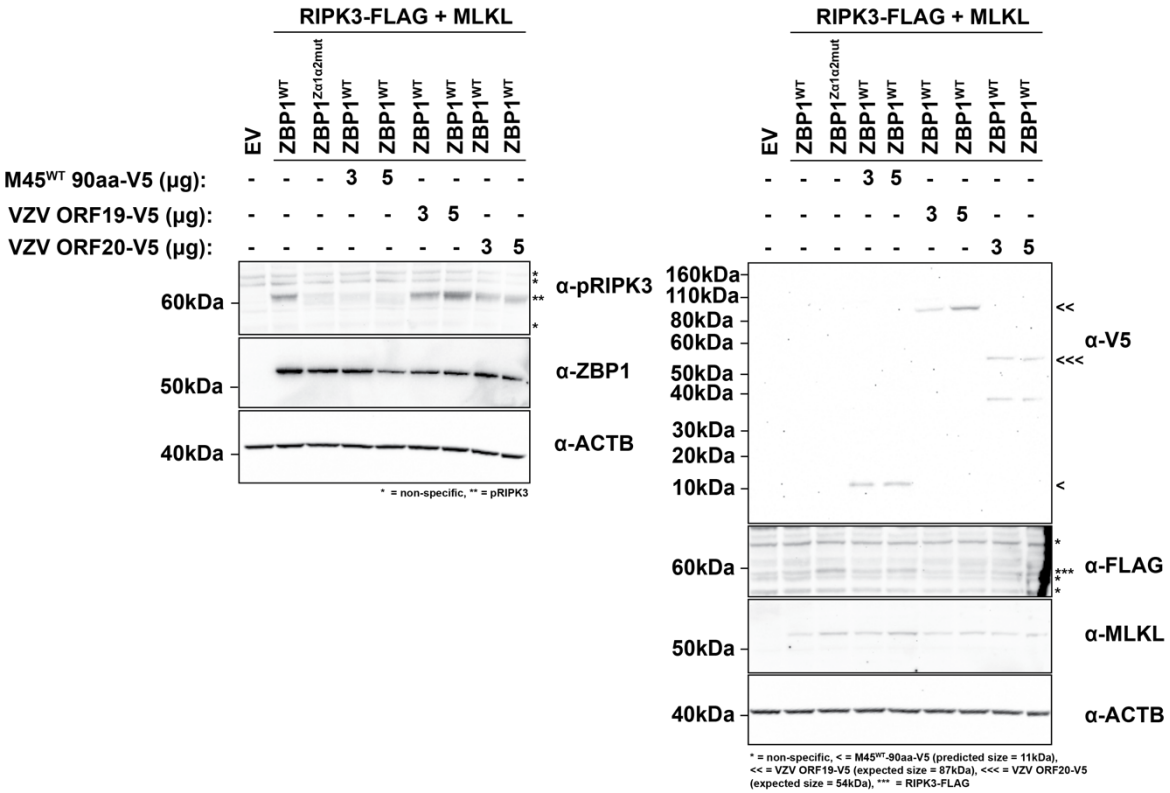


Figure S11. VZV ORFs 19 and 20 do not inhibit ZBP1-mediated ZBD-dependent RIPK3 auto-phosphorylation.

HEK293T cells were co-transfected with plasmids encoding empty vector (EV) or RIPK3, MLKL and ZBP1, with or without a dose titration of plasmid encoding V5-tagged 90-amino acid fragment of M45 ($M45^{WT}$-90aa), VZV ORF19 or VZV ORF20. 24h post-transfection, cells were harvested and lysates analysed by SDS-PAGE and western blotting with anti-pRIPK3 antibody (pSer-227) and the other antibodies indicated. Data are representative of 3 independent experiments (see Figure 36 and Figure S12).

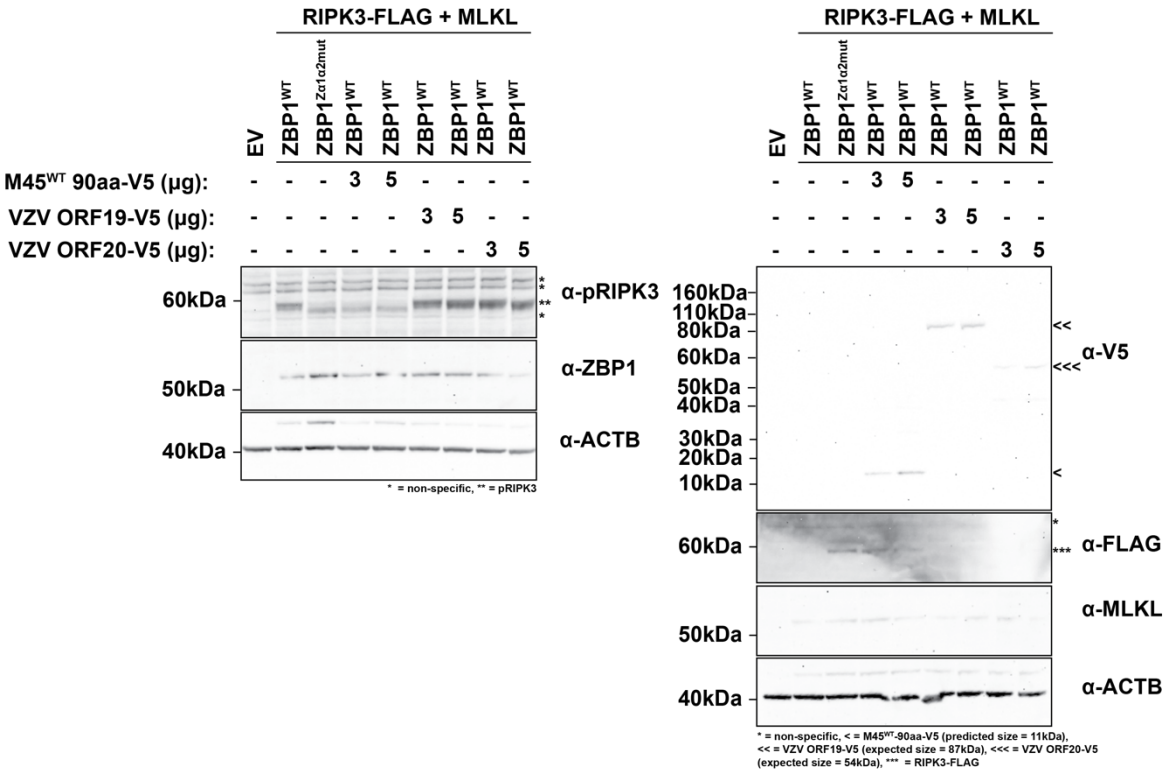


Figure S12. VZV ORFs 19 and 20 do not inhibit ZBP1-mediated ZBD-dependent RIPK3 auto-phosphorylation.

HEK293T cells were co-transfected with plasmids encoding empty vector (EV) or RIPK3, MLKL and ZBP1, with or without a dose titration of plasmid encoding V5-tagged 90-amino acid fragment of M45 ($M45^{WT}$-90aa), VZV ORF19 or VZV ORF20. 24h post-transfection, cells were harvested and lysates analysed by SDS-PAGE and western blotting with anti-pRIPK3 antibody (pSer-227) and the other antibodies indicated. Data are representative of 3 independent experiments (see Figure 36 and Figure S11).

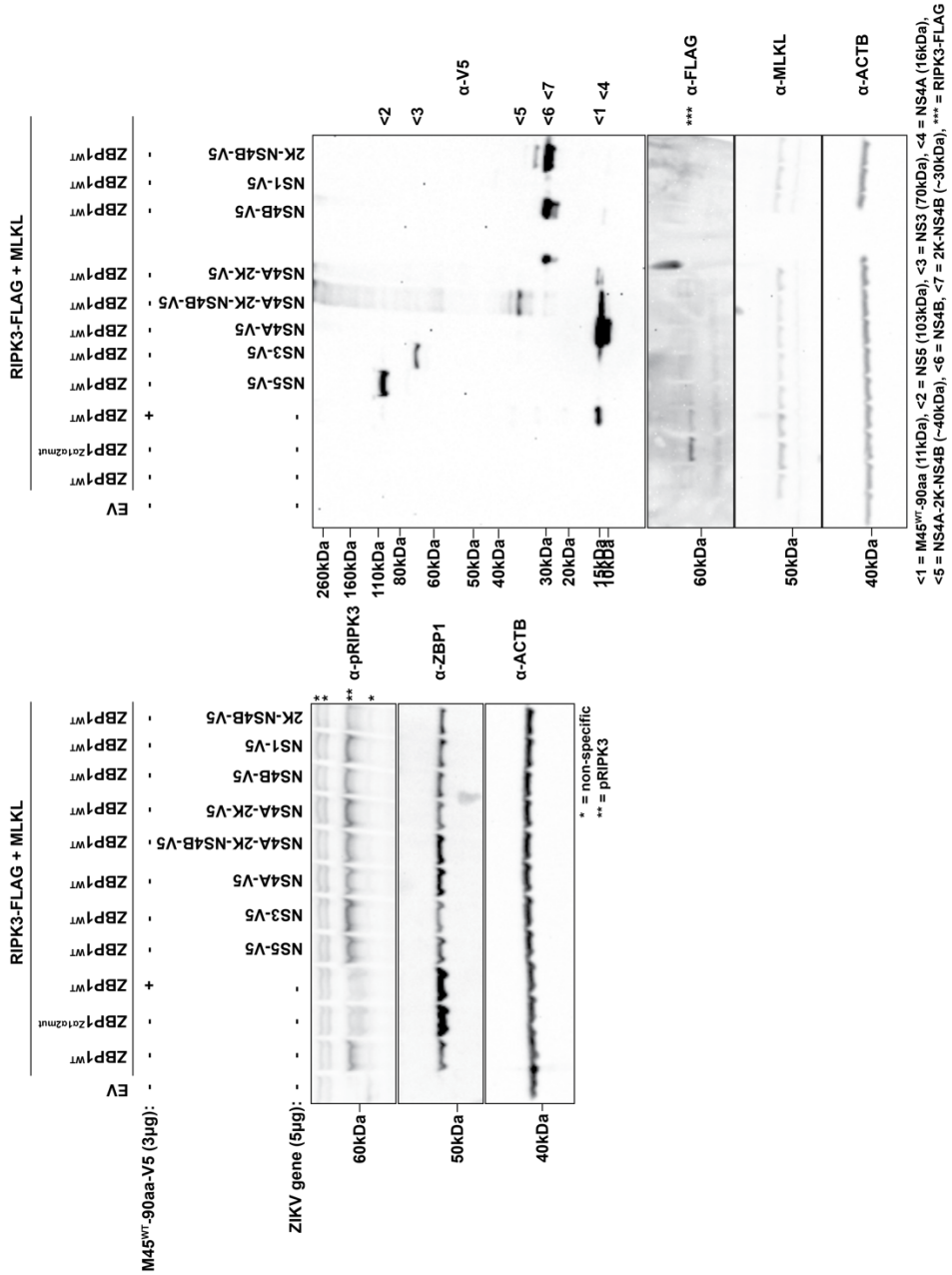


Figure S13. ZIKV proteins NS5, NS3, NS4A, NS4A-2K-NS4B, NS4B and 2K-NS4B do not inhibit ZBP1-mediated ZBD-dependent RIPK3 auto-phosphorylation.

HEK293T cells were co-transfected with plasmids encoding empty vector (EV) or RIPK3, MLKL and ZBP1, with or without a dose titration of plasmid encoding V5-tagged 90-amino acid fragment of M45 ($M45^{WT}$-90aa) or the ZIKV proteins indicated. 24h post-transfection, cells were harvested and lysates analysed by SDS-PAGE and western blotting with anti-pRIPK3 antibody (pSer-227) and the other antibodies indicated. Data are representative of 2 independent experiments (see Figure 37).

APPENDIX II SCIENCE COMMUNICATION & PUBLIC ENGAGEMENT

In an era that many are calling 'post-truth', it is as important as ever that scientific research be transparent and accessible to the general public. During my PhD, I have been very active in communicating science and engaging the public with my research. I will briefly highlight my science communication and public engagement work in this Appendix.

Communication is essential to the scientific process. My PhD research was communicated to scientists in my field through a peer-reviewed publication, on which I am second author, as well as through presentations at regional and international conferences. Specifically, I was selected to give short talks at the Oxford Immunology Symposium in 2018 and at the Keystone Symposium on 'Innate Immune Receptors: Roles in Immunology and Beyond' in 2019 (Taiwan). Moreover, I presented posters at several internal student symposiums as well as at the Keystone Symposium on 'Cells vs Pathogens: Intrinsic Defenses and Counter-defenses' in 2018 (USA). I was awarded the 1st prize for best poster at Oxford University Medical Sciences DPhil Day in 2017.

In addition to communicating my research to fellow scientists, I have made it my mission to enhance public understanding of science through a number of science communication initiatives. My short talks on HIV and influenza landed me in the regional final of the science communication competition FameLab UK in 2016

and, in 2017, I co-founded PubHD Oxford, a series of events hosted in Oxford pubs featuring short talks from PhD students about their research in front of non-expert audiences. I have been writing and editing articles on a broad range of scientific topics for general audiences since the start of my PhD, most notably for the *Science Innovation Union Editorial* and the *Guardian*. In 2018, I was awarded a British Science Association Media Fellowship, which I used to undertake a placement working on the science desk at the *Guardian*. Most recently, I have started a blog on Instagram called Science Sped Up, which features time-lapse videos of scientific experiments in action, alongside general explanations of the science behind them. I additionally launched a students' website for the Infection, Immunology & Translational Medicine DPhil programme as a science communication platform and I was responsible for keeping our laboratory webpages updated.

I believe that scientists have a responsibility to engage the public with the research we do. I have been involved in several online public engagement initiatives as well as in face-to-face engagement activities. In 2018, myself and a colleague were live-streamed from the laboratory speaking about viruses and our research, and answering live questions from our online audience via Facebook. This opportunity arose after I entered a competition that Oxford Sparks, a University portal for public engagement with science, ran across the University. In 2017, I co-developed a public engagement activity to communicate immunology research from the MRC Human Immunology Unit during the annual MRC Festival. I have

additionally hosted A-level student laboratory visits and visited schools in Oxfordshire to speak about my research and immunology in general.

Altogether, I would like to highlight my science communication and public engagement work as an important output of my thesis. I hope my efforts have inspired more people to engage with science and encouraged more scientists to engage the public with their research.

APPENDIX III PUBLICATIONS

The following manuscripts are appended to this thesis:

Maelfait, J., Liverpool, L. , Bridgeman, A., Ragan, K.B., Upton, J.W. & Rehwinkel, J. (2017). Sensing of viral and endogenous RNA by ZBP1/DAI induces necroptosis. *The EMBO journal*, e201796476.

Liverpool, L.*, Maelfait, J.* & Rehwinkel, J. Nucleic acid sensors and programmed cell death (review article). *Journal of Molecular Biology*. Under peer review (unpublished).

* equally contributing authors

Published online: July 17, 2017

Article

SOURCE DATA | TRANSPARENT PROCESS | OPEN ACCESS

THE EMBO JOURNAL

Sensing of viral and endogenous RNA by ZBP1/DAI induces necroptosis

Jonathan Maelfait[1,†,‡,*], Layal Liverpool[1], Anne Bridgeman[1], Katherine B Ragan[2], Jason W Upton[2] & Jan Rehwinkel[1,**]

Abstract

Nucleic acids are potent triggers for innate immunity. Double-stranded DNA and RNA adopt different helical conformations, including the unusual Z-conformation. Z-DNA/RNA is recognised by Z-binding domains (ZBDs), which are present in proteins implicated in antiviral immunity. These include ZBP1 (also known as DAI or DLM-1), which induces necroptosis, an inflammatory form of cell death. Using reconstitution and knock-in models, we report that mutation of key amino acids involved in Z-DNA/RNA binding in ZBP1's ZBDs prevented necroptosis upon infection with mouse cytomegalovirus. Induction of cell death was cell autonomous and required RNA synthesis but not viral DNA replication. Accordingly, ZBP1 directly bound to RNA via its ZBDs. Intact ZBP1-ZBDs were also required for necroptosis triggered by ectopic expression of ZBP1 and caspase blockade, and ZBP1 cross-linked to endogenous RNA. These observations show that Z-RNA may constitute a molecular pattern that induces inflammatory cell death upon sensing by ZBP1.

Keywords ZBP1; DAI; Z-RNA; cytomegalovirus; necroptosis
Subject Categories Immunology; RNA Biology
DOI 10.15252/embj.201796476 | Received 7 January 2017 | Revised 4 June 2017 | Accepted 13 June 2017 | Published online 17 July 2017
The EMBO Journal (2017) 36: 2529–2543

See also: **S Assil & SR Paludan** (September 2017)

Introduction

Nucleic acids form double-stranded helices. Double-stranded (ds) DNA typically adopts the so-called B-conformation, while dsRNA is usually in the A-conformation. Both DNA and RNA can also adopt a Z-form double helix that is characterised by a left-handed helical arrangement, a zigzag pattern of the phosphodiester backbone and the absence of major grooves (Wang *et al*, 1979; Hall *et al*, 1984; Rich & Zhang, 2003). Antibodies raised against Z-form RNA or DNA stain mammalian cells and chromosomes, respectively, suggesting that nucleic acids in this unusual conformation occur naturally in cells (Viegas-Péquignot *et al*, 1983; Zarling *et al*, 1990). However, biological functions of the Z-conformation are only partially understood (Rich & Zhang, 2003; Wang & Vasquez, 2007). Z-DNA is believed to play a role in transcription by relieving torsional strain induced within the DNA template by the movement of RNA polymerases, and Z-DNA may also promote genetic instability (Rich & Zhang, 2003; Wang & Vasquez, 2007). Physiological functions of Z-RNA remain unknown.

Early biochemical and structural studies identified a protein fold called Z-binding domain (ZBD) that specifically binds to Z-DNA but not to B-DNA (Herbert *et al*, 1993; Schwartz *et al*, 1999). This 78-amino-acid domain is also referred to as Zα or Zβ, and subsequent work showed that it not only binds to Z-DNA but also to Z-RNA (Brown *et al*, 2000; Placido *et al*, 2007). ZBDs have been identified in four proteins: ADAR1, ZBP1, E3L and PKZ (Athanasiadis, 2012). ADAR1 and ZBP1 are mammalian proteins implicated in antiviral innate immune responses. E3L is a poxvirus protein known to antagonise this host response. Lastly, PKZ is a fish protein related to mammalian PKR, also involved in antiviral immunity. This suggests an important role of ZBDs in innate antiviral immune responses (Athanasiadis, 2012) and may imply that Z-DNA and/or Z-RNA trigger such a host defence response. Z-form nucleic acids are further implicated in immune responses by the observation that sera from some systemic lupus erythematosus patients contain anti-Z-DNA autoantibodies (Lafer *et al*, 1983).

Z-DNA binding protein 1 (ZBP1, also known as DAI or DLM-1) has two N-terminal ZBDs (Zα1 and Zα2) and two RIP homotypic interaction motifs (RHIMs) (Ha *et al*, 2008; Kaiser *et al*, 2008; Rebsamen *et al*, 2009; Kim *et al*, 2011a,b; Yang *et al*, 2014). ZBP1 had initially been suggested to be a cytosolic B-DNA sensor that induces type I interferons (IFNs) (Takaoka *et al*, 2007). However, this observation could not be confirmed in ZBP1-deficient mice (Ishii *et al*, 2008). Instead, ZBP1 activates NF-κB and triggers necroptosis (Kaiser *et al*, 2008; Rebsamen *et al*, 2009; Upton *et al*, 2012), an inflammatory form of programmed cell death (Wallach *et al*, 2016). NF-κB activation is mediated by RIPK1 and RIPK3 kinases, which bind to ZBP1 via RHIM-RHIM interactions (Kaiser *et al*, 2008; Rebsamen *et al*, 2009). In contrast, ZBP1-dependent

1 Medical Research Council Human Immunology Unit, Radcliffe Department of Medicine, Medical Research Council Weatherall Institute of Molecular Medicine, University of Oxford, Oxford, UK
2 Department of Molecular Biosciences, LaMontagne Center for Infectious Disease, Institute for Cellular and Molecular Biology, University of Texas at Austin, Austin, TX, USA
*Corresponding author. Tel: +32 9 331 3745; E-mail: jonathan.maelfait@irc.vib-ugent.be
**Corresponding author. Tel: +44 1865 222362; E-mail: jan.rehwinkel@imm.ox.ac.uk
†Present address: Laboratory of Immunoregulation and Mucosal Immunology, VIB Center for Inflammation Research, Ghent, Belgium
‡Present address: Department of Internal Medicine, Ghent University, Ghent, Belgium

© 2017 The Authors. Published under the terms of the CC BY 4.0 license

necroptosis depends on RIPK3 recruitment and does not require RIPK1 (Upton *et al*, 2012). RIPK3 phosphorylates and activates the pseudokinase MLKL, which upon oligomerisation ruptures the plasma membrane, leading to cell death (Wallach *et al*, 2016).

Necroptosis mediates host defence by eliminating virus-infected cells (Mocarski *et al*, 2015). Viruses in turn suppress necroptosis. A well-studied example is mouse cytomegalovirus (MCMV) infection (Mocarski *et al*, 2015): MCMV prevents ZBP1- and RIPK3-dependent necroptosis by expression of M45 (Upton *et al*, 2010, 2012). M45 has a RHIM that disrupts the interaction of ZBP1 and RIPK3. MCMV expressing M45 with a mutated RHIM fails to inhibit necroptosis, resulting in death of infected cells (Upton *et al*, 2012). Necroptotic cell death is normally held in check by the proteolytic activity of the pro-apoptotic caspase-8. Cells can be sensitised to RIPK3-dependent necroptosis by genetic loss (Kaiser *et al*, 2011; Oberst *et al*, 2011) or chemical blockade of caspase-8 (Vandenabeele *et al*, 2006). During M45-RHIM-mutant MCMV infection, the viral M36 protein—also known as viral inhibitor of caspase-8-induced apoptosis (vICA)—is believed to predispose cells to necroptosis by blocking caspase-8 (McCormick *et al*, 2003; Ménard *et al*, 2003; Guo *et al*, 2015).

Here, we show that necroptosis triggered by MCMV-M45^{mutRHIM} or by ectopic ZBP1 expression and caspase blockade required binding of nucleic acids to the tandem ZBDs of ZBP1. We generated *Zbp1* knock-in mice carrying four amino acid substitutions that abrogate binding to Z-form nucleic acids. Cells from *Zbp1*-mutant mice are resistant to MCMV-M45^{mutRHIM}-induced necroptosis. During infection, inhibition of RNA transcription but not of viral DNA replication prevented ZBP1-dependent necroptosis and we found that ZBP1 bound to newly synthesised RNA. Furthermore, ZBP1 cross-linked to endogenous RNA and stained cells in an RNase-sensitive manner. In sum, these results show that ZBP1 is an RNA sensor.

Results

Cell death following MCMV-M45^{mutRHIM} infection requires intact ZBP1 ZBDs

We initially wished to confirm the role of ZBP1 in cell death upon virus infection. Expression of ZBP1 was induced by IFN in *Zbp1*$^{+/-}$ but not in *Zbp1*$^{-/-}$ primary mouse embryonic fibroblasts (MEFs; Fig 1A). We then assessed cell viability upon virus infection by determining intracellular ATP levels using CellTiter-Glo reagent. Infection with MCMV-M45^{mutRHIM}, a virus that fails to inhibit ZBP1-RIPK3-dependent necroptosis (Upton *et al*, 2012), induced cell death in *Zbp1*$^{+/-}$ primary MEFs following IFN pre-treatment (Fig 1B). In contrast, viability upon MCMV-M45^{mutRHIM} infection was much higher in IFN-treated *Zbp1*$^{-/-}$ primary MEFs (Fig 1B), despite comparable expression of RIPK3 and MLKL (Fig 1A). We also infected primary MEFs with MCMV-M45^{wt}, which did not cause much cell death in either *Zbp1*$^{+/-}$ or *Zbp1*$^{-/-}$ cells (Fig 1B). As a control, the induction of necroptosis by TNF stimulation in the presence of the caspase inhibitor zVAD (Vercammen *et al*, 1998) (hereafter simply TZ) was independent of ZBP1 (Fig 1B). Similar results were obtained in immortalised MEFs (Fig EV1A and B). These observations are consistent with an earlier report (Upton *et al*, 2012) and demonstrate that death of MCMV-infected cells required ZBP1 and was antagonised by the viral M45 protein.

To test if binding of Z-form nucleic acids to ZBP1 is involved in the induction of cell death during virus infection, we mutated key conserved residues involved in Z-RNA/DNA binding in mouse ZBP1. Based on the structures of the ZBP1 Zα1 and Zα2 domains (Schwartz *et al*, 2001; Ha *et al*, 2008; Kim *et al*, 2011a,b; Yang *et al*, 2014) and on sequence alignments (Fig 1C and D), we introduced N46A and Y50A mutations into Zα1 (Zα1^{mut}), N122A and Y126A substitutions into Zα2 (Zα2^{mut}), and all four mutations together (Zα1α2^{mut}). Mutation of the corresponding residues in ADAR1's Zα ZBD completely abolishes Z-DNA binding without altering protein stability (Schade *et al*, 1999); accordingly, we predicted diminished binding of our ZBP1 mutants to Z-RNA/DNA. Wild-type and Zα1α2^{mut} ZBP1 proteins were equally able to induce an NF-κB reporter upon ectopic expression together with RIPK3 in HEK293T cells, suggesting that the mutant protein folds correctly and retains signalling via its RHIMs (Figs 1E and EV1C).

We reconstituted immortalised *Zbp1*$^{-/-}$ MEFs with ZBP1 3xFLAG-tagged ZBD mutants (Fig 1F). Cell viability following TZ treatment or MCMV-M45^{wt} infection was comparable between parental *Zbp1*$^{-/-}$ and ZBP1-reconstituted cells (Fig 1G). MCMV-M45^{mutRHIM} infection induced pronounced cell death in ZBP1 wild-type reconstituted cells (Fig 1G and H). In contrast, ZBP1-Zα1α2^{mut}-expressing cells displayed higher viability after infection and

Figure 1. Necroptosis during MCMV infection requires nucleic acid binding to the ZBDs of ZBP1.

A, B Primary MEFs of the indicated genotypes were treated or not with 100 U/ml of IFN-A/D for 16 h. (A) Cell extracts were subjected to Western blot analysis using the indicated antibodies. (B) Cells were treated with 30 ng/ml TNF and 20 μM zVAD (TZ) or were infected with the indicated viruses at an MOI of 10. After 16 h, cell viability was assessed using CellTiter-Glo reagent. Values for untreated cells were set to 100%.

C Domain architecture of mouse ZBP1.

D Conservation of key amino acids in ZBP1's ZBDs. ZBP1 sequences from the indicated species were aligned using Clustal Omega and the sequence context of the conserved asparagine and tyrosine residues involved in Z-DNA/RNA binding is shown.

E HEK293T cells were transfected with 50 ng NF-κB firefly luciferase and 25 ng *Renilla* luciferase reporter plasmids, together with expression vectors for RIPK3 (0.2 ng) and HA-STING or ZBP1-3xFLAG (20, 100, 500 ng). Luciferase activity was measured after 24 h, and the ratio of firefly and *Renilla* luciferase was set to 1 for control cells transfected with empty vector. Cell lysates were analysed for expression of the indicated proteins by Western blot (bottom). Asterisk (*) indicates residual signal from the α-HA antibody.

F–I Immortalised *Zbp1*$^{-/-}$ MEFs were reconstituted with the indicated ZBP1 mutants. (F) Cell extracts were subjected to Western blot analysis using the indicated antibodies. (G and H) Cell viability upon TZ treatment or MCMV infection was assessed as in (B). In (G), an MOI of 10 was used. (I) Cell death was monitored upon infection (MOI = 3) or TZ treatment using an in-incubator imaging platform (Incucyte) and the dye Sytox Green that stains dead cells.

Data information: Data are representative of three or more independent experiments. Panels (A, B, E and G–I) represent mean ± SD (n = 3). **P < 0.01, ***P < 0.001; two-way ANOVA. See also Fig EV1.
Source data are available online for this figure.

 © 2017 The Authors

behaved similar to the parental *Zbp1*$^{-/-}$ cells, while ZBP1-Zα1^{mut} and ZBP1-Zα2^{mut} cells showed intermediate phenotypes (Fig 1G and H), with a greater contribution to cell death of the Zα2 domain. Cell death induced by MCMV-M45^{mutRHIM} in wild-type ZBP1-expressing cells was also observed by live-cell microscopy using the dye Sytox-Green, which stains cells that have lost membrane integrity, and cell death was detected from 8 h post-infection onwards (Fig 1I). We then used mouse NIH3T3 fibroblasts, a transformed cell line. Endogenous ZBP1 expression was undetectable by Western blot, but could be induced by IFN treatment (Fig EV1D). We stably transduced NIH3T3 cells to express either 3xFLAG-tagged wild-type or mutant ZBP1 (Fig EV1D and F). Cell viability was comparable between these cells after MCMV-M45^{wt} infection (Fig EV1E) and upon TZ treatment (Fig EV1G and H). Consistent with our results in MEFs, cell viability was decreased in wild-type ZBP1 but not in ZBP1-Zα1α2^{mut}-expressing cells following infection with

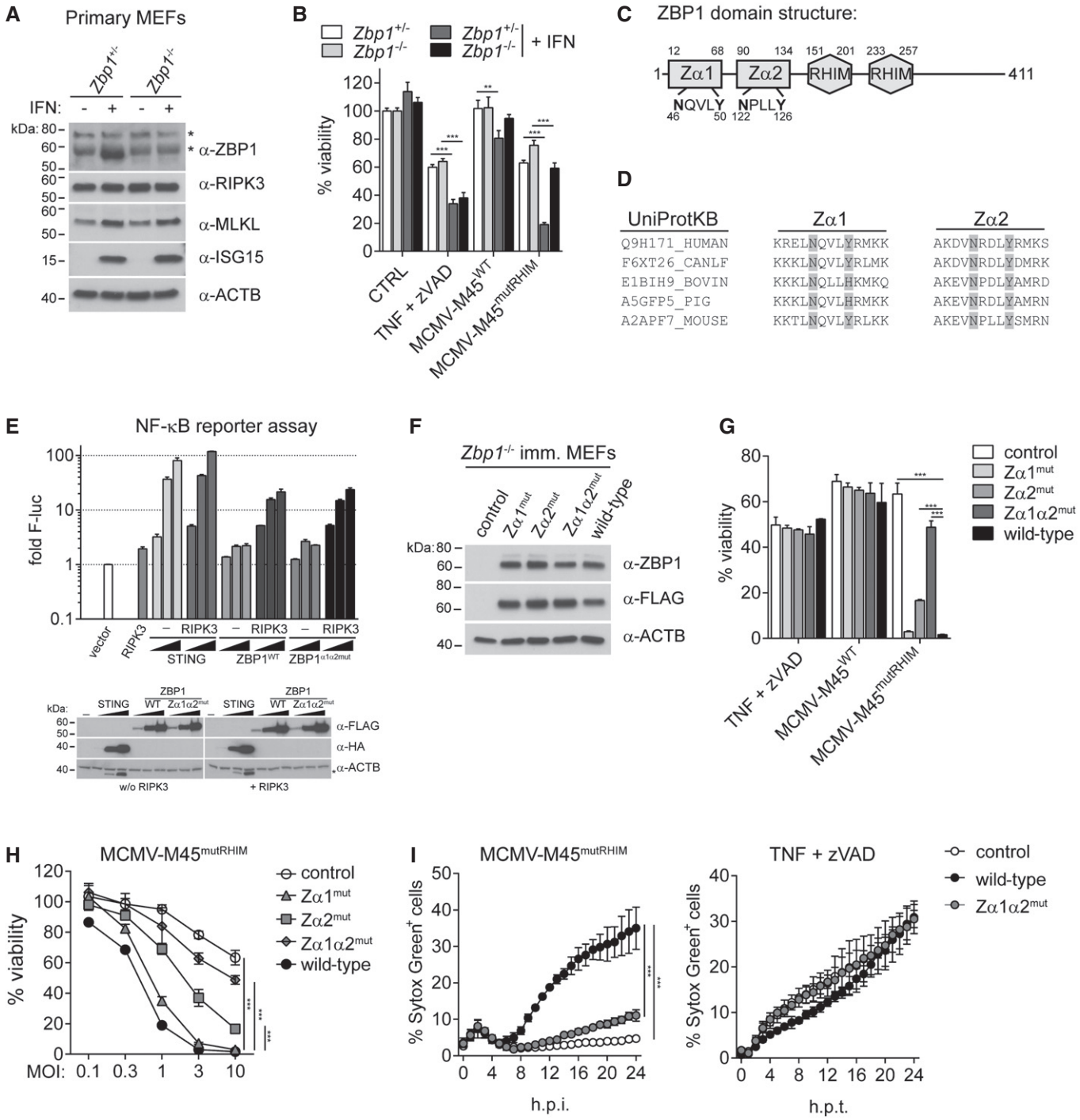


Figure 1.

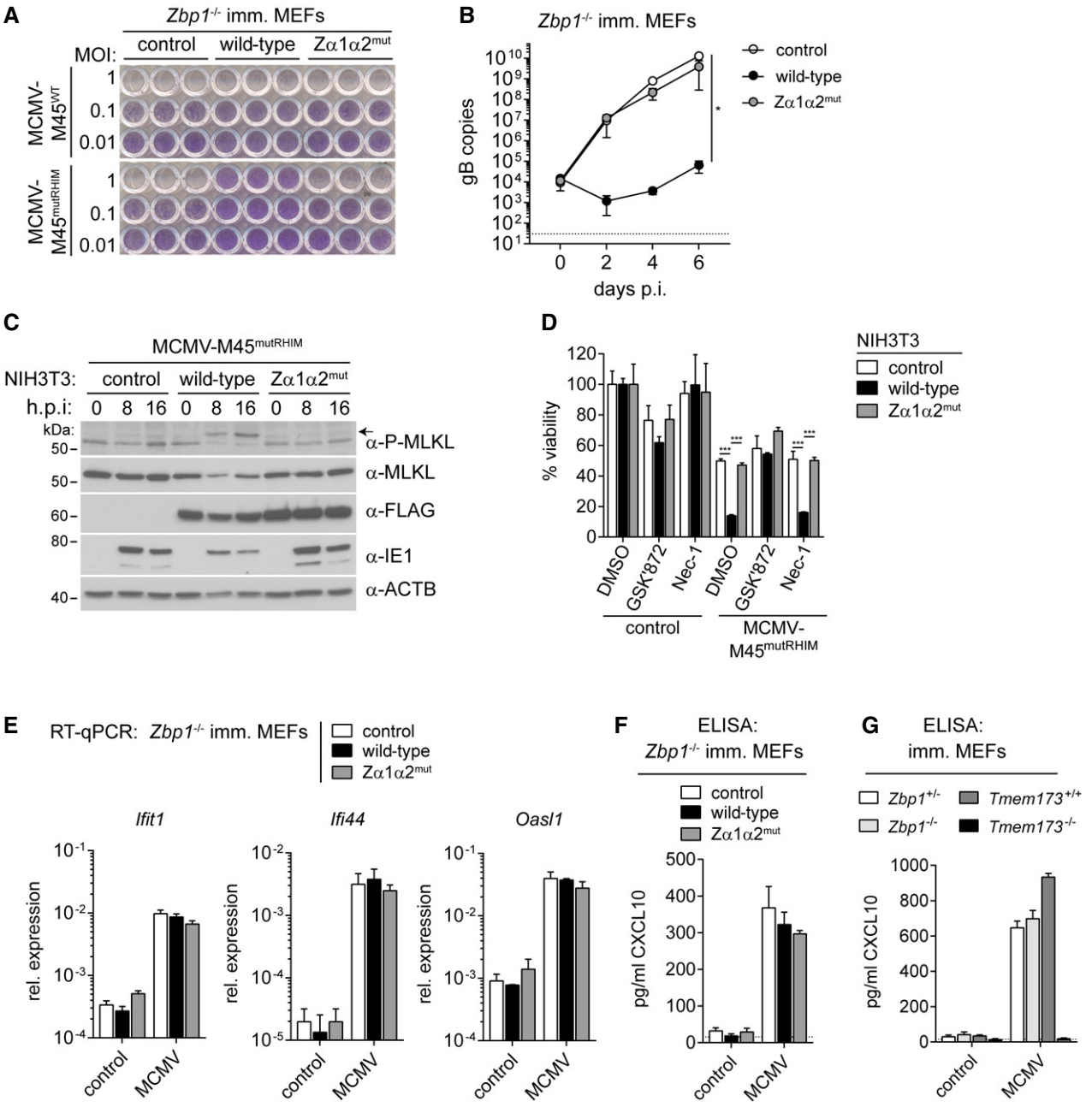


Figure 2. ZBP1 restricts MCMV replication by inducing necroptosis but not IFN expression.

A Immortalised *Zbp1*$^{-/-}$ MEFs reconstituted with wild-type or mutant ZBP1 were infected as indicated. After 5 days, cells were fixed and stained with crystal violet.

B Immortalised *Zbp1*$^{-/-}$ MEFs reconstituted with wild-type or mutant ZBP1 were infected with MCMV-M45^{mutRHIM} at an MOI of 0.01. DNA samples were collected at 0, 2, 4 or 6 days after infection and analysed by qPCR. gB copy numbers were derived from a titration using defined amounts of gB plasmid. The dotted line represents the lower limit of detection.

C NIH3T3 cells reconstituted with wild-type or mutant ZBP1 were infected as indicated using an MOI of 3. After 0, 8 or 16 h, cell lysates were subjected to Western blot analysis under reducing conditions using the indicated antibodies. The arrow indicates phosphorylated MLKL.

D NIH3T3 cells reconstituted with wild-type or mutant ZBP1 were infected with MCMV-M45^{mutRHIM} at an MOI of 10. Cells were simultaneously treated with 3 μM GSK'872 (RIPK3 inhibitor) or 30 μM Nec-1 (RIPK1 inhibitor) or 0.1% DMSO as a control. Cell viability was analysed 24 h after infection as in Fig 1B.

E Immortalised *Zbp1*$^{-/-}$ MEFs reconstituted with wild-type or mutant ZBP1 were infected with MCMV-M45^{mutRHIM} at an MOI of 3. RNA samples were collected 8 h after infection and analysed by RT–qPCR.

F, G CXCL10 was analysed by ELISA in supernatants from MEFs of the indicated genotypes infected with MCMV-M45^{mutRHIM} (MOI = 3; 8 h post-infection). The dotted line represents the lower limit of detection.

Data information: Data are representative of two or more independent experiments. Panels (B and D–G) represent mean ± SD (n = 3). *P < 0.05, ***P < 0.001; two-way ANOVA. See also Fig EV2.
Source data are available online for this figure.

 © 2017 The Authors

MCMV-M45^{mutRHIM} (Fig EV1E–H). Taken together, these observations suggest that induction of cell death by ZBP1 requires intact ZBDs and may imply that nucleic acids in Z-conformation trigger this response.

Nucleic acid recognition by ZBP1 is essential for necroptosis and virus restriction, but not for IFN induction

We next wished to test whether restriction of MCMV infection by ZBP1 depends on the protein's ZBDs. Infection of cells with MCMV results in lytic cell death after several days of culture due to virus replication. Expression of wild-type ZBP1 but not ZBP1-Zα1α2^{mut} protected *Zbp1*$^{-/-}$ MEFs or NIH3T3 cells against MCMV-M45^{mutRHIM}-induced cytopathic effects 5 days post-infection (Figs 2A and EV2A). Furthermore, replication of the virus genome was blunted by wild-type but not by mutant ZBP1 (Fig 2B). These observations show that ZBP1 defended cells against MCMV and that intact ZBP1 ZBDs were required for this.

This block in virus replication may depend on ZBP1-dependent cell death or engagement of an IFN response in infected cells. We first explored how mutations in ZBP1's ZBDs affected MCMV-M45^{mutRHIM}-induced cell death. Previous work suggested that the type of cell death triggered by ZBP1 upon MCMV-M45^{mutRHIM} infection is necroptosis (Upton *et al*, 2012). Upon phosphorylation by RIPK3, MLKL forms trimers and large multimeric complexes, which execute necroptosis by causing plasma membrane permeabilisation (Wallach *et al*, 2016). Phosphorylation of MLKL was only observed in MCMV-M45^{mutRHIM}-infected NIH3T3 cells reconstituted with wild-type ZBP1 and not in ZBP1-Zα1α2^{mut} ZBP1-expressing cells (Fig 2C). Concomitantly, reduced levels of the viral IE1 protein accumulated in cells expressing wild-type ZBP1 (Fig 2C). Furthermore, we observed the formation of MLKL-trimers (Cai *et al*, 2014) in non-reducing SDS–PAGE gels after induction of necroptosis in NIH3T3 cells with TZ (Fig EV2B). Large MLKL oligomers, which did not migrate through the gel, were also observed in the gel-loading pocket (Dondelinger *et al*, 2014; Fig EV2B). MCMV-M45^{wt} infection did not change MLKL electrophoretic mobility (Fig EV2B), which is in line with our earlier observation that this virus does not cause cell death (Fig 1). MCMV-M45^{mutRHIM} infection induced MLKL oligomerisation at 16 h post-infection (Figs 2C and EV2B). These effects were enhanced and accelerated in cells expressing wild-type ZBP1 but not in cells reconstituted with ZBP1-Zα1α2^{mut} (Fig EV2B). Furthermore, the viability of MCMV-M45^{mutRHIM}-infected NIH3T3 cells expressing wild-type ZBP1 was rescued upon treatment with the RIPK3 kinase inhibitor GSK'872 (Fig 2D). As described previously (Upton *et al*, 2010), blocking RIPK1 activity with Nec-1 had no effect on virus-induced cell death (Fig 2D). These observations show that ZBP1 indeed activates necroptosis in this setting.

MCMV-M45^{mutRHIM} infection also induced an IFN response. Expression of the interferon-stimulated genes (ISGs) *Ifit1*, *Ifi44* and *Oasl1* was increased upon infection and was not altered in cells expressing ZBP1 (Fig 2E). Consistent with this observation, the expression and secretion of CXCL10, a chemokine that signifies the induction of an IFN response, were independent of ZBP1 or MCMV M45 protein (Figs 2F and EV2C). Instead, CXCL10 induction was reduced to background levels in *Tmem173*$^{-/-}$ cells that lack STING, a protein involved in cytosolic DNA sensing (Figs 2G and EV2C; Chen *et al*, 2016). Furthermore, overexpression of ZBP1 did not induce an IFNβ reporter in HEK293T cells (Fig EV2D). In sum, these results demonstrate that ZBP1 and its ZBDs were required specifically for the induction of necroptosis upon virus infection and not for the induction of an IFN response.

ZBP1-Zα1α2^{mut} knock-in mice do not restrict MCMV-M45^{mutRHIM} and cells from these animals do not undergo virus-triggered necroptosis

To substantiate our conclusion that intact ZBDs are required for ZBP1-dependent necroptosis, we developed a knock-in mouse in which the endogenous *Zbp1* allele is replaced by *Zbp1-Zα1α2*^{mut} (*Zbp1*^{Zα1α2}) carrying the four point mutations shown in Fig 1C. The generation and validation of this model are detailed in Fig EV3A and B. We obtained primary MEFs by crossing of *Zbp1*$^{+/Zα1α2}$ animals. Similar levels of *Zbp1* mRNA and ZBP1 protein were expressed at baseline and after IFN induction in cells expressing only wild-type ZBP1 (*Zbp1*$^{+/+}$), only mutant ZBP1 (*Zbp1*$^{Zα1α2/Zα1α2}$) or both (*Zbp1*$^{+/Zα1α2}$) (Figs 3A and EV3C). Consistent with our experiments based on ectopic ZBP1 expression (Figs 1 and 2), intact ZBDs of endogenous ZBP1 were required for cell death induced by MCMV-M45^{mutRHIM} (Fig 3B and C). Cell death induced by TZ treatment was not affected by mutations in *Zbp1* (Figs 3B and EV3D). Furthermore, the levels of phosphorylated MLKL and MLKL oligomerisation were reduced in *Zbp1*$^{Zα1α2/Zα1α2}$ primary MEFs upon MCMV-M45^{mutRHIM} infection (Figs 3D and EV3E), but not after TZ treatment (Fig 3E). Finally, virus growth and accumulation of the viral IE1 protein were enhanced in *Zbp1*$^{Zα1α2/Zα1α2}$ primary MEFs (Fig 3D and F). To test whether intact ZBDs are required to restrict virus replication *in vivo*, we infected *Zbp1*$^{Zα1α2/Zα1α2}$ knock-in mice with MCMV-M45^{mutRHIM}. After 5 days, we were able to recover infectious virus from the spleens of eight of 13 infected *Zbp1*$^{Zα1α2/Zα1α2}$ animals, while the spleens of all wild-type and heterozygous mice remained free of virus (Fig 3G). As expected, no differences in splenic virus titres were observed between the genotypes when mice were infected with wild-type MCMV (Fig 3G). These observations provide further evidence that recognition of nucleic acids, potentially in Z-conformation, by ZBP1 is required for the induction of necroptosis and virus restriction.

MCMV-induced necroptosis requires viral RNA synthesis but not DNA replication

To define the molecular requirements of ZBP1 and necroptosis activation in MCMV-infected cells, we co-cultured NIH3T3 cells expressing wild-type and Zα1α2^{mut} ZBP1 at a 2:1 ratio. The latter cells were labelled with a dye prior to co-culture. We infected co-cultures with MCMV-M45^{wt} or MCMV-M45^{mutRHIM} and, after 16 h, determined the ratio of wild-type ZBP1 and ZBP1-Zα1α2^{mut} cells by flow cytometry (Fig 4A). Infection with MCMV-M45^{wt} did not affect the ratio of these cells; however, MCMV-M45^{mutRHIM} infection resulted in selective loss of wild-type ZBP1-expressing cells (Fig 4A). This observation shows that ZBP1-dependent cell death is cell autonomous and further indicates that infection generates an intracellular ZBP1 agonist, conceivably a nucleic acid in Z-conformation.

To determine whether viral DNA replication was required for ZBP1 activation, we treated infected cells with 50 μM of the

© 2017 The Authors

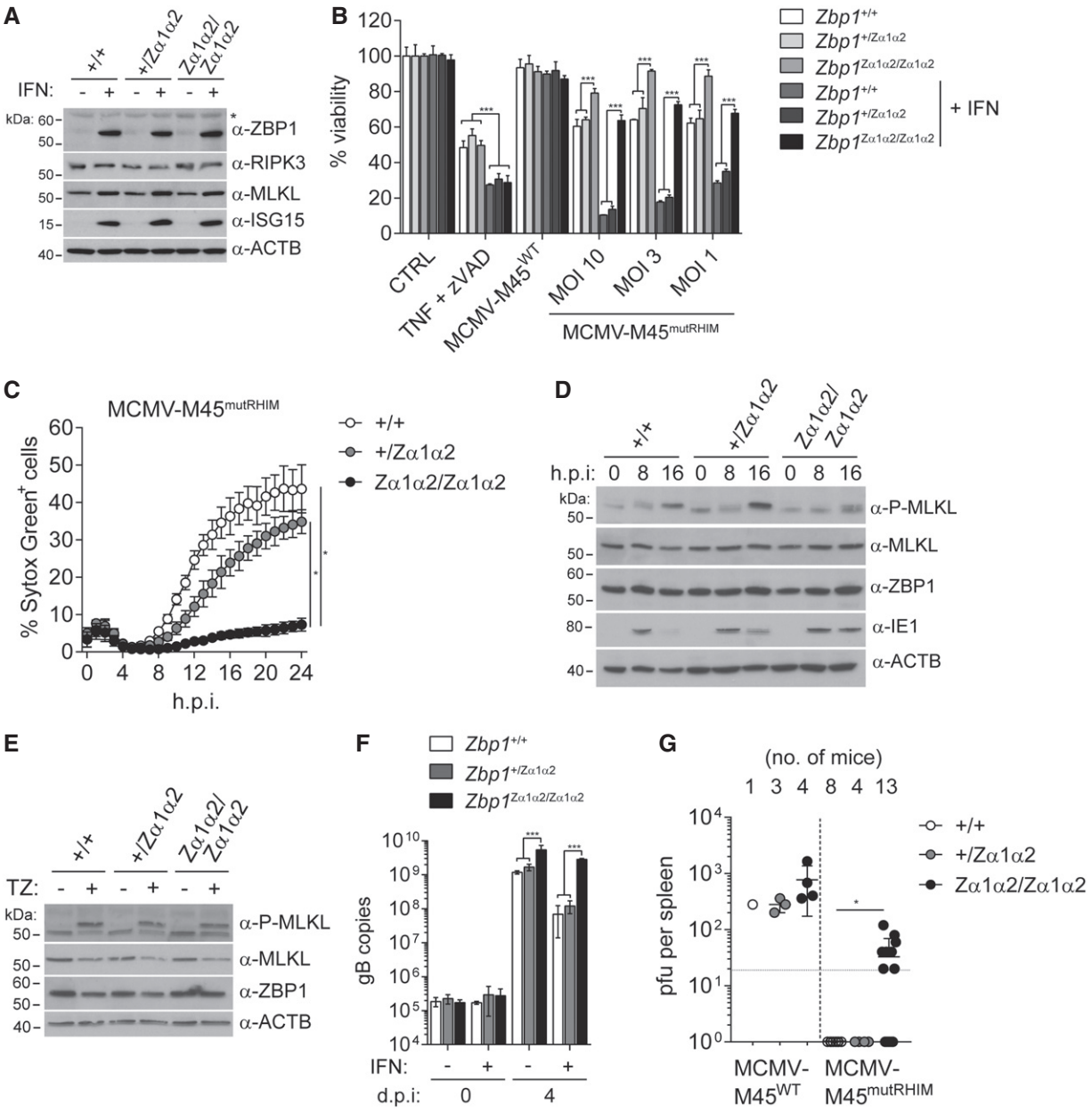


Figure 3. Knock-in of ZBP1-Zα1α2^{mut} abrogates MCMV-triggered necroptosis.

A Primary MEFs of the indicated genotypes were treated or not with 100 U/ml of IFN-A/D for 16 h. Cell extracts were subjected to Western blot analysis using the indicated antibodies. Asterisk (*) indicates a non-specific band.

B Primary MEFs of the indicated genotypes were treated or not with 100 U/ml of IFN-A/D for 16 h. Cells were treated with TZ or were infected with the indicated viruses (WT MCMV: MOI = 3). After 24 h, cell viability was assessed using CellTitre-Glo reagent. Values for untreated control cells were set to 100%.

C Primary MEFs of the indicated genotypes were treated or not with 100 U/ml of IFN-A/D for 16 h. Cell death was monitored upon infection with MCMV-M45^{mutRHIM} (MOI = 3) using an in-incubator imaging platform (Incucyte) and the dye Sytox Green that stains dead cells.

D, E Primary MEFs of the indicated genotypes were treated or not with 100 U/ml of IFN-A/D for 16 h. Cells were infected with MCMV-M45^{mutRHIM} at an MOI of 3 for 0, 8 and 16 h (D) or treated for 8 h with TZ (E), and cell lysates were analysed by Western blot.

F Primary MEFs of the indicated genotypes were treated or not with 100 U/ml of IFN-A/D for 16 h. DNA samples were collected at 0 and 4 days after infection and analysed by qPCR. gB copy numbers were derived from a titration using defined amounts of gB plasmid.

G Zα1α2-mutant Zbp1 knock-in (*Zbp1*$^{Zα1α2/Zα1α2}$), heterozygous (*Zbp1*$^{+/Zα1α2}$) and wild-type (*Zbp1*$^{+/+}$) littermate mice were infected with 2 × 10^6 pfu MCMV-M45^{WT} (one experiment) or MCMV-M45^{mutRHIM} (pooled data from two experiments using independent virus stocks) by intraperitoneal injection. Five days post-infection mice were sacrificed and viral titres in spleens were determined by plaque assay. Each dot represents one mouse. The dotted horizontal line depicts the detection limit.

Data information: If not indicated otherwise, data are representative of two or more independent experiments. Panels (B, C, F and G) show mean ± SD (n = 3 in B, C, F). *P < 0.05, ***P < 0.001; two-way ANOVA (panels B, C and F) and Mann–Whitney t-test (panel G). See also Fig EV3.
Source data are available online for this figure.

 © 2017 The Authors

nucleotide analogue ganciclovir (Smee *et al*, 1995). Although this effectively prevented MCMV replication in NIH3T3 cells and immortalised MEFs (Fig EV4A), virus-induced cell death in wild-type ZBP1-reconstituted cells remained unaffected (Fig 4B). UV inactivation of MCMV-M45^{mutRHIM} abrogated viral replication and expression of viral genes (Figs 4C, and EV4A and B). At the same time, CXCL10 protein and ISG mRNA induction, which are dependent on STING (Figs 2G and EV2C), remained normal (Figs 4C and EV4B). Importantly, UV-treated MCMV did not induce cell death (Fig 4B). Together with the result using the DNA replication inhibitor ganciclovir, this suggested that viral RNA transcription was required for ZBP1-dependent necroptosis. Indeed, inhibition of *de novo* RNA synthesis using actinomycin D (ActD) prevented cell death induced by MCMV-M45^{mutRHIM} in NIH3T3 cells expressing wild-type ZBP1 (Fig 4D). Similarly, ActD but not the translation inhibitor cycloheximide (CHX) blocked MCMV-M45^{mutRHIM} induced cell death in primary MEFs (Fig 4E). We also interfered with expression of the viral immediate early protein IE3 that is required for expression of early and late genes (Angulo *et al*, 2000). siRNA-mediated depletion of IE3 was confirmed using MCMV-IE1/3-GFP infection (Martínez *et al*, 2010; Fig EV4C and D). IE3 depletion led to diminished cell death upon infection of NIH3T3 cells expressing wild-type ZBP1 with MCMV-M45^{mutRHIM} (Fig 4F). MCMV-M45^{mutRHIM} infection predisposes NIH3T3 cells to TNF-induced cell death independent of ZBP1 expression (Fig EV4E). This predisposition is likely due to expression of the MCMV protein M36, which blocks caspase-8 and in combination with TNF treatment triggers necroptosis (Guo *et al*, 2015; Omoto *et al*, 2015). IE3 depletion did not influence cell death triggered by MCMV-M45^{mutRHIM} and TNF, indicating that IE3 depletion did not change sensitisation to necroptosis (Fig EV4F). MCMV induces a potent IFN response (Fig 2E and F), and IFN-induced endogenous transcripts could contribute to ZBP1 activation. To test this, we cultured wild-type ZBP1-reconstituted MEFs in the presence of neutralising antibodies against the type I IFN receptor (anti-IFNAR1). Blockade of IFNAR1 signalling did not affect MCMV-M45^{mutRHIM}-induced cell death, while the expression of the ISGs *Ifit1* and *Ifi44*, but not of *Ifnb*, was reduced upon anti-IFNAR1 treatment (Fig EV4G and H). Taken together, these data show that MCMV RNA transcripts generated in infected cells contribute to the activation of ZBP1 and necroptosis.

To further substantiate this conclusion, we employed the PAR-CLIP protocol (Fig 4G; Hafner *et al*, 2010). In brief, NIH3T3 cells expressing ZBP1-3xFLAG were pulsed with photo-activatable nucleoside analogues (4SU or 6SG) and were then infected with MCMV-M45^{mutRHIM}. Eight hours post-infection, cells were treated with UV-A light (365 nm), which only cross-links newly synthesised RNA that contains 4SU or 6SG to proteins. Cells were lysed and treated with RNase A. In this setting, small fragments of RNA are protected from degradation by cross-linking to proteins. ZBP1 was then immunoprecipitated using α-FLAG antibody and stringent conditions (see Materials and Methods). The RNA-ZBP1 complex was visualised by ^{32}P labelling of the RNA, followed by gel electrophoresis, blotting and autoradiography (Fig 4G). Indeed, we observed bands corresponding to the molecular weight of ZBP1 (60 kDa) when MCMV-infected cells were treated with 4SU or 6SG (Fig 4G). To investigate whether cross-linking of newly synthetised RNA required intact ZBDs, NIH3T3 cells expressing wild-type or mutant ZBP1 were infected with MCMV-M45^{WT} in the presence of 6SG. Wild-type M45-expressing virus was used to prevent loss of wild-type ZBP1-expressing cells due to necroptosis. After cross-linking, we observed enhanced ZBP1-RNA complex formation with wild-type ZBP1 compared to mutant ZBP1, confirming that ZBDs are important for RNA binding (Fig 4H). These finding supports the notion that ZBP1 binds newly synthesised RNA in infected cells.

Ectopic expression of ZBP1 predisposes cells to necroptosis

Surprisingly, we observed that expression of ZBP1 in NIH3T3 cells triggered spontaneous cell death upon caspase inhibition with zVAD (Figs 5A and EV5A). zVAD had a similar, albeit less pronounced, effect in immortalised MEFs (Fig 5A). Cell death in zVAD-treated cells expressing ZBP1 required intact ZBDs (Figs 5A and EV5A). Phosphorylation of MLKL at 16 h post-treatment confirmed that cells died by necroptosis (Fig EV5B). Furthermore, treatment with the RIPK3 inhibitor GSK'872 prevented cell death in zVAD-treated cells (Fig 5B). Viability was also restored by Nec-1 treatment,

Figure 4. ZBP1 binds newly synthesised RNA in MCMV-infected cells.

A NIH3T3 cells expressing mutant ZBP1 were labelled with CellTrace Violet and were then co-cultured with cells expressing wild-type ZBP1 at a 1:2 ratio. Cells were then infected as indicated (MOI 1, 3 and 10) and analysed by flow cytometry after 16 h. Representative FACS histograms (MOI 3) are shown (left), and ratios of wild-type to mutant cell numbers were calculated (right).

B Immortalised *Zbp1*$^{-/-}$ MEFs were infected with MCMV-M45^{mutRHIM} in the presence or not of 50 μM ganciclovir (GCV) or with UV-treated virus at an MOI of 10. After 16 h, cell viability was assessed using CellTitre-Glo reagent. Values for untreated control cells were set to 100%.

C Using supernatants and RNA samples from (B), CXCL10 protein levels and *Ifi44* and *M36* mRNA levels were determined by ELISA and RT–qPCR, respectively.

D Cell death was monitored upon infection of NIH3T3 cells expressing wild-type ZBP1 with MCMV-M45^{mutRHIM} (MOI = 3) using an in-incubator imaging platform (Incucyte) and the dye YOYO-3 that stains dead cells. Actinomycin D (ActD) was added (5 μg/ml) at the indicated time points.

E Primary MEFs of the indicated genotypes were pre-treated with 100 U/ml IFN-A/D for 16 h and were then treated with TZ, CHX (50 μg/ml) or ActD (5 μg/ml) in the presence or absence of MCMV-M45^{mutRHIM}. Cell viability was assessed as in (B).

F NIH3T3 cells expressing wild-type ZBP1 were transfected with the indicated siRNAs and were then infected with MCMV-M45^{mutRHIM}. Cell viability was assessed as in (D).

G Cells were treated with 100 μM 4SU or 6SG and infected with MCMV-M45^{mutRHIM} for 8 h. Binding of newly synthesised RNA to ZBP1 was analysed by PAR-CLIP (see Materials and Methods). Shown is an autoradiogram after electrophoresis and blotting of ZBP1 immunoprecipitates.

H NIH3T3 cells expressing wild-type or mutant ZBP1 were treated with 100 μM 6SG and were infected with MCMV-M45^{WT} at an MOI of 3 for 8 h. Binding of ZBP1 to RNA was analysed as in (G).

Data information: Data are representative of three or more independent experiments. Panels (A–F) show mean ± SD (n = 3). *P < 0.05, **P < 0.01, ***P < 0.001; two-way ANOVA. See also Fig EV4.
Source data are available online for this figure.

© 2017 The Authors

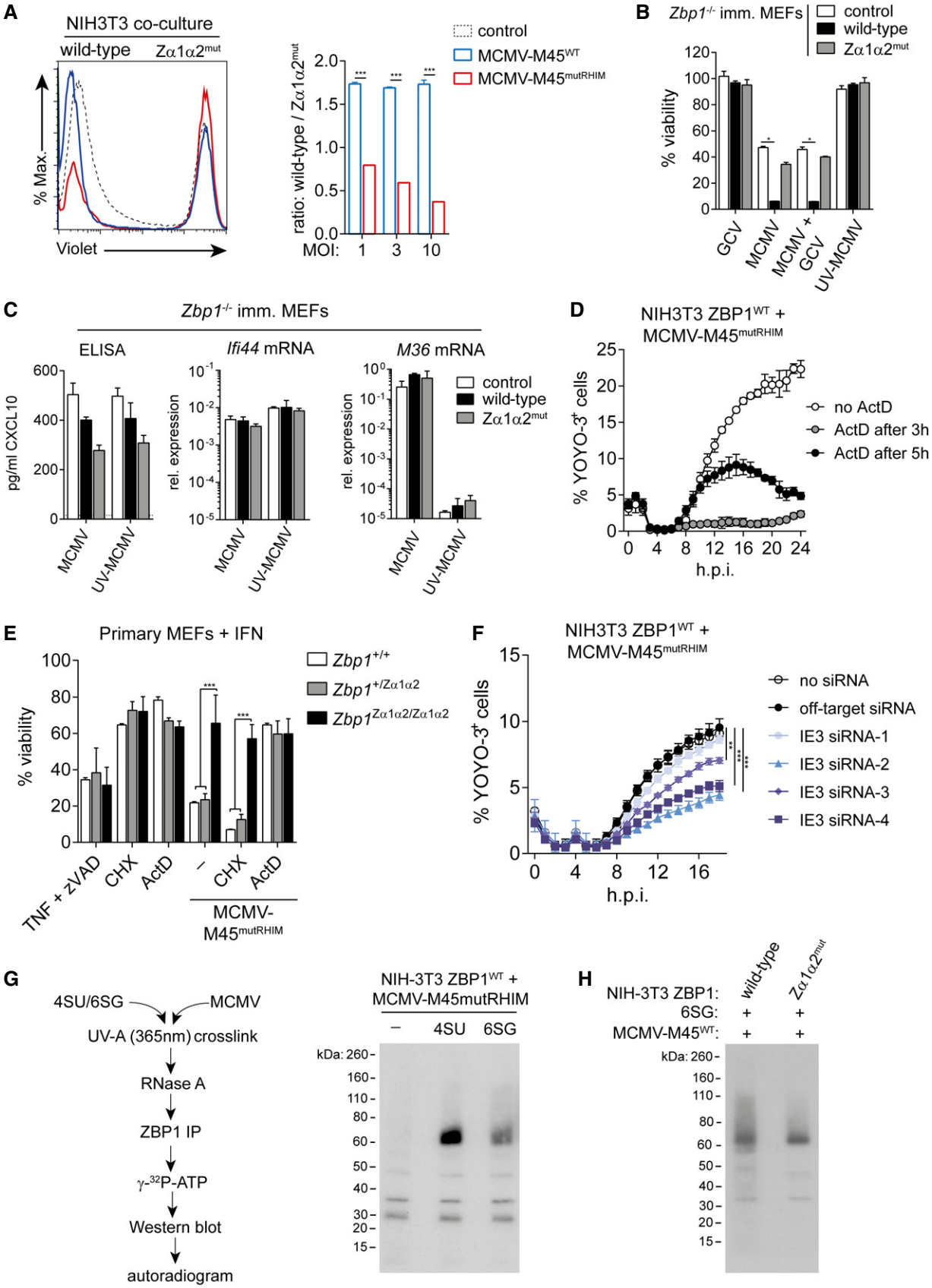


Figure 4.

 © 2017 The Authors

suggesting that spontaneous ZBP1-dependent cell death induced by caspase inhibition additionally requires the activity of RIPK1 (Fig 5B).

Next, using a polyclonal cell population, we generated NIH3T3 clones expressing wild-type ZBP1 at different levels by limiting dilution (Figs 5C, and EV5C and D). Expression of ZBP1 at both low and high levels sensitised cells to killing by MCMV-M45^{mutRHIM} (Fig 5D). In contrast, cell death triggered by ectopic ZBP1 and zVAD required high levels of expression (Fig 5D). To further explore this observation, we transduced cells expressing wild-type or Zα1α2^{mut} ZBP1 with M36 that blocks caspase-8-mediated apoptosis. This led to selective loss of cells expressing wild-type ZBP1 and M36 (Fig 5E). Western blot analysis further indicated that expression of wild-type ZBP1 and M36 was mutually exclusive, indicating death of cells expressing these two proteins together (Fig 5F). Taken together, these observations suggested that cells contain endogenous nucleic acids that engage ZBP1 if present at sufficiently high levels. This then leads to necroptosis in conditions where caspase-8 activity is blocked.

ZBP1 binds endogenous RNA

To further explore the observation that ZBP1 triggers necroptosis in response to endogenous nucleic acids, we used recombinant ZBP1 protein as a staining reagent in uninfected cells. We expressed 3xFLAG-tagged ZBP1 and ZBP1-Zα1α2^{mut} in HEK293T cells and purified the proteins by immunoprecipitation (Fig EV6A). We then incubated uninfected, fixed and permeabilised HEK293T cells with purified ZBP1 protein, followed by staining with a secondary α-FLAG antibody. Cells were analysed by flow cytometry. Recombinant wild-type ZBP1 stained cells, whereas ZBP1-Zα1α2^{mut} showed only background staining (Fig 6A, left panel). Interestingly, the labelling of cells with wild-type ZBP1 was sensitive to RNase but not to DNase treatment (Fig 6A, middle and right panel). These observations suggest that ZBP1, *via* its ZBDs, binds endogenous RNA, potentially in the Z-conformation.

Next, we used cross-link immunoprecipitation (CLIP, Fig 6B) to further explore the binding of endogenous nucleic acids to ZBP1 (Darnell, 2010). In brief, we cross-linked nucleic acids and proteins using UV-C light (254 nm) in uninfected NIH3T3 cells expressing ectopic ZBP1-3xFLAG. Cell extracts were then treated with DNase and/or RNase. This degrades free nucleic acids leaving intact fragments of DNA or RNA cross-linked to proteins. Next, we immunoprecipitated ZBP1 using α-FLAG antibodies (Fig EV6B). Nucleic acids present in the precipitate were then end-labelled using ^{32}P, followed by Western blot and autoradiography (Fig 6B). Using high amounts of RNase A, we observed a major band in the autoradiogram corresponding in size to ZBP1 (sample 3 in Fig 6B). In samples without RNase A, this band was not visible; instead, a smear of higher molecular weight was apparent (sample 1). These patterns were not changed in samples containing DNase I (samples 2 and 4). These findings suggest that ZBP1 binds RNA and not DNA. At the high RNase A concentrations used here, a very short stretch of RNA is likely to be protected by ZBP1, explaining the sharp band in lane 3 in Fig 6B. In the absence of RNase, this band shifted to a slower migrating smear, indicating the presence of longer RNA fragments bound to ZBP1. Indeed, when we used a range of decreasing RNase A concentrations, we observed a concomitant increase in the amount of ^{32}P-labelled material migrating more slowly (Figs 6C and EV6C). Importantly, this shift was markedly reduced when we used uninfected cells expressing ZBP1-Zα1α2^{mut} despite equal efficiency of protein precipitation (Figs 6D and EV6D). Taken together, these data show that ZBP1 binds endogenous RNA but not DNA in uninfected cells.

Discussion

Mammalian cells autonomously detect virus infection (Pichlmair & Reis e Sousa, 2007). Pattern recognition receptors (PRRs) sense virus invasion and recognise pathogen- or danger-associated molecular patterns (Medzhitov, 2009). Upon activation, these receptors induce immune responses, including the production of cytokines such as IFNs, chemokines and inflammatory mediators, as well as the triggering of programmed cell death (Pichlmair & Reis e Sousa, 2007; Mocarski *et al*, 2012, 2015; Lupfer *et al*, 2015). In many instances, nucleic acids such as viral RNA or DNA genomes trigger PRRs (Goubau *et al*, 2013). This raises an important question: How can PRRs distinguish between the RNAs and DNAs abundantly found in healthy, uninfected cells and nucleic acids introduced during infection? Several "solutions" to this problem have been described and include detection of nucleic acids in cellular compartments usually devoid of RNA or DNA, detection of covalent chemical modifications unique to viral RNAs and DNAs, and detection of specific sequences (Goubau *et al*, 2013; Roers *et al*, 2016).

Here, we propose that RNA in the unusual Z-conformation is a molecular pattern recognised by ZBP1. Indeed, we found that intact ZBDs were required for ZBP1-dependent induction of necroptosis in MCMV-infected cells. Several lines of evidence showed that ZBP1 recognises RNA, and not DNA, and that this RNA likely corresponds to viral transcripts newly synthesised after infection. Firstly, the induction of cell death could not be blocked by an inhibitor of the viral DNA polymerase (GCV). Secondly, UV-inactivated virus that failed to generate viral RNA transcripts also did not induce necroptosis. Thirdly, necroptosis induction was sensitive to ActD, which potently inhibits RNA transcription. Fourthly, knock-down of the viral IE3 gene—that drives expression of many other viral genes—reduced cell death. Lastly, PAR-CLIP analysis showed that ZBP1 cross-linked with newly synthesised RNA in infected cells.

Two recent studies published while this manuscript was in preparation suggest that ZBP1 senses influenza A virus (IAV) infection and induces cell death of IAV-infected cells (Kuriakose *et al*, 2016; Thapa *et al*, 2016). Our results confirm these two reports in a different infection model and resolve an important discordance: Thapa *et al* reported that ZBP1 senses IAV RNA (Thapa *et al*, 2016) while Kuriakose *et al* concluded that IAV proteins, particularly PB1 and NP, trigger ZBP1 (Kuriakose *et al*, 2016). Our results strongly suggest that ZBP1 is an RNA sensor. We used stringent cross-link and immunoprecipitation protocols and provide a detailed analysis of ZBP1 mutants unable to bind Z nucleic acids, including a knock-in model. It is conceivable that ZBP1 binds IAV PB1 and NP indirectly via viral RNA as both IAV proteins tightly associate with IAV RNA genomes and transcripts (Eisfeld *et al*, 2015). In the future, it will be interesting to infect ZBP1-Zα1α2^{mut} knock-in mice with IAV to analyse the role of Z-RNA sensing and necroptosis in *in vivo* settings. Moreover, it will be worthwhile to explore other viral

© 2017 The Authors

Published online: July 17, 2017
The EMBO Journal

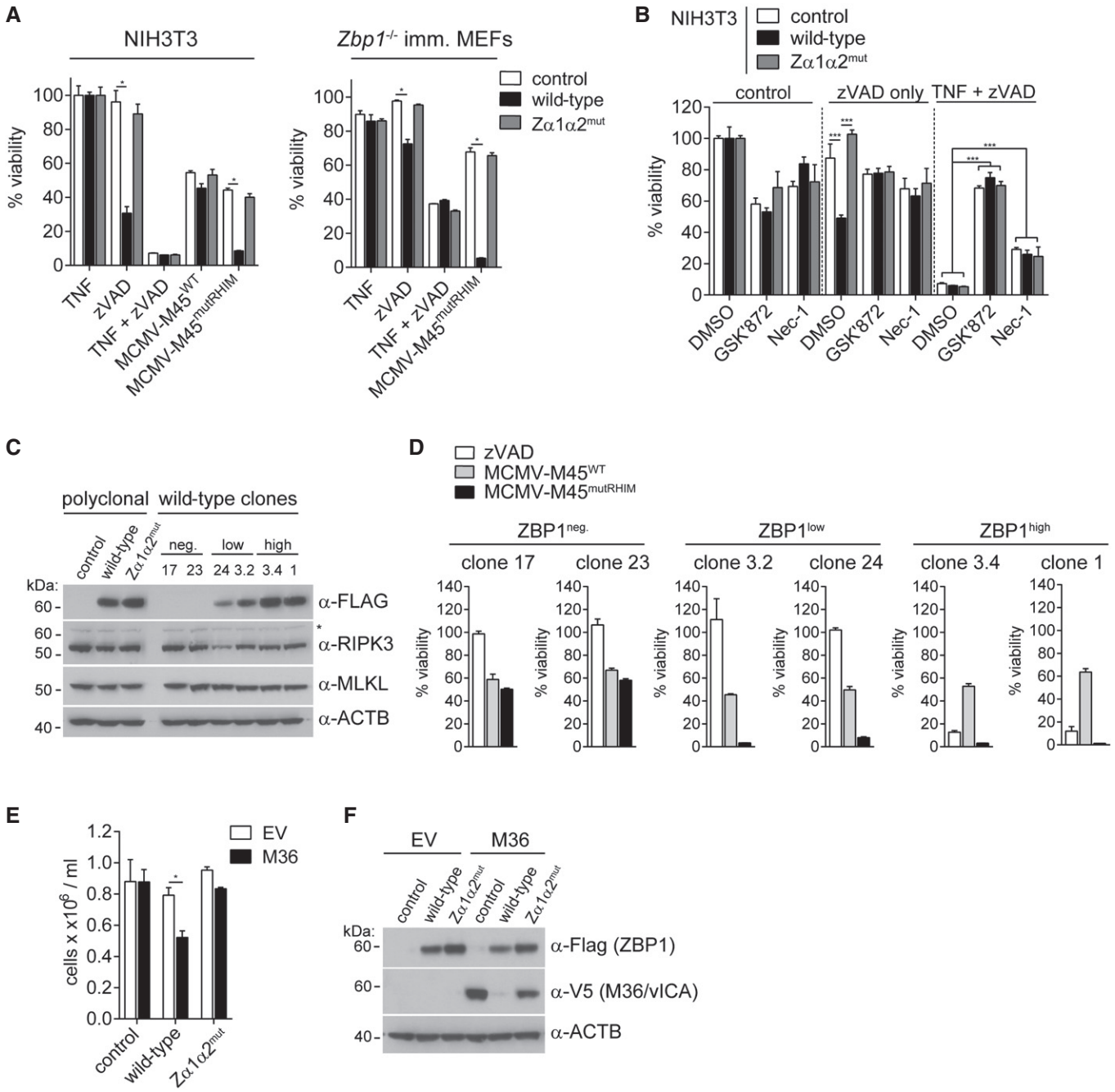


Figure 5. High levels of ectopic ZBP1 expression sensitise cells to necroptosis.

A NIH3T3 cells or immortalised *Zbp1*$^{-/-}$ MEFs expressing wild-type or mutant ZBP1 were treated with 20 μM zVAD alone, 30 ng/ml TNF, or with TZ or were infected as indicated (MOI = 10). Cell viability was assessed as in Fig 1B after 16 h.

B NIH3T3 cells reconstituted with wild-type or mutant ZBP1 were treated with 20 μM zVAD alone or TZ in combination with 3 μM GSK'872 (RIPK3 inhibitor) or 30 μM Nec-1 (RIPK1 inhibitor) or 0.1% DMSO as a control. Cell viability was monitored after 24 h as in Fig 1B.

C Polyclonal and monoclonal NIH3T3 cell lines expressing no, low or high levels of ZBP1 were analysed by Western blot using the indicated antibodies. Asterisk (*) indicates a non-specific band.

D Clonal cell lines from (C) were analysed as in (A).

E *Zbp1*$^{-/-}$-immortalised MEFs expressing wild-type or mutant ZBP1 were transduced with empty or with M36 lentiviral vectors. Cell numbers were determined after 4 days.

F Cells from (E) were tested by Western blot using the indicated antibodies.

Data information: Data are representative of two or more independent experiments. Panels (A, B, D and E) show mean ± SD (n = 3). *P < 0.05, ***P < 0.001; two-way ANOVA. See also Fig EV5.
Source data are available online for this figure.

© 2017 The Authors

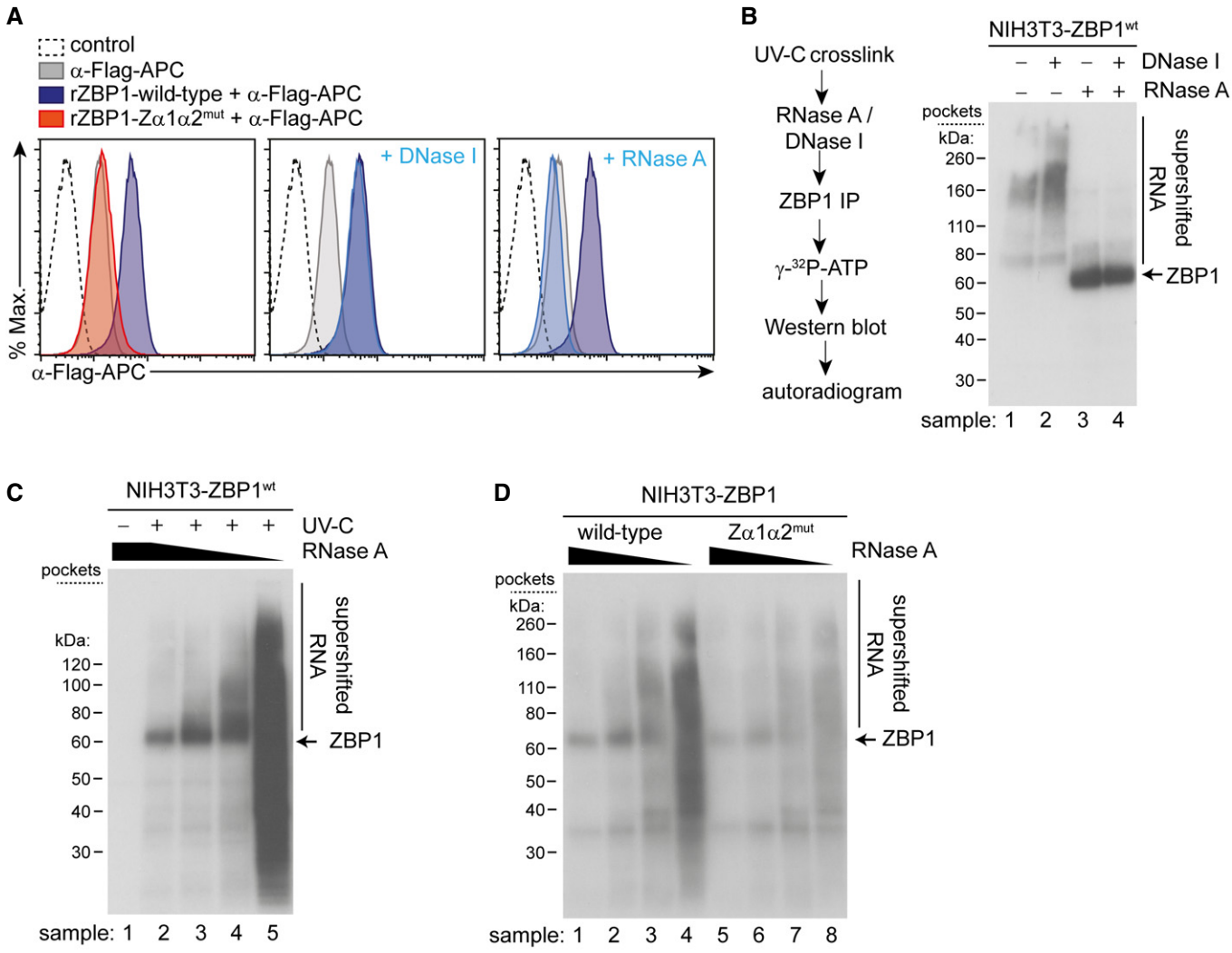


Figure 6. ZBP1 binds endogenous RNA in uninfected cells.

A Fixed and permeabilised HEK293T cells were treated with DNase I or RNase A where indicated. Cells were then incubated with recombinant ZBP1-3xFLAG and were subsequently stained with α-FLAG-APC antibody and analysed by flow cytometry. Histograms representing the APC signal are shown.

B An outline of the CLIP protocol is shown (left). NIH3T3 cells expressing wild-type ZBP1 were subjected to CLIP analysis using 20 U/ml DNase I and/or 20 U/ml RNase A. ZBP1 associated nucleic acids were labelled with ^{32}P and resolved by gel electrophoresis. The autoradiogram is shown (right).

C CLIP was performed as in (B) using different concentrations of RNase A. The autoradiogram shows supershifted RNA-ZBP1 complexes at intermediate RNase A concentrations.

D CLIP analysis was done as in (B) and (C) using NIH3T3 cells expressing wild-type or mutant ZBP1.

Data information: For panels (B–D), sample numbers are indicated at the bottom of each lane. Data are representative of three or more independent experiments. See also Fig EV6.
Source data are available online for this figure.

infections. Indeed, necroptosis is also important during infection with human cytomegalovirus (HCMV) and herpes simplex viruses (HSV) 1 and 2 (Mocarski *et al*, 2015) and, in HIV-1 infection, necroptosis of infected T cells may contribute to pathogenesis (Gaiha *et al*, 2014; Pan *et al*, 2014).

Surprisingly, we found that cells expressing high levels of ZBP1 undergo necroptosis when caspase-8 is blocked and that ZBP1 cross-links to endogenous RNA in uninfected cells. This suggests a model in which ZBP1 continuously senses self-RNA, but only engages the necroptosis machinery when sufficient levels of downstream signalling components such as RIPK3 become available, as is the case when caspase-8 is blocked. Indeed, loss of caspase-8 activity predisposes to RIPK3-dependent necroptosis (Kaiser *et al*, 2011; Oberst *et al*, 2011). Interestingly, ZBP1-dependent cell death in this setting required the activity of both RIPK1 and RIPK3. This is in contrast to MCMV-induced necroptosis, which occurs independently of RIPK1 (Upton *et al*, 2010). This may be important during development and in sterile inflammation. RIPK1-deficient mice display severe developmental defects and die around birth, and genetic ablation of RIPK1 in the skin leads to

© 2017 The Authors

inflammatory phenotypes (Silke *et al*, 2015). These observations have been linked to excessive RIPK3-MLKL-driven necroptosis (Silke *et al*, 2015). Two recent manuscripts showed that the defects of germline or keratinocyte-specific RIPK1-deficient mice are rescued by additional knock-out of ZBP1 (Lin *et al*, 2016; Newton *et al*, 2016). It is tempting to speculate that ZBP1 engages an endogenous Z-RNA in these settings and activates RIPK3 if inhibition by RIPK1 is lost. Our ZBP1-Zα1α2^{mut} knock-in model will be an important tool to address this question.

It will also be interesting to extend our CLIP analysis by deep sequencing of ZBP1-associated nucleic acids. It is possible that ZBP1 binds GC-rich sequences given that GC-rich nucleic acids adopt the Z-conformation in the test tube under high salt conditions (Wang *et al*, 1979; Hall *et al*, 1984). It is noteworthy that in cells Z-RNA may not exist as a pre-formed structure but that this conformation is induced upon binding of ZBP1 and other ZBD-containing proteins to nucleic acids that are prone to adopt this structure, for example, due to their sequence content (Kim *et al*, 2011a). We would also like to point out that the RNA recognised by ZBP1 may correspond to both double-stranded and single-stranded molecules. The former may be the case in MCMV-infected cells, given that herpesviruses produce overlapping transcripts from both DNA strands (Rajcáni *et al*, 2004; Marcinowski *et al*, 2012; Juranic Lisnic *et al*, 2013). The latter may be the case when endogenous RNA is sensed; for example, ribosomal RNAs fold back and form base-paired hairpin structures that may be recognised by ZBDs (Feng *et al*, 2011).

Taken together, we demonstrate that binding of viral RNA to ZBP1 triggers necroptosis in infected cells. Whether these RNA molecules are indeed arranged in the Z-conformation requires further experimental testing. Additionally, endogenous nucleic acids may also adopt this unusual conformation and engage ZBP1. These data indicate that Z-RNA may be molecular pattern and that ZBP1 functions as its receptor, which induces inflammatory cell death.

Materials and Methods

Mice

All mice were on the C57Bl/6 background. *Tmem173*$^{-/-}$ (STING-deficient) mice were a gift from J Cambier (Jin *et al*, 2011). The *Zbp1* gene is located on chromosome 2 (GenBank NM_021394.2; Ensembl ENSMUSG00000027514). ZBP1-Zα1α2^{mut} transgenic mice were generated by Cyagen (see Fig EV3A) and have been designated as Zbp1 < tm1.1Jreh> (MGI:5775152). See Appendix Supplementary Methods for further details. This work was performed in accordance with the UK Animals (Scientific Procedures) Act 1986 and institutional guidelines for animal care. This work was approved by a project license granted by the UK Home Office (PPL No. 40/3583) and was also approved by the Institutional Animal Ethics Committee Review Board at the University of Oxford.

Cell culture

TLA HEK293T (Open Biosystems), NIH3T3 cells (kind gift from C. Reis e Sousa), and immortalised MEFs (generated in this study) were grown in DMEM (Sigma-Aldrich) supplemented with 10% heat-inactivated FCS and 2 mM L-Gln. Cells were grown at 37°C and 5% CO_2. Primary MEFs (kind gift from K. Ishii or generated in this study) were grown in DMEM 10% FCS, 2 mM L-Gln, 100 U/ml penicillin and 0.1 mg/ml streptomycin under low oxygen conditions (3% O_2) at 37°C and 5% CO_2. The absence of mycoplasma contamination was confirmed monthly for all cells.

Plasmids and reagents

Mouse *Zbp1* was cloned from pCMV-SPORT6-Zbp1 (PlasmID clone: MmCD00314236, Harvard Medical School). A 3xFLAG-tag was added C-terminally to ZBP1 and TOPO-TA cloned into the pCR8/GW/TOPO entry vector (ThermoFisher). Zα1 (N46A, Y50A) and Zα2 (N122A, Y126A) mutant ZBP1 were cloned using overlap PCR. MCMV M36 was cloned from cDNA isolated from MCMV-infected NIH3T3 cells. ZBP1 and M36 were then Gateway cloned into pLenti6.3/TO/V5-DEST or pcDNA3.2/V5-DEST using the LR clonase II enzyme mix (ThermoFisher). The oligos used for cloning are listed in Appendix Table S1. The plasmids for human MDA5 (pcDNA3-3xFLAG-hMDA5), the IFNβ firefly luciferase reporter (p125Luc) and *Renilla* luciferase (Rluc) plasmids have been described before (Rehwinkel *et al*, 2010). The mouse RIPK3 expression plasmid (pCMV-SPORT6-mRIPK3) and the NF-κB firefly luciferase reporter plasmid (pConLuc) were a gift from M. Bertrand and G. van Loo, respectively. The expression vector for mouse STING (pcDNA3-HA-mSTING) was a kind gift from R. Vance (Burdette *et al*, 2011). pGEMTeasy-MCMV-gB was a kind gift from E. Beuken. IFN-A/D was purchased from Sigma-Aldrich or R&D Systems. Recombinant mouse TNF was from PeproTech. zVAD (Z-VAD-FMK) was from Enzo Life Sciences. Actinomycin D was from Life Technologies and CHX was from Sigma-Aldrich. Nec-1 was from Enzo Life Sciences, and GSK'872 was from Calbiochem. Neutralising anti-IFNAR1 (clone MAR1-5A3) was from Biolegend.

Virus production and infection

MCMV-M45^{WT} (K181 strain) and MCMV-M45^{mutRHIM} were a kind gift from E. Mocarski (Upton *et al*, 2010). MCMV was propagated in NIH3T3 cells or immortalised *Zbp1*$^{-/-}$ MEFs. See Appendix Supplementary Methods for further details. Lentivirus for ZBP1 and M36 reconstitution was produced in TLA HEK293T cells using pLenti6.3/TO/V5-DEST transducing vectors and the Virapower packaging mix (ThermoFisher).

Cell viability assays

A total of 5,000 NIH3T3 cells or MEFs were seeded per well in 96-well plates. Twenty-four hours later, cells were infected with MCMV or treated with TNF and/or zVAD. Endpoint viability (generally 16 h post-infection/treatment) was determined by CellTiter-Glo (Promega) using a luminometer (GloMax, Promega). For kinetic analysis of cell death, an in-incubator imaging platform was used (IncuCyte ZOOM, Essen Bioscience; 10× objective, 1 scan per well in 96-well plates per hour; samples were imaged in triplicate wells). To measure viability, the cell-impermeant dyes YOYO-3 Iodide (0.25 μM) or Sytox Green (25 nM) (ThermoFisher) were added to the medium prior to imaging. At the end of the experiment, cells in control wells were lysed with 0.0625% Triton X-100 and total number of dye-positive cells were set to 100%. For NIH3T3

 © 2017 The Authors

co-culture experiments, mutant ZBP1-expressing cells were labelled with 5 μM CellTrace Violet (Molecular Probes) for 20 min at 37°C. Cells were washed with medium and plated together with non-labelled wild-type ZBP1-expressing cells in 24 wells. Cells were then infected with MCMV. Sixteen hours post-infection, cells were harvested and the ratio of labelled vs. non-labelled cells was analysed by flow cytometry.

Luciferase reporter assays and CXCL10 ELISA

A total of 150,000 TLA HEK293T cells were seeded in 24-well plates. Cells were transfected with NF-κB (50 ng) or IFNβ firefly (125 ng) and 25 ng of *Renilla* luciferase reporter constructs, and the indicated amounts of expression vectors using FuGENE 6 (Promega). Luciferase activity was measured 24 h after transfection using a luminometer (GloMax, Promega) and Dual-Glo reagents (Promega). CXCL10 ELISA was from eBioscience.

qPCR and RT–qPCR

Cells were lysed in RLT buffer and homogenised using a Qiashredder (Qiagen), and RNA was purified using RNeasy columns with DNase I digestion (Qiagen). cDNA synthesis was performed with SuperScript II reverse transcriptase (Thermo Fisher) and oligo(dT) primers (Ambion). For DNA extraction, cells were lysed in AL-buffer and incubated with proteinase K at 56°C for 10 min, and DNA was purified using DNeasy blood and tissue columns (Qiagen). 15 ng DNA was amplified using TaqMan universal PCR (Applied Biosystems) or EXPRESS SYBR GreenER (ThermoFisher) master mixes on a 7,800 real-time PCR system (Applied Biosystems). mRNA expression data were normalised to GAPDH and analysed by the comparative Ct method. A plasmid carrying a fragment of the MCMV gB gene (pGEMTeasy-MCMV-gB) was used as a standard for determining the viral genome copy numbers (Vliegen *et al*, 2003). The lower detection limit was 30 molecules. The qPCR probes and primers used in this study are detailed in Appendix Table S2.

Western blot

Cells were lysed in 25 mM Tris.HCl pH 7.4, 150 mM NaCl, 2 mM EDTA, 1% Igepal CA-630 (Sigma-Aldrich) and 5% glycerol, protease inhibitors (Cell Signalling) and phosphatase inhibitor cocktail 3 (Sigma). Protein lysates were cleared by centrifugation at 16,000 *g* for 10 min. Alternatively, cells were directly lysed in NuPAGE SDS–PAGE sample loading buffer (ThermoFisher). 50 mM of the reducing agent DTT was added to the lysates, except for non-reducing gels. Protein lysates were run on Bis-Tris SDS–PAGE gels (NuPAGE, ThermoFisher). Primary antibodies used for Western blotting are listed in Appendix Table S3. Anti-rabbit, anti-rat or anti-mouse secondary antibodies coupled to HRP were from GE Healthcare.

Flow cytometry and fluorescence microscopy

For intracellular ZBP1 staining, cells were fixed and permeabilised in Cytofix/Cytoperm (BD biosciences) according to manufacturer's instructions. When recombinant ZBP1 was used (Fig 6A), cells were incubated with 0.3 μg ZBP1-3xFLAG for 1 h in Perm/Wash buffer. In some instances, cells were pre-incubated for 30 min at 37°C with 30 U Purelink RNase A (Invitrogen) or Turbo DNase I (Ambion). Anti-FLAG-APC (Abcam, clone M2) was used to detect ZBP1-FLAG. Samples were analysed in FACS buffer (PBS, 2 mM EDTA, 1% FCS). 1 μg/ml DAPI (Sigma-Aldrich) or Live/Dead Fixable Violet (Molecular Probes) was used to exclude dead cells. Data were acquired on Beckmann Coulter CyAn or BD Biosciences LSRFortessa flow cytometers. FCS files were analysed using FlowJo V.10.0.8. For fluorescence microscopy, polyclonal ZBP1-expressing NIH3T3 cells were seeded on poly-D-lysine (Sigma-Aldrich)-coated coverslips (Lab-Tek). Cells were fixed using 4% paraformaldehyde (ThermoFisher) and blocked and permeabilised for 1 h in PBS + 5% BSA (Sigma-Aldrich) + 0.1% saponin (Sigma-Aldrich). Primary antibody (anti-FLAG-HRP, clone M2, Sigma-Aldrich) and detection antibodies (anti-HRP-Alexa Fluor 594, Jackson Immunoresearch) were incubated for 1 h in PBS + 5% BSA + 0.1% saponin (Sigma-Aldrich). Images were acquired using a Zeiss Axiovert S100 inverted fluorescence microscope.

IE3 knockdown

siRNAs targeting MCMV IE3 were directed against exon 5 of the IE1/3 gene and were designed using siDESIGN Center from Dharmacon (GE Healthcare). siRNAs were ordered from Dharmacon, and the sequences are detailed in Appendix Table S4. A total of 5,000 NIH3T3 cells were seeded per well in 96-well plates. 25 nM siRNAs were transfected using DharmaFECT 1 (Dharmacon, GE Healthcare) according to manufacturer's instructions. One hour later, transfection mix was washed away, and cells were infected with MCMV.

(PAR)-CLIP

PAR-CLIP and CLIP protocols were adapted from (Hafner *et al*, 2010; Huppertz *et al*, 2014). Further details are provided in Appendix Supplementary Methods.

ZBP1 purification

Wild-type and Zα1α2^{mut} mouse ZBP1 were purified based on the protocol published in Sun *et al* (2013). See Appendix Supplementary Methods for further details.

Statistics

Statistical analysis was performed in GraphPad Prism v7.00 as detailed in the figure legends.

Expanded View for this article is available online.

Acknowledgements

The authors thank K. Ishii for *Zbp1*$^{-/-}$ MEFs, E. Mocarski for MCMV-M45^{mutRHIM} virus, A. Pichlmair for the α-ZBP1 antibody and Q. Tang for MCMV-IE1/3-GFP and the α-IE1 antibody. The authors further thank A. Jackson and members of the Rehwinkel laboratory for critical discussions and reading of the manuscript draft. This work was funded by the UK Medical Research Council (MRC core funding of the MRC Human Immunology Unit) and by the Wellcome Trust (grant number 100954). KBR and JWU were funded by the Cancer Prevention and Research Institute of Texas (CPRIT), R1202. JM was a recipient of an EMBO long-term postdoctoral fellowship and was also

© 2017 The Authors

supported by Marie Curie Actions (EMBOCOFUND2010, GA-2010-267146). *Tmem173*$^{-/-}$ mice were provided by J. Cambier and are subject to materials transfer agreements.

Author contributions

JM and JR conceived the study, designed experiments, analysed data and wrote the manuscript. JM performed all experiments. LL and AB provided technical help and analysed data. KBR and JWU provided MCMV-M45^{mutRHIM} virus for the experiment shown in Fig 3G. All authors read and approved the final manuscript.

Conflict of interest

The authors declare that they have no conflict of interest.

References

Angulo A, Ghazal P, Messerle M (2000) The major immediate-early gene ie3 of mouse cytomegalovirus is essential for viral growth. *J Virol* 74: 11129 – 11136

Athanasiadis A (2012) Zalpha-domains: at the intersection between RNA editing and innate immunity. *Semin Cell Dev Biol* 23: 275 – 280

Brown BA, Lowenhaupt K, Wilbert CM, Hanlon EB, Rich A (2000) The zalpha domain of the editing enzyme dsRNA adenosine deaminase binds left-handed Z-RNA as well as Z-DNA. *Proc Natl Acad Sci USA* 97: 13532 – 13536

Burdette DL, Monroe KM, Sotelo-Troha K, Iwig JS, Eckert B, Hyodo M, Hayakawa Y, Vance RE (2011) STING is a direct innate immune sensor of cyclic di-GMP. *Nature* 478: 515 – 518

Cai Z, Jitkaew S, Zhao J, Chiang H-C, Choksi S, Liu J, Ward Y, Wu L-G, Liu Z-G (2014) Plasma membrane translocation of trimerized MLKL protein is required for TNF-induced necroptosis. *Nat Cell Biol* 16: 55 – 65

Chen Q, Sun L, Chen ZJ (2016) Regulation and function of the cGAS–STING pathway of cytosolic DNA sensing. *Nat Immunol* 17: 1142 – 1149

Darnell RB (2010) HITS-CLIP: panoramic views of protein-RNA regulation in living cells. *Wiley Interdiscip Rev RNA* 1: 266 – 286

Dondelinger Y, Declercq W, Montessuit S, Roelandt R, Goncalves A, Bruggeman I, Hulpiau P, Weber K, Sehon CA, Marquis RW, Bertin J, Gough PJ, Savvides S, Martinou J-C, Bertrand MJM, Vandenabeele P (2014) MLKL compromises plasma membrane integrity by binding to phosphatidylinositol phosphates. *Cell Rep* 7: 971 – 981

Eisfeld AJ, Neumann G, Kawaoka Y (2015) At the centre: influenza A virus ribonucleoproteins. *Nat Rev Microbiol* 13: 28 – 41

Feng S, Li H, Zhao J, Pervushin K, Lowenhaupt K, Schwartz TU, Dröge P (2011) Alternate rRNA secondary structures as regulators of translation. *Nat Struct Mol Biol* 18: 169 – 176

Gaiha GD, McKim KJ, Woods M, Pertel T, Rohrbach J, Barteneva N, Chin CR, Liu D, Soghoian DZ, Cesa K, Wilton S, Waring MT, Chicoine A, Doering T, Wherry EJ, Kaufmann DE, Lichterfeld M, Brass AL, Walker BD (2014) Dysfunctional HIV-specific CD8$^+$ T cell proliferation is associated with increased caspase-8 activity and mediated by necroptosis. *Immunity* 41: 1001 – 1012

Goubau D, Deddouche S, Reis e Sousa C (2013) Cytosolic sensing of viruses. *Immunity* 38: 855 – 869

Guo H, Kaiser WJ, Mocarski ES (2015) Manipulation of apoptosis and necroptosis signaling by herpesviruses. *Med Microbiol Immunol* 204: 439 – 448

Ha SC, Kim D, Hwang H-Y, Rich A, Kim Y-G, Kim KK (2008) The crystal structure of the second Z-DNA binding domain of human DAI (ZBP1) in complex with Z-DNA reveals an unusual binding mode to Z-DNA. *Proc Natl Acad Sci USA* 105: 20671 – 20676

Hafner M, Landthaler M, Burger L, Khorshid M, Hausser J, Berninger P, Rothballer A, Ascano M, Jungkamp A-C, Munschauer M, Ulrich A, Wardle GS, Dewell S, Zavolan M, Tuschl T (2010) Transcriptome-wide identification of RNA-binding protein and microRNA target sites by PAR-CLIP. *Cell* 141: 129 – 141

Hall K, Cruz P, Tinoco I, Jovin TM, van de Sande JH (1984) 'Z-RNA'–a left-handed RNA double helix. *Nature* 311: 584 – 586

Herbert AG, Spitzner JR, Lowenhaupt K, Rich A (1993) Z-DNA binding protein from chicken blood nuclei. *Proc Natl Acad Sci USA* 90: 3339 – 3342

Huppertz I, Attig J, D'Ambrogio A, Easton LE, Sibley CR, Sugimoto Y, Tajnik M, König J, Ule J (2014) iCLIP: protein-RNA interactions at nucleotide resolution. *Methods* 65: 274 – 287

Ishii KJ, Kawagoe T, Koyama S, Matsui K, Kumar H, Kawai T, Uematsu S, Takeuchi O, Takeshita F, Coban C, Akira S (2008) TANK-binding kinase-1 delineates innate and adaptive immune responses to DNA vaccines. *Nature* 451: 725 – 729

Jin L, Hill KK, Filak H, Mogan J, Knowles H, Zhang B, Perraud A-L, Cambier JC, Lenz LL (2011) MPYS is required for IFN response factor 3 activation and type I IFN production in the response of cultured phagocytes to bacterial second messengers cyclic-di-AMP and cyclic-di-GMP. *J Immunol* 187: 2595 – 2601

Juranic Lisnic V, Babic Cac M, Lisnic B, Trsan T, Mefferd A, Mukhopadhyay Das C, Cook CH, Jonjić S, Trgovcich J (2013) Dual analysis of the murine cytomegalovirus and host cell transcriptomes reveal new aspects of the virus-host cell interface. *PLoS Pathog* 9: e1003611

Kaiser WJ, Upton JW, Mocarski ES (2008) Receptor-interacting protein homotypic interaction motif-dependent control of NF-kappa B activation via the DNA-dependent activator of IFN regulatory factors. *J Immunol* 181: 6427 – 6434

Kaiser WJ, Upton JW, Long AB, Livingston-Rosanoff D, Daley-Bauer LP, Hakem R, Caspary T, Mocarski ES (2011) RIP3 mediates the embryonic lethality of caspase-8-deficient mice. *Nature* 471: 368 – 372

Kim H-E, Ahn H-C, Lee Y-M, Lee E-H, Seo Y-J, Kim Y-G, Kim KK, Choi B-S, Lee J-H (2011a) The Zβ domain of human DAI binds to Z-DNA via a novel B-Z transition pathway. *FEBS Lett* 585: 772 – 778

Kim K, Khayrutdinov BI, Lee C-K, Cheong H-K, Kang SW, Park H, Lee S, Kim Y-G, Jee J, Rich A, Kim KK, Jeon YH (2011b) Solution structure of the Zbeta domain of human DNA-dependent activator of IFN-regulatory factors and its binding modes to B- and Z-DNAs. *Proc Natl Acad Sci USA* 108: 6921 – 6926

Kuriakose T, Man SM, Malireddi RKS, Karki R, Kesavardhana S, Place DE, Neale G, Vogel P, Kanneganti T-D (2016) ZBP1/DAI is an innate sensor of influenza virus triggering the NLRP3 inflammasome and programmed cell death pathways. *Sci Immunol* 1: aag2045

Lafer EM, Valle RP, Möller A, Nordheim A, Schur PH, Rich A, Stollar BD (1983) Z-DNA-specific antibodies in human systemic lupus erythematosus. *J Clin Invest* 71: 314 – 321

Lin J, Kumari S, Kim C, Van T-M, Wachsmuth L, Polykratis A, Pasparakis M (2016) RIPK1 counteracts ZBP1-mediated necroptosis to inhibit inflammation. *Nature* 540: 124 – 128

Lupfer C, Malik A, Kanneganti T-D (2015) Inflammasome control of viral infection. *Curr Opin Virol* 12: 38 – 46

Marcinowski L, Lidschreiber M, Windhager L, Rieder M, Bosse JB, Rädle B, Bonfert T, Györy I, de Graaf M, Prazeres da Costa O, Rosenstiel P, Friedel CC, Zimmer R, Ruzsics Z, Dölken L (2012) Real-time transcriptional profiling of cellular and viral gene expression during lytic cytomegalovirus infection. *PLoS Pathog* 8: e1002908

Martínez FP, Cosme RSC, Tang Q (2010) Murine cytomegalovirus major immediate-early protein 3 interacts with cellular and viral proteins in viral

 © 2017 The Authors

DNA replication compartments and is important for early gene activation. *J Gen Virol* 91: 2664 – 2676

McCormick AL, Skaletskaya A, Barry PA, Mocarski ES, Goldmacher VS (2003) Differential function and expression of the viral inhibitor of caspase 8-induced apoptosis (vICA) and the viral mitochondria-localized inhibitor of apoptosis (vMIA) cell death suppressors conserved in primate and rodent cytomegaloviruses. *Virology* 316: 221 – 233

Medzhitov R (2009) Approaching the asymptote: 20 years later. *Immunity* 30: 766 – 775

Ménard C, Wagner M, Ruzsics Z, Holak K, Brune W, Campbell AE, Koszinowski UH (2003) Role of murine cytomegalovirus US22 gene family members in replication in macrophages. *J Virol* 77: 5557 – 5570

Mocarski ES, Upton JW, Kaiser WJ (2012) Viral infection and the evolution of caspase 8-regulated apoptotic and necrotic death pathways. *Nat Rev Immunol* 12: 79 – 88

Mocarski ES, Guo H, Kaiser WJ (2015) Necroptosis: the Trojan horse in cell autonomous antiviral host defense. *Virology* 479–480: 160 – 166

Newton K, Wickliffe KE, Maltzman A, Dugger DL, Strasser A, Pham VC, Lill JR, Roose-Girma M, Warming S, Solon M, Ngu H, Webster JD, Dixit VM (2016) RIPK1 inhibits ZBP1-driven necroptosis during development. *Nature* 540: 129 – 133

Oberst A, Dillon CP, Weinlich R, McCormick LL, Fitzgerald P, Pop C, Hakem R, Salvesen GS, Green DR (2011) Catalytic activity of the caspase-8-FLIP(L) complex inhibits RIPK3-dependent necrosis. *Nature* 471: 363 – 367

Omoto S, Guo H, Talekar GR, Roback L, Kaiser WJ, Mocarski ES (2015) Suppression of RIP3-dependent necroptosis by human cytomegalovirus. *J Biol Chem* 290: 11635 – 11648

Pan T, Wu S, He X, Luo H, Zhang Y, Fan M, Geng G, Ruiz VC, Zhang J, Mills L, Bai C, Zhang H (2014) Necroptosis takes place in human immunodeficiency virus type-1 (HIV-1)-infected $CD4^+$ T lymphocytes. *PLoS One* 9: e93944

Pichlmair A, Reis e Sousa C (2007) Innate recognition of viruses. *Immunity* 27: 370 – 383

Placido D, Brown BA, Lowenhaupt K, Rich A, Athanasiadis A (2007) A left-handed RNA double helix bound by the Z alpha domain of the RNA-editing enzyme ADAR1. *Structure* 15: 395 – 404

Rajcáni J, Andrea V, Ingeborg R (2004) Peculiarities of herpes simplex virus (HSV) transcription: an overview. *Virus Genes* 28: 293 – 310

Rebsamen M, Heinz LX, Meylan E, Michallet M-CEC, Schroder K, Hofmann K, Vazquez J, Benedict CA, Tschopp JUR (2009) DAI/ZBP1 recruits RIP1 and RIP3 through RIP homotypic interaction motifs to activate NF-kB. *EMBO Rep* 10: 916 – 922

Rehwinkel J, Tan CP, Goubau D, Schulz O, Pichlmair A, Bier K, Robb N, Vreede F, Barclay W, Fodor E, Reis e Sousa C (2010) RIG-I detects viral genomic RNA during negative-strand RNA virus infection. *Cell* 140: 397 – 408

Rich A, Zhang S (2003) Timeline: Z-DNA: the long road to biological function. *Nat Rev Genet* 4: 566 – 572

Roers A, Hiller B, Hornung V (2016) Recognition of endogenous nucleic acids by the innate immune system. *Immunity* 44: 739 – 754

Schade M, Turner CJ, Lowenhaupt K, Rich A, Herbert A (1999) Structure-function analysis of the Z-DNA-binding domain Zalpha of dsRNA adenosine deaminase type I reveals similarity to the (alpha + beta) family of helix-turn-helix proteins. *EMBO J* 18: 470 – 479

Schwartz T, Rould MA, Lowenhaupt K, Herbert A, Rich A (1999) Crystal structure of the Zalpha domain of the human editing enzyme ADAR1 bound to left-handed Z-DNA. *Science* 284: 1841 – 1845

Schwartz T, Behlke J, Lowenhaupt K, Heinemann U, Rich A (2001) Structure of the DLM-1-Z-DNA complex reveals a conserved family of Z-DNA-binding proteins. *Nat Struct Biol* 8: 761 – 765

Silke J, Rickard JA, Gerlic M (2015) The diverse role of RIP kinases in necroptosis and inflammation. *Nat Immunol* 16: 689 – 697

Smee DF, Barnett BB, Sidwell RW, Reist EJ, Holy A (1995) Antiviral activities of nucleosides and nucleotides against wild-type and drug-resistant strains of murine cytomegalovirus. *Antiviral Res* 26: 1 – 9

Sun L, Wu J, Du F, Chen X, Chen ZJ (2013) Cyclic GMP-AMP synthase is a cytosolic DNA sensor that activates the type I interferon pathway. *Science* 339: 786 – 791

Takaoka A, Wang Z, Choi MK, Yanai H, Negishi H, Ban T, Lu Y, Miyagishi M, Kodama T, Honda K, Ohba Y, Taniguchi T (2007) DAI (DLM-1/ZBP1) is a cytosolic DNA sensor and an activator of innate immune response. *Nature* 448: 501 – 505

Thapa RJ, Ingram JP, Ragan KB, Nogusa S, Boyd DF, Benitez AA, Sridharan H, Kosoff R, Shubina M, Landsteiner VJ, Andrake M, Vogel P, Sigal LJ, tenOever BR, Thomas PG, Upton JW, Balachandran S (2016) DAI senses influenza A virus genomic RNA and activates RIPK3-dependent cell death. *Cell Host Microbe* 20: 552 – 554

Upton JW, Kaiser WJ, Mocarski ES (2010) Virus inhibition of RIP3-dependent necrosis. *Cell Host Microbe* 7: 302 – 313

Upton JW, Kaiser WJ, Mocarski ES (2012) DAI/ZBP1/DLM-1 complexes with RIP3 to mediate virus-induced programmed necrosis that is targeted by murine cytomegalovirus vIRA. *Cell Host Microbe* 11: 290 – 297

Vandenabeele P, Vanden Berghe T, Festjens N (2006) Caspase inhibitors promote alternative cell death pathways. *Sci STKE* 2006: pe44

Vercammen D, Beyaert R, Denecker G, Goossens V, van Loo G, Declercq W, Grooten J, Fiers W, Vandenabeele P (1998) Inhibition of caspases increases the sensitivity of L929 cells to necrosis mediated by tumor necrosis factor. *J Exp Med* 187: 1477 – 1485

Viegas-Péquignot E, Derbin C, Malfoy B, Taillandier E, Leng M, Dutrillaux B (1983) Z-DNA immunoreactivity in fixed metaphase chromosomes of primates. *Proc Natl Acad Sci USA* 80: 5890 – 5894

Vliegen I, Herngreen S, Grauls G, Bruggeman C, Stassen F (2003) Improved detection and quantification of mouse cytomegalovirus by real-time PCR. *Virus Res* 98: 17 – 25

Wallach D, Kang TB, Dillon CP, Green DR (2016) Programmed necrosis in inflammation: toward identification of the effector molecules. *Science* 352: aaf2154

Wang AH, Quigley GJ, Kolpak FJ, Crawford JL, van Boom JH, van der Marel G, Rich A (1979) Molecular structure of a left-handed double helical DNA fragment at atomic resolution. *Nature* 282: 680 – 686

Wang G, Vasquez KM (2007) Z-DNA, an active element in the genome. *Front Biosci* 12: 4424 – 4438

Yang Y, Ramelot TA, Lee H-W, Xiao R, Everett JK, Montelione GT, Prestegard JH, Kennedy MA (2014) Solution structure of the free Zα domain of human DLM-1 (ZBP1/DAI), a Z-DNA binding domain. *J Biomol NMR* 60: 189 – 195

Zarling DA, Calhoun CJ, Feuerstein BG, Sena EP (1990) Cytoplasmic microinjection of immunoglobulin Gs recognizing RNA helices inhibits human cell growth. *J Mol Biol* 211: 147 – 160

License: This is an open access article under the terms of the Creative Commons Attribution 4.0 License, which permits use, distribution and reproduction in any medium, provided the original work is properly cited.

Nucleic Acid Sensors and Programmed Cell Death

Jonathan Maelfait[1,2,*#], Layal Liverpool[3*] and Jan Rehwinkel[3,#]

[1] Laboratory of Immunoregulation and Mucosal Immunology, VIB Center for Inflammation Research, 9052 Ghent, Belgium.

[2] Department of Internal Medicine, Ghent University, 9000 Ghent, Belgium.

[3] Medical Research Council Human Immunology Unit, Medical Research Council Weatherall Institute of Molecular Medicine, Radcliffe Department of Medicine, University of Oxford, Oxford OX3 9DS, UK.

* These authors contributed equally to this work.

Correspondence:
jonathan.maelfait@irc.vib-ugent.be (JM); jan.rehwinkel@imm.ox.ac.uk (JR)

Abstract

Nucleic acids are powerful triggers for innate immune responses. Proteins called RNA and DNA sensors detect foreign nucleic acids, which are derived from microorganisms and, in mammalian cells, include RIG-I, cGAS and AIM2. Upon binding to nucleic acids, these proteins initiate signalling cascades that activate host defence responses. An important aspect of this defence programme is the production of cytokines such as type I interferons and IL-1β. Studies conducted over recent years have revealed that nucleic acid sensors also activate programmed cell death pathways as an innate immune response to infection. Indeed, RNA and DNA sensors induce apoptosis, pyroptosis and necroptosis. Cell death via these pathways prevents replication of pathogens by eliminating the infected cell and can also contribute to the release of cytokines and inflammatory mediators. Interestingly, recent evidence suggests that programmed cell death triggered by nucleic acid sensors also plays an important role in a number of non-infectious pathologies. In addition to non-self DNA and RNA from microorganisms, nucleic acid sensors also recognise endogenous nucleic acids, for example when cells are damaged by genotoxic agents and in certain autoinflammatory diseases. This review article summarises current knowledge on the links between nucleic acid sensing and cell death and explores important open questions for future studies in this area.

Keywords

apoptosis; pyroptosis; necroptosis; RIG-I; cGAS; STING; AIM2; IFI16; TLR9; ZBP1; DAI; TLR3; type I interferon; IL-1β

Introduction

DNA and RNA play fundamental roles in the immune system (Hartmann 2017). Unusual and aberrant nucleic acids are molecular signatures indicative of the presence of microorganisms or of perturbations to cellular homeostasis (Goubau, Deddouche et al. 2013, Roers, Hiller et al. 2016). A variety of mammalian, germ-line encoded proteins, called nucleic acid sensors, bind directly to such DNA and RNA species and then signal for the induction of host defence responses. Examples are the Toll-like receptors (TLRs) 3, 7, 8 and 9, the RIG-I-like receptors (RLRs), cyclic guanosine-monophosphate adenosine-monophosphate synthase (cGAS) and absent in melanoma 2 (AIM2). These proteins have been well studied in the context of infectious insults, particularly viruses. Being obligate intracellular pathogens, viruses need to introduce and replicate their genetic material in the cells they infect. Therefore, nucleic acid sensing is a broadly effective strategy employed by host cells to detect invading viruses. However, healthy cells contain a variety of endogenous DNA and RNA species, necessitating molecular mechanisms that prevent the activation of nucleic acid sensors in the absence of infection. These include: (i) recognition of nucleic acids in subcellular compartments usually devoid of DNA or RNA; (ii) detection of the presence or absence of chemical modifications on viral nucleic acids; (iii) sensing of unusual nucleotide sequences or secondary and tertiary structures; (iv) recognition of changes in DNA or RNA abundance; and (v) elaborate positive and negative feedback loops regulating nucleic acid sensors (Goubau, Deddouche et al. 2013, Hartmann 2017). Stress and damage of cells, as well as mutations – for example, in genes encoding nucleases – can result in a breakdown of these mechanisms and subsequent sensing of endogenous nucleic acids. This is relevant in the context of autoinflammatory diseases and in cancer (Barber 2015, Crow and Manel 2015, Roers, Hiller et al. 2016).

Once activated by DNA or RNA, nucleic acid sensors induce innate immune responses, the best characterised of which is the induction of cytokines. For example, TLRs, RLRs and cGAS all activate signalling cascades that transcriptionally induce the genes encoding type I interferons (IFNs), which are important mediators of antiviral immunity (McNab, Mayer-Barber et al. 2015). Another example is the double-stranded (ds) DNA sensor AIM2, which nucleates the formation of an inflammasome, leading to proteolytic maturation of IL-1β and other cytokines (Man, Karki et al. 2016). Although cytokine production plays an essential role in nucleic acid triggered host

defence, other signalling outputs of nucleic acid sensing have been described. PKR detects dsRNA and then phosphorylates and thereby inhibits eIF2α, a translation initiation factor (Williams 2001). This results in a global shutdown of protein translation in virally infected cells, preventing the production of viral proteins. Much like PKR, OAS family proteins also detect dsRNA following virus infection (Hornung, Hartmann et al. 2014). This results in activation of the enzymatic function of OAS proteins to produce 2'-5' oligoadenylate, which in turn activates RNase L. This nuclease then cleaves cellular and viral RNAs and thereby prohibits replication of RNA viruses.

Another possible consequence of engagement of nucleic acid sensors is the activation of programmed cell death. Indeed, apoptosis, pyroptosis and necroptosis can all be initiated by DNA and RNA sensors. These pathways are summarised in Table 1. "Suicidal" cell death can be advantageous to the host in a number of ways (Danthi 2016, Jorgensen, Rayamajhi et al. 2017, Orzalli and Kagan 2017). Firstly, it prevents replication of intracellular pathogens by elimination of infected cells. Secondly, some types of programmed cell death such as pyroptosis result in the release of cytokines, particularly IL-1β. Thirdly, when cell death involves damage to the plasma membrane, as is the case during necroptosis and pyroptosis, intracellular molecules such as ATP are released into the extracellular space and serve as damage associated molecular patterns. Finally, cell corpses can entrap and thereby disable pathogenic microorganisms (Jorgensen, Rayamajhi et al. 2017).

In this article, we discuss recent examples of how nucleic acid sensors couple to programmed cell death, focussing on some of the key questions in the field: What are the mechanisms of self versus non-self discrimination by nucleic acid sensors in the context of cell death? What are the molecules driving cell death downstream of nucleic acid sensors? What is the importance of cell death instructed by DNA and RNA sensors to host defence against pathogens, in cancer and during autoinflammation? We will first explore DNA sensors and then RNA sensors in separate chapters.

DNA sensors

Innate immune DNA sensors are DNA-binding proteins that detect perturbations in cellular DNA homeostasis and activate cell-autonomous innate immune signalling cascades (Ablasser and Chen 2019). These perturbations can be

caused by infection, through the introduction of foreign DNA into the cell, or by damage or mislocalisation of self DNA, which is usually compartmentalised in organelles. DNA sensors activate a wide range of innate immune responses. DNA sensing is particularly important in the context of viral infection where a key innate immune response is the induction of type I IFNs, which signal in an autocrine and paracrine manner to establish an anti-viral state (McNab, Mayer-Barber et al. 2015). As such, type I IFNs not only restrict viruses in the infected cell but also limit the spread of viruses to surrounding cells. In addition to type I IFN induction, several DNA sensors and proteins involved in downstream signalling activate programmed cell death as an innate immune response to infection. This section will focus on the role of DNA sensors in the activation of programmed cell death pathways.

AIM2

The inflammasome is a large protein complex that facilitates activation of caspase-1 by auto-proteolytic cleavage. Active caspase-1 in turn cleaves and thereby matures the pro-inflammatory cytokines IL-18 and IL-1β (Schroder and Tschopp 2010). Inflammasome activation also results in the induction of pyroptosis, a caspase-1-dependent inflammatory form of cell death (Table 1). Pyroptosis involves cell swelling, lysis and ultimately the release of cytoplasmic content (Shi, Gao et al. 2017).

Absent in melanoma 2 (AIM2) is a DNA sensor that activates the inflammasome (Burckstummer, Baumann et al. 2009, Fernandes-Alnemri, Yu et al. 2009, Hornung, Ablasser et al. 2009, Roberts, Idris et al. 2009). AIM2 is cytosolic and contains a pyrin domain and a HIN200 domain. HIN200 domains are positively charged and bind to dsDNA in a sequence independent manner (Jin, Perry et al. 2012). Upon dsDNA binding, the pyrin domain of AIM2 interacts with the pyrin domain of the key inflammasome adaptor apoptosis-related speck-like protein (ASC). ASC can now nucleate an inflammasome using its caspase activation and recruitment domain (CARD) to interact with the CARD of pro-caspase-1, triggering its autocatalytic cleavage to release active caspase-1. This occurs in a large protein complex, the so-called “ASC speck” that can be readily visualised by microscopy (Juruj, Lelogeais et al. 2013, Man, Karki et al. 2015, Meunier, Wallet et al. 2015). Active caspase-1 subsequently catalyses the processing of pro-IL-18 and pro-IL-1β into the mature cytokines (Figure 1A). The active forms of these pro-inflammatory cytokines mediate downstream inflammation and immune responses and, given that they are not released

by the canonical secretory pathway *via* the Golgi apparatus, it is thought that their release is dependent on pyroptosis (Lamkanfi and Dixit , Sharma and Kanneganti 2016, Shi, Gao et al. 2017) (Place and Kanneganti 2019).

The mechanism by which pyroptosis is actually initiated remained a mystery until the discovery of gasdermin D (GSDMD) (Kayagaki, Stowe et al. 2015, Shi, Zhao et al. 2015) as a substrate cleaved by caspase-1. Full-length GSDMD is in an auto-inhibited, inactive conformation. Cleavage by caspase-1 leads to the release of an N-terminal GSDMD fragment (p30) that forms pores in the cell membrane and thereby initiates pyroptotic cell death (Kayagaki, Stowe et al. 2015, Shi, Zhao et al. 2015, Liu, Zhang et al. 2016, Shi, Gao et al. 2017). GSDMD-mediated cytolysis is negatively regulated by the endosomal sorting complexes required for transport (ESCRT) machinery, which can initiate repair of damaged membranes (Ruhl, Shkarina et al. 2018). GSDMD is also regulated at the transcriptional level by IRF2, which binds to a region within the gene promoter to mediate transcriptional activation (Kayagaki, Lee et al. 2019). GSDMD deficiency abrogates pyroptosis in response to poly(dA:dT), a synthetic dsDNA that is sensed by AIM2 (Kayagaki, Stowe et al. 2015, Shi, Zhao et al. 2015). Of note, AIM2 has been implicated as a sensor of cytosolic DNA from invading DNA viruses and bacteria, as well as self-derived cytosolic DNA (Muruve, Petrilli et al. 2008, Hornung, Ablasser et al. 2009, Choubey and Panchanathan 2017). AIM2 has also been implicated in sensing of influenza A virus (IAV) infection (Zhang, Luo et al. 2017). IAV is an RNA virus. Interestingly, this study (Zhang, Luo et al. 2017) demonstrates that dsDNA released into the lungs of infected mice, presumably from dying cells, is sensed by AIM2 to activate caspase-1 and IL-1β. Recognition of self-derived DNA by AIM2 is also important in the context of radiation induced DNA damage (Hu, Jin et al. 2016). Ionising radiation induces double-stranded breaks in DNA. AIM2 localises to these double-stranded DNA breaks in the cell nucleus, and the resulting inflammasome activation and cell death causes tissue damage in mice (Hu, Jin et al. 2016). In human myeloid cells, where AIM2 has been shown to be dispensable for DNA-mediated inflammasome activation, DNA sensing via the cGAS-STING pathway induces NLRP3-dependent lysosomal cell death and release of IL-1β (Gaidt, Ebert et al. 2017).

In addition to pyroptosis, AIM2 has recently been implicated in apoptosis. AIM2 is so-called because it was originally identified as a tumour suppressor, absent in melanoma (DeYoung, Ray et al. 1997). Indeed, loss-of-function mutations in *AIM2*

are present in more than half of the tumours from patients with bowel cancers, including colorectal cancers (Woerner, Kloor et al. 2005, Woerner, Kloor et al. 2007). A recent study (Chen, Wang et al. 2017) demonstrated a pro-apoptotic and anti-proliferative effect of AIM2, and further suggested that this is antagonised by the pro-survival phosphatidylinositol-3-kinase (PI3K)/protein kinase B (Akt) pathway in colorectal cancer cells. The molecular mechanisms by which AIM2 activates apoptosis in this context remain to be elucidated. AIM2 can also induce apoptosis during infection. AIM2 sensing of *Toxoplasma* infection signals the activation of GSDMD-independent, ASC and caspase-8 dependent apoptosis (Fisch, Bando et al. 2019).

IFI16

Much like AIM2, IFNγ-inducible protein 16 (IFI16) comprises HIN200 and pyrin domains. AIM2, IFI16 and other proteins constitute the AIM2-like receptor (ALR) family that has undergone species-specific diversification (Brunette, Young et al. 2012). IFI16 has been suggested to function as a DNA sensor for both the induction of type I IFN (Unterholzner, Keating et al. 2010, Almine, O'Hare et al. 2017, Jønsson, Laustsen et al. 2017) and the inflammasome (Kerur, Veettil et al. 2011). IFI16 can be both nuclear and cytoplasmic and in its nuclear localisation has been suggested to sense herpes viral genomic DNA to activate the inflammasome (Kerur, Veettil et al. 2011, Ansari, Dutta et al. 2015, Dutta, Dutta et al. 2015). IFI16 becomes acetylated upon recognition of viral DNA in the nucleus and is transported into the cytoplasm in complex with breast cancer 1 (BRCA1) (Dutta, Dutta et al. 2015). Here, the complex activates the inflammasome by interacting with ASC to mediate caspase-1 activation and IL-1β maturation (Figure 1A). This forms a key innate immune response to virus infection as evidenced by the fact that Kaposi's sarcoma herpes virus (KSHV) has evolved a mechanism of antagonising this by targeting IFI16 for degradation (Roy, Dutta et al. 2016).

IFI16 has further been implicated in pyroptosis of human immunodeficiency virus type-1 (HIV-1)-infected CD4 T-cells (Monroe, Yang et al. 2014). Acquired immunodeficiency syndrome is caused by the progressive depletion of CD4 T-cells as a consequence of HIV-1 infection. CD4 T-cell depletion is associated with inflammasome formation and subsequent caspase-1 activation and pyroptotic cell death (Doitsh, Galloway et al. 2014). These CD4 T-cells are generally quiescent, uninfected by-stander cells, which primarily reside in lymphoid organs (Doitsh, Cavrois et al.

2010). The restriction factor SAMHD1 is active in non-cycling cells, including quiescent CD4 T-cells, reducing their permissiveness to HIV-1 (Baldauf, Pan et al. 2012, Descours, Cribier et al. 2012). Non-productive HIV-1 infection of these cells results in an accumulation of incomplete reverse transcripts in the cytosol. IFI16 was identified as a sensor of this HIV-1 DNA using an unbiased proteomic screen of tonsillar HIV-infected CD4 T-cell lysates (Monroe, Yang et al. 2014) . Indeed, IFI16 silencing or pharmacological inhibition of reverse transcription in resting human CD4 T-cells prevents caspase-1 activation and cell death following abortive HIV-1 infection. This study further reports that IFI16 is localised in the cytosol of resting human tonsillar CD4 T-cells and that IFI16 immunoprecipitates with HIV-1 Nef DNA (Monroe, Yang et al. 2014).

A subsequent study (Galloway, Doitsh et al. 2015) by the same group demonstrated that IFI16-mediated pyroptosis is dependent on the mode of viral spread. Specifically, direct cell-to-cell spread as opposed to cell-free transmission of virus is required to induce cell death of abortively infected CD4 T-cells. Furthermore, neither AIM2 (see above) nor STING (see below) silencing rescues cell death in HIV-1 infected tonsillar T-cells (Monroe, Yang et al. 2014). These observations suggest that cell type and differentiation state, as well as the route of virus entry, and perhaps other aspects of viral life cycles, play important roles in determining the how dsDNA is sensed and the ensuing downstream consequences.

cGAS-STING

The DNA sensor cGAS is essential for the type I IFN response to cytosolic dsDNA derived from microorganisms (Ablasser and Chen 2019). Active cGAS synthesises the second messenger cyclic guanosine monophosphate-adenosine monophosphate (cGAMP) (Wu, Sun et al. 2013), hence its nomenclature, cGAMP synthase. cGAMP binds to and activates stimulator of IFN genes (STING). Active STING then engages TANK-binding kinase 1 (TBK1), which in turn phosphorylates the transcription factor IFN regulatory factor 3 (IRF3), leading to type I IFN gene transcription (Ablasser and Chen 2019) (Figure 1B). Interestingly, cGAS has been implicated in some auto-inflammatory diseases and may therefore sense endogenous DNA in these settings (Ablasser, Hemmerling et al. 2014, Gao, Li et al. 2015, Gray, Treuting et al. 2015, Mackenzie, Carroll et al. 2016, Maelfait, Bridgeman et al. 2016). Furthermore, the cGAS-STING pathway is known to play an important role in anti-

cancer immunity and facilitates tumour-specific adaptive immune responses (Li and Chen 2018, Ng, Marshall et al. 2018). STING agonists have been proposed as adjuvants for vaccinations and cancer therapy (Corrales, Glickman et al. 2015).

Several recent studies demonstrate that programmed cell death, particularly apoptosis, can be activated downstream of the cGAS-STING pathway. Tang *et al.* show that natural and artificial STING agonists, including variants of cGAMP, induce intrinsic apoptosis in malignant B-cells (Tang, Zundell et al. 2016). This is characterised by decreased expression of the mitochondrial apoptosis inhibitor protein MCL-1 and increased cleavage of caspases 3 and 9 as well as PARP, consistent with intrinsic apoptosis (Tang, Zundell et al. 2016) (Figure 1B). STING agonist induced apoptosis is not re-capitulated by treatment with recombinant IFNβ suggesting that this is unlikely to be an indirect effect of signalling through the type I IFN receptor. In T-cells, STING activation blocks proliferation and triggers cell death characterised by increased expression of pro-apoptotic genes (Cerboni, Jeremiah et al. 2017, Larkin, Ilyukha et al. 2017) (Gulen, Koch et al. 2017). Mechanistically, disruption of calcium homeostasis mediated by STING in T-cells activates ER stress and consequent cell death (Wu, Chen et al. 2019). Another piece of evidence connecting the cytosolic DNA sensing pathway to apoptosis stems from the observation that human fibroblasts undergo STING-dependent apoptosis upon detection of DNA from herpes simplex virus 1 (HSV-1) and human cytomegalovirus (HCMV) (Diner, Lum et al. 2016). Somewhat analogous to the situation in resting T-cells infected with HIV, it has been suggested that reverse transcription intermediates trigger cell death in Human T Cell Leukemia Virus Type 1 (HTLV1) infected monocytes (Sze, Belgnaoui et al. 2013). In this case, however, the type of cell death is apoptosis rather than pyroptosis and, instead of IFI16, STING is required (Sze, Belgnaoui et al. 2013). In hepatocytes, endoplasmic reticulum stress triggers apoptosis in a STING- and IRF3-dependent manner (Petrasek, Iracheta-Vellve et al. 2013, Iracheta-Vellve, Petrasek et al. 2016). It will be interesting to determine whether cGAS is required, too, or whether this represents a function of STING independent of upstream nucleic acid sensing (Dunphy, Flannery et al. 2018). Finally, cGAMP induces STING-dependent cell death in the monocytic cell line THP1, although the type of cell death remains open (Cerboni, Jeremiah et al. 2017).

The cGAS-STING pathway can additionally signal necroptosis activation, as well as activate alternatives to cell death. Intracellular DNA sensing by cGAS in bone marrow-derived macrophages activates both type I IFN and TNF signalling pathways,

which synergise to activate RIPK3-driven necroptosis (Brault, Olsen et al. 2018). Moreover, cGAS-STING signalling downstream of mitochondrial DNA sensing can promote necroptosis via a type I IFN dependent mechanism (Chen, Tong et al. 2018). Mitochondrial DNA released during apoptosis has been shown to activate the cGAS-STING pathway, causing type I IFN to be secreted by dying cells (McArthur, Whitehead et al. 2018). In addition to programmed cell death induction, the cGAS-STING pathway has also been implicated in the induction of autophagy (Wassermann, Gulen et al. 2015, Watson, Bell et al. 2015) (Nassour, Radford et al. 2019) and in the regulation of cellular senescence (Dou, Ghosh et al. 2017, Glück, Guey et al. 2017, Yang, Wang et al. 2017) (Figure 1B). It will be interesting for future studies to determine how STING signalling can toggle between these alternatives to cell death, transcriptional responses leading to type I IFN expression and apoptosis induction.

TLR9

Toll-like receptor 9 (TLR9) is an endosomal DNA sensor that mediates MyD88-dependent transcriptional responses, including by NF-κB and IRF7 activation (Kumagai, Takeuchi et al. 2008). TLR9 has also been linked to cell death. TLR9 is strongly activated by DNA molecules containing CpG dinucleotides, which are commonly found in bacteria but are usually methylated in vertebrates (Hacker, Redecke et al. 2002). In a 2010 study (Brignole, Marimpietri et al. 2010), stimulation of neuroblastoma cells with TLR9 ligands was found to induce apoptosis. Indeed, treatment with CpG induces cell death that is characterised by cleavage of caspase 3 and 7 and, which is rescued by the pan-caspase inhibitor zVAD-FMK (Brignole, Marimpietri et al. 2010). The authors additionally observed depolarisation of the mitochondrial membrane potential consistent with intrinsic apoptosis. Down-regulation of TLR9 using RNA interference protects dendritic cells from CpG induced apoptosis. In nude mice with neuroblastoma, treatment with CpG prolongs long-term survival suggesting an important potential application for CpG oligonucleotides in cancer therapy (Brignole, Marimpietri et al. 2010). The use of nude mice, which lack a fully functioning adaptive immune system, is consistent with T-cell-independent cytolysis of the cancer cells. A number of other studies have linked TLR9 with apoptosis induction and revealed that TLR9 is not only pro-apoptotic, but also blocks apoptosis depending on the cellular context (Fischer, Rehm et al. 2005, Zheng, Asprodites et al. 2008, He, Li et al. 2011, El Kebir, Damlaj et al. 2014, Xiang, Yan et al. 2015). For

instance, murine macrophages exposed to environmental stress undergo increased apoptosis and a 2015 study (Xiang, Yan et al. 2015) found that deficiency of TLR9 attenuates macrophage apoptosis and is associated with down-regulation of caspase-3 and PARP cleavage. More recently, TLR9 activation has been implicated in immunopathogenic necrosis during ischaemic acute kidney injury, and in non-apoptotic hepatocyte death mediated by RIPK1 (Han, Li et al. 2018, Saito, Hikita et al. 2019). Altogether, these results reinforce the notion that the links between nucleic acid sensors and cell death are highly cell-type specific.

RNA sensors

Much like the DNA sensors discussed in the previous chapter, RNA sensors respond to foreign nucleic acids derived from invading microorganisms or to unusual endogenous RNA molecules (Goubau, Deddouche et al. 2013). Given the presence of normal cellular RNA in many different subcellular compartments, mechanisms of self versus non-self discrimination are particularly important for RNA sensors to avoid spontaneous responses. Here, we discuss programmed cell death as a consequence of the engagement of RNA sensors.

RLRs

RIG-I-like receptors (RLRs) are a family of cytosolic RNA sensors (Goubau, Deddouche et al. 2013). All three members of this protein family (RIG-I, MDA5 and LGP2) have a helicase domain and a so-called C-terminal domain, both of which bind to RNA. Additionally, RIG-I and MDA5 have two N-terminal CARD domains. Binding of immunostimulatory RNAs to the CTD and helicase domains of RIG-I and MDA5 results in conformational changes that expose their CARD domains, which then interact with the CARD domain found in MAVS. This mitochondrial protein is an essential adaptor for RLRs and mediates downstream signalling, for example the induction of type I IFNs (Goubau, Deddouche et al. 2013) (Figure 2A). The third RLR, LGP2, lacks CARD domains and regulates the function of RIG-I and MDA5 (Goubau, Deddouche et al. 2013).

In addition to their essential role in type I IFN induction during virus infection, RLRs have also been described to induce apoptosis. RLR activation can be triggered experimentally by cytosolic delivery of synthetic RNA agonists such as poly(I:C), which engages MDA5 and RIG-I, or 5’-triphosphate containing, base-paired RNAs that

activate RIG-I (Goubau, Deddouche et al. 2013). Transfection of such RNAs into the cytosol of cells not only results in type I IFN production but also in the induction of apoptosis (Poeck, Besch et al. 2008, Rintahaka, Wiik et al. 2008, Besch, Poeck et al. 2009). If activated naturally by virus infection, RLR-triggered apoptosis can be beneficial to the host by eliminating infected cells (Chattopadhyay, Yamashita et al. 2011). However, inappropriate RLR activation by self RNA can be immunopathogenic and, thus, RLR activation is tightly regulated (Dias Junior, Sampaio et al. 2019). The RNA editing enzyme adenosine deaminase acting on RNA 1 (ADAR1) has been implicated in the regulation of RNA sensing by MDA5 (Ahmad, Mu et al. 2018). ADAR1 deficiency has been associated with spontaneous activation of MDA5-mediated apoptosis induction, as well as induction of type I IFN and activation of translational arrest (Chung, Calis et al. 2018). Interesting translational approaches have been suggested to harness RLR-mediated apoptosis to eliminate cells persistently infected with viruses and to kill cancer cells (van den Boorn and Hartmann 2013, Li, Kaiser et al. 2016, Yu, Wang et al. 2016) (Elion, Jacobson et al. 2018). Stimulation of RIG-I in breast cancer cells activates pyroptosis, in addition to extrinsic apoptosis, thereby promoting anti-tumour immune responses (Elion, Jacobson et al. 2018). In addition to apoptosis and pyroptosis, RIG-I signalling has been implicated in the activation of RIPK3-mediated necroptosis driven by cooperative type I IFN and TNF signalling (Brault, Olsen et al. 2018).

Mechanistically, apoptosis triggered by RLRs requires MAVS and IRF3, much like IFN induction (Besch, Poeck et al. 2009, Chattopadhyay, Marques et al. 2010). However, MAVS has been suggested to form two functionally distinct complexes with IRF3. One mediates IRF3 phosphorylation by TBK1 and subsequent transcriptional induction of type I IFNs. The other complex additionally contains TRAF2, TRAF6 and the linear ubiquitin chain assembly complex (LUBAC) and modifies IRF3 by addition of linear ubiquitin chains (Chattopadhyay, Marques et al. 2010, Chattopadhyay, Kuzmanovic et al. 2016). IRF3 then translocates to mitochondria and together with the pro-apoptotic protein Bax triggers the cell intrinsic apoptosis pathway and cytochrome C release from mitochondria (Chattopadhyay, Marques et al. 2010, Chattopadhyay, Kuzmanovic et al. 2016). This pathway has been designated as “RIG-I-like receptor-induced IRF3 mediated pathway of apoptosis (RIPA)” (Chattopadhyay and Sen 2017) (Figure 2A). It will be interesting to determine whether this pathway of IRF3-mediated apoptosis is specific to the RLR pathway or is also activated downstream of other

nucleic acid sensors that signal to IFN induction via IRF3; for example, apoptosis initiated by cGAS and STING may involve a similar IRF3-dependent mechanism (Sze, Belgnaoui et al. 2013). Intriguingly, MDA5 may not only be involved in triggering apoptosis but also in the execution of apoptosis; this has been suggested to involve cleavage of MDA5 (Kovacsovics, Martinon et al. 2002).

ZBP1

Z-DNA binding protein 1 (ZBP1, also known as DAI and DLM-1) was described as an antiviral cytosolic DNA sensor inducing type I IFNs, hence its widely used name DNA-dependent activator of IFN-regulatory factors (DAI) (Takaoka, Wang et al. 2007). Studies in *Zbp1*$^{-/-}$ mice, however, did not support these early findings (Ishii, Kawagoe et al. 2008); ZBP1-deficient primary mouse embryonic fibroblasts and bone marrow-derived dendritic cells respond normally to dsDNA transfection into the cytosol and ZBP1 knockout mice show no defects in T cell-mediated and humoral immune responses when immunized with DNA vaccines, which depend on TBK1 and type I IFN signalling (Ishii, Kawagoe et al. 2008). Moreover, overexpression of ZBP1 in HEK293T cells does only modestly stimulates reporter constructs under control of promoter elements from type I IFN genes (Kaiser, Upton et al. 2008, Lippmann, Rothenburg et al. 2008, Rebsamen, Heinz et al. 2009). Importantly, seminal studies by the Chen lab have identified cGAS as a major cytosolic DNA sensor inducing type I IFNs and antiviral immunity (Ablasser and Chen 2019).

These observations pointed to a different antiviral mechanism of action. Mocarski and colleagues were the first to show that ZBP1 induces necroptosis when cells are infected with the β-herpesvirus murine cytomegalovirus (MCMV) (Upton, Kaiser et al. 2012). ZBP1 contains two tandem RIP homotypic interaction motifs (RHIMs) (Kaiser, Upton et al. 2008, Rebsamen, Heinz et al. 2009). ZBP1 associates with and activates the kinase RIPK3 via RHIM-RHIM interactions, leading to phosphorylation of the pseudokinase MLKL, which upon oligomerization forms pores in the plasma membrane causing necroptosis of the infected cell (Wallach, Kang et al. 2016) (Figure 2B). Interestingly, ZBP1-mediated cell death occurs independently of RIPK1 (Upton, Kaiser et al. 2010) setting it apart from TNF-induced necroptosis, which requires the kinase activity of RIPK1 (Silke, Rickard et al. 2015). MCMV encodes viral inhibitor of RIP kinase activation (vIRA, also known as M45), which contains its own RHIM and suppresses the execution of necroptosis by preventing ZBP1-RIPK3

interactions (Brune, Menard et al. 2001, Upton, Kaiser et al. 2010, Upton, Kaiser et al. 2012) (Pham, Shanmugam et al. 2019). Detection by ZBP1 is also important *in vivo* as replication of M45 RHIM-mutant MCMV is severely attenuated in wild-type mice, while it efficiently infects mice deficient for RIPK3 or ZBP1 (Upton, Kaiser et al. 2010, Upton, Kaiser et al. 2012).

It is not clear whether caspase-8 blockade is required for the sensitisation of cells to MCMV M45-mutant induced ZBP1-dependent necroptosis as is the case for necroptosis triggered through the TNF-receptor or as discussed later by TLR3 (Vercammen, Beyaert et al. 1998, Kaiser, Sridharan et al. 2013). MCMV may predispose some types of cells to ZBP1-induced necroptosis through the expression of viral inhibitor of caspase activation (vICA, also known as M36) (Menard, Wagner et al. 2003), which suppresses caspase-8 activation and apoptosis (Cicin-Sain, Ruzsics et al. 2008, Ebermann, Ruzsics et al. 2012). This appears to be the case in endothelial cells; however, macrophages that are infected with MCMV expressing non-functional M45 and M36 (which fails to block ZBP1-mediated necroptosis and caspase-8 induced apoptosis) still retain the ability to induce RIPK3/MLKL-dependent necroptosis, albeit independently of ZBP1 (Daley-Bauer, Roback et al. 2017).

ZBP1 also acts an innate sensor inducing cell death following Influenza A (IAV) and B virus infection (Kuriakose, Man et al. 2016, Thapa, Ingram et al. 2016). During influenza virus infection, ZBP1 signalling is positively regulated by the transcription factor IRF1 (Kuriakose, Zheng et al. 2018). In primary mouse embryonic fibroblasts and bone marrow-derived macrophages ZBP1 nucleates a RIPK3-containing complex that contains MLKL, triggering necroptosis, and FADD, which induces caspase-8 mediated apoptosis (Kuriakose, Man et al. 2016, Nogusa, Thapa et al. 2016, Thapa, Ingram et al. 2016). In LPS-primed macrophages, ZBP1 drives NLRP3 inflammasome activation, pyroptosis and IL-1β secretion (DeFilippis, Alvarado et al. 2010, Kuriakose, Man et al. 2016, Kesavardhana, Kuriakose et al. 2017) (Figure 2B). It is not clear how both apoptosis and necroptosis co-exist in cell cultures infected with IAV as these events are generally considered hierarchical and mutually exclusive (Weinlich, Oberst et al. 2017). Also, whether this phenomenon is regulated by viral factors that antagonize programmed cell death as is the case for MCMV remains to be determined. Two groups have independently shown that IAV replication is enhanced in ZBP1-deficient mice suggesting that ZBP1-mediated cell death is an effective antiviral strategy *in vivo* (Kuriakose, Man et al. 2016, Thapa, Ingram et al. 2016). These

studies, however, report differently on the survival outcome after challenge with a lethal dose of IAV. This discrepancy may be due to the fact that different contributions of immunopathology, host tolerance and viral resistance are a common source of variation in IAV survival studies (Ayres and Schneider 2012, Medzhitov, Schneider et al. 2012).

Most studies on ZBP1 so far have been conducted in the mouse system. ZBP1/RIPK3-dependent antiviral cell death in human cells is less well characterised, however, in an unbiased systemic approach to determine the antiviral effects of more than 350 interferon-stimulated genes, human ZBP1 was shown to prevent replication of multiple RNA and DNA viruses, including Coxsackie B virus, Sindbis virus, Hepatitis C virus and Vaccinia virus (Schoggins, Wilson et al. 2011, Schoggins, MacDuff et al. 2014). Human ZBP1 has additionally been shown to be involved in the detection of human herpes viruses (DeFilippis, Alvarado et al. 2010) (Furr, Chauhan et al. 2011, Pham, Kwon et al. 2013). More recently, human ZBP1 has been specifically implicated as a sensor of vaccinia virus, IAV and herpes simplex virus (HSV) for activation of RIPK3-driven antiviral necroptosis (Hartmann, Albrecht et al. 2017, Koehler, Cotsmire et al. 2017, Guo, Gilley et al. 2018).

In addition to its role during virus infection, ZBP1 has been shown to activate RIPK3/MLKL-mediated necroptosis in cells lacking RIPK1 (Lin, Kumari et al. 2016, Newton, Wickliffe et al. 2016). RIPK1-deficient mice die shortly after birth as a consequence of unchecked caspase-8-dependent apoptosis and RIPK3/MLKL-mediated necroptosis (Newton and Manning 2016). The RHIM-domain of RIPK1 selectively suppresses necroptosis as embryos in which the RHIM of RIPK1 is mutated develop RIPK3/MLKL-dependent dermal inflammation, but do not exhibit typical abnormalities associated with aberrant caspase-8 activation (Lin, Kumari et al. 2016, Newton, Wickliffe et al. 2016). Crossing these mice to ZBP1 knockout animals rescues their perinatal lethality. ZBP1-induced necroptosis also drives skin inflammation in mice in which RIPK1 expression was specifically abrogated in keratinocytes (Lin, Kumari et al. 2016). In the absence of a functional RIPK1 RHIM, ZBP1 was shown to interact with RIPK3 and induce its auto-phosphorylation; however, the authors did not detect ZBP1-RIPK1 interactions (Lin, Kumari et al. 2016, Newton, Wickliffe et al. 2016) and the precise mechanism of action of how RIPK1 prevents ZBP1 activation remains unknown.

What stimulates ZBP1 activation during viral infection and inflammation associated with RIPK1-deficiency? ZBP1 contains two N-terminal Zα domains (Zα1

and Zα2). These domains are found in a few different proteins and specifically bind to double stranded RNA or DNA in the 'zig-zag' or Z-conformation (Athanasiadis 2012). IAV RNA genomes co-immunoprecipitate with ZBP1 and ZBP1 has been shown to co-localise with IAV viral nucleoprotein complexes (Thapa, Ingram et al. 2016, Kesavardhana, Kuriakose et al. 2017). We and others have recently shown that upon MCMV infection IE3-mediated transcription - but not translation - of viral genes contributes to activation of ZBP1, and that newly synthesised RNA cross-links to ZBP1 (Maelfait, Liverpool et al. 2017, Sridharan, Ragan et al. 2017). These observations suggest that ZBP1 is an RNA sensor. Furthermore, ZBP1 readily crosslinks to endogenous RNA in uninfected cells (Maelfait, Liverpool et al. 2017). ZBP1 can additionally mediate IFN-induced necroptosis in the absence of infection, including during cell cycle arrest (Frank, Tuppi et al. 2019, Yang, Liang et al. 2019). Blockade of caspase-8 activity upon ectopic expression of ZBP1 induces cell death (Maelfait, Liverpool et al. 2017). Therefore, sensing of endogenous RNA by ZBP1 may contribute to the inflammatory disease seen in RIPK1 or caspase-8 deficient mice (Newton and Manning 2016).

Activation of ZBP1 is dependent on its Zα-domains, which specifically bind to Z-form dsRNA (Z-RNA) and not to A-form dsRNA (Kuriakose, Man et al. 2016, Thapa, Ingram et al. 2016, Maelfait, Liverpool et al. 2017, Sridharan, Ragan et al. 2017) (Guo, Gilley et al. 2018). Importantly, Zα-domains are essential *in vivo* as knock-in mice, which express ZBP1 carrying point mutations in both Zα-domains that abrogate binding to Z-RNA, do not restrict M45-mutant MCMV, similar to complete ZBP1 knockout animals (Maelfait, Liverpool et al. 2017). Under physiological conditions Z-RNA is unstable (Hall, Cruz et al. 1984) and the transition of A-form dsRNA into Z-RNA in living cells requires stabilisation, for example through protein-RNA interactions. This may be the case in IAV viral ribonucleoprotein complexes, where the winding of IAV genomes around viral nucleoproteins may induce the Z-conformation (Eisfeld, Neumann et al. 2015). Alternatively, certain dsRNA helices are more prone to form Z-RNA due to their sequence content (Deigendesch, Koch-Nolte et al. 2006). Indeed, alternating CG-, rather than AT-sequences more readily transition into Z-form nucleic acids (Wang, Hakoshima et al. 1984). MCMV and human CMV genomes are rich in CG-repeats and contain overlapping transcription units on both DNA strands, which give rise to viral dsRNA that may adopt the Z conformation. Collectively, these

observations suggest that Z-RNA constitutes a molecular pattern that activates ZBP1 and induces cell death.

TLR3

Toll-like receptor 3 (TLR3) is expressed on the cell surface and in the endosomal compartment and recognises dsRNA and poly(I:C) (Alexopoulou, Holt et al. 2001, Blasius and Beutler 2010). TLR3 signals via TIR domain-containing adapter inducing IFNβ (TRIF) and, through NF-κB and IRF3, stimulates production of pro-inflammatory cytokines and type I IFNs (Yamamoto, Sato et al. 2002, Hoebe, Du et al. 2003, Oshiumi, Matsumoto et al. 2003, Yamamoto, Sato et al. 2003) (Figure 2C). TRIF contains a C-terminal RHIM and interacts with RIPK1 to activate NF-κB (Meylan, Burns et al. 2004). RIPK1 can also form a complex with FADD and caspase-8 to induce apoptosis (Kaiser and Offermann 2005, Weber, Kirejczyk et al. 2010, Feoktistova, Geserick et al. 2011, Estornes, Toscano et al. 2012). In macrophages, simultaneous TLR3 stimulation and inhibition of translation results in cell death accompanied by caspase-8-mediated cleavage and release of IL-1β, independently of caspase-1 (Maelfait, Vercammen et al. 2008). When caspase-8 activity is compromised, TLR3 signals via RIPK3 and MLKL, independently of RIPK1, to induce necroptosis (He, Liang et al. 2011, Kaiser, Sridharan et al. 2013) (Figure 2C).

TLR3 is highly expressed in a subset of dendritic cells specialised in cross-presentation of extracellular antigens (Alloatti, Kotsias et al. 2016). In these cells, TLR3 induces important co-stimulatory signals for the induction of cytotoxic T cell responses against virus-infected cells (Schulz, Diebold et al. 2005). The dsRNA ligands that stimulate TLR3 during virus infection may originate from genomes of dsRNA viruses, dsRNA replication intermediates or overlapping transcripts of large DNA viruses (Weber, Wagner et al. 2006, Blasius and Beutler 2010). Mutations in *TLR3* or *TRIF* are associated with encephalitis after infection with HSV-1 (Zhang, Jouanguy et al. 2007, Sancho-Shimizu, Perez de Diego et al. 2011) or IAV (Hidaka, Matsuo et al. 2006). Furthermore, in IAV infected mice, TLR3 contributes to immunopathology (Le Goffic, Balloy et al. 2006) and triggers cell death in the lungs (Zinngrebe, Rieser et al. 2016). Cells from patients with homozygous loss-of-function mutations in RIPK1 exhibit impaired pro-inflammatory signalling via TLR3 and the TNF receptor, resulting in dysregulated cytokine secretion and a predisposition to necroptosis (Cuchet-Lourenço, Eletto et al. 2018).

TLR3 has been shown to induce cell death of epithelial cells in the small intestine in response to direct poly(I:C) administration (McAllister, Lakhdari et al. 2013) or after release of RNA from cells damaged by ionising radiation (Takemura, Kawasaki et al. 2014). Moreover, RNA released by HaCaT cells following treatment with sub-lethal ultraviolet B radiation increases sensitivity to TLR3-mediated apoptosis induced by poly(I:C) (Otkur, Liu et al. 2018). Indeed, endogenous dsRNA released from dying cells can act as a danger signal (Kariko, Ni et al. 2004) driving both beneficial and detrimental inflammatory responses that occur during tissue damage. For example, stimulation of TLR3 by non-coding RNAs released from dying keratinocytes aids tissue repair after exposure of the skin to ultraviolet light (Borkowski, Kuo et al. 2015) or wounding (Lai, Di Nardo et al. 2009, Nelson, Reddy et al. 2015). In contrast, TLR3 signalling contributes to tissue damage in mouse models of acute respiratory distress syndrome (Murray, Knight et al. 2008), myocardial infarction (Lu, Ren et al. 2014) and sepsis (Cavassani, Ishii et al. 2008). An important question for future work will be whether TLR3-mediated production of pro-inflammatory cytokines or TLR3-induced cell death, or both, causes these phenotypes.

In some cases, TLR3-induced cell death aggravates disease by contributing to a self-propagating cycle of inflammation. Mice deficient for the LUBAC subunit Sharpin develop chronic proliferative dermatitis (Seymour, Hasham et al. 2007). These animals develop severe skin inflammation (HogenEsch, Gijbels et al. 1993) due to early TNF-induced cell death of keratinocytes in the absence of an intact LUBAC (Kumari, Redouane et al. 2014, Rickard, Anderton et al. 2014). The release of endogenous dsRNA from dying cells subsequently triggers TLR3-mediated cell death driving skin inflammation with increasing severity. Accordingly, crossing Sharpin-deficient mice to TLR3 knockouts prevented cell death in the skin and ameliorated disease (Zinngrebe, Rieser et al. 2016). Interestingly, TRIF signalling was reported to contribute to skin inflammation in epidermis specific RIPK1 knockout animals, suggesting a role for TLR3 (or TLR4, another TLR that signals via TRIF) in autoinflammatory skin disease (Dannappel, Vlantis et al. 2014), although it appears that the relative contribution of ZBP1 in this setting is greater than that of TRIF (Dannappel, Vlantis et al. 2014, Lin, Kumari et al. 2016).

Age-related macular degeneration (AMD) is a complex human disease leading to progressive retinal deterioration ultimately causing blindness (Ambati, Atkinson et al. 2013). Choroidal neovascularisation followed by vascular leakage damages the

retinal pigment epithelium (RPE). Surprisingly, small interfering RNAs (siRNAs) targeting vascular endothelial growth factor-A (VEGFA), which are clinically tested to prevent angiogenesis, act through a TLR3-mediated cell death pathway and inhibit neovascularisation in a sequence independent manner (Kleinman, Yamada et al. 2008). Indeed, siRNAs can serve as agonists of TLR3 expressed on the cell surface of both blood vessels and lymphatic endothelial cells and induce apoptosis in these cells (Cho, Albuquerque et al. 2009). It should be noted that the application of siRNA-TLR3 induced cytotoxicity - at least in AMD - should be approached with caution as this process also induced the degeneration of the RPE itself (Kleinman, Kaneko et al. 2012).

Taken together, programmed cell death induced by TLR3 stimulation occurs in the forms of apoptosis and necroptosis. Sensing of viral or endogenous dsRNA by TLR3 contributes to beneficial host responses such as tissue repair and cytotoxic T cell activation, but it also triggers inflammatory disease. Finally, ligands that induce TLR3-mediated cell death can be harnessed for their therapeutic potential for example in AMD and possibly also for treatment of cancers (Glavan and Pavelic 2014) (Alkurdi, Virard et al. 2018).

Outlook

The examples discussed in this review illustrate intimate connections between innate immune nucleic acid sensors and programmed cell death pathways. Recent work has demonstrated that cell death often rivals more classical responses such as cytokine production in terms of importance to host defence against infectious or inflammatory insults. At the same time, it has also become clear that these connections are highly complex and variable, depending for example on disease context and cell type. Our understanding of how divergent signalling outcomes such as transcription of cytokine genes and cell death are coordinated is at its infancy. Post-translational modifications such as linear ubiquitin appear to play an important role in this decision (Chattopadhyay, Kuzmanovic et al. 2016, Zinngrebe, Rieser et al. 2016).

In addition to the three types of programmed cell death discussed here (Table 1), other cell death pathways such as NETosis, paraptosis, oxeiptosis and ferroptosis play important roles in host-pathogen interactions (Jorgensen, Rayamajhi et al. 2017, Monel, Compton et al. 2017) (Dixon, Lemberg et al. 2012, Holze, Michaudel et al. 2018). It will be interesting to study the role of nucleic acids sensors as putative upstream activators of these pathways. Moreover, the list of nucleic acid sensors

612 coupling to cell death presented in this article is not exhaustive; for example, several
613 NOD-like receptors have been reported to sense nucleic acids, sometimes working
614 together with helicase proteins. This includes NLRP9b, which senses RNA in
615 conjunction with DHX9, as well as NLRP3 that responds to IAV RNA (Allen, Scull et
616 al. 2009, Zhu, Ding et al. 2017). It seems clear that nucleic acid sensing and cell death
617 will remain a fertile area for future research for many years to come.
618

619 **Acknowledgements**

620 JR acknowledges funding from the UK Medical Research Council and the
621 Wellcome Trust. LL acknowledges funding from the Wellcome Trust (109024/Z/15/Z).
622 JM was a recipient of an EMBO long-term postdoctoral fellowship and was also
623 supported by Marie Curie Actions (EMBOCOFUND2010, GA-2010-267146). The
624 authors apologise to colleagues whose work could not be cited due to space limitations.
625

626 **Conflict of Interest**

627 The authors declare no conflict of interests.
628

References

- Ablasser, A. and Z. J. Chen (2019). "cGAS in action: Expanding roles in immunity and inflammation." Science **363**(6431): eaat8657.

- Ablasser, A., I. Hemmerling, J. L. Schmid-Burgk, R. Behrendt, A. Roers and V. Hornung (2014). "TREX1 deficiency triggers cell-autonomous immunity in a cGAS-dependent manner." J Immunol **192**(12): 5993-5997.

- Ahmad, S., X. Mu, F. Yang, E. Greenwald, J. W. Park, E. Jacob, C. Z. Zhang and S. Hur (2018). "Breaching Self-Tolerance to Alu Duplex RNA Underlies MDA5-Mediated Inflammation." Cell **172**(4): 797-810.e713.

- Alexopoulou, L., A. C. Holt, R. Medzhitov and R. A. Flavell (2001). "Recognition of double-stranded RNA and activation of NF-kappaB by Toll-like receptor 3." Nature **413**(6857): 732-738.

- Alkurdi, L., F. Virard, B. Vanbervliet, K. Weber, F. Toscano, M. Bonnin, N. Le Stang, S. Lantuejoul, O. Micheau, T. Renno, S. Lebecque and Y. Estornes (2018). "Release of c-FLIP brake selectively sensitizes human cancer cells to TLR3-mediated apoptosis." Cell Death Dis **9**(9): 874.

- Allen, I. C., M. A. Scull, C. B. Moore, E. K. Holl, E. McElvania-TeKippe, D. J. Taxman, E. H. Guthrie, R. J. Pickles and J. P. Ting (2009). "The NLRP3 inflammasome mediates in vivo innate immunity to influenza A virus through recognition of viral RNA." Immunity **30**(4): 556-565.

- Alloatti, A., F. Kotsias, J. G. Magalhaes and S. Amigorena (2016). "Dendritic cell maturation and cross-presentation: timing matters!" Immunol Rev **272**(1): 97-108.

- Almine, J. F., C. A. J. O'Hare, G. Dunphy, I. R. Haga, R. J. Naik, A. Atrih, D. J. Connolly, J. Taylor, I. R. Kelsall, A. G. Bowie, P. M. Beard and L. Unterholzner (2017). IFI16 and cGAS cooperate in the activation of STING during DNA sensing in human keratinocytes. Nature Communications, The Author(s) SN -. **8:** 14392.

- Ambati, J., J. P. Atkinson and B. D. Gelfand (2013). "Immunology of age-related macular degeneration." Nat Rev Immunol **13**(6): 438-451.

- Ansari, M. A., S. Dutta, M. V. Veettil, D. Dutta, J. Iqbal, B. Kumar, A. Roy, L. Chikoti, V. V. Singh and B. Chandran (2015). Herpesvirus Genome Recognition Induced Acetylation of Nuclear IFI16 Is Essential for Its Cytoplasmic Translocation, Inflammasome and IFN-beta Responses. PLoS Pathog. **11:** e1005019.

- Athanasiadis, A. (2012). "Zalpha-domains: at the intersection between RNA editing and innate immunity." Semin Cell Dev Biol **23**(3): 275-280.

- Ayres, J. S. and D. S. Schneider (2012). "Tolerance of infections." Annu Rev Immunol **30**: 271-294.

- Baldauf, H.-M., X. Pan, E. Erikson, S. Schmidt, W. Daddacha, M. Burggraf, K. Schenkova, I. Ambiel, G. Wabnitz, T. Gramberg, S. Panitz, E. Flory, N. R. Landau, S. Sertel, F. Rutsch, F. Lasitschka, B. Kim, R. König, O. T. Fackler and O. T. Keppler (2012). SAMHD1 restricts HIV-1 infection in resting CD4(+) T cells. Nat Med, Nature Publishing Group. **18:** 1682-1687.

- Barber, G. N. (2015). "STING: infection, inflammation and cancer." Nat Rev Immunol **15**(12): 760-770.

- Besch, R., H. Poeck, T. Hohenauer, D. Senft, G. Hacker, C. Berking, V. Hornung, S. Endres, T. Ruzicka, S. Rothenfusser and G. Hartmann (2009). "Proapoptotic signaling induced by RIG-I and MDA-5 results in type I interferon-independent apoptosis in human melanoma cells." J Clin Invest **119**(8): 2399-2411.

- Blasius, A. L. and B. Beutler (2010). "Intracellular toll-like receptors." Immunity **32**(3): 305-315.

- Borkowski, A. W., I. H. Kuo, J. J. Bernard, T. Yoshida, M. R. Williams, N. J. Hung, B. D. Yu, L. A. Beck and R. L. Gallo (2015). "Toll-like receptor 3 activation is required for normal skin barrier repair following UV damage." J Invest Dermatol **135**(2): 569-578.

- Brault, M., T. M. Olsen, J. Martinez, D. B. Stetson and A. Oberst (2018). "Intracellular Nucleic Acid Sensing Triggers Necroptosis through Synergistic Type I IFN and TNF Signaling." J Immunol **200**(8): 2748-2756.

- Brignole, C., D. Marimpietri, D. Di Paolo, P. Perri, F. Morandi, F. Pastorino, A. Zorzoli, G. Pagnan, M. Loi, I. Caffa, G. Erminio, R. Haupt, C. Gambini, V. Pistoia and M. Ponzoni (2010). Therapeutic targeting of TLR9 inhibits cell growth and induces apoptosis in neuroblastoma. Cancer Res, American Association for Cancer Research. **70:** 9816-9826.

- Brune, W., C. Menard, J. Heesemann and U. H. Koszinowski (2001). "A ribonucleotide reductase homolog of cytomegalovirus and endothelial cell tropism." Science **291**(5502): 303-305.

- Brunette, R. L., J. M. Young, D. G. Whitley, I. E. Brodsky, H. S. Malik and D. B. Stetson (2012). "Extensive evolutionary and functional diversity among mammalian AIM2-like receptors." J Exp Med **209**(11): 1969-1983.

- Burckstummer, T., C. Baumann, S. Bluml, E. Dixit, G. Durnberger, H. Jahn, M. Planyavsky, M. Bilban, J. Colinge, K. L. Bennett and G. Superti-Furga (2009). "An orthogonal proteomic-genomic screen identifies AIM2 as a cytoplasmic DNA sensor for the inflammasome." Nat Immunol **10**(3): 266-272.

- Cavassani, K. A., M. Ishii, H. Wen, M. A. Schaller, P. M. Lincoln, N. W. Lukacs, C. M. Hogaboam and S. L. Kunkel (2008). "TLR3 is an endogenous sensor of tissue necrosis during acute inflammatory events." J Exp Med **205**(11): 2609-2621.

- Cerboni, S., N. Jeremiah, M. Gentili, U. Gehrmann, C. Conrad, M. C. Stolzenberg, C. Picard, B. Neven, A. Fischer, S. Amigorena, F. Rieux-Laucat and N. Manel (2017). "Intrinsic antiproliferative activity of the innate sensor STING in T lymphocytes." J Exp Med **214**(6): 1769-1785.

- Chattopadhyay, S., T. Kuzmanovic, Y. Zhang, J. L. Wetzel and G. C. Sen (2016). "Ubiquitination of the Transcription Factor IRF-3 Activates RIPA, the Apoptotic Pathway that Protects Mice from Viral Pathogenesis." Immunity **44**(5): 1151-1161.

- Chattopadhyay, S., J. T. Marques, M. Yamashita, K. L. Peters, K. Smith, A. Desai, B. R. Williams and G. C. Sen (2010). "Viral apoptosis is induced by IRF-3-mediated activation of Bax." Embo j **29**(10): 1762-1773.

- Chattopadhyay, S. and G. C. Sen (2017). "RIG-I-like receptor-induced IRF3 mediated pathway of apoptosis (RIPA): a new antiviral pathway." Protein Cell **8**(3): 165-168.

- Chattopadhyay, S., M. Yamashita, Y. Zhang and G. C. Sen (2011). "The IRF-3/Bax-mediated apoptotic pathway, activated by viral cytoplasmic RNA and DNA, inhibits virus replication." J Virol **85**(8): 3708-3716.

- Chen, D., J. Tong, L. Yang, L. Wei, D. B. Stolz, J. Yu, J. Zhang and L. Zhang (2018). "PUMA amplifies necroptosis signaling by activating cytosolic DNA sensors." Proceedings of the National Academy of Sciences **115**(15): 3930-3935.

- Chen, J., Z. Wang and S. Yu (2017). AIM2 regulates viability and apoptosis in human colorectal cancer cells via the PI3K/Akt pathway. Onco Targets Ther. **10:** 811-817.

- Cho, W. G., R. J. Albuquerque, M. E. Kleinman, V. Tarallo, A. Greco, M. Nozaki, M. G. Green, J. Z. Baffi, B. K. Ambati, M. De Falco, J. S. Alexander, A. Brunetti, S. De Falco and J. Ambati (2009). "Small interfering RNA-induced TLR3 activation inhibits blood and lymphatic vessel growth." Proc Natl Acad Sci U S A **106**(17): 7137-7142.

- Choubey, D. and R. Panchanathan (2017). "Absent in Melanoma 2 proteins in SLE." Clin Immunol **176**: 42-48.

- Chung, H., J. J. A. Calis, X. Wu, T. Sun, Y. Yu, S. L. Sarbanes, V. L. Dao Thi, A. R. Shilvock, H. H. Hoffmann, B. R. Rosenberg and C. M. Rice (2018). "Human ADAR1 Prevents Endogenous RNA from Triggering Translational Shutdown." Cell **172**(4): 811-824.e814.

- Cicin-Sain, L., Z. Ruzsics, J. Podlech, I. Bubic, C. Menard, S. Jonjic, M. J. Reddehase and U. H. Koszinowski (2008). "Dominant-negative FADD rescues the in vivo fitness of a cytomegalovirus lacking an antiapoptotic viral gene." J Virol **82**(5): 2056-2064.

- Corrales, L., L. H. Glickman, S. M. McWhirter, D. B. Kanne, K. E. Sivick, G. E. Katibah, S. R. Woo, E. Lemmens, T. Banda, J. J. Leong, K. Metchette, T. W. Dubensky, Jr. and T. F. Gajewski (2015). "Direct Activation of STING in the Tumor Microenvironment Leads to Potent and Systemic Tumor Regression and Immunity." Cell Rep **11**(7): 1018-1030.

- Crow, Y. J. and N. Manel (2015). "Aicardi-Goutieres syndrome and the type I interferonopathies." Nat Rev Immunol **15**(7): 429-440.

- Cuchet-Lourenço, D., D. Eletto, C. Wu, V. Plagnol, O. Papapietro, J. Curtis, L. Ceron-Gutierrez, C. M. Bacon, S. Hackett, B. Alsaleem, M. Maes, M. Gaspar, A. Alisaac, E. Goss, E. AlIdrissi, D. Siegmund, H. Wajant, D. Kumararatne, M. S. AlZahrani, P. D. Arkwright, M. Abinun, R. Doffinger and S. Nejentsev (2018). "Biallelic RIPK1 mutations in humans cause severe immunodeficiency, arthritis, and intestinal inflammation." Science **361**(6404): 810-813.

- Daley-Bauer, L. P., L. Roback, L. N. Crosby, A. L. McCormick, Y. Feng, W. J. Kaiser and E. S. Mocarski (2017). "Mouse cytomegalovirus M36 and M45 death suppressors cooperate to prevent inflammation resulting from antiviral programmed cell death pathways." Proc Natl Acad Sci U S A **114**(13): E2786-E2795.

- Dannappel, M., K. Vlantis, S. Kumari, A. Polykratis, C. Kim, L. Wachsmuth, C. Eftychi, J. Lin, T. Corona, N. Hermance, M. Zelic, P. Kirsch, M. Basic, A. Bleich, M. Kelliher and M. Pasparakis (2014). "RIPK1 maintains epithelial homeostasis by inhibiting apoptosis and necroptosis." Nature **513**(7516): 90-94.

- Danthi, P. (2016). "Viruses and the Diversity of Cell Death." Annu Rev Virol **3**(1): 533-553.

- DeFilippis, V. R., D. Alvarado, T. Sali, S. Rothenburg and K. Fruh (2010). "Human cytomegalovirus induces the interferon response via the DNA sensor ZBP1." J Virol **84**(1): 585-598.

- Deigendesch, N., F. Koch-Nolte and S. Rothenburg (2006). "ZBP1 subcellular localization and association with stress granules is controlled by its Z-DNA binding domains." Nucleic Acids Res **34**(18): 5007-5020.

- Descours, B., A. Cribier, C. Chable-Bessia, D. Ayinde, G. Rice, Y. Crow, A. Yatim, O. Schwartz, N. Laguette and M. Benkirane (2012). SAMHD1 restricts HIV-1 reverse transcription in quiescent CD4(+) T-cells. Retrovirology, BioMed Central Ltd. **9:** 87.

- DeYoung, K. L., M. E. Ray, Y. A. Su, S. L. Anzick, R. W. Johnstone, J. A. Trapani, P. S. Meltzer and J. M. Trent (1997). "Cloning a novel member of the human interferon-inducible gene family associated with control of tumorigenicity in a model of human melanoma." Oncogene **15**(4): 453-457.

- Dias Junior, A. G., N. G. Sampaio and J. Rehwinkel (2019). "A Balancing Act: MDA5 in Antiviral Immunity and Autoinflammation." Trends Microbiol **27**(1): 75-85.

- Diner, B. A., K. K. Lum, J. E. Toettcher and I. M. Cristea (2016). Viral DNA Sensors IFI16 and Cyclic GMP-AMP Synthase Possess Distinct Functions in Regulating Viral Gene Expression, Immune Defenses, and Apoptotic Responses during Herpesvirus Infection. mBio. **7**.

- Dixon, S. J., K. M. Lemberg, M. R. Lamprecht, R. Skouta, E. M. Zaitsev, C. E. Gleason, D. N. Patel, A. J. Bauer, A. M. Cantley, W. S. Yang, B. Morrison, 3rd and B. R. Stockwell (2012). "Ferroptosis: an iron-dependent form of nonapoptotic cell death." Cell **149**(5): 1060-1072.

- Doitsh, G., M. Cavrois, K. G. Lassen, O. Zepeda, Z. Yang, M. L. Santiago, A. M. Hebbeler and W. C. Greene (2010). "Abortive HIV infection mediates CD4 T cell depletion and inflammation in human lymphoid tissue." Cell **143**(5): 789-801.

- Doitsh, G., N. L. K. Galloway, X. Geng, Z. Yang, K. M. Monroe, O. Zepeda, P. W. Hunt, H. Hatano, S. Sowinski, I. Munoz-Arias and W. C. Greene (2014). "Cell death by pyroptosis drives CD4 T-cell depletion in HIV-1 infection." Nature **505**(7484): 509-514.

- Dou, Z., K. Ghosh, M. G. Vizioli, J. Zhu, P. Sen, K. J. Wangensteen, J. Simithy, Y. Lan, Y. Lin, Z. Zhou, B. C. Capell, C. Xu, M. Xu, J. E. Kieckhaefer, T. Jiang, M. Shoshkes-Carmel, K. M. A. A. Tanim, G. N. Barber, J. T. Seykora, S. E. Millar, K. H. Kaestner, B. A. Garcia, P. D. Adams and S. L. Berger (2017). "Cytoplasmic chromatin triggers inflammation in senescence and cancer." Nature **550**: 402.

- Dunphy, G., S. M. Flannery, J. F. Almine, D. J. Connolly, C. Paulus, K. L. Jonsson, M. R. Jakobsen, M. M. Nevels, A. G. Bowie and L. Unterholzner (2018). "Non-canonical Activation of the DNA Sensing Adaptor STING by ATM and IFI16

807 Mediates NF-kappaB Signaling after Nuclear DNA Damage." Mol Cell **71**(5): 745-
808 760.e745.

809 • Dutta, D., S. Dutta, M. V. Veettil, A. Roy, M. A. Ansari, J. Iqbal, L. Chikoti, B.
810 Kumar, K. E. Johnson and B. Chandran (2015). BRCA1 Regulates IFI16 Mediated
811 Nuclear Innate Sensing of Herpes Viral DNA and Subsequent Induction of the
812 Innate Inflammasome and Interferon-beta Responses. PLoS Pathog. **11:** e1005030.

813 • Ebermann, L., Z. Ruzsics, C. A. Guzman, N. van Rooijen, R. Casalegno-Garduno,
814 U. Koszinowski and L. Cicin-Sain (2012). "Block of death-receptor apoptosis
815 protects mouse cytomegalovirus from macrophages and is a determinant of
816 virulence in immunodeficient hosts." PLoS Pathog **8**(12): e1003062.

817 • Eisfeld, A. J., G. Neumann and Y. Kawaoka (2015). "At the centre: influenza A
818 virus ribonucleoproteins." Nat Rev Microbiol **13**(1): 28-41.

819 • El Kebir, D., A. Damlaj and J. G. Filep (2014). Toll-like receptor 9 signaling delays
820 neutrophil apoptosis by increasing transcription of Mcl-1. PLoS ONE. **9:** e87006.

821 • Elion, D. L., M. E. Jacobson, D. J. Hicks, B. Rahman, V. Sanchez, P. I. Gonzales-
822 Ericsson, O. Fedorova, A. M. Pyle, J. T. Wilson and R. S. Cook (2018).
823 "Therapeutically Active RIG-I Agonist Induces Immunogenic Tumor Cell Killing
824 in Breast Cancers." Cancer Res **78**(21): 6183-6195.

825 • Estornes, Y., F. Toscano, F. Virard, G. Jacquemin, A. Pierrot, B. Vanbervliet, M.
826 Bonnin, N. Lalaoui, P. Mercier-Gouy, Y. Pacheco, B. Salaun, T. Renno, O.
827 Micheau and S. Lebecque (2012). "dsRNA induces apoptosis through an atypical
828 death complex associating TLR3 to caspase-8." Cell Death Differ **19**(9): 1482-
829 1494.

830 • Feoktistova, M., P. Geserick, B. Kellert, D. P. Dimitrova, C. Langlais, M. Hupe, K.
831 Cain, M. MacFarlane, G. Hacker and M. Leverkus (2011). "cIAPs block
832 Ripoptosome formation, a RIP1/caspase-8 containing intracellular cell death
833 complex differentially regulated by cFLIP isoforms." Mol Cell **43**(3): 449-463.

834 • Fernandes-Alnemri, T., J. W. Yu, P. Datta, J. Wu and E. S. Alnemri (2009). "AIM2
835 activates the inflammasome and cell death in response to cytoplasmic DNA."
836 Nature **458**(7237): 509-513.

837 • Fisch, D., H. Bando, B. Clough, V. Hornung, M. Yamamoto, A. R. Shenoy and E.
838 M. Frickel (2019). "Human GBP1 is a microbe-specific gatekeeper of macrophage
839 apoptosis and pyroptosis." Embo j.

840 • Fischer, S. F., M. Rehm, A. Bauer, F. Hofling, S. Kirschnek, M. Rutz, S. Bauer, H.
841 Wagner and G. Hacker (2005). Toll-like receptor 9 signaling can sensitize
842 fibroblasts for apoptosis. Immunol Lett. **97:** 115-122.

- Frank, T., M. Tuppi, M. Hugle, V. Dötsch, S. J. L. van Wijk and S. Fulda (2019). "Cell cycle arrest in mitosis promotes interferon-induced necroptosis." Cell Death & Differentiation.

- Furr, S. R., V. S. Chauhan, M. J. Moerdyk-Schauwecker and I. Marriott (2011). "A role for DNA-dependent activator of interferon regulatory factor in the recognition of herpes simplex virus type 1 by glial cells." J Neuroinflammation **8**: 99.

- Gaidt, M. M., T. S. Ebert, D. Chauhan, K. Ramshorn, F. Pinci, S. Zuber, F. O'Duill, J. L. Schmid-Burgk, F. Hoss, R. Buhmann, G. Wittmann, E. Latz, M. Subklewe and V. Hornung (2017). "The DNA Inflammasome in Human Myeloid Cells Is Initiated by a STING-Cell Death Program Upstream of NLRP3." Cell **171**(5): 1110-1124.e1118.

- Galloway, N. L. K., G. Doitsh, K. M. Monroe, Z. Yang, I. Muñoz-Arias, D. N. Levy and W. C. Greene (2015). Cell-to-Cell Transmission of HIV-1 Is Required to Trigger Pyroptotic Death of Lymphoid-Tissue-Derived CD4 T Cells. Cell Reports. **12:** 1555-1563.

- Gao, D., T. Li, X. D. Li, X. Chen, Q. Z. Li, M. Wight-Carter and Z. J. Chen (2015). "Activation of cyclic GMP-AMP synthase by self-DNA causes autoimmune diseases." Proc Natl Acad Sci U S A **112**(42): E5699-5705.

- Glavan, T. M. and J. Pavelic (2014). "The exploitation of Toll-like receptor 3 signaling in cancer therapy." Curr Pharm Des **20**(42): 6555-6564.

- Glück, S., B. Guey, M. F. Gulen, K. Wolter, T. W. Kang, N. A. Schmacke, A. Bridgeman, J. Rehwinkel, L. Zender and A. Ablasser (2017). "Innate immune sensing of cytosolic chromatin fragments through cGAS promotes senescence." Nat Cell Biol **19**(9): 1061-1070.

- Goubau, D., S. Deddouche and C. Reis e Sousa (2013). "Cytosolic sensing of viruses." Immunity **38**(5): 855-869.

- Gray, E. E., P. M. Treuting, J. J. Woodward and D. B. Stetson (2015). "Cutting Edge: cGAS Is Required for Lethal Autoimmune Disease in the Trex1-Deficient Mouse Model of Aicardi-Goutieres Syndrome." J Immunol **195**(5): 1939-1943.

- Gulen, M. F., U. Koch, S. M. Haag, F. Schuler, L. Apetoh, A. Villunger, F. Radtke and A. Ablasser (2017). "Signalling strength determines proapoptotic functions of STING." Nature Communications **8**(1): 427.

- Guo, H., R. P. Gilley, A. Fisher, R. Lane, V. J. Landsteiner, K. B. Ragan, C. M. Dovey, J. E. Carette, J. W. Upton, E. S. Mocarski and W. J. Kaiser (2018). "Species-independent contribution of ZBP1/DAI/DLM-1-triggered necroptosis in host defense against HSV1." Cell Death & Disease **9**(8): 816.

- Hacker, G., V. Redecke and H. Hacker (2002). "Activation of the immune system by bacterial CpG-DNA." Immunology **105**(3): 245-251.

- Hall, K., P. Cruz, I. Tinoco, Jr., T. M. Jovin and J. H. van de Sande (1984). "'Z-RNA'--a left-handed RNA double helix." Nature **311**(5986): 584-586.

- Han, S. J., H. Li, M. Kim, M. J. Shlomchik and H. T. Lee (2018). "Kidney Proximal Tubular TLR9 Exacerbates Ischemic Acute Kidney Injury." J Immunol **201**(3): 1073-1085.

- Hartmann, B. M., R. A. Albrecht, E. Zaslavsky, G. Nudelman, H. Pincas, N. Marjanovic, M. Schotsaert, C. Martínez-Romero, R. Fenutria, J. P. Ingram, I. Ramos, A. Fernandez-Sesma, S. Balachandran, A. García-Sastre and S. C. Sealfon (2017). "Pandemic H1N1 influenza A viruses suppress immunogenic RIPK3-driven dendritic cell death." Nature Communications **8**(1): 1931.

- Hartmann, G. (2017). "Nucleic Acid Immunity." Adv Immunol **133**: 121-169.

- He, L., H. Li, L. Chen, J. Miao, Y. Jiang, Y. Zhang, Z. Xiao, G. Hanley, Y. Li, X. Zhang, G. LeSage, Y. Peng and D. Yin (2011). Toll-like receptor 9 is required for opioid-induced microglia apoptosis. PLoS ONE. **6:** e18190.

- He, S., Y. Liang, F. Shao and X. Wang (2011). "Toll-like receptors activate programmed necrosis in macrophages through a receptor-interacting kinase-3-mediated pathway." Proc Natl Acad Sci U S A **108**(50): 20054-20059.

- Hidaka, F., S. Matsuo, T. Muta, K. Takeshige, T. Mizukami and H. Nunoi (2006). "A missense mutation of the Toll-like receptor 3 gene in a patient with influenza-associated encephalopathy." Clin Immunol **119**(2): 188-194.

- Hoebe, K., X. Du, P. Georgel, E. Janssen, K. Tabeta, S. O. Kim, J. Goode, P. Lin, N. Mann, S. Mudd, K. Crozat, S. Sovath, J. Han and B. Beutler (2003). "Identification of Lps2 as a key transducer of MyD88-independent TIR signalling." Nature **424**(6950): 743-748.

- HogenEsch, H., M. J. Gijbels, E. Offerman, J. van Hooft, D. W. van Bekkum and C. Zurcher (1993). "A spontaneous mutation characterized by chronic proliferative dermatitis in C57BL mice." Am J Pathol **143**(3): 972-982.

- Holze, C., C. Michaudel, C. Mackowiak, D. A. Haas, C. Benda, P. Hubel, F. L. Pennemann, D. Schnepf, J. Wettmarshausen, M. Braun, D. W. Leung, G. K. Amarasinghe, F. Perocchi, P. Staeheli, B. Ryffel and A. Pichlmair (2018). "Oxeiptosis, a ROS-induced caspase-independent apoptosis-like cell-death pathway." Nat Immunol **19**(2): 130-140.

- Hornung, V., A. Ablasser, M. Charrel-Dennis, F. Bauernfeind, G. Horvath, D. R. Caffrey, E. Latz and K. A. Fitzgerald (2009). "AIM2 recognizes cytosolic dsDNA and forms a caspase-1-activating inflammasome with ASC." Nature **458**(7237): 514-518.

- Hornung, V., R. Hartmann, A. Ablasser and K. P. Hopfner (2014). "OAS proteins and cGAS: unifying concepts in sensing and responding to cytosolic nucleic acids." Nat Rev Immunol **14**(8): 521-528.

- Hu, B., C. Jin, H.-B. Li, J. Tong, X. Ouyang, N. M. Cetinbas, S. Zhu, T. Strowig, F. C. Lam, C. Zhao, J. Henao-Mejia, O. Yilmaz, K. A. Fitzgerald, S. C. Eisenbarth, E. Elinav and R. A. Flavell (2016). The DNA-sensing AIM2 inflammasome controls radiation-induced cell death and tissue injury. Science (New York, N.Y.), American Association for the Advancement of Science. **354:** 765-768.

- Iracheta-Vellve, A., J. Petrasek, B. Gyongyosi, A. Satishchandran, P. Lowe, K. Kodys, D. Catalano, C. D. Calenda, E. A. Kurt-Jones, K. A. Fitzgerald and G. Szabo (2016). "Endoplasmic Reticulum Stress-induced Hepatocellular Death Pathways Mediate Liver Injury and Fibrosis via Stimulator of Interferon Genes." J Biol Chem **291**(52): 26794-26805.

- Ishii, K. J., T. Kawagoe, S. Koyama, K. Matsui, H. Kumar, T. Kawai, S. Uematsu, O. Takeuchi, F. Takeshita, C. Coban and S. Akira (2008). "TANK-binding kinase-1 delineates innate and adaptive immune responses to DNA vaccines." Nature **451**(7179): 725-729.

- Jin, T., A. Perry, J. Jiang, P. Smith, J. A. Curry, L. Unterholzner, Z. Jiang, G. Horvath, V. A. Rathinam, R. W. Johnstone, V. Hornung, E. Latz, A. G. Bowie, K. A. Fitzgerald and T. S. Xiao (2012). "Structures of the HIN domain:DNA complexes reveal ligand binding and activation mechanisms of the AIM2 inflammasome and IFI16 receptor." Immunity **36**(4): 561-571.

- Jønsson, K. L., A. Laustsen, C. Krapp, K. A. Skipper, K. Thavachelvam, D. Hotter, J. H. Egedal, M. Kjolby, P. Mohammadi, T. Prabakaran, L. K. Sørensen, C. Sun, S. B. Jensen, C. K. Holm, R. J. Lebbink, M. Johannsen, M. Nyegaard, J. G. Mikkelsen, F. Kirchhoff, S. R. Paludan and M. R. Jakobsen (2017). IFI16 is required for DNA sensing in human macrophages by promoting production and function of cGAMP. Nature Communications, The Author(s) SN -. **8:** 14391 EP -.

- Jorgensen, I., M. Rayamajhi and E. A. Miao (2017). "Programmed cell death as a defence against infection." Nat Rev Immunol **17**(3): 151-164.

- Juruj, C., V. Lelogeais, R. Pierini, M. Perret, B. F. Py, Y. Jamilloux, P. Broz, F. Ader, M. Faure and T. Henry (2013). "Caspase-1 activity affects AIM2 speck formation/stability through a negative feedback loop." Front Cell Infect Microbiol **3**: 14.

- Kaiser, W. J. and M. K. Offermann (2005). "Apoptosis induced by the toll-like receptor adaptor TRIF is dependent on its receptor interacting protein homotypic interaction motif." J Immunol **174**(8): 4942-4952.

- Kaiser, W. J., H. Sridharan, C. Huang, P. Mandal, J. W. Upton, P. J. Gough, C. A. Sehon, R. W. Marquis, J. Bertin and E. S. Mocarski (2013). "Toll-like receptor 3-mediated necrosis via TRIF, RIP3, and MLKL." J Biol Chem **288**(43): 31268-31279.

- Kaiser, W. J., J. W. Upton and E. S. Mocarski (2008). "Receptor-interacting protein homotypic interaction motif-dependent control of NF-kappa B activation via the DNA-dependent activator of IFN regulatory factors." J Immunol **181**(9): 6427-6434.

- Kariko, K., H. Ni, J. Capodici, M. Lamphier and D. Weissman (2004). "mRNA is an endogenous ligand for Toll-like receptor 3." J Biol Chem **279**(13): 12542-12550.

- Kayagaki, N., B. L. Lee, I. B. Stowe, O. S. Kornfeld, K. O'Rourke, K. M. Mirrashidi, B. Haley, C. Watanabe, M. Roose-Girma, Z. Modrusan, S. Kummerfeld, R. Reja, Y. Zhang, V. Cho, T. D. Andrews, L. X. Morris, C. C. Goodnow, E. M. Bertram and V. M. Dixit (2019). "IRF2 transcriptionally induces GSDMD expression for pyroptosis." Sci Signal **12**(582).

- Kayagaki, N., I. B. Stowe, B. L. Lee, K. O'Rourke, K. Anderson, S. Warming, T. Cuellar, B. Haley, M. Roose-Girma, Q. T. Phung, P. S. Liu, J. R. Lill, H. Li, J. Wu, S. Kummerfeld, J. Zhang, W. P. Lee, S. J. Snipas, G. S. Salvesen, L. X. Morris, L. Fitzgerald, Y. Zhang, E. M. Bertram, C. C. Goodnow and V. M. Dixit (2015). "Caspase-11 cleaves gasdermin D for non-canonical inflammasome signalling." Nature **526**(7575): 666-671.

- Kerur, N., M. V. Veettil, N. Sharma-Walia, V. Bottero, S. Sadagopan, P. Otageri and B. Chandran (2011). IFI16 acts as a nuclear pathogen sensor to induce the inflammasome in response to Kaposi Sarcoma-associated herpesvirus infection. Cell Host & Microbe. **9:** 363-375.

- Kesavardhana, S., T. Kuriakose, C. S. Guy, P. Samir, R. K. S. Malireddi, A. Mishra and T. D. Kanneganti (2017). "ZBP1/DAI ubiquitination and sensing of influenza vRNPs activate programmed cell death." J Exp Med.

- Kleinman, M. E., H. Kaneko, W. G. Cho, S. Dridi, B. J. Fowler, A. D. Blandford, R. J. Albuquerque, Y. Hirano, H. Terasaki, M. Kondo, T. Fujita, B. K. Ambati, V. Tarallo, B. D. Gelfand, S. Bogdanovich, J. Z. Baffi and J. Ambati (2012). "Short-interfering RNAs induce retinal degeneration via TLR3 and IRF3." Mol Ther **20**(1): 101-108.

- Kleinman, M. E., K. Yamada, A. Takeda, V. Chandrasekaran, M. Nozaki, J. Z. Baffi, R. J. Albuquerque, S. Yamasaki, M. Itaya, Y. Pan, B. Appukuttan, D. Gibbs,

Z. Yang, K. Kariko, B. K. Ambati, T. A. Wilgus, L. A. DiPietro, E. Sakurai, K. Zhang, J. R. Smith, E. W. Taylor and J. Ambati (2008). "Sequence- and target-independent angiogenesis suppression by siRNA via TLR3." Nature **452**(7187): 591-597.

- Koehler, H., S. Cotsmire, J. Langland, K. V. Kibler, D. Kalman, J. W. Upton, E. S. Mocarski and B. L. Jacobs (2017). "Inhibition of DAI-dependent necroptosis by the Z-DNA binding domain of the vaccinia virus innate immune evasion protein, E3." Proc Natl Acad Sci U S A **114**(43): 11506-11511.

- Kovacsovics, M., F. Martinon, O. Micheau, J. L. Bodmer, K. Hofmann and J. Tschopp (2002). "Overexpression of Helicard, a CARD-containing helicase cleaved during apoptosis, accelerates DNA degradation." Curr Biol **12**(10): 838-843.

- Kumagai, Y., O. Takeuchi and S. Akira (2008). "TLR9 as a key receptor for the recognition of DNA." Adv Drug Deliv Rev **60**(7): 795-804.

- Kumari, S., Y. Redouane, J. Lopez-Mosqueda, R. Shiraishi, M. Romanowska, S. Lutzmayer, J. Kuiper, C. Martinez, I. Dikic, M. Pasparakis and F. Ikeda (2014). "Sharpin prevents skin inflammation by inhibiting TNFR1-induced keratinocyte apoptosis." Elife **3**.

- Kuriakose, T., S. M. Man, R. K. Malireddi, R. Karki, S. Kesavardhana, D. E. Place, G. Neale, P. Vogel and T. D. Kanneganti (2016). "ZBP1/DAI is an innate sensor of influenza virus triggering the NLRP3 inflammasome and programmed cell death pathways." Sci Immunol **1**(2).

- Kuriakose, T., M. Zheng, G. Neale and T. D. Kanneganti (2018). "IRF1 Is a Transcriptional Regulator of ZBP1 Promoting NLRP3 Inflammasome Activation and Cell Death during Influenza Virus Infection." J Immunol **200**(4): 1489-1495.

- Lai, Y., A. Di Nardo, T. Nakatsuji, A. Leichtle, Y. Yang, A. L. Cogen, Z. R. Wu, L. V. Hooper, R. R. Schmidt, S. von Aulock, K. A. Radek, C. M. Huang, A. F. Ryan and R. L. Gallo (2009). "Commensal bacteria regulate Toll-like receptor 3-dependent inflammation after skin injury." Nat Med **15**(12): 1377-1382.

- Lamkanfi, M. and Vishva M. Dixit "Mechanisms and Functions of Inflammasomes." Cell **157**(5): 1013-1022.

- Larkin, B., V. Ilyukha, M. Sorokin, A. Buzdin, E. Vannier and A. Poltorak (2017). "Cutting Edge: Activation of STING in T Cells Induces Type I IFN Responses and Cell Death." J Immunol **199**(2): 397-402.

- Le Goffic, R., V. Balloy, M. Lagranderie, L. Alexopoulou, N. Escriou, R. Flavell, M. Chignard and M. Si-Tahar (2006). "Detrimental contribution of the Toll-like

receptor (TLR)3 to influenza A virus-induced acute pneumonia." PLoS Pathog **2**(6): e53.

- Li, P., P. Kaiser, H. W. Lampiris, P. Kim, S. A. Yukl, D. V. Havlir, W. C. Greene and J. K. Wong (2016). "Stimulating the RIG-I pathway to kill cells in the latent HIV reservoir following viral reactivation." Nat Med **22**(7): 807-811.

- Li, T. and Z. J. Chen (2018). "The cGAS-cGAMP-STING pathway connects DNA damage to inflammation, senescence, and cancer." J Exp Med **215**(5): 1287-1299.

- Lin, J., S. Kumari, C. Kim, T. M. Van, L. Wachsmuth, A. Polykratis and M. Pasparakis (2016). "RIPK1 counteracts ZBP1-mediated necroptosis to inhibit inflammation." Nature **540**(7631): 124-128.

- Lippmann, J., S. Rothenburg, N. Deigendesch, J. Eitel, K. Meixenberger, V. van Laak, H. Slevogt, D. N'Guessan P, S. Hippenstiel, T. Chakraborty, A. Flieger, N. Suttorp and B. Opitz (2008). "IFNbeta responses induced by intracellular bacteria or cytosolic DNA in different human cells do not require ZBP1 (DLM-1/DAI)." Cell Microbiol **10**(12): 2579-2588.

- Liu, X., Z. Zhang, J. Ruan, Y. Pan, V. G. Magupalli, H. Wu and J. Lieberman (2016). "Inflammasome-activated gasdermin D causes pyroptosis by forming membrane pores." Nature **535**(7610): 153-158.

- Lu, C., D. Ren, X. Wang, T. Ha, L. Liu, E. J. Lee, J. Hu, J. Kalbfleisch, X. Gao, R. Kao, D. Williams and C. Li (2014). "Toll-like receptor 3 plays a role in myocardial infarction and ischemia/reperfusion injury." Biochim Biophys Acta **1842**(1): 22-31.

- Mackenzie, K. J., P. Carroll, L. Lettice, Z. Tarnauskaite, K. Reddy, F. Dix, A. Revuelta, E. Abbondati, R. E. Rigby, B. Rabe, F. Kilanowski, G. Grimes, A. Fluteau, P. S. Devenney, R. E. Hill, M. A. Reijns and A. P. Jackson (2016). "Ribonuclease H2 mutations induce a cGAS/STING-dependent innate immune response." Embo j **35**(8): 831-844.

- Maelfait, J., A. Bridgeman, A. Benlahrech, C. Cursi and J. Rehwinkel (2016). "Restriction by SAMHD1 Limits cGAS/STING-Dependent Innate and Adaptive Immune Responses to HIV-1." Cell Rep **16**(6): 1492-1501.

- Maelfait, J., L. Liverpool, A. Bridgeman, K. Ragan, J. Upton and J. Rehwinkel (2017). "Sensing of viral and endogenous RNA by ZBP1/DAI induces necroptosis." The EMBO Journal.

- Maelfait, J., E. Vercammen, S. Janssens, P. Schotte, M. Haegman, S. Magez and R. Beyaert (2008). "Stimulation of Toll-like receptor 3 and 4 induces interleukin-1beta maturation by caspase-8." J Exp Med **205**(9): 1967-1973.

- Man, S. M., R. Karki and T. D. Kanneganti (2016). "DNA-sensing inflammasomes: regulation of bacterial host defense and the gut microbiota." Pathog Dis **74**(4): ftw028.

- Man, S. M., R. Karki, R. K. Malireddi, G. Neale, P. Vogel, M. Yamamoto, M. Lamkanfi and T. D. Kanneganti (2015). "The transcription factor IRF1 and guanylate-binding proteins target activation of the AIM2 inflammasome by Francisella infection." Nat Immunol **16**(5): 467-475.

- McAllister, C. S., O. Lakhdari, G. Pineton de Chambrun, M. G. Gareau, A. Broquet, G. H. Lee, S. Shenouda, L. Eckmann and M. F. Kagnoff (2013). "TLR3, TRIF, and caspase 8 determine double-stranded RNA-induced epithelial cell death and survival in vivo." J Immunol **190**(1): 418-427.

- McArthur, K., L. W. Whitehead, J. M. Heddleston, L. Li, B. S. Padman, V. Oorschot, N. D. Geoghegan, S. Chappaz, S. Davidson, H. San Chin, R. M. Lane, M. Dramicanin, T. L. Saunders, C. Sugiana, R. Lessene, L. D. Osellame, T.-L. Chew, G. Dewson, M. Lazarou, G. Ramm, G. Lessene, M. T. Ryan, K. L. Rogers, M. F. van Delft and B. T. Kile (2018). "BAK/BAX macropores facilitate mitochondrial herniation and mtDNA efflux during apoptosis." Science **359**(6378): eaao6047.

- McNab, F., K. Mayer-Barber, A. Sher, A. Wack and A. O'Garra (2015). "Type I interferons in infectious disease." Nat Rev Immunol **15**(2): 87-103.

- Medzhitov, R., D. S. Schneider and M. P. Soares (2012). "Disease tolerance as a defense strategy." Science **335**(6071): 936-941.

- Menard, C., M. Wagner, Z. Ruzsics, K. Holak, W. Brune, A. E. Campbell and U. H. Koszinowski (2003). "Role of murine cytomegalovirus US22 gene family members in replication in macrophages." J Virol **77**(10): 5557-5570.

- Meunier, E., P. Wallet, R. F. Dreier, S. Costanzo, L. Anton, S. Ruhl, S. Dussurgey, M. S. Dick, A. Kistner, M. Rigard, D. Degrandi, K. Pfeffer, M. Yamamoto, T. Henry and P. Broz (2015). "Guanylate-binding proteins promote activation of the AIM2 inflammasome during infection with Francisella novicida." Nat Immunol **16**(5): 476-484.

- Meylan, E., K. Burns, K. Hofmann, V. Blancheteau, F. Martinon, M. Kelliher and J. Tschopp (2004). "RIP1 is an essential mediator of Toll-like receptor 3-induced NF-kappa B activation." Nat Immunol **5**(5): 503-507.

- Monel, B., A. A. Compton, T. Bruel, S. Amraoui, J. Burlaud-Gaillard, N. Roy, F. Guivel-Benhassine, F. Porrot, P. Genin, L. Meertens, L. Sinigaglia, N. Jouvenet, R. Weil, N. Casartelli, C. Demangel, E. Simon-Loriere, A. Moris, P. Roingeard, A. Amara and O. Schwartz (2017). "Zika virus induces massive cytoplasmic

vacuolization and paraptosis-like death in infected cells." EMBO J **36**(12): 1653-1668.

- Monroe, K. M., Z. Yang, J. R. Johnson, X. Geng, G. Doitsh, N. J. Krogan and W. C. Greene (2014). IFI16 DNA sensor is required for death of lymphoid CD4 T cells abortively infected with HIV. Science (New York, N.Y.), American Association for the Advancement of Science. **343:** 428-432.

- Murray, L. A., D. A. Knight, L. McAlonan, R. Argentieri, A. Joshi, F. Shaheen, M. Cunningham, L. Alexopolou, R. A. Flavell, R. T. Sarisky and C. M. Hogaboam (2008). "Deleterious role of TLR3 during hyperoxia-induced acute lung injury." Am J Respir Crit Care Med **178**(12): 1227-1237.

- Muruve, D. A., V. Petrilli, A. K. Zaiss, L. R. White, S. A. Clark, P. J. Ross, R. J. Parks and J. Tschopp (2008). "The inflammasome recognizes cytosolic microbial and host DNA and triggers an innate immune response." Nature **452**(7183): 103-107.

- Nassour, J., R. Radford, A. Correia, J. M. Fuste, B. Schoell, A. Jauch, R. J. Shaw and J. Karlseder (2019). "Autophagic cell death restricts chromosomal instability during replicative crisis." Nature **565**(7741): 659-663.

- Nelson, A. M., S. K. Reddy, T. S. Ratliff, M. Z. Hossain, A. S. Katseff, A. S. Zhu, E. Chang, S. R. Resnik, C. Page, D. Kim, A. J. Whittam, L. S. Miller and L. A. Garza (2015). "dsRNA Released by Tissue Damage Activates TLR3 to Drive Skin Regeneration." Cell Stem Cell **17**(2): 139-151.

- Newton, K. and G. Manning (2016). "Necroptosis and Inflammation." Annu Rev Biochem **85**: 743-763.

- Newton, K., K. E. Wickliffe, A. Maltzman, D. L. Dugger, A. Strasser, V. C. Pham, J. R. Lill, M. Roose-Girma, S. Warming, M. Solon, H. Ngu, J. D. Webster and V. M. Dixit (2016). "RIPK1 inhibits ZBP1-driven necroptosis during development." Nature **540**(7631): 129-133.

- Ng, K. W., E. A. Marshall, J. C. Bell and W. L. Lam (2018). "cGAS-STING and Cancer: Dichotomous Roles in Tumor Immunity and Development." Trends Immunol **39**(1): 44-54.

- Nogusa, S., R. J. Thapa, C. P. Dillon, S. Liedmann, T. H. Oguin, 3rd, J. P. Ingram, D. A. Rodriguez, R. Kosoff, S. Sharma, O. Sturm, K. Verbist, P. J. Gough, J. Bertin, B. M. Hartmann, S. C. Sealfon, W. J. Kaiser, E. S. Mocarski, C. B. Lopez, P. G. Thomas, A. Oberst, D. R. Green and S. Balachandran (2016). "RIPK3 Activates Parallel Pathways of MLKL-Driven Necroptosis and FADD-Mediated Apoptosis to Protect against Influenza A Virus." Cell Host Microbe **20**(1): 13-24.

- Orzalli, M. H. and J. C. Kagan (2017). "Apoptosis and Necroptosis as Host Defense Strategies to Prevent Viral Infection." Trends Cell Biol.

- Oshiumi, H., M. Matsumoto, K. Funami, T. Akazawa and T. Seya (2003). "TICAM-1, an adaptor molecule that participates in Toll-like receptor 3-mediated interferon-beta induction." Nat Immunol **4**(2): 161-167.

- Otkur, W., W. Liu, J. Wang, X. Jia, D. Huang, F. Wang, T. Hayashi, S. I. Tashiro, S. Onodera and T. Ikejima (2018). "Sub-lethal ultraviolet B irradiation and Poly I:C treatment synergistically induced apoptosis of HaCaT cells through NF-kappaB pathway." Mol Immunol **99**: 19-29.

- Petrasek, J., A. Iracheta-Vellve, T. Csak, A. Satishchandran, K. Kodys, E. A. Kurt-Jones, K. A. Fitzgerald and G. Szabo (2013). "STING-IRF3 pathway links endoplasmic reticulum stress with hepatocyte apoptosis in early alcoholic liver disease." Proc Natl Acad Sci U S A **110**(41): 16544-16549.

- Pham, C. L., N. Shanmugam, M. Strange, A. O'Carroll, J. W. Brown, E. Sierecki, Y. Gambin, M. Steain and M. Sunde (2019). "Viral M45 and necroptosis-associated proteins form heteromeric amyloid assemblies." EMBO Rep **20**(2).

- Pham, T. H., K. M. Kwon, Y. E. Kim, K. K. Kim and J. H. Ahn (2013). "DNA sensing-independent inhibition of herpes simplex virus 1 replication by DAI/ZBP1." J Virol **87**(6): 3076-3086.

- Place, D. E. and T.-D. Kanneganti (2019). "Cell death–mediated cytokine release and its therapeutic implications." The Journal of Experimental Medicine **216**(7): 1474-1486.

- Poeck, H., R. Besch, C. Maihoefer, M. Renn, D. Tormo, S. S. Morskaya, S. Kirschnek, E. Gaffal, J. Landsberg, J. Hellmuth, A. Schmidt, D. Anz, M. Bscheider, T. Schwerd, C. Berking, C. Bourquin, U. Kalinke, E. Kremmer, H. Kato, S. Akira, R. Meyers, G. Hacker, M. Neuenhahn, D. Busch, J. Ruland, S. Rothenfusser, M. Prinz, V. Hornung, S. Endres, T. Tuting and G. Hartmann (2008). "5'-Triphosphate-siRNA: turning gene silencing and Rig-I activation against melanoma." Nat Med **14**(11): 1256-1263.

- Rebsamen, M., L. X. Heinz, E. Meylan, M. C. Michallet, K. Schroder, K. Hofmann, J. Vazquez, C. A. Benedict and J. Tschopp (2009). "DAI/ZBP1 recruits RIP1 and RIP3 through RIP homotypic interaction motifs to activate NF-kappaB." EMBO Rep **10**(8): 916-922.

- Rickard, J. A., H. Anderton, N. Etemadi, U. Nachbur, M. Darding, N. Peltzer, N. Lalaoui, K. E. Lawlor, H. Vanyai, C. Hall, A. Bankovacki, L. Gangoda, W. W. Wong, J. Corbin, C. Huang, E. S. Mocarski, J. M. Murphy, W. S. Alexander, A. K. Voss, D. L. Vaux, W. J. Kaiser, H. Walczak and J. Silke (2014). "TNFR1-dependent cell death drives inflammation in Sharpin-deficient mice." Elife **3**.

- Rintahaka, J., D. Wiik, P. E. Kovanen, H. Alenius and S. Matikainen (2008). "Cytosolic antiviral RNA recognition pathway activates caspases 1 and 3." J Immunol **180**(3): 1749-1757.

- Roberts, T. L., A. Idris, J. A. Dunn, G. M. Kelly, C. M. Burnton, S. Hodgson, L. L. Hardy, V. Garceau, M. J. Sweet, I. L. Ross, D. A. Hume and K. J. Stacey (2009). "HIN-200 proteins regulate caspase activation in response to foreign cytoplasmic DNA." Science **323**(5917): 1057-1060.

- Roers, A., B. Hiller and V. Hornung (2016). "Recognition of Endogenous Nucleic Acids by the Innate Immune System." Immunity **44**(4): 739-754.

- Roy, A., D. Dutta, J. Iqbal, G. Pisano, O. Gjyshi, M. A. Ansari, B. Kumar and B. Chandran (2016). Nuclear Innate Immune DNA Sensor IFI16 Is Degraded during Lytic Reactivation of Kaposi's Sarcoma-Associated Herpesvirus (KSHV): Role of IFI16 in Maintenance of KSHV Latency. Journal of Virology. **90:** 8822-8841.

- Ruhl, S., K. Shkarina, B. Demarco, R. Heilig, J. C. Santos and P. Broz (2018). "ESCRT-dependent membrane repair negatively regulates pyroptosis downstream of GSDMD activation." Science **362**(6417): 956-960.

- Saito, Y., H. Hikita, Y. Nozaki, Y. Kai, Y. Makino, T. Nakabori, S. Tanaka, R. Yamada, M. Shigekawa, T. Kodama, R. Sakamori, T. Tatsumi and T. Takehara (2019). "DNase II activated by the mitochondrial apoptotic pathway regulates RIP1-dependent non-apoptotic hepatocyte death via the TLR9/IFN-beta signaling pathway." Cell Death Differ **26**(3): 470-486.

- Sancho-Shimizu, V., R. Perez de Diego, L. Lorenzo, R. Halwani, A. Alangari, E. Israelsson, S. Fabrega, A. Cardon, J. Maluenda, M. Tatematsu, F. Mahvelati, M. Herman, M. Ciancanelli, Y. Guo, Z. AlSum, N. Alkhamis, A. S. Al-Makadma, A. Ghadiri, S. Boucherit, S. Plancoulaine, C. Picard, F. Rozenberg, M. Tardieu, P. Lebon, E. Jouanguy, N. Rezaei, T. Seya, M. Matsumoto, D. Chaussabel, A. Puel, S. Y. Zhang, L. Abel, S. Al-Muhsen and J. L. Casanova (2011). "Herpes simplex encephalitis in children with autosomal recessive and dominant TRIF deficiency." J Clin Invest **121**(12): 4889-4902.

- Schoggins, J. W., D. A. MacDuff, N. Imanaka, M. D. Gainey, B. Shrestha, J. L. Eitson, K. B. Mar, R. B. Richardson, A. V. Ratushny, V. Litvak, R. Dabelic, B. Manicassamy, J. D. Aitchison, A. Aderem, R. M. Elliott, A. Garcia-Sastre, V. Racaniello, E. J. Snijder, W. M. Yokoyama, M. S. Diamond, H. W. Virgin and C. M. Rice (2014). "Pan-viral specificity of IFN-induced genes reveals new roles for cGAS in innate immunity." Nature **505**(7485): 691-695.

- Schoggins, J. W., S. J. Wilson, M. Panis, M. Y. Murphy, C. T. Jones, P. Bieniasz and C. M. Rice (2011). "A diverse range of gene products are effectors of the type I interferon antiviral response." Nature **472**(7344): 481-485.

- Schroder, K. and J. Tschopp (2010). "The inflammasomes." Cell **140**(6): 821-832.

- Schulz, O., S. S. Diebold, M. Chen, T. I. Naslund, M. A. Nolte, L. Alexopoulou, Y. T. Azuma, R. A. Flavell, P. Liljestrom and C. Reis e Sousa (2005). "Toll-like receptor 3 promotes cross-priming to virus-infected cells." Nature **433**(7028): 887-892.

- Seymour, R. E., M. G. Hasham, G. A. Cox, L. D. Shultz, H. Hogenesch, D. C. Roopenian and J. P. Sundberg (2007). "Spontaneous mutations in the mouse Sharpin gene result in multiorgan inflammation, immune system dysregulation and dermatitis." Genes Immun **8**(5): 416-421.

- Sharma, D. and T. D. Kanneganti (2016). "The cell biology of inflammasomes: Mechanisms of inflammasome activation and regulation." J Cell Biol **213**(6): 617-629.

- Shi, J., W. Gao and F. Shao (2017). "Pyroptosis: Gasdermin-Mediated Programmed Necrotic Cell Death." Trends Biochem Sci **42**(4): 245-254.

- Shi, J., Y. Zhao, K. Wang, X. Shi, Y. Wang, H. Huang, Y. Zhuang, T. Cai, F. Wang and F. Shao (2015). "Cleavage of GSDMD by inflammatory caspases determines pyroptotic cell death." Nature **526**(7575): 660-665.

- Silke, J., J. A. Rickard and M. Gerlic (2015). "The diverse role of RIP kinases in necroptosis and inflammation." Nat Immunol **16**(7): 689-697.

- Sridharan, H., K. B. Ragan, H. Guo, R. P. Gilley, V. J. Landsteiner, W. J. Kaiser and J. W. Upton (2017). "Murine cytomegalovirus IE3-dependent transcription is required for DAI/ZBP1-mediated necroptosis." EMBO Rep.

- Sze, A., S. M. Belgnaoui, D. Olagnier, R. Lin, J. Hiscott and J. van Grevenynghe (2013). "Host restriction factor SAMHD1 limits human T cell leukemia virus type 1 infection of monocytes via STING-mediated apoptosis." Cell Host Microbe **14**(4): 422-434.

- Takaoka, A., Z. Wang, M. K. Choi, H. Yanai, H. Negishi, T. Ban, Y. Lu, M. Miyagishi, T. Kodama, K. Honda, Y. Ohba and T. Taniguchi (2007). "DAI (DLM-1/ZBP1) is a cytosolic DNA sensor and an activator of innate immune response." Nature **448**(7152): 501-505.

- Takemura, N., T. Kawasaki, J. Kunisawa, S. Sato, A. Lamichhane, K. Kobiyama, T. Aoshi, J. Ito, K. Mizuguchi, T. Karuppuchamy, K. Matsunaga, S. Miyatake, N. Mori, T. Tsujimura, T. Satoh, Y. Kumagai, T. Kawai, D. M. Standley, K. J. Ishii, H. Kiyono, S. Akira and S. Uematsu (2014). "Blockade of TLR3 protects mice from lethal radiation-induced gastrointestinal syndrome." Nat Commun **5**: 3492.

- Tang, C.-H. A., J. A. Zundell, S. Ranatunga, C. Lin, Y. Nefedova, J. R. Del Valle and C.-C. A. Hu (2016). Agonist-Mediated Activation of STING Induces Apoptosis in Malignant B Cells. Cancer Res, American Association for Cancer Research. **76:** 2137-2152.

- Thapa, R. J., J. P. Ingram, K. B. Ragan, S. Nogusa, D. F. Boyd, A. A. Benitez, H. Sridharan, R. Kosoff, M. Shubina, V. J. Landsteiner, M. Andrake, P. Vogel, L. J. Sigal, B. R. tenOever, P. G. Thomas, J. W. Upton and S. Balachandran (2016). "DAI Senses Influenza A Virus Genomic RNA and Activates RIPK3-Dependent Cell Death." Cell Host Microbe **20**(5): 674-681.

- Unterholzner, L., S. E. Keating, M. Baran, K. A. Horan, S. B. Jensen, S. Sharma, C. M. Sirois, T. Jin, E. Latz, T. S. Xiao, K. A. Fitzgerald, S. R. Paludan and A. G. Bowie (2010). IFI16 is an innate immune sensor for intracellular DNA. Nat Immunol. **11:** 997-1004.

- Upton, J. W., W. J. Kaiser and E. S. Mocarski (2010). "Virus inhibition of RIP3-dependent necrosis." Cell Host Microbe **7**(4): 302-313.

- Upton, J. W., W. J. Kaiser and E. S. Mocarski (2012). "DAI/ZBP1/DLM-1 complexes with RIP3 to mediate virus-induced programmed necrosis that is targeted by murine cytomegalovirus vIRA." Cell Host Microbe **11**(3): 290-297.

- van den Boorn, J. G. and G. Hartmann (2013). "Turning tumors into vaccines: co-opting the innate immune system." Immunity **39**(1): 27-37.

- Vercammen, D., R. Beyaert, G. Denecker, V. Goossens, G. Van Loo, W. Declercq, J. Grooten, W. Fiers and P. Vandenabeele (1998). "Inhibition of caspases increases the sensitivity of L929 cells to necrosis mediated by tumor necrosis factor." J Exp Med **187**(9): 1477-1485.

- Wallach, D., T. B. Kang, C. P. Dillon and D. R. Green (2016). "Programmed necrosis in inflammation: Toward identification of the effector molecules." Science **352**(6281): aaf2154.

- Wang, A. H., T. Hakoshima, G. van der Marel, J. H. van Boom and A. Rich (1984). "AT base pairs are less stable than GC base pairs in Z-DNA: the crystal structure of d(m5CGTAm5CG)." Cell **37**(1): 321-331.

- Wassermann, R., M. F. Gulen, C. Sala, S. G. Perin, Y. Lou, J. Rybniker, J. L. Schmid-Burgk, T. Schmidt, V. Hornung, S. T. Cole and A. Ablasser (2015). "Mycobacterium tuberculosis Differentially Activates cGAS- and Inflammasome-Dependent Intracellular Immune Responses through ESX-1." Cell Host Microbe **17**(6): 799-810.

- Watson, R. O., S. L. Bell, D. A. MacDuff, J. M. Kimmey, E. J. Diner, J. Olivas, R. E. Vance, C. L. Stallings, H. W. Virgin and J. S. Cox (2015). The Cytosolic Sensor cGAS Detects Mycobacterium tuberculosis DNA to Induce Type I Interferons and Activate Autophagy. Cell Host & Microbe. **17:** 811-819.

- Weber, A., Z. Kirejczyk, R. Besch, S. Potthoff, M. Leverkus and G. Hacker (2010). "Proapoptotic signalling through Toll-like receptor-3 involves TRIF-dependent activation of caspase-8 and is under the control of inhibitor of apoptosis proteins in melanoma cells." Cell Death Differ **17**(6): 942-951.

- Weber, F., V. Wagner, S. B. Rasmussen, R. Hartmann and S. R. Paludan (2006). "Double-stranded RNA is produced by positive-strand RNA viruses and DNA viruses but not in detectable amounts by negative-strand RNA viruses." J Virol **80**(10): 5059-5064.

- Weinlich, R., A. Oberst, H. M. Beere and D. R. Green (2017). "Necroptosis in development, inflammation and disease." Nat Rev Mol Cell Biol **18**(2): 127-136.

- Williams, B. R. (2001). "Signal integration via PKR." Sci STKE **2001**(89): re2.

- Woerner, S. M., M. Kloor, A. Mueller, J. Rueschoff, N. Friedrichs, R. Buettner, M. Buzello, P. Kienle, H.-P. Knaebel, E. Kunstmann, C. Pagenstecher, H. K. Schackert, G. Moslein, H. Vogelsang, M. von Knebel Doeberitz and J. F. Gebert (2005). Microsatellite instability of selective target genes in HNPCC-associated colon adenomas. Oncogene. **24:** 2525-2535.

- Woerner, S. M., M. Kloor, Y. Schwitalle, H. Youmans, M. v. K. Doeberitz, J. Gebert and S. Dihlmann (2007). The putative tumor suppressor AIM2 is frequently affected by different genetic alterations in microsatellite unstable colon cancers. Genes Chromosomes Cancer. **46:** 1080-1089.

- Wu, J., Y. J. Chen, N. Dobbs, T. Sakai, J. Liou, J. J. Miner and N. Yan (2019). "STING-mediated disruption of calcium homeostasis chronically activates ER stress and primes T cell death." J Exp Med **216**(4): 867-883.

- Wu, J., L. Sun, X. Chen, F. Du, H. Shi, C. Chen and Z. J. Chen (2013). "Cyclic GMP-AMP is an endogenous second messenger in innate immune signaling by cytosolic DNA." Science **339**(6121): 826-830.

- Xiang, Y., H. Yan, J. Zhou, Q. Zhang, G. Hanley, Y. Caudle, G. LeSage, X. Zhang and D. Yin (2015). The role of toll-like receptor 9 in chronic stress-induced apoptosis in macrophage. PLoS ONE. **10:** e0123447.

- Yamamoto, M., S. Sato, H. Hemmi, K. Hoshino, T. Kaisho, H. Sanjo, O. Takeuchi, M. Sugiyama, M. Okabe, K. Takeda and S. Akira (2003). "Role of adaptor TRIF in

the MyD88-independent toll-like receptor signaling pathway." Science **301**(5633): 640-643.

- Yamamoto, M., S. Sato, K. Mori, K. Hoshino, O. Takeuchi, K. Takeda and S. Akira (2002). "Cutting edge: a novel Toll/IL-1 receptor domain-containing adapter that preferentially activates the IFN-beta promoter in the Toll-like receptor signaling." J Immunol **169**(12): 6668-6672.

- Yang, D., Y. Liang, S. Zhao, Y. Ding, Q. Zhuang, Q. Shi, T. Ai, S. Q. Wu and J. Han (2019). "ZBP1 mediates interferon-induced necroptosis." Cell Mol Immunol.

- Yang, H., H. Wang, J. Ren, Q. Chen and Z. J. Chen (2017). "cGAS is essential for cellular senescence." Proc Natl Acad Sci U S A **114**(23): E4612-e4620.

- Yu, X., H. Wang, X. Li, C. Guo, F. Yuan, P. B. Fisher and X. Y. Wang (2016). "Activation of the MDA-5-IPS-1 Viral Sensing Pathway Induces Cancer Cell Death and Type I IFN-Dependent Antitumor Immunity." Cancer Res **76**(8): 2166-2176.

- Zhang, H., J. Luo, J. F. Alcorn, K. Chen, S. Fan, J. Pilewski, A. Liu, W. Chen, J. K. Kolls and J. Wang (2017). "AIM2 Inflammasome Is Critical for Influenza-Induced Lung Injury and Mortality." J Immunol **198**(11): 4383-4393.

- Zhang, S. Y., E. Jouanguy, S. Ugolini, A. Smahi, G. Elain, P. Romero, D. Segal, V. Sancho-Shimizu, L. Lorenzo, A. Puel, C. Picard, A. Chapgier, S. Plancoulaine, M. Titeux, C. Cognet, H. von Bernuth, C. L. Ku, A. Casrouge, X. X. Zhang, L. Barreiro, J. Leonard, C. Hamilton, P. Lebon, B. Heron, L. Vallee, L. Quintana-Murci, A. Hovnanian, F. Rozenberg, E. Vivier, F. Geissmann, M. Tardieu, L. Abel and J. L. Casanova (2007). "TLR3 deficiency in patients with herpes simplex encephalitis." Science **317**(5844): 1522-1527.

- Zheng, L., N. Asprodites, A. H. Keene, P. Rodriguez, K. D. Brown and E. Davila (2008). TLR9 engagement on CD4 T lymphocytes represses gamma-radiation-induced apoptosis through activation of checkpoint kinase response elements. 14th Conference on retroviruses and opportunistic infections (CROI). **111:** 2704-2713.

- Zhu, S., S. Ding, P. Wang, Z. Wei, W. Pan, N. W. Palm, Y. Yang, H. Yu, H. B. Li, G. Wang, X. Lei, M. R. de Zoete, J. Zhao, Y. Zheng, H. Chen, Y. Zhao, K. A. Jurado, N. Feng, L. Shan, Y. Kluger, J. Lu, C. Abraham, E. Fikrig, H. B. Greenberg and R. A. Flavell (2017). "Nlrp9b inflammasome restricts rotavirus infection in intestinal epithelial cells." Nature **546**(7660): 667-670.

- Zinngrebe, J., E. Rieser, L. Taraborrelli, N. Peltzer, T. Hartwig, H. Ren, I. Kovacs, C. Endres, P. Draber, M. Darding, S. von Karstedt, J. Lemke, B. Dome, M. Bergmann, B. J. Ferguson and H. Walczak (2016). "--LUBAC deficiency perturbs TLR3 signaling to cause immunodeficiency and autoinflammation." J Exp Med **213**(12): 2671-2689.

1353

Tables, Figures and Figure legends

Table 1. Overview of apoptosis, pyroptosis and necroptosis.

	Apoptosis	Pyroptosis	Necroptosis
Cellular events	cell shrinkage DNA fragmentation apoptotic bodies	pore formation loss of plasma membrane integrity swollen cellular organelles	
Inflammation	non-inflammatory	pro-inflammatory	
Key proteins*	caspase-3	ASC caspase-1 GSDMD	RIPK3 MLKL
DNA sensors*	cGAS-STING TLR9	AIM2 IFI16	
RNA sensors*	RIG-I MDA5	NLRP3 NLRP9b	TLR3 ZBP1

(*) selected examples, please see text for further details

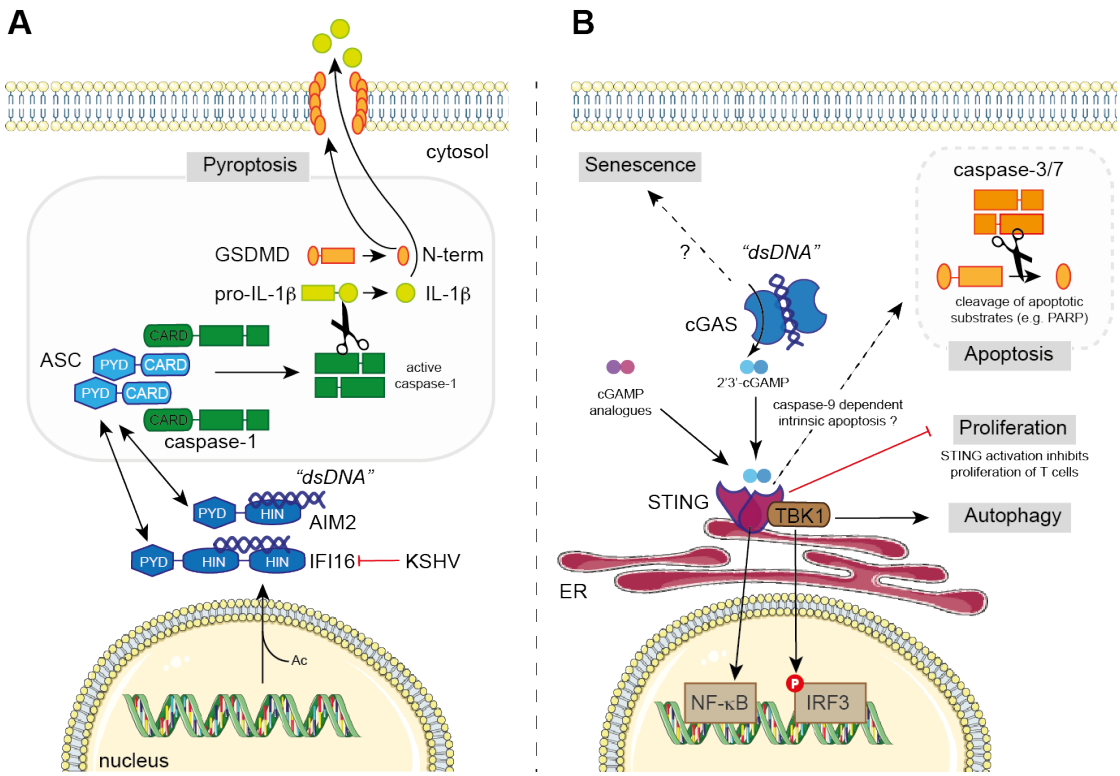


Figure 1. Cell death pathways triggered by DNA sensors.

(A) The AIM2-like receptors AIM2 and IFI16 recognise dsDNA and induce pyroptosis. AIM2 resides in the cytosol, while IFI16 can sense viruses such as KSHV in the nucleus. Acetylation (Ac) of IFI16 promotes its nuclear export. KSHV antagonises IFI16 by inducing its proteasomal degradation. AIM2 and IFI16 bind to dsDNA via their HIN200 domains (HIN) and subsequently recruit ASC via Pyrin domain (PYD) interactions. ASC contains a CARD domain, which interacts with the CARD of pro-caspase-1, forming a large molecular weight complex called the 'ASC-speck'. Autocatalytic cleavage of pro-caspase-1 results in the formation of active caspase-1, which cleaves GSDMD releasing the cytotoxic N-terminal fragment (p30) that forms pores in the cell membrane. Caspase-1 also cleaves pro-IL1β, leading to the maturation into its biologically active form.

(B) The cGAS/STING pathway detects the presence of dsDNA inside the cytosol and promotes antiviral immunity by inducing type I IFN production. Upon binding of dsDNA, cGAS synthetises the cyclic di-nucleotide cGAMP, a ligand for the ER-resident protein STING. cGAMP analogues, bacterial cyclic di-nucleotides and certain chemically synthesised molecules such as DMXAA can also bind STING. Activated STING recruits the kinase TBK1, which phosphorylates the transcription factor IRF3.

IRF3 then dimerises and translocates to the nucleus where it controls type I IFN gene expression. STING also induces the activation of the pro-inflammatory transcription factor NF-κB. Engagement of cGAS/STING can also induce cell death presumably via the cell-intrinsic caspase-9 mediated apoptotic pathway. Active caspase-9 activates the executioner caspases 3 and 7. Other outcomes of cGAS/STING stimulation include cellular senescence, inhibition of T cell proliferation and autophagy. The signalling pathways that control these processes are poorly characterised.

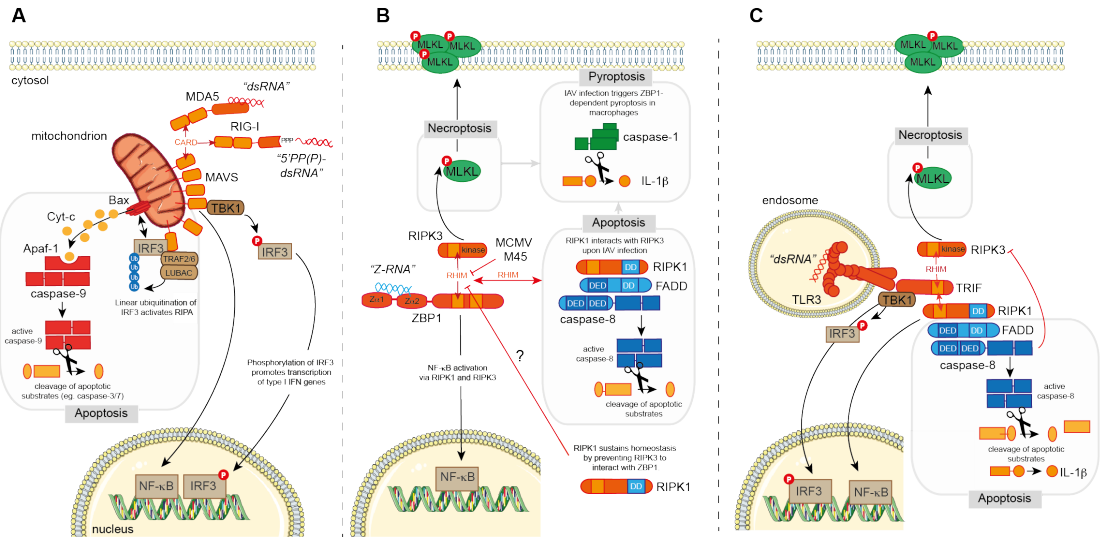


Figure 2. Cell death pathways triggered by RNA sensors.

(A) The RLRs RIG-I and MDA5 recognise 5' di- or triphosphorylated short stretches of base-paired RNA and long complex dsRNA, respectively. Stimulation of RIG-I and MDA5 exposes their CARDs, which interact with the CARD of MAVS. MAVS forms a multimeric complex localised at the mitochondria, from where two distinct signalling pathways diverge. One complex contains the kinase TBK1, which phosphorylates and activates the IRF3 transcription factor, which in turn controls expression type I IFN. MAVS also stimulates the activation of the pro-inflammatory transcription factor NF-κB. A second complex forms with TRAF2, TRAF6 and LUBAC and activates the RLR-induced IRF3 mediated pathway of apoptosis (RIPA). LUBAC adds linear ubiquitin chains onto IRF3, which activates the pro-apoptotic protein Bax. This leads to leakage of cytochrome-c out of the mitochondria. Cytochrome-c binds to and activates the pro-apoptotic protein Apaf-1, which induces the cleavage of the pro-enzyme of caspase-9 into the active form.

(B) ZBP1 contains two N-terminal Z-nucleic acid binding domains (Zα1 and Zα2) through which it binds to Z-form dsRNA (Z-RNA). Upon activation, ZBP1 interacts with RIPK3 via homotypic RHIM interactions. ZBP1 contains two tandem RHIMs (RHIM-A and RHIM-B), of which only RHIM-A is required for this interaction. RIPK3 then phosphorylates MLKL, which upon oligomerisation triggers necroptosis by inducing permeabilisation of the cell membrane. In cells infected with IAV, RIPK3 also associates with RIPK1. RIPK1 contains a death domain (DD) through which it recruits FADD. FADD associates with caspase-8 through death-effector domain (DED) interactions leading to caspase-8 activation and apoptosis. In macrophages, ZBP1-

mediated necroptosis or apoptosis triggers the formation of a caspase-1 inflammasome leading to maturation of IL-1β. ZBP1 can also induce NF-κB activation and this requires RIPK1 or RIPK3. The RHIM of RIPK1 prevents ZBP1-mediated necroptosis during development and in keratinocytes. The mechanism through which RIPK1 prevents such 'spontaneous' ZBP1 activation is unknown.

(C) TLR3 is expressed on the cell surface (not shown) and in endosomes. The ligand-binding domain of TLR3 faces the endosomal lumen and binds to dsRNA. TLR3 signals via TRIF that contains a RHIM, allowing recruitment of RIPK1 and RIPK3. Interactions with RIPK1 stimulate NF-κB activation and pro-inflammatory gene expression. TRIF also signals via TBK1 and IRF3 promoting type I IFN gene expression. RIPK1 can also associate with FADD and caspase-8 to induce apoptosis. Active caspase-8 can directly cleave pro-IL1β into its biologically active form in TLR3-stimulated macrophages. When caspase-8 activation is compromised, RIPK3 is recruited to TRIF and induces necroptosis by activating MLKL, independently of RIPK1.